

WestminsterResearch

<http://www.westminster.ac.uk/research/westminsterresearch>

Engineering of recombinant antimalaria antibodies for application in paratransgenesis.

Bernard Q. Anani

School of Life Sciences

This is an electronic version of a PhD thesis awarded by the University of Westminster. © The Author, 2011.

This is an exact reproduction of the paper copy held by the University of Westminster library.

The WestminsterResearch online digital archive at the University of Westminster aims to make the research output of the University available to a wider audience. Copyright and Moral Rights remain with the authors and/or copyright owners.

Users are permitted to download and/or print one copy for non-commercial private study or research. Further distribution and any use of material from within this archive for profit-making enterprises or for commercial gain is strictly forbidden.

Whilst further distribution of specific materials from within this archive is forbidden, you may freely distribute the URL of WestminsterResearch: (<http://westminsterresearch.wmin.ac.uk/>).

In case of abuse or copyright appearing without permission e-mail repository@westminster.ac.uk

**ENGINEERING OF RECOMBINANT
ANTIMALARIA ANTIBODIES FOR
APPLICATION IN PARATRANSGENESIS**

Bernard Q. Anani

A THESIS SUBMITTED IN PARTIAL FULFILMENT OF THE REQUIREMENTS
OF THE UNIVERSITY OF WESTMINSTER FOR THE DEGREE OF DOCTOR
OF PHILOSOPHY

OCTOBER 2011

Abstract

Malaria, transmitted by *Anopheles* mosquitoes is responsible for millions of deaths worldwide, especially in the developing countries. The emergence of drug resistant parasites and insecticide resistant vectors has stimulated efforts to develop novel genetic strategies to modify the insect vector and reduce its competence to transmit the parasite. One proposed approach is the genetic manipulation of insect's midgut symbionts to express anti-parasite molecules.

Recombinant antibodies that target specific antigens expressed on the parasites' surface could be used as anti-parasite molecules, especially if they could not only bind but agglutinate the target. The murine antibody 4B7 binds to Pfs25 epitope expressed on the zygote and ookinete stages of the parasite. Pf-NPNA-1 is a human antibody that specifically binds to the NPNA (Asn-Pro-Asn-Ala) repeats of the circumsporozoite protein expressed on the sporozoite stage of the malaria parasite. This study aimed to characterise these antibodies for their application in symbiont control. For this purpose, the antibodies have been codon optimised for bacterial expression and formatted as single chain variable fragments (scFv).

Synthetic genes encoding the scFv 4B7 and Pf-NPNA-1 were constructed, with varying linker length, in the V_H-V_L and V_L-V_H orientation. The scFvs were cloned into different expression plasmids to evaluate a suitable expression system. The orientation of the variable domains on secretion of the scFv 4B7 was investigated. No secretion was observed for the scFv 4B7 in the V_H-V_L orientation. For the reverse orientation, scFv 4B7 (V_L-V_H) was poorly secreted with no antigen binding. Secretion was observed for a variant of scFv 4B7 but this did not show significant antigen binding. Pf-NPNA-1 scFv constructs, in the V_H-V_L orientation, were efficiently secreted and showed detectable binding to antigen. Multimeric assembly of the scFv constructs was evaluated by varying the linker length. 4B7 and Pf-NPNA-1 scFv constructs exhibited monomeric, dimeric and multimeric assembly. Fusion of the human kappa constant domain to the scFvs resulted in formation of monomeric and higher ordered forms. Transfer of the scFv gene fragments into a broad-host vector facilitated evaluation of recombinant antibody expression in the acetic acid bacterium, *Asaia* SF2.1.

In summary, the results from this study demonstrate the potential utility of the antibodies, 4B7 and Pf-NPNA-1, as anti-parasite molecules for blockade of malaria transmission via mosquito midgut symbionts.

Acknowledgements

Firstly and foremost, my sincere appreciation to my director of studies, Dr. Angray S. Kang, for his immense support, guidance, advice and patience throughout my studies. I am grateful for his contributions of time, ideas, and funding to make my Ph.D experience productive and stimulating.

I would also like to thank Dr. Ian Harmer, my second supervisor, for his helpful comments. Special thanks to Dr. Anatoliy Markiv for his constructive criticism and assistance with Vector NTI and fluorescent microscope.

I am grateful to Dr. John McCarfferty, Dr. Mark Clements, Dr. Takafumi Tsuboi and Dr. David Millich for provision of pSANG10-3F and pET41b(+) vectors, Pfs25 and (NPNA)₃ antigens, respectively. The immunofluorescence assay would not have been possible without the *P. falciparum* sporozoites provided by Dr. Lisa Ranford-Cartwright.

My colleagues in the laboratory have contributed immensely to my personal and professional time at Westminster. I would like to acknowledge Dr. Victor Ujor, Dr. Shameem Fawdar, Tang Jie and Armaghan Azizi for their friendship and encouragement. Other past and present group members that I have had the pleasure to work with or alongside of are Anne Langheinze and Alessia Cagnetti. I am also thankful to the technical staff for their assistance, especially Dr. Thakor Tandel and Vanita Patel.

I am also grateful to the University of Westminster for granting me the Cavendish Research Scholarship.

And finally to my parents, Dr. and Mrs. Anani, my siblings Francisca and Francis, and my nephew John for their continued support and prayers.

TABLE OF CONTENTS

	Page
Title	i
Abstract	ii
Acknowledgement	iii
Table of contents	iv
List of Figures	vii
List of Tables	x
Abbreviations	xi
CHAPTER 1: General Introduction	1
1.1 Introduction	2
1.2 Application of biological agents for control of malaria	10
1.2.1 Fungal biopesticides	11
1.2.2 Transgenesis	14
1.2.3 Paratransgenesis	17
1.3 Effector molecules	23
1.4 Prokaryotic expression of scFv fragments	29
1.5 Thesis aim and objectives	30
CHAPTER 2: Materials and Methods	32
2.1 Materials and methods	33
2.1.1 General chemicals and reagents	33
2.1.2 Bacterial strains	33
2.1.3 Antibiotic stock solutions	33
2.1.4 Buffers and media	33
2.1.5 Antibodies and Enzymes	34
2.1.5.1 Restriction Enzymes	34
2.1.5.2 Antibodies	34
2.1.6 DNA Vectors	35
2.2 Molecular biology methods	35
2.2.1 Separation of DNA using agarose gel electrophoresis	35

Table of contents

2.2.2 Gel purification of PCR products and plasmid DNA	36
2.2.3 Restriction endonuclease digestion	33
2.2.4 Ligation of DNA fragments	37
2.2.5 Preparation of <i>E. coli</i> chemical competent cells	37
2.2.6 Transformation of <i>E. coli</i> using the heat-shock method	38
2.2.7 PCR colony screening	38
2.2.8 Preservation of bacterial cultures	39
2.2.9 Plasmid DNA extraction	39
2.2.10 DNA quantification and Sequencing	40
2.3 Construction of scFv expression vectors	41
2.3.1 Construction of scFv expression vectors pBAK.1 and pBAK.1Hk	41
2.3.2 Cloning of synthetic DNA Constructs	41
2.3.3 Construction of 4B7 V _L -V _H scFv-0, scFv-20, scFv-0Hk and scFv-20Hk	42
2.3.4 Site directed mutagenesis of 4B7 scFv	45
2.3.5 Construction of Pf-NPNA V _H -V _L scFv-0, scFv-12, scFv-0Hk and scFv-12Hk	47
2.4 Protein expression and purification of recombinant proteins	49
2.4.1 Expression and purification of (NPNA) ₉ -MKC antigen	49
2.4.2 Soluble expression of recombinant scFv and scFv-Hk antibodies	49
2.4.3 Isolation and purification of periplasmic extracts	50
2.4.4 Desalting of IMAC purified proteins	51
2.4.5 Anion exchange chromatography (AEC)	51
2.4.6 Cation exchange chromatography (CEC)	51
2.4.7 Sodium Dodecyl Sulphate Polyacrylamide Gel Electrophoresis	52
2.4.8 Coomassie Brilliant Blue staining of protein gels	53
2.4.9 Bradford assay	53
2.4.10 Western blotting	54
2.4.11 Enzyme-linked immunosorbent assay (DeLisa <i>et al.</i>)	54
2.4.12 Size-exclusion chromatography (SEC)	56

Table of contents

2.4.13 Indirect Immunofluorescence Assay (IFA) on <i>P. falciparum</i> sporozoites	56
2.4.14 Statistical Analysis	57
2.5 Preliminary evaluation of Pf-NPNA-1 and 4B7 scFvs in <i>Asaia</i> SF2.1	58
2.5.1 Assessment of antibiotic resistance	58
2.5.2 Preparation of Electrocompetent <i>Asaia</i> sp.	58
2.5.3 Expression of Pf-NPNA-1 and 4B7 scFvs in <i>Asaia</i> sp.	59
2.5.4 Isolation and purification of Pf-NPNA-1 (scFv-0 and 12) and 4B7 scFv-0	59
CHAPTER 3: Results	61
3.1 Introduction to results	62
3.2 Construction of scFv expression vectors pBAK.1 and pBAK.1Hk	63
3.2.1 Cloning of 4B7 scFv-1 V _H -V _L gene into pBAK.1 and pBAK.1Hk	65
3.2.2 Cloning of 4B7 scFv-0 and scFv-20 V _L - V _H genes into pSANG10-3F and pBAK.1Hk	67
3.2.3 ELISA for functional analysis of 4B7 scFv-0 and scFv-20	71
3.2.4 Site directed mutagenesis of 4B7 (V _L - V _H) scFv-0 and scFv-20	73
3.2.5 ELISA of 4B7 (AJ) scFv-0 (V _L - V _H) and scFv-20 (V _L - V _H)	79
3.3 Discussion on expression and characterisation of 4B7 scFv	81
3.3.2 Site-directed mutagenesis of scFv 4B7 framework residues	85
3.3.3 Assessment of 4B7 scFv-0 and 20 multimer formation	87
3.3.4 Effect of HuCk on 4B7 scFv expression	89
3.4 Results for expression and characterisation of Pf-NPNA-1	92
3.4.1 Cloning, expression and purification of (NPNA) ₉ -MKC antigen	92
3.4.2 Cloning of Pf-NPNA-1 scFv-0 and scFv-12 V _H - V _L genes into pBAK.1, pSANG10-3F	94
3.4.3 Cloning of Pf-NPNA-1 scFv-0 V _H -V _L	95
3.4.4 ELISA for functional analyses of Pf-NPNA-1 scFv-0 and scFv-12	100
3.4.5 Indirect Immunofluorescence Assay (IFA) on <i>P. falciparum</i> Sporozoites	105

Table of contents

CHAPTER 4: Expression of scFv 4B7 and Pf-NPNA-1 in <i>Asaia</i>	110
4.1 The genus <i>Asaia</i>	111
4.2 Assessment of antibiotic resistance	113
4.3 Expression of recombinant proteins in <i>Asaia</i> SF2.1	114
4.3.2 Carbon utilisation of <i>Asaia</i>	116
4.3.3 Cloning of 4B7 and Pf-NPNA-1 scFvs into pMAK031 2P	117
4.4 Discussion on recombinant expression of scFvs in <i>Asaia</i> SF2.1	123
CHAPTER 5: General Discussion and Conclusion	127
5.1 Discussion	128
CHAPTER 6: Conclusion and Future prospects	134
6.1 Conclusion	135
6.2 Future work	136
6.2.1 Multimeric assembly of scFv	136
6.2.2 Homology modelling and affinity enhancement of scFv 4B7	137
6.2.3 Extracellular secretion of recombinant scFvs in <i>Asaia</i> sp. SF2.1	138
6.2.4 Evaluation of scFv expression in <i>Anopheles</i> and its impact on parasite load	139
REFERENCES	140
APPENDIX	161
PUBLICATION	199

List of Figures

	Page
Figure 1.1: Global distribution of malaria with low and high areas of transmission	2
Figure 1.2: Plasmodium life cycle in the vertebrate host and mosquito	3
Figure 1.3: Parasite losses and amplification in the mosquito	5
Figure 1.4: Superimposed structures of Pfs25 and Pvs25	7
Figure 1.5: Schematic representation of the PfCS protein	9
Figure 1.6: Nomenclature of engineered antibody fragments in comparison with native IgG	25
Figure 1.7: Molecular models of scFv monomer, dimer and trimer	29
Figure 2.1: Design and construction of 4B7 scFv-0 (V_L - V_H)	43
Figure 2.2: Design and construction of 4B7 scFv-20 (V_L - V_H)	44
Figure 2.3: Design and construction of 4B7 scFv-0 mutants (V_H Q20R and V_H T94F)	45
Figure 2.4: Design and construction of 4B7 scFv-0 mutants (V_L L85F, V_L G86A, V_L Q3E, V_L I5T and V_H L114V)	46
Figure 2.5: Design and construction of Pf-NPNA-1 scFv-0 (V_H - V_L)	47
Figure 3.1: Cloning strategy and restriction maps of pET41b(+), pET41b(+) _{Hk} , pORFES and pBAK.1 _{Hk}	64
Figure 3.2: Cloning strategy and restriction maps of pET41b(+), pORFES and pBAK.1	55
Figure 3.3: SDS-PAGE analysis under reducing conditions and Western blotting of small scale purification 4B7 scFv-1 V_H - V_L	66
Figure 3.4: Expression and purification of 4B7 scFv-0 and scFv-20	68
Figure 3.5: AEC of 4B7 scFv-0 and scFv-20 using pSANG10-3F plasmid	61
Figure 3.6: Expression and purification of 4B7 scFv-0 and 20 using pBAK.1 _{Hk} plasmid	70
Figure 3.7: AEC of 4B7 scFv-0 and 20 using pBAK.1 _{Hk} plasmid	70
Figure 3.8: Specificity evaluation of 4B7 pSANG10-3F expressed scFv-0 and scFv-20 to Pfs25	71

Figure 3.9: Specificity of soluble 4B7 scFv-0 and scFv-20 expressed from pBAK.1Hk to Pfs25	72
Figure 3.10: Amino acid sequence alignment of two variants of 4B7 scFv	73
Figure 3.11: Expression and purification of 4B7 (AJ) scFv-0 and scFv-20 using pSANG10-3F plasmid	74
Figure 3.12: Western blot of IMAC purified proteins electrophoresed under reducing and non-reducing conditions	75
Figure 3.13: Anion exchange chromatography of 4B7 scFv-20 a 1 mL HiTrap Q Sepharose column	76
Figure 3.14: Size exclusion HPLC on a calibrated Hi-Load 16/60 Superdex column of purified 4B7 scFv-20.	77
Figure 3.15: Expression and purification of 4B7 (AJ) scFv-0HK	78
Figure 3.16: Expression and purification of 4B7 (AJ) scFv-20HK	78
Figure 3.17: Specificity evaluation of 4B7 (AJ) pSANG10-3F expressed scFv-0 and scFv-20 to Pfs25	79
Figure 3.18: Specificity of soluble 4B7 (AJ) scFv-0 and scFv-20 expressed from pBAK.1Hk to Pfs25	80
Figure 3.19: Ni-NTA purification of (NPNA) ₉ -MKC antigen	92
Figure 3.20: SDS-PAGE analysis of Ni-NTA affinity purified (NPNA) ₉ -MKC antigen	93
Figure 3.21: SDS-PAGE and Western blotting of small scale purification of Pf-NPNA-1V _H – V _L scFv-12	94
Figure 3.22: Expression and purification of Pf-NPNA-1 scFv-0 and 12 using pBAK.1plasmid	96
Figure 3.23: CEC of Pf-NPNA-1 scFv-0 and 12 using pBAK1 plasmid	96
Figure 3.24: Expression and purification of Pf-NPNA-1 scFv-0 and 12 using pSANG10-3F plasmid	97
Figure 3.25: Western blot of expressed and purified Pf-NPNA-1 scFv-0 and scFv-12 using pSANG10-3F	98
Figure 3.26: Expression and purification of Pf-NPNA-1 scFv-0 and 12 using pBAK.1Hk plasmid	99

List of Figures

Figure 3.27: CEC of Pf-NPNA-1 scFv-0 and 12 using pBAK.1Hk plasmid	99
Figure 3.28: Specificity of soluble Pf-NPNA-1 scFv-0 and scFv-12 expressed from pBAK.1Hk to (NPNA) ₉ -MKC	101
Figure 3.29: Specificity of soluble Pf-NPNA-1 scFv-0 and scFv-12 expressed from pSANG10-3F to WHcAg	102
Figure 3.30: Specificity of soluble Pf-NPNA-1 scFv-0 and scFv-12 expressed from pBAK.1 to WHcAg	103
Figure 3.31: Specificity of soluble Pf-NPNA-1 scFv-0 and scFv-12 expressed from pBAK.1Hk to WHcAg	104
Figure 3.32: Indirect Immunofluorescence Assay of Pf-NPNA-1 scFv-0 and scFv-12	105
Figure 3.33: Sequence alignment of the <i>pefB</i> signal sequence from pSANG10-3F and pBAK.1	108
Figure 4.1: Assessment of kanamycin resistance of <i>Asaia</i> SF2.1	113
Figure 4.2: Vector map of plasmid pMAK031 2P with a GFP gene	114
Figure 4.3: Fluorescence images of <i>E. coli</i> (A) and <i>Asaia sp</i> SF2.1 (B) transformed with pMAK031(2P)-GFP	115
Figure 4.4: Growth profile of pMAK031 2P 4B7 scFv-0 transformed <i>Asaia sp</i> SF1 on different carbon sources	116
Figure 4.5: Restriction enzyme digestion of pMAK031 2P-GFP	117
Figure 4.6: Impact of production time on expression scFv in small scale culture of <i>Asaia</i>	118
Figure 4.7: Purification and Western blot of <i>E. coli</i> and <i>Asaia</i> expressed and purified 4B7(AJ) scFv-0	119
Figure 4.8: Purification and SDS-PAGE of <i>Asaia</i> expressed Pf-NPNA-1 scFv-0	120
Figure 4.9: Purification and SDS-PAGE of <i>Asaia</i> expressed Pf-NPNA-1 scFv-12	121
Figure 4.10: Western blot of purified Pf-NPNA-1 scFv-0 and 12 from <i>Asaia sp.</i> SF2.1 with different signal peptides	122
Figure 4.11: Specificity evaluation of Pf-NPNA-1 pMAK031 2P expressed scFv-0 and scFv-12 to WHcAg	122

List of Tables	Page
Table 1.1: Stage-specific differences in <i>Plasmodium</i> parasite numbers	6
Table 1.2: Bacteria microbiota from different mosquito species	22
Table 1.3: Effector target, molecule and target parasite for engineering <i>Plasmodium</i> resistance in mosquitoes	24
Table 1.4: Signal sequences used for the secretory production of recombinant proteins in <i>E. coli</i>	27
Table 2.1: Amplification program for PCR colony screening	38
Table 2.2: PCR cycle profile for the amplification of 4B7 scFv-1 variable domains and assembly of scFv-0 and scFv-20	42
Table 2.3: Primer sequences used for the amplification of 4B7 scFv variable domains and for assembly of the scFv-0 and scFv-20	44
Table 2.4: Primer sequences for site directed mutagenesis of 4B7 scFv-1 (V _L -V _H)	46
Table 2.5: Primer sequences used for the amplification Pf-NPNA-1 scFv-12 variable domains and for assembly of the scFv-0	47
Table 2.6: Reagents used for SDS-PAGE	52
Table 2.7: Outline of ELISA procedure on Nunc 96-well plates	55
Table 3.1: Amino acid substitutions in FR of 4B7 scFv and properties of the substituted residues	73

The abbreviations used in this study are as follows:

Abbreviation	Full name
AEC	Anion exchange chromatography
AgCP	<i>A. gambiae</i> carboxypeptidase
AP	Alkaline phosphatase
BCIP	5-bromo-4-chloro-3-indolylphosphate
BSA	Bovine serum albumin
cDNA	complementary Deoxyribonucleic acid
CDR	Complementarity determining region
CEC	Cation exchange chromatography
CSP	Circumsporozoite protein
DAB	3,3-Diaminobenzidine
2-DE	Two-dimensional electrophoresis
DNV	Denosonucleosis viruses
DNP	Dinitrophenyl
Dsb	Disulfide-binding proteins
EDTA	Ethylenediaminetetraacetic acid
ELISA	Enzyme linked immunosorbent assay
EGF-like	Epidermal growth factor-like
FITC	Fluorescein isothiocyanate
FR	Framework region
GFP	Green fluorescent protein
GLY	Glycerol yeast
GPI	Glycosyl phosphatidylinositol
HRP	Horseradish peroxidase
HuCk	Human kappa constant domain
HSPG	Heparan sulphate proteoglycans
IFA	Indirect Immunofluorescence Assay
IgG	Immunoglobulin G
IMAC	Immobilised metal affinity chromatography
IPTG	Isopropyl- β -d-thiogalactopyranoside
LB	Luria Bertani

MAb	Monoclonal antibody
MAEBL	Membrane apical erythrocyte binding-like
MalE	Maltose-binding protein
<i>Medea</i>	Maternal-effect dominant embryonic arrest
MKC	Mouse kappa constant
mRNA	messenger Ribonucleic acid
NBT	Nitroblue tetrazolium
Ni	Nickel
PAGE	Polyacrylamide gel electrophoresis
PBS	Phosphate buffered saline
PBST	Phosphate buffered saline Tween-20
PCR	Polymerase chain reaction
<i>PeIB</i>	Pectate lyase B
Pfs25	<i>Plasmodium falciparum</i> ookinete surface protein
PhoA	Alkaline phosphatase
PLA2	Phospholipase A2
PM	Peritrophic matrix
pNPP	Para-nitrophenyl phosphate
PVDF	Polyvinylidene difluoride
OmpA	Outer-membrane protein A
OmpC	Outer-membrane protein C
RNaseA	Ribonuclease A
SC	Start codon
scFv	Single chain fragment variable
SD	Shine Dalgarno
SDS	Sodium lauryl sulfate
SM1	Salivary gland and midgut peptide 1
SP	Signal peptide
SOB	Super optimal broth
SOC	SOB with catabolite repression
TAE	Tris-acetate-EDTA
TE	Tris EDTA
TEs	Transposable elements

Abbreviation

TS	Tris sucrose
TRAP	Thrombospondin related adhesive protein
UV	Ultra violet
V _H	Variable heavy chain domain
V _L	Variable light chain domain
VLP	Virus-like particle
WHcAg	Woodchuck Hepatitis virus core antigen

Chapter 1

General Introduction

1.1 INTRODUCTION

Malaria, caused by the protozoan apicomplexan parasite of the genus *Plasmodium* and transmitted by *Anopheles* mosquitoes, still poses a global public health problem in the developing world, where more than a third (2.4 billion) of the world's population resides (Malkin *et al.*, 2006) (Figure 1.1). Of the five *Plasmodium* species (*P. falciparum*, *P. malariae*, *P. vivax*, *P. ovale*, *P. knowlesi*) that infect humans, *P. falciparum* is the most virulent (Moorthy *et al.*, 2004; Singh *et al.*, 2004). A child dies every 30 seconds and in 2008 a worldwide estimation of 250 million clinical cases resulted in 850,000 deaths of which 89% were in Africa (Malaria Report, 2010). Current control strategies such as the use of long-lasting insecticide treated nets and artemisinin combination therapy have reduced malaria transmission in some areas (Bhattarai *et al.*, 2007; Ndiaye *et al.*, 2009; Otten *et al.*, 2009). However, the problem has been compounded by the increase in vector resistance to insecticides (Martinez-Torres *et al.*, 1998; Hemingway *et al.*, 2004; Pinto *et al.*, 2007) and emergence of multidrug-resistant *P. falciparum* parasites (Fidock *et al.*, 2000; Sidhu *et al.*, 2002; Picot *et al.*, 2009; Witkowski *et al.*, 2010). Although a promising vaccine is in development (Sacarlal *et al.*, 2009; Vekemans *et al.*, 2009), there is still an urgent need for additional and novel control strategies to augment current approaches. Novel control strategies include transgenic mosquitoes that are refractory to infection, application of biological agents that are capable of disrupting parasite life cycle or their engineering to secrete anti-parasite molecules, within the mosquito, that inhibit parasite development and the development of new insecticidal compounds.

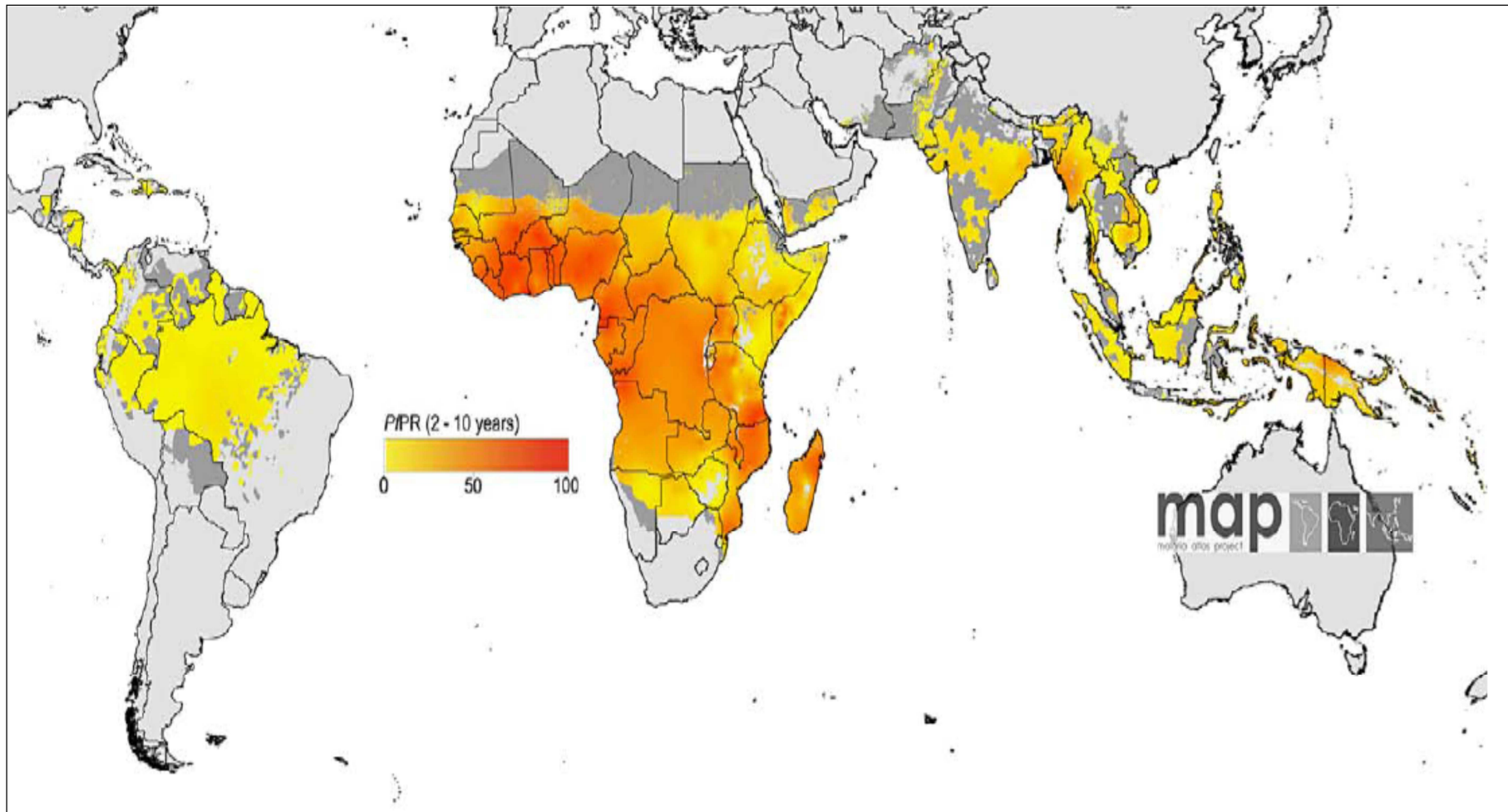


Figure 1.1: Global distribution of malaria with low to high transmission areas. *P. falciparum* malaria transmission is displayed as a continuum of yellow to red 0% - 100% (map legend). The medium grey and grey areas are the unstable and stable areas of transmission, respectively (Hay *et al.*, 2009).

In order to appreciate the difficulties associated with the development of control strategies for malaria transmission, an understanding of the life cycle and developmental stages including the complex series of interactions between parasite, host and vector is required.

All *Plasmodium* parasites require two hosts for their development. For the human malaria parasite (Figure 1.2) *P. falciparum*, acquisition of the parasite occurs when an infected female mosquito injects sporozoites with saliva into the skin during feeding. The sporozoites enter the blood stream and are transported to the liver where they invade hepatocytes and multiply asexually (exoerythrocytic schizogony) to form merozoites (Garcia *et al.*, 2006). Merozoites released from the hepatocytes actively invade erythrocytes to undergo further multiplication and enlarge into ring shaped uninucleate cells, termed trophozoites. The trophozoites then divide asexually into multinucleate schizonts, which subsequently divide into mononucleated merozoites.

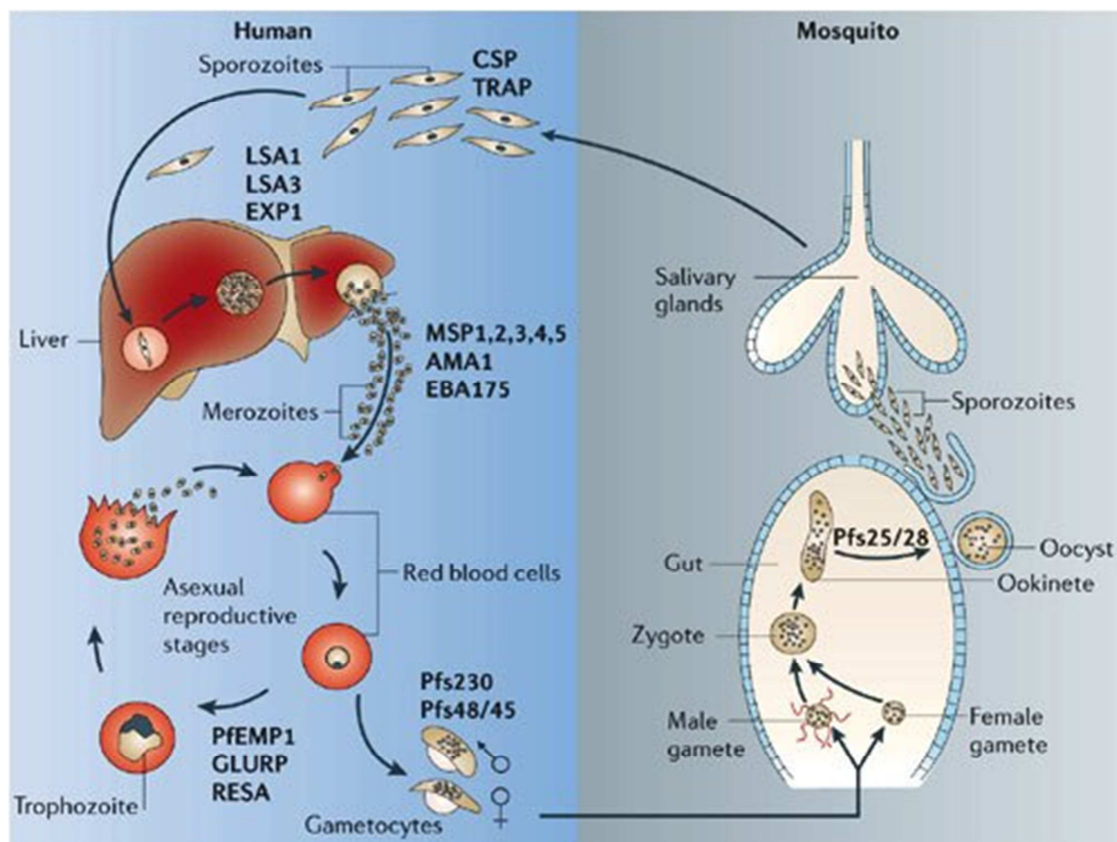


Figure 1.2: Plasmodium life cycle in the vertebrate host and mosquito. The different antigens expressed during the developmental stages are highlighted (Winzeler, 2006).

The erythrocyte eventually ruptures, releasing 8–32 new merozoites, which can infect new erythrocytes. This stage marks the period when an infected person experiences periodic cycles of fever and chill lasting about 42–48 hours (Bannister and Mitchell, 2003; Winzeler, 2006). The merozoites which do not infect new erythrocytes undergo gametocytogenesis, during which they differentiate into male and female gametocytes. Subsequently, the mosquito takes up the mature sexual forms during a blood meal, and sexual reproduction of the parasite occurs in the insect's midgut (Kappe *et al.*, 2004).

Within the mosquito vector, *Plasmodium* undergoes a complex developmental process differentiating into six distinct morphological forms: female and male gametes, zygote, ookinete, oocyst and sporozoite. Within minutes of being taken up, the gametocytes differentiate into male and female gametes. The male gametocytes (microgametes) undergo exflagellation, releasing eight haploid gametes. Fertilisation of the male and female (macrogamete) gametes ensues, leading to the formation of zygotes (Ghosh *et al.*, 2000). Gametogenesis, the transformation and differentiation of the zygotes into motile ookinetes follows. The ookinetes then migrate through the blood meal; traverse the peritrophic matrix (PM), a chitinous membrane that surrounds the blood bolus. To cross the PM the parasite secretes a chitinase (Huber *et al.*, 1991). Inhibition of chitinase activity by allosamidin prevents the parasites from invading the midgut epithelium (Shahabuddin *et al.*, 1993).

After crossing the PM, the ookinetes encounter another barrier – the midgut epithelia. In order to invade the midgut epithelia, ookinetes must attach themselves to the surface of the midgut microvilli (Ghosh *et al.*, 2000). The ookinetes enter the epithelial cells, attach to the basal lamina where they differentiate into oocysts. The oocysts undergo multiple rounds of asexual replication resulting in the production of sporozoites. Each mature oocyst contains thousands of sporozoites that are released into the haemocoel and eventually invade the salivary glands (specifically distal lateral and medial lobes) (Shahabuddin and Costero, 2001; James, 2003; Moreira *et al.*, 2004a). A number of laboratory studies have shown evidences to suggest that the attachment and invasion of salivary glands is a receptor-mediated process.

For instance, Rosenberg (1985) demonstrated the inability of *P. knowlesi* sporozoites to invade the salivary glands of *A. freeborni* but able to invade those of *A. dirus* (Rosenberg, 1985). Furthermore, polyclonal sera raised against *Aedes aegypti* salivary glands inhibited sporozoite invasion (Warburg *et al.*, 1992; Barreau *et al.*, 1995; Barreau *et al.*, 1999; Brennan *et al.*, 2000). Finally, *A. stephensi* sporozoites were inhibited from invading *P. berghei* salivary glands by the 12 amino acid peptide SM1 (Ghosh *et al.*, 2001). Thus, it is apparent that successful establishment of *Plasmodium* in the mosquito is dependent on recognition of mosquito midgut and salivary epithelia.

During its development in the mosquito, the parasite encounters various barriers: physical (membranes and receptors), biochemical (proteases, chitinases) and physiological (immunological factors). As a result large increases in parasite losses (3,000-160,000) occur during the transition of the parasites from the blood meal to the PM, the midgut epithelium and into the haemocoel (Shahabuddin and Costero, 2001) (Figure 1.3).

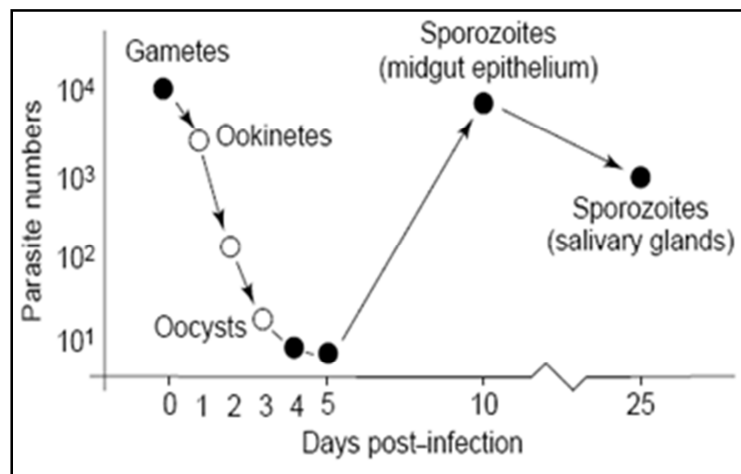


Figure 1.3: Parasite losses and amplification in the mosquito. Parasite numbers during the critical steps of transformation of gametes to ookinetes and of ookinetes to oocysts. The initial number of ingested parasites was estimated to be 10⁴. Adapted from (Blandin and Levashina, 2004).

This loss is more evident during the zygote to ookinete transition (Vaughan *et al.*, 1994). For every 1000 *P. berghei* gametocytes ingested, only two viable ookinetes successfully develop and invade the midgut which subsequently

develop into mature oocysts (Alavi *et al.*, 2003). These decreases in parasite numbers are listed Table 1.1.

	Stage of development		Reference
	Gametocyte to ookinete (decrease)	Ookinete to oocyst (decrease)	
<i>P. falciparum</i>			
<i>An. gambiae</i>	316-fold	100-fold	(Vaughan <i>et al.</i> , 1994)
<i>An. gambiae</i>	40-fold	69-fold	(Vaughan <i>et al.</i> , 1992)
<i>An. stephensi</i>	490-fold	250-fold	(Vaughan <i>et al.</i> , 1992)
<i>An. dirus</i>	1,223-fold	192-fold	(Vaughan <i>et al.</i> , 1992)
<i>P. vivax</i>			
<i>An. dirus</i>	35-fold	5-fold	(Zollner <i>et al.</i> , 2006)
<i>P. gallinaceum</i>			
<i>An. gambiae</i>	4,635-fold	5-fold	(Alavi <i>et al.</i> , 2003)
<i>An. stephensi</i>	9,972-fold	127-fold	(Alavi <i>et al.</i> , 2003)
<i>P. berghei</i>			
<i>An. gambiae</i>	470-fold	54-fold	(Alavi <i>et al.</i> , 2003)
<i>An. stephensi</i>	531-fold	6-fold	(Alavi <i>et al.</i> , 2003)

Table 1.1: Stage-specific differences in *Plasmodium* parasite numbers in *Anopheles* mosquitoes (Adapted and modified from Ghosh *et al.*, 2000).

Clearly, the studies cited indicate the importance of the ookinete to oocyst transition on the successful development of the parasite within the mosquito. Thus, the low numbers of the ookinetes makes them an attractive stage to target in blocking parasite transmission. Efficient blocking of the parasite will require identification of parasite ligands or proteins expressed on the parasite surface that mediate cell adhesion. The sporogonic development of *Plasmodium* is characterised by distinct morphological forms, which express proteins on their surface. These proteins have been implicated in parasite

survival within the midgut, recognition, attachment and penetration of the midgut epithelium.

P. falciparum sexual stage antigen Pfs25 (Figure 1.4) and its homologue in *P. vivax*, Pvs25, are members of the P25 family of cysteine-rich 25 kDa antigens expressed on the surface of zygotes, ookinetes and young oocysts. Structural homology of this protein has been observed in the human, bird and rodent *Plasmodium* parasites (Barr *et al.*, 1991; Duffy *et al.*, 1993; Duffy and Kaslow, 1997; Tsuboi *et al.*, 1997).

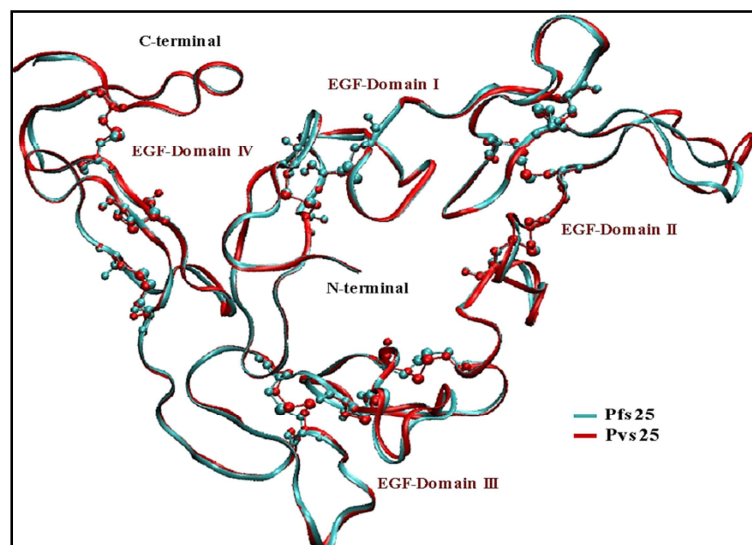


Figure 1.4: Superimposed structures of Pfs25 (cyan colour) and Pvs25 (red colour). Conserved cysteines are represented as CPK representations. (Adapted from (Sharma, 2008))

They are characterised by an N-terminal signal peptide that precedes four tandem epidermal growth factor-like (EGF) domains and a C-terminal glycosylphosphatidylinositol that anchors the protein to the parasite surface. P25 proteins contain 22 cysteine residues, capable of forming 11 potential disulphide bonds (Stowers *et al.*, 2000; Saxena *et al.*, 2007). The P25 protein is involved in parasite recognition of and attachment to the mosquito midgut (Tomas *et al.*, 2001; Siden-Kiamos and Louis, 2004). Using knockout parasites of *P. berghei*, lacking the P25 protein, Tomas *et al.* (2001) showed that P25 plays an important role in parasite survival in the harsh proteolytic environment of the midgut by providing a protective sheath around the

parasite, permitting penetration of the epithelium and transformation of the ookinetes into oocysts.

P25 proteins are only expressed in the mosquito midgut and not in the vertebrate host and thus, have not been under selection pressure by the host immune system. Though insects have long been recognised to have effective innate (cellular and humoral) defense mechanisms they, however, lack the memory and specific recognition that are characteristic of the vertebrate immune system (Dong *et al.*, 2006). The sequences of field isolates of *P. falciparum* and *P. vivax*, unlike blood stage antigens, show limited polymorphisms making P25 a potential target for blockade of transmission (Duffy and Kaslow, 1997). Studies conducted in mice and rhesus monkeys have shown that Pfs25 expressed in yeast is able to elicit antibodies that block development of *P. falciparum* oocysts in the midgut of the mosquito vector. (Barr *et al.*, 1991; Stowers *et al.*, 2000; Arakawa *et al.*, 2005; Miura *et al.*, 2007). Pfs25 antigen is a leading candidate for transmission blocking vaccines and Phase I clinical trials in humans have confirmed safety as a vaccine candidate (Kaslow, 2002; Wu *et al.*, 2008). The third EGF-like domain contains a portion of a B-cell epitope and is the target of monoclonal antibodies 4B7 (Barr *et al.*, 1991), ID2, IC7 (Quakyi *et al.*, 1995) and 32F81 (Vermeulen *et al.*, 1985).

Another parasite antigen that is a potential target for blockade of malaria transmission is the circumsporozoite (CS) protein expressed on the surface of sporozoites. This 45 kDa protein covers the entire surface of the sporozoites and is the most extensively characterised of the sporozoite proteins (Nagasawa *et al.*, 1987; Boulanger *et al.*, 1988; Nagasawa *et al.*, 1988; Kappe *et al.*, 2004). Two other sporozoite antigens that have well been characterised are the thrombospondin-related anonymous protein (TRAP), and membrane apical erythrocyte binding-like (MAEBL) (Garcia *et al.*, 2006).

CS protein shows structural homology in all species, consisting of three main domains. A striking feature of the *P. falciparum* CS (Figure 1.5) protein is the central domain, which is a major B-cell epitope, consisting of 37 tandem

repeats of asparagine-proline-asparagine-alanine (NPNA) and 4 repeats of asparagine-valine-aspartic acid-proline (NVDP). The central repeat tetramer peptide (Asn-Pro-Asn-Ala)_n, (NPNA)_n of CS protein is 100% conserved among *P. falciparum* isolates (Zavala *et al.*, 1985a; Kappe *et al.*, 2004; Garcia *et al.*, 2006). It has been suggested that the high number of repeats precludes the development of mutants which will evade recognition by a target antibody (Chappel *et al.*, 2004b). CS protein is flanked at the amino and carboxyl terminals by region I and II, respectively. The protein is anchored to the parasite surface by a glycosyl phosphatidylinositol (GPI) anchor. Region I consists of the conserved sequence KLKQP and has been shown to be involved in invasion of the mosquito's salivary glands (Sidjanski *et al.*, 1997). Region II, however, consists of 18 amino acids and is involved in binding to heparan sulphate proteoglycans (HSPGs) present on the surface of hepatocytes (Kappe *et al.*, 2004).

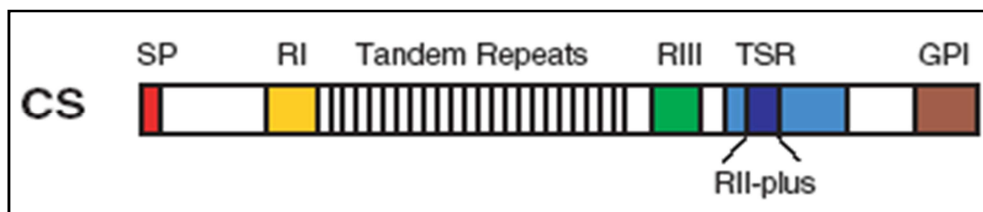


Figure 1.5: Schematic representation of the PfCS protein: SP, signal peptide; RI, region I; RII-plus, region II-plus; RIII, region III; TSR, thrombospondin type I repeat domain; GPI, glycosyl phosphatidylinositol (Kappe *et al.*, 2004).

Many reports have implicated CS protein in oocyst development and sporozoite differentiation (Menard *et al.*, 1997), maintenance of species specificity during infection (Rathore *et al.*, 2003), attachment and invasion of liver cells (Frevert *et al.*, 1993; Rathore *et al.*, 2003), inhibition of host cell protein synthesis (Frevert *et al.*, 1998) and facilitation of sporozoite passage into salivary glands of the mosquito (Sidjanski *et al.*, 1997). Anti-CS protein antibodies have blocked salivary gland invasion by *P. gallinaceum* sporozoites (Warburg *et al.*, 1992; Barreau *et al.*, 1995; de Lara Capurro *et al.*, 2000). Additional evidence suggests that a recombinant CS protein preferentially bound salivary glands but not Malpighian tubules or ovaries and this binding was inhibited by the peptide LRKPKHKKLKQPADG, which corresponds to the

conserved region I (Sidjanski *et al.*, 1997). In subsequent experiments, the recombinant CS protein and the peptide inhibited sporozoite entry into salivary glands (Myung *et al.*, 2004).

The immunodominance of CS protein was shown when rodents, monkeys and humans vaccinated with radiation-attenuated sporozoites were protected against malaria infection or re-infection (Nussenzweig *et al.*, 1967; Clyde *et al.*, 1973; Clyde, 1975; Hoffman *et al.*, 2002). The sporozoites though attenuated are capable of invading hepatocytes but do not develop fully to the merozoite stage. The presence of the partially developed parasites elicits an immune response which is mainly antibody mediated. This protection is sterile and long lasting compared to naturally acquired immunity, which allows intermittent episodes of infection to occur (Carvalho *et al.*, 2002). Antibodies to the repeat epitope (NPNA) prevent infection by blocking entry of sporozoites into hepatocytes. High levels of anti-PfCSP repeat antibodies have been shown to correlate with protection in areas where malaria is endemic (Hoffman *et al.*, 1986; Ballou *et al.*, 1987; Jones *et al.*, 1993). The CS protein has been incorporated in the RTS,S vaccine currently in phase III clinical trials (Ballou, 2009; Sacarlal *et al.*, 2009; Vekemans *et al.*, 2009).

1.2 Application of biological agents for control of malaria

Traditionally, success in the management of vector-borne diseases has been achieved through the controlled reduction of vector populations by use of insecticides. However, the continued application of insecticides has been hampered by increase in insecticide resistance. With recent progress in molecular biology, biocontrol measures are being developed to reduce vector capacity to transmit disease. This is based on the use of naturally occurring microorganisms. Insects, generally can be infected by a range of microorganisms: fungi, protozoa, viruses and bacteria.

1.2.1 Fungal biopesticides

The use of fungal isolates, such as *Bacillus thuringiensis* and *Bacillus sphaericus*, against mosquito larvae have been attempted in numerous studies in the past (Padua *et al.*, 1980; Lacey and Undeen, 1986; Federici, 1995; Scholte *et al.*, 2004). However, the renewed use of fungi against adult mosquitoes is based on the past successes and effectiveness of indoor residual spraying to reduce vector populations. Since the strategy involves spraying mosquitoes' resting sites with suspensions of fungal spores, infection of the insect host only occurs through external contact and not by ingestion. The fungal conidia upon contact with the insect's cuticle germinate and grow hyphae which penetrate the insect body. Within the insect's haemocoel numerous organic compounds, such as destruxins, are produced that cause internal damage and paralysis. Nutrient depletion eventually results in the death of the insect (Howard *et al.*, 2010). However, the time taken to kill the host may vary from 2 to 5 days or weeks based on the host-pathogen combination and environmental factors (Blanford and Thomas, 2001; Elliot *et al.*, 2002).

It has been suggested that malaria transmission rates are more dependent on the changes in adult mosquito survival rather than on changes in the survival of larval forms (Bukhari *et al.*, 2010; Howard *et al.*, 2010; Knols *et al.*, 2010). Targeting adult females before they are capable of transmitting parasite would result in less exertion of the high selection pressure usually associated with the use of insecticides. Furthermore, the likelihood of resistance development is reduced due to the multiple modes of action of the fungus and the slow speed of kill (mosquitoes killed within 14 days). In addition, an entomological inoculation rate model estimated that the application of fungi as biopesticides may result in a reduction of annual mosquito bites per person from 262 to 64 (Scholte *et al.*, 2005).

It was the independent work of Blanford *et al.* (2005) and Scholte *et al.* (2005) demonstrated the pathogenic effect of two entomopathogenic fungi, *Metarhizium anisopliae* and *Beauveria bassiana*, on adult mosquitoes.

Besides their effect on mosquito survival, they have also been demonstrated to inhibit parasite development in the mosquito (only 8% of infected mosquitoes had infectious parasites compared to 35% of control which were only infected with *Plasmodium*) (Blanford *et al.*, 2005) and reduction in mosquito feeding propensity and fecundity (Scholte *et al.*, 2006). In laboratory setting, Scholte *et al.* (2004) demonstrated horizontal transfer of *Metarhizium anisopliae* from infected males to females. In addition, a recent study has demonstrated increased susceptibility of insecticide resistant Anopheles mosquitoes to the insecticides permethrin and dichlorodiphenyltrichloroethane after preinfection with *B. bassiana* or *M. anisopliae* (Farenhorst *et al.*, 2009). It has also been shown that pyrethroid resistant *A. gambiae* mosquitoes were more susceptible to *B. bassiana* and *M. anisopliae* infections than their non-resistant counterparts (Howard *et al.*, 2010). Subsequently, combinations of the insecticide, permethrin, with fungal formulations of *B. bassiana* and *M. anisopliae* were observed to have synergistic effects on the survival of mosquitoes. Simultaneous application of both agents had a higher effect than the use of a single agent (Farenhorst *et al.*, 2010). More recently, transgenic strains of *M. anisopliae* have been engineered to express anti-parasite molecules, which target the sporozoite stages of the parasite, in the haemolymph of the mosquito. The anti-parasite molecules, SM1 (a midgut and salivary gland peptide that blocks sporozoites invasion of salivary glands), Pf-NPNA-1 (a single chain antibody that agglutinates sporozoites) and scorpine (an antimicrobial toxin) reduced sporozoite numbers by 71%, 85% and 90%, respectively. Sporozoite numbers were further reduced by 98% when an SM1-scorpine fusion protein was expressed (Fang *et al.*, 2011).

Numerous technical hurdles are yet to be surmounted despite the success achieved in the pioneering of a transgenic fungus capable of disrupting malaria transmission. Fungal spore viability, fungal specificity, infectivity and persistence of spores under field conditions and development of resistance have not been adequately evaluated (Howard *et al.*, 2010; Knols *et al.*, 2010). Howard *et al.* (2010) are of the view that any potential application method be evaluated in the field due to the biological nature of fungal spores. The ubiquitous nature of these fungi in the environment coupled with the lack of

specificity, their ability to infect a wide range of insects, may pose both environmental and health risks. However, the low survival rate of fungal spores when exposed to UV radiation and high temperatures may dampen this concern. Yet to be adequately investigated is the potential health risks immuno-compromised people, who are inhabitants of malaria endemic regions, may encounter due to exposure to fungal spores (Farenhorst and Knols, 2007).

A major concern is the development of antifungal resistance. In the study by Blanford *et al.* (2005), using the murine malaria model and the fungus *B. bassiana*, the mosquito host was killed within two weeks, which is approximately the time the malaria parasite takes to develop into infectious sporozoites. This slow speed of kill, it has been suggested, will impose a limited selection pressure on the mosquitoes and reduce the development of antifungal resistance (Knols and Thomas, 2006). The likelihood of resistance development may also be limited as fungi can attack the mosquitoes by secreting chitinase, proteases and toxins (Hajek and St Leger, 1994). However, the two weeks within which the mosquito is killed, is long enough for the female *Anopheles* to acquire, develop and transmit the malaria parasite.

Secondly, environmental factors such as temperature may also affect the growth of the fungi with a direct effect on its killing speed. This stems from the fact that studies using fungi as biopesticides for control of locust and grasshoppers have reported varying field results (Blanford *et al.*, 1998; Blanford and Thomas, 1999; Klass *et al.*, 2007). These have been associated with changes in environmental temperature. Though Blanford and colleagues have reported no changes in the speed of kill due to changes in the thermal behaviour of *A. stephensi* mosquitoes, Kikankie and colleagues are of the view that the temperature effect on the germination and growth rate within the mosquito warrants further study (Blanford *et al.*, 2009; Kikankie *et al.*, 2010).

Another issue with use of fungi as biocontrol agents is the viability of the conidia. Scholte *et al.* (2005) estimated that a 63% decrease in viability occurs after 3 weeks when applied to surfaces. Thus, surfaces would have to be re-

treated regularly, a requirement which is unsustainable during large scale implementation. Other barriers, such as fungal specificity and the development of resistance in the mosquitoes, need to be addressed before its widespread application (Kanzok and Jacobs-Lorena, 2006).

Due to the aforementioned problems associated with the use of fungi as biocontrol agents, two other alternative strategies, transgenesis and paratransgenesis, are under development to control spread of the disease. These strategies, in contrast to the fungal biocontrol approach, do not aim to kill the arthropod vector but reduce its competence to support parasite development and transmission.

1.2.2 Transgenesis

Application of genetically modified mosquitoes to reduce or replace vector populations offers great opportunities for the control of mosquito-borne diseases. The genetic modification involves the introduction into the mosquito genome, genes whose products impair *Plasmodium* development. This has been made possible by advances in germ-line transformation of mosquitoes (Catteruccia *et al.*, 2000), identification of effector molecules that interfere with parasite development (Possani *et al.*, 1998; de Lara Capurro *et al.*, 2000; Ghosh *et al.*, 2001; Zieler *et al.*, 2001; Arrighi *et al.*, 2002; Nirmala and James, 2003) and characterisation of tissue-specific promoters to express the effector molecule (Kokoza *et al.*, 2000; Moreira *et al.*, 2000). These milestones have led to the stable transformation of a number of *Anopheles* mosquitoes and more recently *A. gambiae* (Grossman *et al.*, 2001; Ito *et al.*, 2002; Nolan *et al.*, 2002; Perera *et al.*, 2002).

To evaluate the feasibility of this approach, some *Anopheles* mosquitoes have been transformed to express effector molecules. Ito and colleagues were the first to develop a transgenic mosquito that was refractory to *P. berghei*. The transgenic *A. stephensi* was transformed with a *piggyBac* transposable

element that expressed SM1 (Ghosh *et al.*, 2001), a 12 amino acid disulphide loop (PCQRAIFQSICN) peptide that binds to the distal lobe of the salivary gland and to the luminal side of the midgut epithelium required for parasite invasion, under the control of *A. gambiae* carboxypeptidase (AgCP) promoter. In this study, *P. berghei* oocyst formation was inhibited by 81.6% (Ito *et al.*, 2002). The *piggyBac* element was isolated from the cabbage looper moth, *Trichoplusia ni*, and has been used to transform a variety of insects.

Subsequently, expression of the bee venom phospholipase A2 (PLA2) in *A. stephensi* resulted in 87% inhibition of oocyst formation compared to controls without PLA2. In addition, PLA2 transgenic mosquitoes failed to transmit parasites to naïve mice (Moreira *et al.*, 2002). By replacing the AgCP promoter with an Ag peritrophin promoter to drive PLA2 expression, the *P. berghei* oocyst formation was inhibited by 80% (Abraham *et al.*, 2005). Transgenic *A. gambiae* expressing cecropin A under the control of the *Aedes aegypti* CP promoter reduced *P. berghei* oocyst formation by 60% compared to nontransgenic controls (Kim *et al.*, 2004). However, cecropin A expression was not observed in the midgut of transgenic mosquitoes. *P. gallinaceum* oocyst intensity was inhibited by 65% to 70% when *Aedes aegypti* was transformed with *piggyBac* expressing defensin A under the control of the Ag peritrophin promoter (Shin *et al.*, 2003).

Despite the significant progress made in the development of transgenic mosquitoes, the approach faces numerous challenges which must be addressed before its application in the natural environment. Firstly, there is an urgent need to develop transgenic mosquitoes capable of inhibiting development of human malaria parasites. This has been achieved for mouse parasite, *P. berghei* (Ito *et al.*, 2002; Moreira *et al.*, 2002) and avian malaria parasite, *P. gallinaceum* (Rodrigues *et al.*, 2008). More recently, Corby-Harris *et al.* (2010) have reported a 95.6% inhibition of *P. falciparum* parasites in the midgut of transgenic *A. stephensi* compared to nontransgenic mosquitoes. Over-expression of the signalling protein, Akt, under the control of the AgCP promoter significantly decreased *P. falciparum* development and mosquito lifespan after a blood meal (Corby-Harris *et al.*, 2010). Akt signalling protein

forms a key component of the insulin/insulin-like growth factor 1 signalling cascade, which regulates innate immunity and lifespan of vertebrates and non-vertebrates (Corby-Harris *et al.*, 2010).

Introduction of such engineered strains of mosquitoes with anti-pathogen refractory phenotypes into the native population would require an effective drive mechanism to spread the genes coding for refractoriness. Of the several genetic drive mechanisms, transposable elements (TEs) were the first to gain increased attention based on the successful worldwide spread of the *Drosophila P* element (Anxolabehere *et al.*, 1988). However, initial attempts to introduce TEs into *Anopheles* mosquitoes have failed (Marshall and Taylor, 2009). Despite their extensive use TEs may not be unsuitable for use as a drive system due to the loss or deletion of internal sequences during replication, decline in activity due to increasing size of refractory genes and inactivation due to accumulation of mutations (Riehle and Jacobs-Lorena, 2005; Marshall and Taylor, 2009). Other drive mechanisms currently being investigated include *Medea* (maternal-effect dominant embryonic arrest), homing endonuclease genes and the intracellular bacteria *Wolbachia* (Marshall and Taylor, 2009; Coutinho-Abreu *et al.*, 2010).

To overcome the limitations of TEs, the *Streptomyces* phage phiC31 integrase system, previously used for *Drosophila melanogaster* and *Aedes aegypti*, was recently used for successful site-specific transformation of *An. gambiae*. Site-specific integration of Vida-3, an antimicrobial peptide that is active against early sporogonic stages and developing oocysts, into the phage phiC31 target site and its expression under the AgCP promoter in the midgut of *An. gambiae* resulted in 85% reduction in *Plasmodium yoelii nigeriensis* parasite intensity. There were, however, variations in the protection conferred against *P. falciparum* due to inconsistencies in the infection rates between experiments (Meredith *et al.*, 2011). As proof-of-principle, the authors are of the view that, future applications of the system will require several modifications to enhance efficiency and extensive fitness studies.

Another important constraint associated with the release of transgenic mosquitoes into the environment is the potential fitness cost imposed by the transgene (Marrelli *et al.*, 2006). However, laboratory studies have suggested that the nature of the refractory gene product is crucial for fitness. In the study by Moreira and colleagues, no fitness load was observed for transgenic mosquitoes expressing the SM1 peptide whereas mosquitoes expressing PLA2 were less fit and less fertile compared to nontransgenic ones (Moreira *et al.*, 2004b).

Although proof-of-concept studies have established the feasibility of developing transgenic mosquitoes, it may take many years before they can be released into wild populations. An effective drive mechanism has not yet been identified and no progress has been attained in developing a transgenic mosquito refractory to human malaria parasites. Due to the many challenges facing the development of transgenic mosquitoes, an alternative approach which utilises symbiotic bacteria to deliver anti-pathogen molecules, is also being developed. The paratransgenic approach has many advantages over transgenic mosquitoes. Firstly, it is compatible with current insecticide control programs. Secondly, the logistics involved in the genetic manipulation of bacteria and their growth in large quantities is simplified. Release of large quantities poses fewer risks compared to large scale release of transgenic mosquitoes. Thirdly, multiple effector molecules could be delivered using a mixture of genetically manipulated bacteria. Finally, the nature of the effector gene could be changed at any time during a control program (Durvasula *et al.*, 1997; Riehle and Jacobs-Lorena, 2005).

1.2.3 Paratransgenesis

Common to both paratransgenesis and transgenesis is the potential to reduce the competence of the host-vector to enable parasite development (Conte, 1997; Beard *et al.*, 1998; Beard *et al.*, 2001; Beard *et al.*, 2002). In contrast to transgenesis, the paratransgenic approach alters the host's ability to transmit disease by genetically manipulating symbiotic microorganisms to express and

secrete effector molecules (i.e., recombinant anti-parasite molecules) that inhibit parasite invasion or development in the midgut (Riehle *et al.*, 2003). Viral and bacterial symbionts have been included in numerous studies (Durvasula *et al.*, 1999; de Lara Capurro *et al.*, 2000; Yoshida *et al.*, 2001; Riehle *et al.*, 2007; Durvasula *et al.*, 2008; Ren *et al.*, 2008). Beard *et al.* (1992) suggested that the successful implementation of this approach depends on six main criteria:

- i) identification of culturable microbes amenable to genetic manipulation
- ii) existence of methods for isolating and transforming microbes
- iii) transformation of the symbiotic bacteria must result in stable mutants without the loss of reproductive fitness
- iv) genetic manipulation of the symbiont should not render them virulent, either to the vector or other organisms in the environment
- v) identification and engineering of anti-parasite or effector molecules that block parasite uptake and transmission in the arthropods,
- vi) spread of the transgene into natural vector populations to a level that is able to interrupt parasite transmission.

This approach was initially developed and successfully used to suppress the transmission of Chagas' disease (Beard *et al.*, 1992). The symbiotic bacteria, *Rhodococcus rhohnii*, transformed with a shuttle vector encoding the gene for ceprocin A was introduced into the vector, *Rhodnius prolixus*. The expressed ceprocin A inhibited the development of *Trypanosoma cruzi* parasites by 99% without any fitness cost on the insect (Durvasula *et al.*, 1997). Subsequently, a functional anti-progesterone antibody was expressed in the midgut of the vectors *R. prolixus* (Durvasula *et al.*, 1999) and *Triatoma infestans* (Durvasula *et al.*, 2008), respectively.

Application of this strategy against African trypanosomes transmitted by tsetse flies has shown promising results. In the case of tsetse flies, the symbiont (*Sodalis glossinidius*) was transformed with a plasmid encoding green fluorescent protein (pGFPuv). Females bearing the pGFPuv plasmid vertically

transmitted it to their progeny, an indication of transstadial transfer of the symbiont across tsetse populations (Cheng and Aksoy, 1999; Aksoy *et al.*, 2008). Recombinant *Sodalis* expressing a *Glossina* attacin, an antimicrobial peptide effective against gram-negative bacteria and protozoa, significantly reduced parasite levels when fed a trypanosomal blood meal (Aksoy, 2003). This approach has gained widespread attention and is being developed to be used against the Mexican fruit fly *Anastrepha ludens*, which threatens citrus fruits (Kuzina *et al.*, 2001), the glassy-winged sharp shooter, *Homalodisca coagulata*, which is a vector for *Xylella fastidiosa*, the bacterium that causes Pierce's disease of grape vines (Bextine *et al.*, 2004), the kala azar vector, *Phlebotomus argentipes*, which transmits leishmaniasis (Hillesland *et al.*, 2008) and in the brine shrimp *Artemia franciscana* (Subhadra *et al.*, 2010) for control of infectious diseases in shrimp aquaculture.

The feasibility of a paratransgenic approach in *Anopheles* mosquitoes has been demonstrated in three laboratory studies (de Lara Capurro *et al.*, 2000; Yoshida *et al.*, 2001; Riehle *et al.*, 2007). A viral paratransgenesis approach was undertaken by de Lara-Capurro *et al.* (2000) and used to successfully block transmission of the avian malaria parasite, *P. gallinaceum*. A single chain variable fragment (scFv) N2H6D5, that targets *P. gallinaceum* circumsporozoite protein (CSP) was expressed from a Sindbis virus vector and shown to reduce the number of parasites in the salivary glands by 99% (de Lara Capurro *et al.*, 2000). Although this viral system was used to evaluate scFv N2H6D5 as an effector molecule, the variability in mosquito infections with the Sindbis virus vector would limit its application in transmission blocking studies. Furthermore, Sindbis viruses may not be suitable for use in paratransgenesis due to their broad specificity (Coutinho-Abreu *et al.*, 2010). They have been shown to infect a broad range of insect genera and vertebrates (Carlson *et al.*, 1995; Blair *et al.*, 2000).

Alternatively, genetically modified densovirus (DNV), which are icosahedral parvoviruses with non-enveloped single stranded DNA, are being evaluated for application in paratransgenesis. Numerous characteristics make

DNV suitable vectors for this approach (Carlson *et al.*, 1995; Carlson *et al.*, 2006; Ren *et al.*, 2008). They:

- i) can be genetically manipulated
- ii) have narrow host range making them highly specific
- iii) are environmentally stable
- iv) are horizontally and vertically transmitted from infected adults to larvae
- v) can kill mosquito larvae in a dose-dependent manner and decrease life span of surviving adults.

DNV were previously not considered for use in paratransgenesis with the main mosquito vector, *A. gambiae*, due to lack of infection when larvae were exposed to the *Aedes aegypti* DNV (Ward *et al.*, 2001). However, a DNV was recently isolated from *A. gambiae* and genetically modified to express GFP in *A. gambiae*. The recombinant DNVs were detected in the midgut, fat body and ovaries and transmitted to other generations (observed in 20% of F₂ and F₃ generations) (Ren *et al.*, 2008). Although a transducing system for *A. gambiae* DNV has been established, its potential to express anti-*Plasmodium* effector molecules is yet to be determined.

Bacteria have also gained widespread application for use in paratransgenesis. An identified culturable bacterium may be well adapted to the mosquito midgut and would not face stiff competition from other bacteria (Riehle and Jacobs-Lorena, 2005). Secondly, it has been observed that the bacterial population increases immediately after a blood meal. Pumpuni *et al.* (1996) observed an 11-fold and 40-fold increase in bacteria numbers of *A. gambiae* and *A. stephensi*, respectively, 24 h after a blood meal. Thirdly, reduction in oocysts density of *P. falciparum* (Pumpuni *et al.*, 1993; Pumpuni *et al.*, 1996) and *P. vivax* (Gonzalez-Ceron *et al.*, 2003) infections has been associated with gram-negative bacteria.

Yoshida *et al.* (2001) evaluated *in vivo* the parasitic activity of a scFv immunotoxin on oocysts formation. The immunotoxin consisted of Shiva-1, a

synthetic peptide analogue of Cecropins that was previously shown to inhibit *P. falciparum in vitro* (Jaynes *et al.*, 1988) and 13.1 scFv (Winger *et al.*, 1988; Yoshida *et al.*, 1999) directed against the *P. berghei* Pbs21 protein. A laboratory strain of *E. coli* was transformed with a plasmid expressing the scFv-immunotoxin and shown to inhibit oocyst formation by up to 95% (Yoshida *et al.*, 2001) when fed to *Anopheles stephensi*. However, the *E. coli* control without the scFv immunotoxin also blocked sporogonic development by 76%. The inhibition of *Plasmodium* development by gram negative bacteria has been reported (Pumpuni *et al.*, 1993; Pumpuni *et al.*, 1996; Gonzalez-Ceron *et al.*, 2003) and associated with elicitation of mosquito innate immune responses (Dimopoulos *et al.*, 1997).

In the study of Riehle *et al.* (2007) a recombinant *E. coli* was engineered to secrete and display two anti-parasite molecules, SM1 (Ghosh *et al.*, 2001) and phospholipase A2 (PLA2) whose mode of action is unknown but has been suggested to modify the membrane properties of the midgut epithelium (Zieler *et al.*, 2001; Moreira *et al.*, 2002). *A. stephensi* mosquitoes harbouring the engineered bacterium showed reduction (SM1 41%; PLA2 23%) in the development of *P. berghei* oocysts compared to control mosquitoes without the effector molecule. However, *E. coli* had a short life span (2 days) within the mosquito's midgut. Thus, the paratransgenic approach requires identification of bacteria that can survive in the midgut over the life span of the mosquito.

To be considered suitable for use in a paratransgenic approach, an ideal bacterium must meet certain criteria:

- i) should be dominant among insect-associated microbiota;
- ii) readily applicable to genetic characterisation and manipulation;
- iii) ease of cultivation in cell-free media;
- iv) co-localisation with the infectious agent in the relevant insect organs (gut and salivary glands);
- v) widespread distribution in the preadult and adult insect body;
- vi) capable of cross-colonising different hosts;

The mosquito midgut is known to be inhabited by a range of bacterial species (Pumpuni *et al.*, 1996; Straif *et al.*, 1998; Gonzalez-Ceron *et al.*, 2003; Riehle *et al.*, 2003; Lindh *et al.*, 2005; Favia *et al.*, 2007; Lindh *et al.*, 2008; Rani *et al.*, 2009). Some of the bacteria isolated from midgut of *Anopheles* mosquitoes (laboratory and field isolates) are listed in Table 1.2. In most of these studies, the midgut identified bacteria could not be cultivated in the laboratory.

Mosquito species	Bacterial species		Reference
	Gamma-proteobacteria	Enterobacteriaceae	
<i>A. stephensi</i>	<i>Pseudomonas cepacia</i> <i>Flavobacterium</i> spp	<i>Serratia marcescens</i> <i>P. agglomerans</i>	Pumpuni <i>et al.</i> (1993) Rani <i>et al.</i> (2009)
<i>A. stephensi</i>	<i>Asaia</i> sp.		Favia <i>et al.</i> (2007)
<i>A. albimanus</i>	<i>Flavobacterium</i> spp.	<i>Pantoea agglomerans</i>	Pumpuni <i>et al.</i> (1996)
		<i>S. marcescens</i> <i>Enterobacter cloacae</i> <i>Enterobacter amnigenus</i>	Gonzalez-Ceron <i>et al.</i> (2003)
<i>A. gambiae</i> (Giles)	<i>Ps. cepacia</i> <i>Ps. gladioli</i>	<i>P. agglomerans</i> <i>Serratia</i> spp.	Pumpuni <i>et al.</i> (1996)
<i>A. gambiae</i>	<i>Thorsellia anopheles</i> <i>Rhodococcus cornyebacteriodes</i>	<i>Aeromonas</i> sp. <i>Enterobacteriaceae</i> sp.	Lindh <i>et al.</i> (2005)
	<i>Bacillus cereus</i> <i>Bacillus mucoides</i>	<i>Escherichia coli</i> <i>Pantoea agglomerans</i>	Straif <i>et al.</i> (1998)
<i>A. funestus</i>	<i>Janibacter anophelis</i>		Lindh <i>et al.</i> (2005)
	<i>Bacillus megaterium</i> <i>Gluconobacter cerinus</i>	<i>Pantoea agglomerans</i> <i>Salmonella choleraesuis</i>	Straif <i>et al.</i> (1998)
<i>Ae. aegypti</i>	<i>Elizabethkingia meningoseptica</i>	<i>Pantoea stewartii</i> <i>S. marcescens</i>	Lindh <i>et al.</i> (2008)

Table 1.2: Bacteria microbiota from different mosquito species

Recently an acetic acid bacterium, *Asaia* sp., was identified, shown to be stably associated with larvae and adults of *A. stephensi* and dominated the

mosquito microbiota (Favia *et al.*, 2007). Genetically modified *Asaia* expressing GFP was capable of colonising the gut, salivary glands (which are important compartments for the developmental stages of the parasite) and male and female reproductive organs. The fluorescently tagged strains were transmitted vertically from mother to progeny, horizontally (through feeding) and paternally by venereal transfer from male to female (Favia *et al.*, 2007; Damiani *et al.*, 2008). *Asaia* sp. has been isolated from laboratory and field samples of *An. gambiae* and GFP-tagged *Asaia* reintroduced into *An. gambiae*. The GFP-tagged bacteria showed similar distribution in both *A. stephensi* and *A. gambiae* (Damiani *et al.*, 2010). It has been shown to colonise insects of two distant genera: *Diptera* (*A. stephensi*, *A. maculipennis*, *A. gambiae*, *Ae. aegypti*) and *Hemiptera* (*Scaphoideus titanus*, the leafhopper vector of phytoplasma that causes Flavescence Dorée in grapevines) (Crotti *et al.*, 2009). These characteristics of *Asaia* satisfy the prerequisites of a paratransgenic approach making it an attractive bacterium for delivery of anti-parasite molecules.

1.3 Effector molecules

A key component that determines the success of paratransgenesis is the identification of an appropriate effector molecule. An ideal effector molecule should block parasite development or kill it with 100% efficiency and should not impose any fitness cost to the mosquito (Jacobs-Lorena, 2003). Nirmala and James (2003) categorised effector molecules into five groups based on their targets.

These targets include parasite ligands, mosquito tissue receptors, and parasite expressed proteins required for invasion of mosquito midgut tissues, components of the immune system and antiparasite toxins. Effector molecules identified that are specific to these targets and the parasites investigated are listed in Table 1.3.

Effector strategy (target)	Molecule	Target parasite	Reference
Parasite ligands	Pbs21 scFv 13.1	<i>P. berghei</i>	(Yoshida <i>et al.</i> , 1999)
	CSP N2 scFv	<i>P. gallinaceum</i>	(de Lara Capurro <i>et al.</i> , 2000)
	4B7, Pfs25 MAb	<i>P. falciparum</i>	(Barr <i>et al.</i> , 1991), (Stowers <i>et al.</i> , 2000)
	CSP 2A10 CSP Pf-NPNA-1	<i>P. falciparum</i> <i>P. falciparum</i>	(Nardin <i>et al.</i> , 1982) (Chappel <i>et al.</i> , 2004b)
Tissue recognition (receptors)	Lectins, MAbs	<i>P. gallinaceum</i> <i>P. berghei</i>	(Barreau <i>et al.</i> , 1995), (Yoshida <i>et al.</i> , 2007)
	SM1 peptide	<i>P. berghei</i> <i>P. falciparum</i>	(Ito <i>et al.</i> , 2002)
	Snake phospholipase A2 ^a	<i>P. gallinaceum</i> , <i>P. falciparum</i>	(Zieler <i>et al.</i> , 2001)
	Bee phospholipase A2 ^a	<i>P. berghei</i>	(Moreira <i>et al.</i> , 2002)
	Gomesin	<i>P. berghei</i> <i>P. falciparum</i>	(Moreira <i>et al.</i> , 2007)
	Vida-3	<i>P. berghei</i>	(Arrighi <i>et al.</i> , 2002)
Parasite gene expression	Chitinase	<i>P. gallinaceum</i>	(Vinetz <i>et al.</i> , 1999)
	Aminopeptidase N	<i>P. berghei</i> <i>P. falciparum</i>	(Dinglasan <i>et al.</i> , 2007)
Immune response effectors	Magainins and cecropins	Variety of <i>P. sp.</i>	(Gwadz <i>et al.</i> , 1989)
	Defensins	<i>P. gallinaceum</i>	(Shahabuddin <i>et al.</i> , 1998)
	scFv 13.1 plus Shiva-1	<i>P. berghei</i>	(Yoshida <i>et al.</i> , 2001)
	Nitric oxide synthase	<i>P. berghei</i>	(Luckhart <i>et al.</i> , 1998)
Antiparasite toxins	Scorpine	<i>P. berghei</i>	(Conde <i>et al.</i> , 2000)

Table 1.3: Effector target, molecule and target parasite for engineering *Plasmodium* resistance in mosquitoes. ^aMolecules could also function as toxins. scFv: single chain fragment variable; MAb: monoclonal antibody. Adapted and modified from (Nirmala and James, 2003).

Though insects have an array of inducible immunity molecules they, however, lack a defence system that is immunoglobulin mediated. Among the numerous effector molecules identified, single chain fragment variable (scFv) show promise for use in control of malaria and other vector-borne diseases (Vinetz *et al.*, 1999; de Lara Capurro *et al.*, 2000; Yoshida *et al.*, 2001). scFv fragments (Figure 1.6) consist of the variable heavy (V_H) and light chain (V_L)

domains of an antibody that are linked with a hydrophobic and flexible peptide linker (15 – 20 amino acids) (Bird *et al.*, 1988). Their simple structure, small size, ease of manipulation and specificity make them attractive candidates in selecting an effector molecule. In addition, they retain the binding properties of their parent antibody.

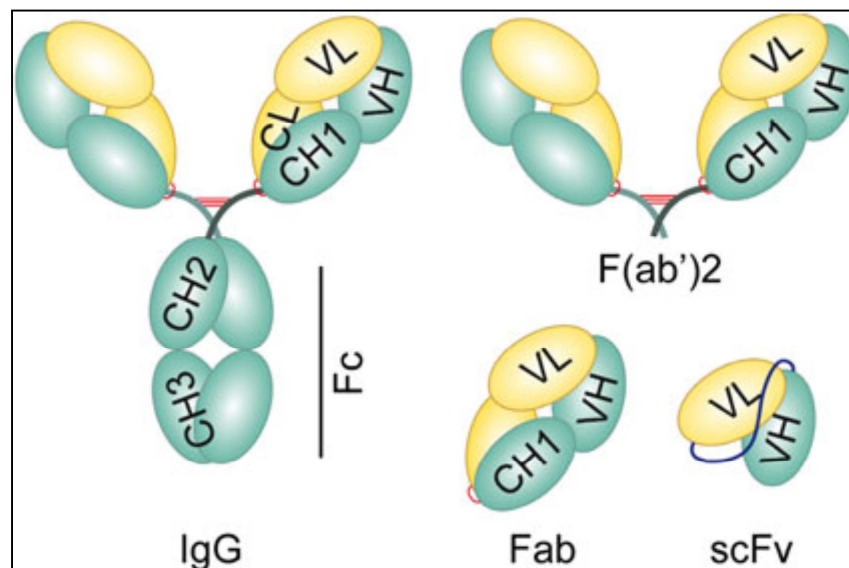


Figure 1.6: Nomenclature of engineered antibody fragments in comparison with native IgG. Each oval represents an immunoglobulin folding domain. Disulfide bonds are represented as red lines, and the polypeptide linker of the scFv is represented by a blue connecting ribbon. VL indicates variable domain light chain; VH, variable domain heavy chain; CL, constant domain light chain; CH, constant domain heavy chain; Fc, Fc fusion; IgG, immunoglobulin G; F(ab')₂, dimeric antigen binding fragment; Fab, antigen binding fragment; scFv, single chain antigen binding fragment (Peterson *et al.*, 2006).

Pettigrew and O'Neill (1997) were of the view that application of scFv for paratransgenesis may lead to development of resistant mosquito strains. However, they stressed that identification of antibodies that target surface ligands or epitopes of proteins required by the pathogen for cell attachment or invasion of host tissues would be a way to overcome the problem (Pettigrew and O'Neill, 1997). Two target antigens, Pfs25, a sexual stage antigen expressed on the surface of ookinetes and Pf-CS protein, abundantly expressed on the surface of sporozoites are the focus of this study. Both target antigens exhibit characteristics that make them suitable candidates to which neutralising antibodies have been generated (Barr *et al.*, 1991; Chappel *et al.*, 2004b). Pfs25 has limited antigenic variation and most importantly it is

only expressed in the mosquito midgut thus, has not undergone prior immune selection (Gwadz *et al.*, 1989; Shi *et al.*, 1992; Duffy and Kaslow, 1997). The ookinete stage is considered as a weak link during parasite development as only a few develop from the thousands of gametocytes ingested (Ghosh *et al.*, 2000; Riehle *et al.*, 2003). Thus, the low number of ookinetes coupled with the limited polymorphism makes Pfs25 a good target to block parasite development within the midgut.

With the Pf-CS protein, the central repeat tetramer peptide (Asn-Pro-Asn-Ala)_n, (NPNA)_n is 100% conserved among *P. falciparum* species (Kappe *et al.*, 2004). In addition, Pf-CS protein facilitates sporozoite passage into salivary glands of the mosquito (Sidjanski *et al.*, 1997). The ookinete and the sporozoite stages of the parasite are temporally and spatially separated (2 weeks) such that an antibody developed against the ookinetes would not function against sporozoites. As previously stated, the paratransgenic approach allows for the introduction of multiple effector molecules anytime during control programs. As a result, any parasites that may have escaped during the ookinete stage and eventually develop into sporozoites would be inhibited from invading the salivary glands to cause infection. Hence, the parasites are blocked at two fronts, ookinete and sporozoite stages.

Targeting two antigens within the same mosquito is based on results of earlier paratransgenic models. Complete inhibition (100 %) of pathogen transmission has not been attained as these model systems utilised single effector molecules (de Lara Capurro *et al.*, 2000; Yoshida *et al.*, 2001; Riehle *et al.*, 2007). The application of two or more effector molecules may have an additive effect resulting in complete interruption of parasite transmission. This strategy would further delay the appearance of resistant pathogens. Recently, Kokoza *et al.* (2010) provided a proof of principle for complete disruption of parasite transmission in transgenic *Aedes aegypti* mosquitoes by co-expression of two antimicrobial peptides (AMPs), Cecropin A and Defensin A. Over-expression of the AMPs, under the control of the *vitellogenin* promoter, and their cooperativity led to transgenic mosquitoes being resistant to infection by the pathogenic bacterium *Pseudomonas aeruginosa*.

Furthermore, *P. gallinaceum* oocysts numbers in the midgut were dramatically reduced resulting in the absence of sporozoites in the salivary glands (Kokoza *et al.*, 2010).

With the advent of recombinant DNA technology and display methods such as phage, ribosome and yeast display, MAbs may be isolated against almost any target antigen from a non-immune or immune library (Skerra and Pluckthun, 1988; Huse *et al.*, 1989; Sastry *et al.*, 1989; Johnson and Bird, 1991). A number of transmission blocking antibodies have been developed against Pfs25: 4B7 (Barr *et al.*, 1991) 32F81 (Vermeulen *et al.*, 1985), IC7 and ID2 (Quakyi *et al.*, 1995) of which 4B7 is the most potent. MAb 4B7 recognized the third EGF-like domain (Stura *et al.*, 1994b; Stowers *et al.*, 2000). The binding site was mapped to the sequence, ILDTSNPVKTGV, located at the apex of the B loop of the third EGF-like domain (Stura *et al.*, 1994b). MAb 4B7 binds to its native protein in a conformation dependent manner as it recognises non-reduced Pfs25 strongly and reduced Pfs25 weakly (Barr *et al.*, 1991). The variable domains of 4B7 have been sequenced (Stura *et al.*, 1994a).

To the central repeats of Pf-CS protein the antibodies IG3.4, 5G5.3, 2F1.1, IB2.2, 5C1.1 (Burkot *et al.*, 1991), 2A10 (Nardin *et al.*, 1982) and Pf-NPNA-1 (Chappel *et al.*, 2004b) have been isolated. With the exception of Pf-NPNA-1, the other antibodies are murine antibodies. These murine antibodies may not be suitable for use in paratransgenesis as they may elicit immune responses in humans bitten by mosquitoes carrying them in their salivary glands. A more appropriate antibody would be the human monoclonal antibody (MAb) Pf-NPNA-1, which was cloned from a protected individual by repertoire cloning and antibody phage display (Chappel *et al.*, 2004b). It is the most characterised having moderate affinity (~1-5 μ M) for its target peptide antigen and able to inhibit sporozoites in an *in vitro* invasion assay in a dose dependent manner (20, 10, 5, 2.5 μ g/ml conferring 68, 74, 58 and 44% inhibition respectively) (Chappel *et al.*, 2004a). The antibody specifically labelled *P. falciparum* in an immunofluorescent assay (Chappel *et al.*, 2004b).

Both 4B7 and Pf-NPNA-1 are candidates for targeting *P. falciparum* in *Anopheles* mosquitoes.

Although the small size of scFv confers many advantages compared to a whole antibody, they are devoid of any biological functions (effector and complement) because they lack the Fc portion of a whole antibody. In addition, scFv with linkers greater than 12 amino acids (aa) exhibit low avidity due to their monovalent antigen binding kinetics (Holliger *et al.*, 1993). However, effector function could be incorporated or mimicked by generating a bifunctional, bivalent or multivalent molecule. Yoshida *et al.* (2001) constructed a bifunctional molecule by fusing the lytic peptide Shiva-1 to the scFv 13.1. They demonstrated enhanced effect of the immunotoxin (scFv 13.1-Shiva-1) on *P. berghei* oocysts compared with the scFv 13.1 or Shiva-1 peptide alone (Yoshida *et al.*, 2001).

Bivalent or multivalent scFv can be generated by shortening the linker connecting the variable domains. Generally, the V_H and V_L domains of scFvs with linkers greater than 12 aa, take on their natural Fv orientation and are not constrained (Holliger *et al.*, 1993; Kortt *et al.*, 1994). However, as the linker length is shortened below 12 aa, the V_H domain is prevented from interacting with its attached V_L . Interaction, however, occurs between the V_H and V_L domains of one scFv with the V_H and V_L domains of a second scFv to form a monospecific dimeric molecule (Holliger *et al.*, 1993) or multivalent multimers (Iliades *et al.*, 1997; Kortt *et al.*, 1997; Atwell *et al.*, 1999; Le Gall *et al.*, 1999; Dolezal *et al.*, 2000; Power *et al.*, 2003). Further reduction in linker length by directly linking the V_H and V_L domains results in a trimeric molecule termed a triabody (Iliades *et al.*, 1997; Kortt *et al.*, 1997). Thus multimerisation of the scFv is governed by the length of the linker joining the variable domains. The multimerisation of scFv (monomer, dimer and trimer) is depicted by the molecular models of the B72.3 monoclonal antibody in Figure 1.6. Generating scFv that are capable of multimeric assembly would further enhance their application in paratransgenesis. It is proposed that avidity effects due to the multimeric status of the scFv will improve agglutination of the parasites and thus potentially arrest development within the mosquito.

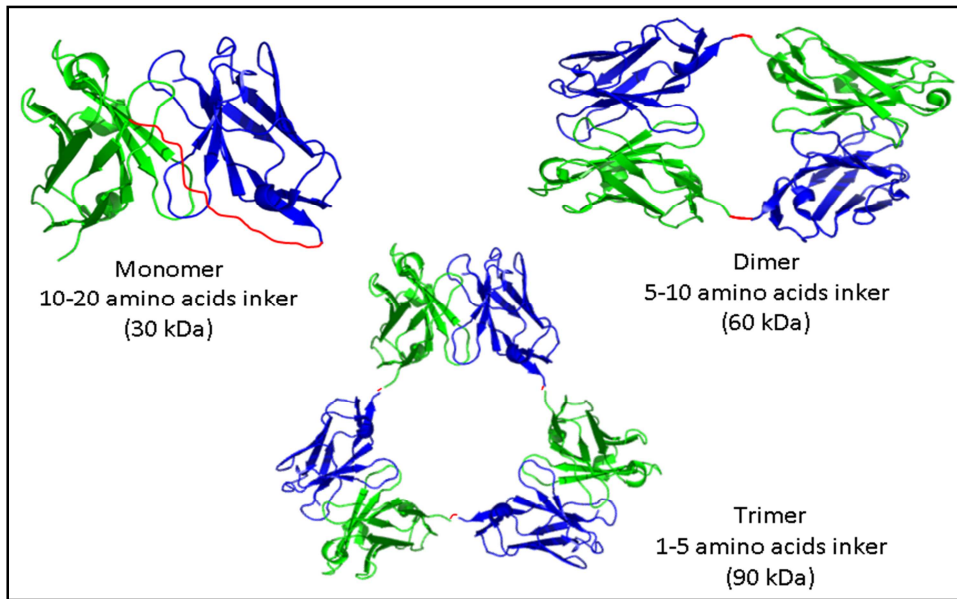


Figure 1.7: Molecular models of scFv monomer, dimer and trimer. The linker between V_H (green) and V_L (blue) domains is coloured red (Provided by Dr. A. Markiv).

1.4 Prokaryotic expression of scFv fragments

scFv fragments contain disulphide bonds that contribute to their stability and biological activity. To ensure the correct pairing of the cysteines and proper folding of the disulfide bonds, the eukaryotic folding and assembly of antibodies and their subsequent translocation into the endoplasmic reticulum can be mimicked by secretion of the scFv into the oxidising environment of the periplasm (Better *et al.*, 1988; Skerra and Pluckthun, 1988) or extracellular medium (Wu *et al.*, 1993; Fernandez *et al.*, 2000; Fernandez and de Lorenzo, 2001) of bacterial cells. The formation of the disulphide bonds within the periplasm is facilitated by the presence of the disulfide-binding proteins (DsbA, DsbB, DsbC, and DsbD) (Bardwell, 1994; Collet and Bardwell, 2002; Choi and Lee, 2004). Periplasmic or extracellular secreted scFv fragments would be advantageous to the paratransgenic approach because the secreted antibodies will be in direct contact with the infectious agent.

The secretion of a scFv from the cytoplasm into the periplasm or extracellular medium requires the presence of a signal peptide (SP). The SP fused to the N-terminus of the scFv gene facilitates the translocation of the premature

protein from the cytoplasm into the periplasm. Subsequent cleavage of the SP, by a signal peptidase, results in a mature protein with an authentic N-terminal methionine (Makrides, 1996). Numerous studies have employed the use of different leader peptides (Table 1.4) for efficient transportation of scFv to the periplasm.

Signal sequences	Amino acid sequences
<i>PeiB</i> (pectate lyase B) from <i>Erwinia carotovora</i>	MK YLLPTAAAGLLLLAAQPAMA
<i>OmpA</i> (outer-membrane protein A)	MKKT AIAIAVALAGFATVAQA
<i>PhoA</i> (alkaline phosphatase)	MKQ STIALALLPLLFTPVTKA
<i>MalE</i> (maltose-binding protein)	MKIKT GARILALSALTTMMFSASALA
<i>OmpC</i> (outer-membrane protein C)	MKVKV LSELLVPALLVAGAANA

Table 1.4: Signal sequences used for the secretory production of recombinant proteins in *E. coli*. The N-domains of signal sequences are shown in bold while the C-domains are underlined (Adopted from Choi and Lee, 2004).

SPs differ in their primary sequences but share some structural features. SPs are composed of three main regions: basic N-terminal consisting of 1-3 positively charged residues; hydrophobic region composed of 10-15 hydrophobic amino acid residues and a C-terminal (serving as the cleavage site) consists of 5-7 less hydrophobic amino acid residues (Choi and Lee, 2004). According to Makrides (1996), the efficient translocation of the target protein across the inner membrane is dependent on the primary structure of the protein to be secreted and the secretory machinery. Secretion of some recombinant antibodies may interfere with the secretory machinery of the cell and may be toxic to the host cell.

1.5 Thesis aim and objectives

Malaria affects millions of people worldwide and traditional control measures have not helped eradicate the disease. Thus, new control strategies are being investigated and developed to control transmission of the disease.

Paratransgenesis, which utilises symbiotic microorganisms to secrete effector molecules, shows promise. Model systems have demonstrated the feasibility of the approach; however, there is the need for identification and evaluation of suitable effector molecules capable of neutralising the pathogen. The antibodies 4B7 and Pf-NPNA-1, which target Pfs25 and Pf-CS proteins expressed on the surface of ookinetes and sporozoites respectively, have been identified as suitable effector molecules. However, there is the need to evaluate these effector molecules in a prokaryotic system. Thus, the aim of this project is the engineering and characterisation of anti-malaria antibodies, scFvs 4B7 and Pf-NPNA-1, which target Pfs25 and CS protein, respectively. Four main objectives will be undertaken to achieve this aim.

Firstly, both antibodies will be constructed in the scFv format with different linker lengths. The effect of linker length on multimerisation behaviour will be investigated. scFv orientation on antibody secretion will also be assessed.

Secondly, expression and secretion of the scFv constructs will be evaluated. Studies with scFv fragments have demonstrated that not all antibodies secrete. In addition the level of expression of scFv is dependent on the primary sequence and yields may even vary between closely related sequences (Knappik and Pluckthun, 1995; Wall and Pluckthun, 1999). As a result the level of secretion of all the scFv constructs will be compared.

Thirdly, purified scFv protein will be assessed for antigen binding. It has been demonstrated that not all multimeric scFvs or monovalent scFvs have functional antigen binding sites (Johnson and Bird, 1991; Kipriyanov *et al.*, 1997; de Haard *et al.*, 1998; Le Gall *et al.*, 1999).

Fourthly, the scFvs evaluated for expression, secretion and antigen binding will be transferred into a broad-range host vector to evaluate expression in the symbiotic bacterium *Asaia sp.*

Chapter 2

Materials and Methods

2.1 Materials and methods

2.1.1 General chemicals and reagents

All reagents were of analytical grade and purchased from Sigma-Aldrich (Poole, Dorset, UK). A full list is given in the Appendix.

2.1.2 Bacterial strains

E. coli XL1-Blue [*recA1 endA1 gyrA96 thi-1 hsdR17 supE44 relA1 lac* [F' *proAB lacIqZΔM15 Tn10* (Tet^r)K12] (Stratagene) was used for plasmid propagation. *E. coli* BL21 (DE3) pRARE, F' *ompT gal dcm lon hsdS_B(r_B⁻ m_B⁻)* λ(DE3 [*lacI lacUV5-T7 gene 1 ind1 sam7 nin5*] used for scFv expression was from Novagen (San Diego, CA). λDE3 denotes the lysogenic gene of T7 bacteriophage gene I, encoding T7 RNA polymerase under the control of the *lac* UV5 promoter. pRARE contains tRNA genes for the rare codons arginine (argU, argW), isoleucine (ileX), glycine (glyT), leucine (leuW), proline (proL), methionine (metT), threonine (thrU, thrT) and tyrosine (tyrU). This strain is deficient in both *lon* and *ompT* proteases.

2.1.3 Antibiotic stock solutions

The following antibiotics were prepared: kanamycin 10 mg/ml in MilliQ water, tetracycline 625 µg/ml in 100% ethanol and chloramphenicol 34 mg/ml in 100% ethanol. Stock solutions were filter sterilised and stored at -20°C until needed. Final working concentrations were kanamycin 50 µg/ml, tetracycline 12.5 µg/ml and chloramphenicol 34 µg/ml.

2.1.4 Buffers and media

Luria Bertani (LB) broth was prepared using 1% w/v Bacto tryptone, 0.5 % w/v yeast extract and 1% w/v NaCl (pH 7.4), autoclaved (121°C, 15min) and stored at room temperature.

LB agar plates were prepared using 1% w/v Bacto tryptone, 0.5 % w/v yeast extract and 1% w/v NaCl and 1.5% w/v Bacto agar (pH 7.4). The suspension was autoclaved, cooled to 50°C in a water bath and antibiotic added to the required concentration. The molten agar (25 ml each) was poured into Petri dishes, allowed to set and stored at 4°C.

Super Optimal Broth (SOB) (Hanahan, 1983) was prepared using 2% w/v Bacto tryptone, 0.5% w/v yeast extract, 10 mM NaCl, 2.5 mM KCl, 10 mM MgSO₄ (pH 7.0) and autoclaved. To prepare SOC (SOB with catabolite repression), MgCl₂ (1M) and filter sterilised 20% glucose were added to SOB to final concentrations of 10 mM and 20 mM, respectively. Aliquots of 1 ml were stored at -20°C.

2.1.5 Antibodies and Enzymes

2.1.5.1 Restriction Enzymes

The restriction modification endonucleases: *NcoI*, *NdeI*, *NotI*, *XbaI*, *XhoI* and T4 DNA ligase were purchased from New England BioLabs (Hitchin, Herts, UK) and used with the buffers provided according to the manufacturer's recommendation.

2.1.5.2 Antibodies

Rabbit anti-hexa-histidine tag antibody conjugated to horseradish peroxidase (HRP) (Abcam, UK; Cat. No. ab1187) was used in Western blots for detection of His-tagged proteins according to manufacturer's recommendations. Murine monoclonal anti-polyhistidine-alkaline phosphatase (AP) antibody (Sigma, UK; Cat. No. A5588, clone HIS-1) was used in ELISA for the detection of His-tagged proteins. A rabbit anti-tri FLAG antibody (Sigma, UK; Cat. No. F7425) was used primary antibody and goat anti-rabbit IgG conjugated to AP (Sigma, UK; Cat. No. A9919) as secondary antibody was used for detection recombinant proteins on membranes and in ELISA. Goat anti-Human kappa

light chains (bound and free) antibody conjugated to AP (Sigma, UK; Cat. No. A3813) was used for the detection of the human kappa light chain. Fluorescein isothiocyanate (FITC) (Abcam, UK; Cat. No. ab 1270) anti-His antibody was used detection of antibody binding to Pf-CS protein.

2.1.6 DNA Vectors

The pET-41b(+) plasmid (Novagen, UK) was modified for the construction of the scFv expression vectors. It lacks an N-terminal signal peptide but contains multiple cloning sites and an octa His-tag to facilitate the purification and detection of fusion proteins. Other plasmids, pUC-19 4B7, pUC-19 Pf-NPNA-1 and pUC57-(NPNA)₉-MKC were provided by Dr. Anatoliy Markiv and Dr. Angray Kang. The pSANG-103F plasmid was provided by Dr. John McCafferty (Martin *et al.*, 2006).

2.2 Molecular biology methods

2.2.1 Separation of DNA using agarose gel electrophoresis

Digested plasmid DNA and PCR products were separated by agarose gel electrophoresis (Sambrook, 2001). Agarose gels were prepared in 1X TAE buffer (40 mM Tris-HCl, pH 8.2, 1 mM EDTA and 20 mM acetic acid) at 1% w/v and 1.5% w/v depending on size of the target DNA. Ethidium bromide was added at a concentration of 0.2 µg/mL. The DNA samples were mixed with 6X sample buffer (0.4% w/v Orange G, 0.03% w/v Bromophenol blue, 0.03% w/v xylene cyanol FF, 15% w/v Ficoll 400 in TAE buffer, pH 8.2) before loading on gel. The gel was run at 100 V for 1 hour. For further cloning and sequencing, the DNA was excised from the gel using long wavelength UV light (315-400 nm) whereas short wavelength UV light (200-280 nm) was used to take images of gels.

2.2.2 Gel purification of PCR products and plasmid DNA

The desired DNA fragment was excised with a sterile scalpel and purified using the GenElute purification kit (Sigma, UK) according to the manufacturer's recommendations. Briefly, to 1 volume of gel (100 mg~ 100 μ L) was added three volumes (300 μ L) of solubilisation buffer (5.5 M guanidine thiocyanate, 20 mM Tris-HCl, pH 6.6, 0.0025% w/v Cresol Red) in a 1.5 mL Eppendorf tube. The tube was incubated in a 50°C water bath for 10 min to allow complete solubilisation of the gel slice, after which 1 volume (100 μ L) of isopropanol was added and mixed to homogeneity. The solubilised gel was loaded onto the binding column assembled in a 1.5 mL Eppendorf tube and centrifuged for 1 min at 13,000 rpm. The flow through was discarded and binding column assembled as before. To wash the column 700 μ L of PE buffer (2mM Tris-HCl, pH 7.5, 20 mM NaCl, and 80% v/v ethanol) was added to the column and centrifuged at 13,000 rpm for 1 min. The flow through was discarded and the column centrifuged for 1 min at 13,000 rpm to remove any residual wash buffer. To elute the DNA, the binding column was transferred to a fresh 1.5 mL Eppendorf tube, 30 μ L of nuclease free water added, incubated at RT for 1 min and centrifuged at 13,000 rpm for 1 min. The eluted DNA was stored at -20°C.

2.2.3 Restriction endonuclease digestion

Plasmid DNA and PCR products were double digested to generate compatible sticky ends and to release inserts for the purposes of cloning. The composition of the restriction endonuclease reaction mixture in a 1.5 mL Eppendorf tube was: 30 μ L of DNA (8 μ g), 5 μ L of 10X NEB digestion buffer (optimal for both enzymes), 0.5 μ L of BSA (10 mg/mL), 1 μ L of each enzyme and 12.5 μ L of nuclease free water. The reaction mixture was gently mixed and incubated at 37°C for 3 h. The digested products were electrophoresed on a 1 or 1.5% agarose gel and purified.

2.2.4 Ligation of DNA fragments

The ligation reaction was composed of the following: 2 μL of 10X T4 DNA ligase buffer, 1 μL of T4 DNA ligase (NEB, UK), 1 μL of digested plasmid (50 ng), 10 μL of digested insert (150 ng) and reaction mixture made up to 20 μL with nuclease free water (Invitrogen, UK). The reaction mixture was left to incubate at room temperature (RT) for 1 hour, transferred onto ice and used to transform *E. coli* competent cells. Control ligations without digested insert were also set up.

2.2.5 Preparation of *E. coli* chemical competent cells

A single colony was inoculated into 10 mL of LB media supplemented with antibiotic specific for the cell type. *E. coli* XL1 blue cells were supplemented with tetracycline (12.5 $\mu\text{g}/\text{mL}$) and BL21DE3 pRARE with chloramphenicol (34 $\mu\text{g}/\text{mL}$). The cultures were grown overnight (16 hours) at 37°C with shaking at 250 rpm. The overnight culture was used to inoculate 200 mL of prewarmed LB medium (supplemented with chloramphenicol for BL21DE3 pRARE and no antibiotics for XL1 blue cells) and grown at 37°C with vigorous shaking 250 rpm until the OD_{600} was 0.4 - 0.5. The culture was incubated on ice for 30 min and aliquoted into four prechilled 50 mL centrifuge tubes (Fisher Scientific, UK). The cells were harvested by centrifugation for 7 min at 3500 rpm (3120 $\times g$) (4°C) using a Sorvall Super T21 centrifuge equipped with a ST-H750 swing bucket. The supernatant was discarded and the cells, in each tube, resuspended in 12.5 mL of cold 0.1 M MgCl_2 . Centrifugation was repeated as before, supernatant discarded and the cells, in each tube, resuspended in 25 mL of cold 0.1 M CaCl_2 and left to incubate on ice for 30 min. The cell suspension was centrifuged; the supernatant discarded and cells in each tube resuspended in 700 μL of 0.1 M CaCl_2 and 300 μL of 50% glycerol. The cell suspensions were pooled, aliquoted 50 μL into prechilled 1.5 mL sterile microcentrifuge (Eppendorf) tubes on ice and stored at -80°C.

2.2.6 Transformation of *E. coli* using the heat-shock method

Chemically prepared competent cells were transformed according to the procedure of Sambrook and Russell (2001) with modifications. An aliquot of the competent cells prepared above were thawed on ice for 5 min and 1 μ L of super coiled plasmid or 10 μ L of ligation mixture added and incubated for 5 min on ice. The cells were heat shocked at 42°C in a water bath for 1 min and quickly transferred onto ice for 5 min. SOC medium (250 μ L) was added and transformants selected on LB agar plates supplemented with the appropriate antibiotic. For ligation products, the transformants were plated out after growing transformed cells, supplemented with SOC, for 1 hour at 37°C.

2.2.7 PCR colony screening

Individual bacterial colonies were picked with a sterile 10 μ L pipette tip and added into 10 μ L of nuclease free water in a 1.5 mL Eppendorf tube. 3 μ L of the suspended colony was added to 22 μ L of PCR master mix (5 μ L of 5X Taq&Go, 1.25 μ L each 10 μ M forward and reverse primers, 14.5 μ L of nuclease free water). PCR was carried out in a MJ Mini gradient thermal cycler (Bio-Rad, UK) set with the thermal cycling conditions outlined in Table 2.1

Cycles	Temperature (°C)	Time
1	95	5 min
22	95	1 min
	55	30 s
	72	1 min/kb
1	72	10 min
	4	∞

Table 2.1: Amplification program for PCR colony screening

The amplified products were examined on a 1.5% agarose gel. For colonies confirmed for the presence of insert, the remaining bacterial suspension, 7 μ L was used to inoculate 10 mL of LB broth, grown for 16 h at 37°C with shaking at 250 rpm.

2.2.8 Preservation of bacterial cultures

For long term storage of bacterial cultures, 700 μ L of an overnight culture grown from a single colony was mixed with 300 μ L of sterile 50% v/v glycerol in a 1.5 mL Eppendorf tube. The tube was labelled and stored at -80°C.

2.2.9 Plasmid DNA extraction

Plasmid DNA was extracted from 10 mL bacterial cultures grown overnight in antibiotic selective LB medium following Qiagen's plasmid purification protocol with slight modifications. Buffers were prepared in-house and the silica membrane spin columns were obtained from Epoch Biolabs (Texas, USA). The overnight bacterial culture was centrifuged at 3500 rpm for 10 min, the supernatant discarded and the bacterial cells resuspended in 500 μ L of buffer P1 (50 mM Tris-base, pH 8.0, 10 mM EDTA, 50 μ g/mL RNaseA). The suspension was then transferred (250 μ L) into two 1.5 mL sterile microcentrifuge tubes to which 250 μ L of buffer P2 (0.2 M NaOH, 1% SDS) was added to lyse the cells and the tubes inverted 10 times. To neutralise the lysis buffer 350 μ L of buffer N3 (4 M guanidine hydrochloride, 0.5 M potassium acetate, pH 4.2, 192 mM acetic acid) was added to each tube and mixed immediately by inverting the tubes 10 times. The tubes were centrifuged at 13,000 rpm for 10 min to pellet genomic DNA, cell membrane and proteins. The supernatant was applied to a spin column and the column centrifuged at 13,000 rpm for 1 min. The flow through was discarded and the spin column washed by addition of 500 μ L buffer PB (5 M guanidine hydrochloride, 20 mM Tris-base, pH 6.6, 38% ethanol v/v) and centrifuged at 13,000 rpm for 1 min. The flow through was discarded and the spin column

was again washed with 750 μL of buffer PE (20 mM NaCl, 2 mM Tris-base, pH 7.5, 80% ethanol v/v) and centrifuged twice at 13,000 rpm for 1 min to remove any residual ethanol. The spin column was transferred to a sterile 1.5 mL microcentrifuge tube; 30 μL of nuclease free water (Invitrogen, UK) was added to the centre of the spin column and allowed to incubate for 1 min at RT. The plasmid DNA was eluted by centrifugation at 13,000 rpm for 1 min and stored at -20°C .

2.2.10 DNA quantification and Sequencing

The concentration of plasmid DNA was determined by preparing a 100 fold dilution (2 μL of DNA: 198 μL of TE) of plasmid DNA in TE buffer (10 mM Tris-HCl, 1mM EDTA pH 8.0). The diluted DNA was transferred into an Eppendorf Uvette and the absorbance measured at 260 and 280 nm using an Eppendorf Biophotometer (Eppendorf, UK). The absorbance at 280 nm gave an indication of the level of protein contamination. The absorbance ratios at 260 nm and 280 nm of the DNA preparations were in the range of 1.7 – 2.0. An aliquot (100 ng/ μL) of the plasmid DNA was sent for sequencing at the Wolfson Institute for Biomedical Research Core Facility, University College London.

2.3 Construction of scFv expression vectors

2.3.1 Construction of scFv expression vectors pBAK.1 and pBAK.1Hk

DNA manipulations were carried out according to Sambrook and Russell (2001). The plasmid, pBAK.1Hk was constructed by using pET41b(+) (Novagen) as the parent plasmid. The gene encoding human kappa constant domain (HuCk) without the terminal cysteine was amplified from the phage display library, BRM1388 (Chappel *et al.*, 2004b) using the primers **BAK1** (5'-ACT **GCG GCC GCA** CCA TCT GTC TTC ATC TTC-3') and **BAK2** (5'-AGA AGC TTG **CTC GAG** TCC CCT GTT GAA GCT CTT TGT GAC-3') which append *NotI* and *XhoI* restriction sites (in bold), respectively. The amplification reaction consisted of 5 μ L of 5X Taq & Go, 1.25 μ L of each 10 μ M primer (5' and 3'), 1 μ L of template DNA and 16.5 μ L nuclease free water. PCR was carried out as outlined in Table 2.1

The PCR product (~300 bp) was gel purified, digested and ligated into a *NotI*-*XhoI* digested pET41b(+) yielding pET41bHk. Modified plasmid pORFES (with a *pelB* leader sequence) (Stratmann and Kang, 2005) was digested with *XbaI*-*NotI* and ligated into a similarly digested pET41bHk to yield pBAK.1Hk. The expression plasmid was then confirmed by DNA sequencing (Wolfson Institute for Biomedical Research Core Facility, University College London, UK). Ligation of the *XbaI*-*NotI* digested fragment from modified pORFES directly into a similarly digested pET41b(+) yielded the expression vector pBAK.1. The expression vectors both have a *pelB* leader sequence and an octa-histidine tag.

2.3.2 Cloning of synthetic DNA Constructs

Synthetic codon optimised (NPNA)₉MKC (mouse kappa constant domain), 4B7 scFv-1, Pf-NPNA-1 scFv-12 genes were purchased from GenScript, USA. The scFv constructs were cloned from their respective cloning vectors as *NcoI/NotI* into pBAK.1, pBAK.1Hk and pSANG10-3F expression plasmids. The (NPNA)₉MKC construct was cloned as *NcoI/XhoI* fragment into pBAK.1.

The ligation mixture was transformed into competent XL1Blue cells and transformants selected at 37°C on LB agar plates supplemented with kanamycin. Transformants were screened by colony PCR (Section 2.2.6).

2.3.3 Construction of 4B7 V_L-V_H scFv-0, scFv-20, scFv-0Hk and scFv-20Hk

To generate the 4B7 scFv-0 and scFv-20 (V_L-V_H), the V_H and V_L gene fragments of 4B7 scFv-1 (V_H-V_L) were PCR-amplified using the primers **4B7VHF** and **4B7VHNot** for V_H and **4B7VLNco** and **4B7VLR** for V_L. The amplification reaction consisted of 5 µL of 5X Taq & Go, 1.25 µL of each 10 µM primer (5' and 3'), 1 µL of template DNA and 16.5 µL nuclease free water. The PCR amplifications were conducted as outlined in Table 2.1. The resulting PCR products were gel purified and constructed into an scFv-0 by overlap extension PCR (Horton *et al.*, 1989). The resulting fragment has *Nco*I and *Not*I restriction sites at the 5' and 3' ends, respectively. The scFv-0 was then digested with *Nco*I and *Not*I restriction enzymes and cloned into the expression vectors pBAK.1, pSANG10-3F and pBAK.1Hk. The strategy for the design and construction of 4B7 scFv-0 V_L-V_H is shown in Figure 2.1.

Cycles	Temperature (°C)	Time
1	95	5 min
22	95	1 min
	55*	30 s
	72	1 min
1	72	10 min
	4	∞

Table 2.2: PCR cycle profile for the amplification of 4B7 scFv-1 variable domains and assembly of scFv-0 and scFv-20. The annealing temperature, shown by the asterisks, was kept constant for the amplification of variable domains and assembly of scFvs.

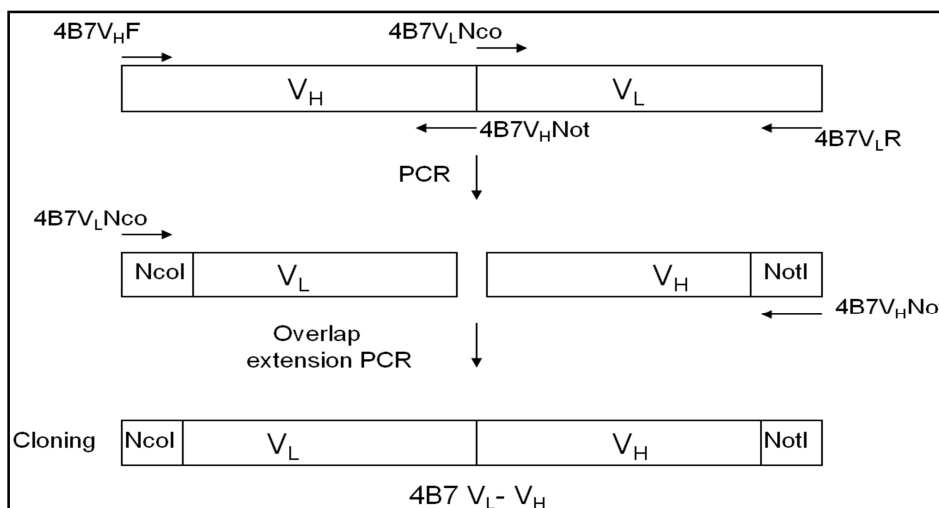


Figure 2.1: Design and construction of 4B7 scFv-0 (V_L-V_H). The variable domains of 4B7 scFv-1 V_H-V_L were amplified by PCR. Two successive PCR products were assembled to generate the full length 4B7 scFv-0 V_L-V_H which was cloned into the pET-based vectors via *NcoI* and *NotI* sites.

To generate 4B7 scFv-20, pSANG10-3F 4B7 scFv-0 (V_L-V_H) was used as template. The variable fragments were amplified using the primers **4B7VLNcoF** and **4B7VLLink5R** for V_L (generating V_LLink5) and **4B7VHLink5F** and **4B7VHNotR** for V_H (generating V_HLink5). The V_LLink5 and V_HLink5 PCR products were gel purified and the V_HLink5 purified product used in a second PCR with the primers **4B7VLVHLink30** and **4B7VHNotR** to generate V_HLink30. The gel purified PCR products of V_LLink5 and V_HLink30 were linked by overlap extension PCR. The purified product was then digested as previously described for 4B7 scFv-0 (V_L-V_H). 4B7 scFv-20 was also cloned into the expression vector pBAK.1, pSANG10-3F and pBAK.1Hk. The strategy for the design and construction of 4B7 scFv-20 V_L-V_H is shown in Figure 2.2. Constructs were confirmed by DNA sequencing. Sequences of primers are outlined in Table 2.4.

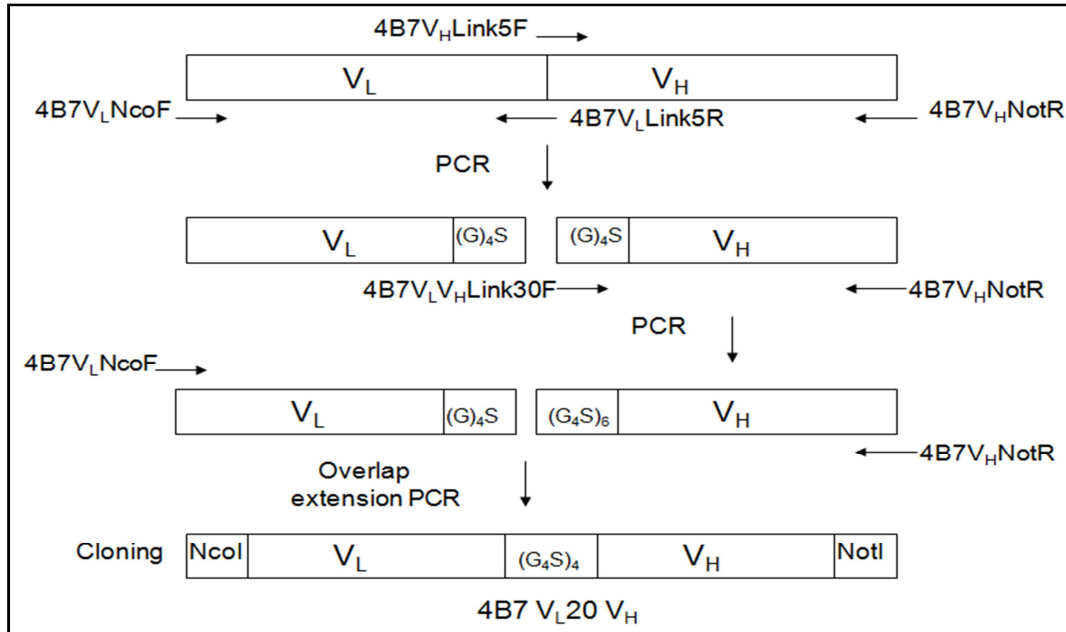


Figure 2.2: Design and construction of 4B7 scFv-20 (V_L-V_H). The variable domains of 4B7 scFv-0 V_L-V_H were amplified by PCR. Three successive PCR products were assembled to generate the full length 4B7 scFv-0 V_L-V_H which was cloned into the pET-based vectors via *NcoI* and *NotI* sites. G-S: glycine-serine linker.

Primer	Sequence 5' – 3'
4B7VHNot	AAGCTT GCGGCCG CGCTGCTCACGGTCAGGGTGGTG CCCTGGCC
4B7VLNcoI	GCCATGG CCGATATTCAGATGATTCAGAGCCCGAC
4B7VLR	CGCTTTATTTTCCAGTTTGGTGCCGCTGCC
4B7VHF	GAAGTGAAACTGGTGGAAAGCGGCGGGCGGC
4B7VHLink5F	GGAGGTGGCGGAAGCGAAGTGAAGTGGTGGAAAGC GGCGGCGGC
4B7VLLink5R	CTACCGCCACCTCCCGCTTTAATTTCCAGTTTGGTG CCGCTGCC
4B7VLVHLink30	GGAGGTGGCGGTAGTGGAGGTGGCGGAAGCGGAGG TGGCGGTAGTGGAGGTGGCGGAAGCGGAGGTGGCG GTAGTGGAGGTGGCGGAAGC

Table 2.3: Primer sequences used for the amplification of 4B7 scFv variable domains and for assembly of the scFv-0 and scFv-20. Restriction sites are in bold.

2.3.4 Site directed mutagenesis of 4B7 scFv

Site directed mutagenesis was essentially performed as described by (Zheng *et al.*, 2004). The strategies for mutagenesis are depicted in Figures 2.3 and 2.4. Partially overlapping primers were designed to introduce mutations at target sequences. PCR conditions were as described in Section 2.3.3. The plasmid pSANG10-3F 4B7 scFv-0 V_L - V_H was used as template. A range of PCR products were assembled to construct the 4B7 scFv-0 mutant. In Figure 2.3 three successive PCR products were assembled to generate the scFv-0 V_H Q20R and V_H T94F mutations. The template was then used to generate the mutations V_L L85F, V_L G86A, V_L Q3E, V_L I5T and V_H L114V. The amplification reaction for introduction of all mutations consisted of 5 μ L of 5X Taq & Go, 1.25 μ L of each 10 μ M primer (5' and 3'), 1 μ L of template DNA and 16.5 μ L nuclease free water. The PCR amplifications were set with the conditions as outlined in Section 2.3.3.

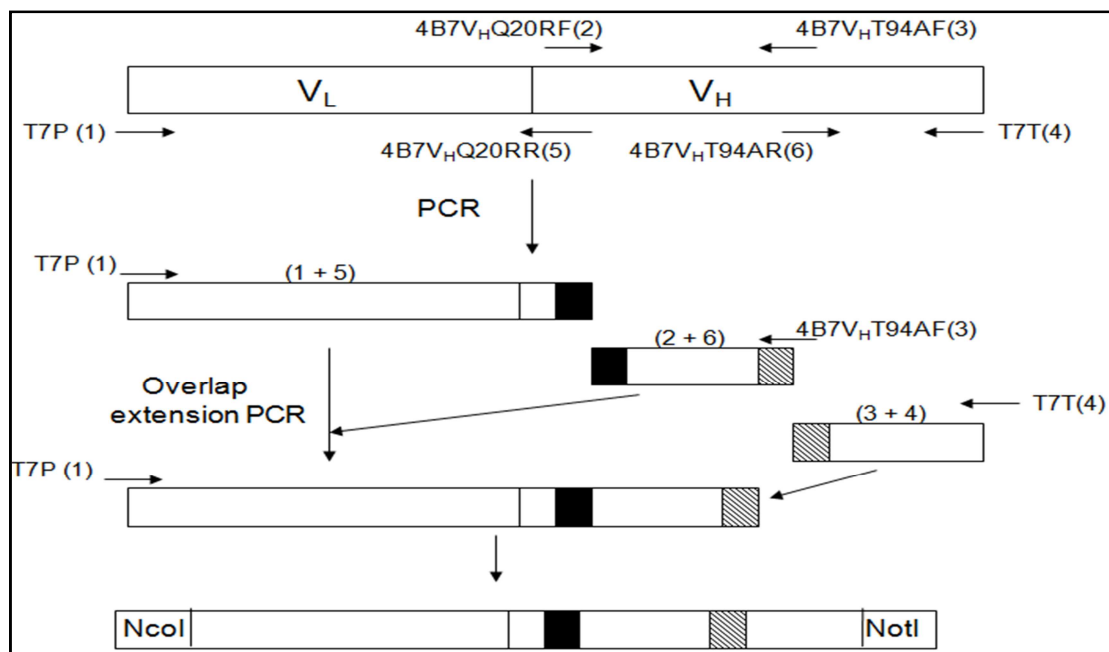


Figure 2.3: Design and construction of 4B7 scFv-0 mutants (V_H Q20R and V_H T94F). Mutations were introduced by PCR using partially overlapping primers. Three successive PCR products were assembled to generate the scFv-0 V_H Q20R and V_H T94F mutations.

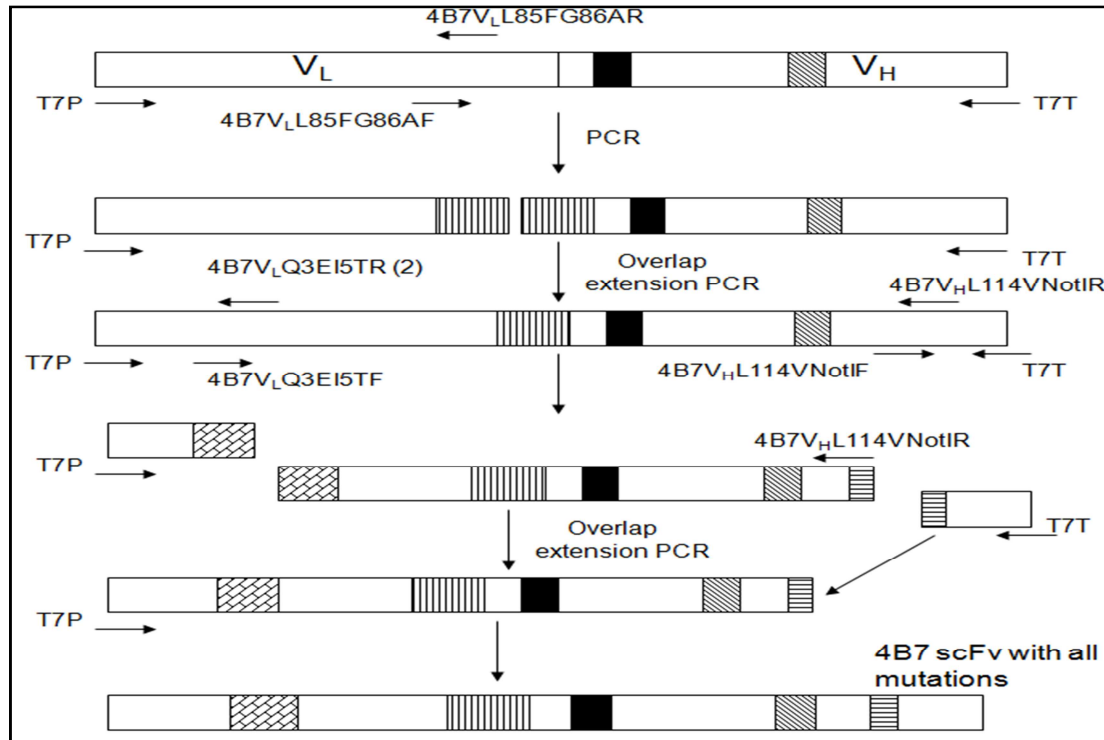


Figure 2.4: Design and construction of 4B7 scFv-0 mutants (V_L L85F, V_L G86A, V_L Q3E, V_L I5T and V_H L114V). Two PCR products were used to generate the V_L L85F and V_L G86A mutants. The template for this mutant was then used to generate the V_L Q3E, V_L I5T and V_H L114V mutations.

<i>Primer</i>	<i>Sequence 5' – 3'</i>
4B7VLQ3EI5TF	GATATTGAGATGACCCAGAGCCCGAGCAGCATGTTTGGC
4B7VLQ3EI5TR	GCTCTGGGTCATCTCAATATCGGCCATGGCCGGCTGGGC
4B7VLL85FG86AF	GCGAAGATTTTGCCGATTATTATTCCTGCAGCGCAAC
4B7VLL85FG86AR	GCAATAATAATCGGCAAATCTTCGCTTTCCAGGCTGC
4B7VHQ20RF	GCGGCAGCCGAAACTGAGCTGCGCGGCGAGCGGC
4B7VHQ20RR	GCTCAGTTTGCGGCTGCCGCCCGGCTGCACCAGGCC
4B7VHT94AF	GAAGATAACCGCCATGTATTATTGCGCGCGCGGC
4B7VHT94AR	GCAATAACATGGCGGTATCTTCGCTGCGCAG
4B7VH	GGCACCACCGTGACCGTGAGCAGCGCGGCCGCATCCGC
4B7VHL114VNotIR	GCGGATGCGGCCGCGCTGCTCACGGTCACGGTGGTGCC

Table 2.4: Primer sequences for site directed mutagenesis of 4B7 scFv-1 (V_L - V_H).

2.3.5 Construction of Pf-NPNA V_H - V_L scFv-0, scFv-12, scFv-0Hk and scFv-12Hk

To generate the NPNA scFv-0 synthetic gene, the V_H and V_L gene fragments were PCR-amplified using the primers (Table 2.5) for V_H , **NcoF** and **PfVHR**, and for V_L , **PfVLF** and **NotR**. The amplification reaction consisted of 5 μ L of 5X Taq & Go, 1.25 μ L of each 10 μ M primer (5' \rightarrow 3'), 1 μ L of template DNA and 16.5 μ L nuclease free water. The PCR amplification was set with the conditions as outlined for Section 2.3.3.

Primer	Sequence 5' – 3'
NcoF	TCT AGA GCG GCC CAG CCG GCC ATG GCC
PfVHR	GCT GCT CAC GGT CAC CAG GGT GCC
PfVLF	GAA ATT GTG CTG ACC CAG AGC CCG
NotR	ATT ACG CCA AGC TT G CGG CCG C

Table 2.5: Primer sequences used for the amplification Pf-NPNA-1 scFv-12 variable domains and for assembly of the scFv-0. Restriction sites are in bold.

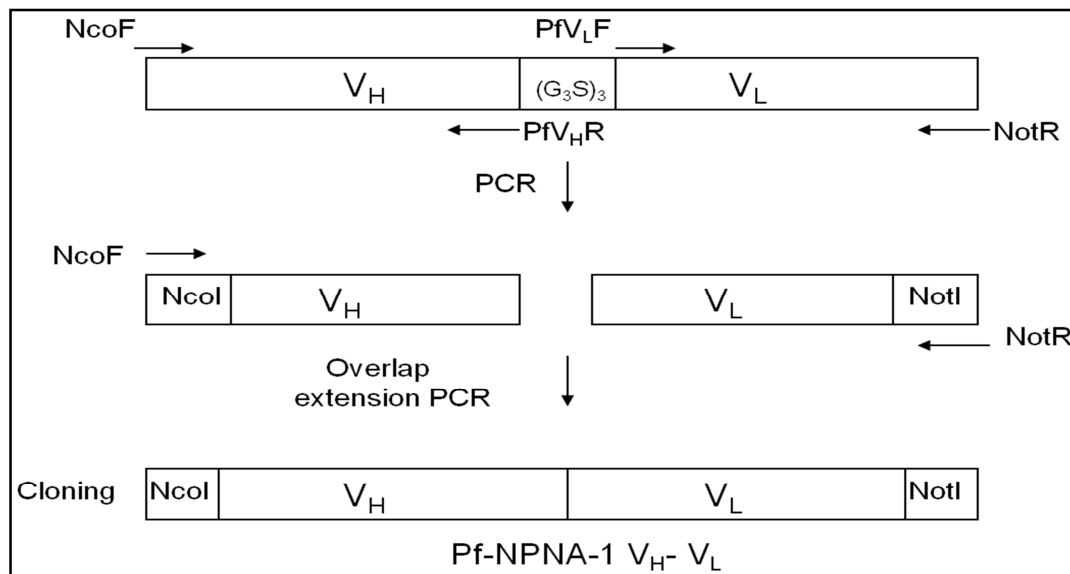


Figure 2.5: Design and construction of Pf-NPNA-1 scFv-0 (V_H - V_L). The variable domains of Pf-NPNA-1 scFv-12 V_H - V_L were amplified by PCR. Two successive PCR products were assembled to generate the full length Pf-NPNA-1 scFv-0 which was cloned into the pET-based vectors via *NcoI* and *NotI* sites.

The resulting PCR products were gel purified and joined into an scFv-0 by overlap extension PCR using the primers **NcoF** and **NotR** (Horton *et al.*, 1989). The reaction mixture for the overlap extension PCR was composed of 5 μ L of 5X Taq & Go, 1.25 μ L of each 10 μ M primer (5' and 3'), 2 μ L each of purified V_H and V_L and 14.5 μ L of nuclease free water. The PCR amplifications were set with the conditions outlined in Table 2.2. The strategy for the design and construction of 4B7 scFv-20 V_L - V_H is shown in Figure 2.5. The scFv-0 and scFv-12 were then digested with *NcoI* and *NotI* restriction enzymes and cloned into the expression vectors pBAK.1, pSANG10-3F and pBAK.1Hk.

2.4 Protein expression and purification of recombinant proteins

2.4.1 Expression and purification of (NPNA)₉-MKC antigen

Five colonies of BL21DE3 pRARE transformed with the plasmid pBAK1-(NPNA)₉-MKC were cultured in 10 mL of LB supplemented with kanamycin (50 µg/mL) and chloramphenicol (34 µg/mL) and grown overnight at 37°C with shaking, 250 rpm. The overnight culture was used to inoculate 200 mL of pre-warmed LB, supplemented with the appropriate antibiotics and grown until an OD_{600nm} of 0.5–0.6. Isopropyl-β-d-thiogalactopyranoside (IPTG) was added to a final concentration of 0.3 mM and the culture was grown for up to 3 hours. The cells were then harvested in a Sorvall Super T21 bench top centrifuge (SL-250T rotor) at 5000 rpm (9520 x g) for 20 min at 4°C. The supernatant was decanted and the pellet resuspended in 5 mL of lysis buffer (100 mM NaHPO₄, 10 mM Tris, 8 M Urea, pH 8) and subjected to 6 sonication cycles of 30s each (20 kHz uniform sonic waves at 40% power). The suspension was incubated on ice for 1 hour and the insoluble material removed by centrifugation (SL-50T rotor) for 30 min at 18000 rpm (39800 x g). The supernatant containing the recombinant protein was purified using an AKTA prime plus (GE Healthcare, UK) equipped with a 1 mL HiTrap Chelating column charged with Ni²⁺. The cleared lysate (5 mL) was loaded onto the column previously equilibrated with 5 column volumes of binding buffer (100 mM NaHPO₄, 500 mM NaCl, 10 mM Imidazole, pH 8) at a flow rate of 1 mL/min. The loaded column was washed with 5 column volumes of wash buffer (100 mM NaHPO₄, 500 mM NaCl, 20 mM Imidazole, pH 8) Bound proteins were then eluted within 1 mL aliquots with elution buffer (100 mM NaHPO₄, 500 mM NaCl, 500 mM Imidazole, pH 8). The purified recombinant antigen was analysed by SDS-PAGE.

2.4.2 Soluble expression of recombinant scFv and scFv-Hk antibodies

All the scFv constructs were evaluated for expression in the periplasm of *E. coli* using the expression vectors pBAK1, pSANG10-3F and pBAK1Hk (for

high level expression) under the control of the T7 promoter. For large scale expression the constructs were transformed into *E. coli* BL21DE3 pRARE cells (Novagen) selected on LB agar plates supplemented with the appropriate antibiotics. Transformants were cultured overnight at 37°C in 50 mL LB broth containing 50µg/ml kanamycin and 34 mg/ml chloramphenicol. The overnight culture was diluted 20 fold into 1 litre of LB broth containing 50 µg/ml kanamycin and 34 µg/ml chloramphenicol grown at 37°C until an OD₆₀₀ of 0.5 – 0.6. scFv expression was then induced by adding IPTG (isopropyl-beta-D-thiogalactopyranoside) to a final concentration of 0.3mM, with growth continued overnight at 20°C.

2.4.3 Isolation and purification of periplasmic extracts

Periplasmic expressed scFvs were isolated by osmotic shock as follows: overnight induced cultures were harvested by centrifugation at 5000 rpm for 20 mins. Cell pellets were resuspended in 1/20th volume of TS (30mM Tris-HCl, 20% sucrose pH 8.0) supplemented with 0.5mM EDTA (ethylenediaminetetraacetic acid) and 0.1mM PMSF (phenylmethylsulphonyl fluoride) and incubated on ice for 30 minutes. The suspension was centrifuged (8000 rpm, 20mins at 4°C; SL-250T rotor), the supernatant retained and the pellet resuspended in same volume of 5mM MgSO₄ and left to incubate on ice for 30 minutes. The supernatants from the TES and MgSO₄ treatments were pooled and centrifuged at 13,000 rpm (24750 x *g*) for 20 mins. The cleared supernatant was then passed through a 0.2µm filter and stored at 4°C and used for purification on a Ni-NTA affinity resin.

The recombinant scFv expressed proteins were purified in two stages: first by ion metal affinity chromatography (IMAC) on a 1 mL nickel agarose column fitted to a peristaltic pump and subsequently by ion exchange chromatography on a 1 mL HiTrapTM SP FF column (cation exchange) or HiTrapTM Q FF column (anion exchange). For IMAC purification, the 1 mL Ni column was equilibrated with 5 column volumes of binding buffer (100 mM NaHPO₄, 500 mM NaCl, 10 mM Imidazole, pH 8). The osmotic shock lysates, made up to

the composition of the binding buffer by a 1:1 ratio with 2X binding buffer, was loaded onto the column with the aid of a peristaltic pump at a flow rate of 1 mL/min. The column was washed with 5 column volumes of wash buffer (100 mM NaHPO₄, 500 mM NaCl, 20 mM Imidazole, pH 8). Bound protein eluted with 5 column volumes of elution buffer (100 mM NaHPO₄, 500 mM NaCl, 500 mM Imidazole, pH 8) in 1 mL fractions and analysed by SDS-PAGE.

2.4.4 Desalting of IMAC purified proteins

Desalting of IMAC purified proteins was performed on an AKTA prime plus (GE Healthcare, Amersham) using a 40 mL Sephadex G-25 column. A 2 mL fraction of IMAC purified proteins were applied onto the column pre-equilibrated with 3 column volumes of 20 mM Tris-HCl pH 8.0. The proteins were eluted with 2 column volumes of 20 mM Tris-HCl pH 8.0 in 0.5 mL fractions.

2.4.5 Anion exchange chromatography (AEC)

AEC was performed on an AKTA Prime Plus using a 1 mL HiTrapTM Q FF anion exchange column (GE Healthcare, Amersham, UK) following manufactures protocol. Five mL of the desalted protein was loaded on the column equilibrated with buffer A (20 mM Tris-HCl, pH 8.0). Proteins were eluted over a linear salt gradient with buffer B (20 mM Tris-HCl, 1 M NaCl, pH 8.0). Fractions were pooled, concentrated with Amicon protein concentrators (MWCO 10 kDa) and analysed by SDS-PAGE.

2.4.6 Cation exchange chromatography (CEC)

CEC was performed on an AKTA Prime Plus using a 1 mL HiTrapTM SP FF cation exchange column (GE Healthcare, Amersham, UK) following manufactures protocol. Five mL of the desalted protein was loaded on the column equilibrated with buffer A (50 mM sodium acetate, pH 5.5). Proteins

were eluted over a linear salt gradient with buffer B (50 mM sodium acetate, 1 M NaCl, pH 5.5). Fractions were pooled, concentrated with Amicon protein concentrators (MWCO 10 kDa) and analysed by SDS-PAGE.

2.4.7 Sodium Dodecyl Sulphate Polyacrylamide Gel Electrophoresis (SDS-PAGE)

Sodium dodecyl sulphate polyacrylamide gel electrophoresis (SDS-PAGE) was performed as described by (Laemmli, 1970). Proteins were electrophoresed on a 12% gel under reducing conditions.

Resolving gel (12%)	
MilliQ water	3.9 ml
1.5 M Tris-base pH 8.8	2.6 ml
10% SDS	100 μ l
40% Acrylamide/Bis (29:1)	3.0 ml
10% Ammonium persulphate	100 μ l
TEMED	20 μ l
Stacking gel (4%)	
MilliQ water	3.45 ml
0.5 M Tris-base pH 6.8	625 μ l
10% SDS	50 μ l
40% Acrylamide/Bis (29:1)	500 μ l
10% Ammonium persulphate	50 μ l
TEMED	10 μ l

Table 2.6: Reagents used for SDS-PAGE

To cast the gel with dimensions of 8 cm (W) x 7.3 cm (H), clean glass plates and spacers (0.75 mm) were assembled in a gel holder on a casting stand. The resolving gel mixture (3.5 ml) was poured between the glass plates, overlaid with water and left to polymerise for 10 minutes. The water was poured off, 1 ml of stacking gel added and a 10-well comb inserted

immediately. The gel was left to polymerise for 10 minutes. The protein samples were then prepared by mixing 15 μ l of sample with 5 μ l of 4X sample buffer (50 mM Tris-HCl pH 6.8, 2% SDS, 5% β -mercaptoethanol, 0.05% Bromophenol blue, and 10% Glycerol) heated at 100°C for 5 minutes, centrifuged (13000 rpm, 1 min) and loaded on the gel. The gel was run at 200 V for 40 min with 1X SDS running buffer (14.4 g/L Glycine, 3.03 g/L Tris Base and 1 g/L SDS). The procedure was performed using a Mini-Protean Tetra cell electrophoresis system (Bio-Rad Laboratories, UK).

To analyse multimerisation of scFvs a semi-native SDS-PAGE was run. For semi-native SDS-PAGE, the sample buffer lacked β -mercaptoethanol but contained SDS (1 %) and the samples were not boiled. The gel was run at 120 V for 3 hours at 4°C with 1X SDS running buffer containing 0.1% SDS.

2.4.8 Coomassie Brilliant Blue staining of protein gels

The separated proteins from SDS-PAGE were visualised by Coomassie Brilliant Blue R-250 staining (Kurien and Scofield, 1998). The gel was stained in 0.025% w/v Coomassie Brilliant Blue R-250 in 10% v/v acetic acid by microwaving until boiling followed by 1 min on rocking table. The gel was destained in 10% v/v acetic acid in a microwave until the solution had boiled.

2.4.9 Bradford assay

Protein concentration was estimated by using Bradford assay (Bradford, 1976) with bovine serum albumin (BSA) as the protein standard. The assay was performed as follows: 20 μ L of protein solution was added to 780 μ L of PBS and 200 μ L of Bradford reagent. The mixture was vortexed and incubated at room temperature for 10 min and the absorbance read at 595 nm using a NovaSpec II spectrophotometer (GE Healthcare, UK). The BSA standards were prepared in the range 0 – 400 μ g/ml in the same buffer as the proteins to be assayed.

2.4.10 Western blotting

SDS-PAGE separated proteins were blotted onto polyvinylidene difluoride (PVDF) (Millipore, UK) membrane using a Trans-Blot semi-dry transfer cell system (Bio-Rad Laboratories, UK) using the method of (Towbin *et al.*, 1979). The gel and membranes were soaked in transfer buffer (25 mM Tris-HCl, 192 mM Glycine, 20% v/v methanol) for 15 min to remove electrophoresis salts and detergents. The PVDF membrane was activated by immersing in methanol for 15 sec, transferred into MilliQ water for 2 min and into transfer buffer for 15mins. The pre-wetted PVDF membrane was placed on top of four chromatography papers (Fisher Scientific, UK), cut to gel dimension. The equilibrated gel was then placed on the PVDF membrane and overlaid with four chromatography papers. Air bubbles were excluded in between stacks by rolling a pipette over the surface each paper or membrane. Protein transfer was performed at 25 V for 20 min. After the transfer, the membrane was blocked overnight at 4°C with 10 ml of 5% dry non-fat milk in PBS. For detection of C-terminal His tag fusion proteins, a rabbit polyclonal hexahistidine tag antibody conjugated to HRP (1:10000) (Abcam, UK) was used. Novex sharp prestained marker (Invitrogen, UK) was used as molecular weight standard.

2.4.11 Enzyme-linked immunosorbent assay

The recombinant virus-like particle (VLP) of Woodchuck Hepatitis virus core antigen (WHcAg) containing the *P. falciparum* sporozoite major repeat motif [NANPNVDP(NANP)₃] peptide and recombinant Pfs25 (3D7) antigen were kind gifts from Prof. David Millich and Dr. Takafumi Tsuboi, respectively. The recombinant (NPNA)₉-MKC antigen, in which the NPNA peptide sequence is fused to mouse kappa constant (MKC) was expressed and purified as described in Section 2.4.1. A solid phase ELISA was used to evaluate the antigen-binding activity of the purified scFvs. Briefly, Nunc MaxiSorp flat bottom polystyrene plates (Fisher, UK) were coated with recombinant antigen (100 ng/100 µL/ well) in carbonate buffer (0.1 M Na₂CO₃ and 0.1 M NaHCO₃,

pH 9.5) at 4°C for 16 h. The (NPNA)₉-MKC antigen was used at 1 µg/100 µL/well. Subsequently, the ELISA plates were washed three times with 200 µL of phosphate buffered saline (PBS) -Tween 20 (0.05%) and blocked with 5% bovine serum albumin (BSA) in PBS for 1 h at room temperature (RT). Purified scFvs were diluted 2-fold in 1% BSA in PBST (0.1% Tween 20), such that final composition of Tween 20 was 0.05%, and stored on ice. After washing three times with PBST, 100 µL of the diluted IMAC purified scFvs were added to the wells, in triplicates, and incubated at RT for 2 hours. Three negative controls were set up as outlined in Table 2.9. In the first two controls, 1% BSA in PBST or a non-specific antibody (for 4B7 scFvs the Pf-NPNA-1 scFvs were used and vice-versa) were added to antigen coated wells. In the third control, the specific scFv antibody, for which the ELISA was carried out, was added to wells previously coated with 5% BSA in carbonate buffer.

Coated wells	Test	Buffer composition (final)
Antigen coated wells	Test antibody	0.5% BSA, 0.05% Tween20, PBS
	Control antibody	0.5% BSA, 0.05% Tween20, PBS
	BSA	1% BSA, 0.1% Tween20, PBS
BSA coated wells	Test antibody	0.5% BSA, 0.05% Tween20, PBS

Table 2.7: Outline of ELISA procedure on Nunc 96-well plates.

The plates were washed five times with PBST followed by three washings with PBS only. The bound scFvs, expressed from pBAK.1 with a C-terminal octa-His tag, were detected by incubation at RT for 1 h with 100 µL of monoclonal anti-His-AP antibody (1:10,000). For pSANG10-3F expressed scFvs, a rabbit anti-tri FLAG antibody (1: 50,000) was used as primary antibody and goat anti-rabbit IgG-AP (1: 50,000) as secondary antibody. Goat anti-Human kappa light chains (bound and free) –AP antibody (1: 30,000) was used for the detection of pBAK.1Hk expressed scFv. After the last washing step, the plates were developed with p-nitrophenol phosphate (SIGMAFAST™ pNPP tablet, Sigma, UK) substrate in 0.2 M Tris buffer pH 8.0 containing 5 mM MgCl₂. The plates were read at 405 nm. Results were expressed as OD units.

2.4.12 Size-exclusion chromatography (SEC)

SEC was performed on an AKTA Prime Plus using a HiLoad 16/60 Superdex 200 size-exclusion column (GE Healthcare) equilibrated with degassed phosphate buffered saline (PBS). The flow rate was 1 ml/min, and the absorbance of the eluted protein was monitored at 280 nm. The column was calibrated with the following protein standards: β -amylase (200 kDa), bovine serum albumin (66 kDa), carbonic anhydrase (29 kDa) and cytochrome C (12.4 kDa).

2.4.13 Indirect Immunofluorescence Assay (IFA) on *P. falciparum* sporozoites

The binding of purified Pf-NPNA-1 scFv-0 and scFv-12 proteins to native circumsporozoite protein (CSP) was assessed in an IFA (Chappel *et al.*, 2004). Acetone-fixed smears of *P. falciparum* X5 (progeny clone of a cross between 3D7 and HB3, provided by Prof. Lisa Ranford-Cartwright) salivary gland sporozoites on glass slides were blocked with 50 μ L of 5% BSA in PBS for 1 hour at 37°C. Slides were washed twice for 5 min with PBST. All other incubations were carried out at 37°C in a humid chamber. The scFv antibodies were diluted in PBST (1:1), applied to the slides and incubated for 2 h. A control slide was set up with 1% BSA. The slides were washed 5 times for 3 min with PBST and fluorescein isothiocyanate (FITC) anti-His antibody diluted 1:500 in 1%BSA-PBST applied for 1 h. Slides were washed, mounted in Vectashield anti-fade (Vector Laboratories) reagent and parasites visualized by fluorescence microscopy with a Zeiss Axioskop fluorescent microscope equipped with a 100X oil immersion objective.

2.4.14 Statistical Analysis

Unpaired T-test, by using Graphpad T-test calculator software, was used to determine the level of significance of the observed binding activities of the expressed proteins (<http://www.graphpad.com/quickcalcs/ttest1.cfm>). *P* values < 0.05 were considered significant.

2.5 Preliminary evaluation of Pf-NPNA-1 and 4B7 scFvs in *Asaia* SF2.1

2.5.1 Assessment of antibiotic resistance

Minimum inhibitory concentration was determined by streaking untransformed bacterial cells on GLY agar (25 g/L glycerol, 10 g/L yeast extract and 15 g/L agar, pH 5) containing increasing concentrations of kanamycin (25, 50, 100, 150, 200 and 300 µg/mL).

2.5.2 Preparation of Electrocompetent *Asaia* sp.

Competent cells were prepared according to the method of Mostafa *et al.* (2002) with slight modifications. A single colony of *Asaia* sp. was inoculated into 10 mL GLY medium (25 g/L glycerol, 10 g/L yeast extract, pH 5) and grown overnight at 30°C with aeration (150 rpm). The overnight culture was inoculated into 200 mL of prewarmed GLY and grown at 30°C with aeration (150 rpm) until the OD₆₀₀ was 0.5 - 0.8. After 15 min of incubation on ice, cells were transferred into chilled centrifuge tubes (4 x 50 mL) and harvested (5000 rpm, 10 min, 4°C). The supernatant was discarded and each pellet resuspended in 25 mL of cold 1 mM Hepes (pH 7.0). This step was repeated and the pellets resuspended in 25 mL of cold 10% (v/v) glycerol and harvested by centrifugation. The pellets were again resuspended in 25 mL of cold 10% glycerol, harvested and finally resuspended in 1/100 culture volume of 10% (vol/vol) glycerol. Competent cells were aliquoted (100 µL) and stored at -80°C.

For electroporation, 100 µL of the competent cells were mixed with 10 µL (50 ng/µL) of plasmid DNA and then transferred to an ice-cold electroporation cuvette (1-mm electrode gap) (Sigma, UK). After incubation for 2 min on ice, the cells were exposed to a single electrical pulse with a Gene-Pulser Xcell apparatus (Bio-Rad Laboratories, Richmond, CA) set at 25 µF, 200 Ω and 1800 V. Immediately following the electrical discharge, 200 µL of GLY medium was added, cells were incubated at 30°C for 3 h and plated on GLY agar (25

g/L glycerol, 10 g/L yeast extract and 15 g/L agar, pH 5) containing 200 µg/mL kanamycin. Plates were incubated for 48 hrs and transformants screened by colony PCR.

2.5.3 Expression of Pf-NPNA-1 and 4B7 scFvs in *Asaia* sp.

Small scale expressions were initially conducted to evaluate the optimal expression of the scFvs. *Asaia* sp. was electroporated with the constitutive expression vector pMAK031 (2P) harbouring the Pf-NPNA-1 and 4B7 scFv cassettes. After 48 h of incubation transformants were PCR screened for the presence of scFv insert. Positively screened transformants were inoculated into 10 mL of GLY medium supplemented with kanamycin (200 µg/ml) and grown with shaking at 30°C for 4 days. Aliquots (1 mL) of bacterial culture were taken at days 2, 3 and 4 and centrifuged at 13,000 rpm for 1 min. The supernatants were discarded and the cell pellets saved to determine optimal day for scFv expression. Glycerol stocks were prepared samples collected on day 2 and stored at -80°C.

For large scale expression, glycerol stocks of Pf-NPNA-1 scFv-0, 12 and 4B7 scFv-0 were inoculated into 10 mL of GLY containing kanamycin (200 µg/ml) and grown overnight at 30°C. The overnight culture was diluted into 200 mL of GLY supplemented with kanamycin and grown for 2 days at 30°C with aeration (150 rpm). The bacterial cells were centrifuged at 5000 rpm for 15 min at 4°C and stored at -20°C.

2.5.4 Isolation and purification of Pf-NPNA-1 (scFv-0 and 12) and 4B7 scFv-0

The bacterial pellets were thawed and resuspended in 5 mL of TS buffer (30mM Tris-HCl, 20% sucrose pH 8.0) supplemented with 0.1mM PMSF. The cell were incubated on ice for 30 minutes and sonicated six times for 30 sec (20 kHz uniform sonic waves at 40% power) to lyse the cells. To remove cell debris, the lysate was centrifuged at 18,000 rpm for 20 min at 4°C. The

supernatant was transferred to a fresh tube on ice and use for the purification of the recombinants scFv by IMAC.

Purification was performed on an ÄKTA prime (GE Healthcare, UK) connected to a 1 mL HiTrap Chelating column charged with Ni²⁺. The cleared lysate (5 mL) was loaded onto the column previously equilibrated with 5 column volumes of binding buffer (100 mM NaHPO₄, 500 mM NaCl, 10 mM Imidazole, pH 8) at a flow rate of 1 mL/min. The loaded column was washed with 5 column volumes of wash buffer (100 mM NaHPO₄, 500 mM NaCl, 20 mM Imidazole, pH 8). Bound proteins were then eluted within 1 mL aliquots with elution buffer (100 mM NaHPO₄, 500 mM NaCl, 500 mM Imidazole, pH 8). The purified recombinant scFvs were analysed by SDS-PAGE under reducing and non-reducing conditions.

Chapter 3

Results

***E. coli* expression of scFv 4B7
and Pf-NPNA-1**

3.0 RESULTS

3.1 Introduction to results

This chapter comprises experiments to express and characterise two scFvs in *E. coli*. The scFv used for these investigations are the anti-Pfs25 murine antibody, 4B7 and the human anti-CSP repeat antibody Pf-NPNA-1. For the purpose of inclusion of these antibodies as effector molecules in symbiont control, initial evaluation must be undertaken in *E. coli* and subsequently in the chosen symbiotic bacterium.

Functionality of antibodies is dependent on the proper formation of the intrachain disulphide bonds. Thus, the expression vectors were designed to translocate the recombinant scFv into the oxidising milieu of the periplasm, where disulphide bond formation occurs (Better *et al.*, 1988; Skerra and Pluckthun, 1988). To enhance the solubility of the recombinant scFv, expression was undertaken at a low temperature of 20°C. The expression and characterisation results are divided into two sections.

Expression and characterisation of 4B7 scFv-0 and scFv-20 in *E. coli*

The murine MAb 4B7 was chosen because of its transmission blocking properties. The codon optimised 4B7 scFv was expressed in both $V_H - V_L$ and $V_L - V_H$ orientations, purified and tested for functionality. Multimer formations by purified recombinant scFvs were assessed.

Expression and characterisation of Pf-NPNA-1 scFv-0 and scFv-12 in *E. coli*

The human anti-CSP repeat antibody, Pf-NPNA-1, was expressed in the $V_H - V_L$ format, purified and functional activity evaluated. A recombinant antigen, (NPNA)₉MKC, which has nine repeats of NPNA fused to MKC (mouse kappa constant domain), was expressed and specificity of the purified Pf-NPNA-1 scFvs tested against it.

Expression of 4B7 and Pf-NPNA-1 scFvs in *Asaia* sp

Subsequently, the 4B7 and Pf-NPNA-1 scFvs were cloned into a broad-host range plasmid for expression and secretion in the symbiotic bacteria *Asaia* sp. Furthermore, functional analysis analyses of the secreted proteins were then evaluated.

3.2 Construction of scFv expression vectors pBAK.1 and pBAK.1Hk

The pET-based expression vectors pBAK.1 and pBAK.1HK were constructed to allow tightly regulated periplasmic expression of scFv and scFv-Hk. The vectors employ a T7 promoter, a *pe/B* signal peptide (SP), to direct secretion of the expressed protein into the periplasm of *E. coli*, and an octa-His tag, at the C-terminus, to facilitate purification and detection. The expression cassette has unique *Nco*I, *Not*I and *Xho*I restriction sites for directional cloning and insertion of scFv DNA fragments.

To construct pBAK.1Hk the light chain human kappa constant gene (HuCk) was amplified with the primers BAK.1 and BAK.2, which appended *Not*I and *Xho*I restriction sites at the 5' and 3' ends, respectively. The PCR product (Figure 3.1B) was digested with the restriction enzymes *Not*I and *Xho*I and cloned into pET41b(+) to give pET41b(+)Hk. The presence of the insert was confirmed by colony PCR. The pET41b(+)Hk plasmid was isolated and digested with *Xba*I and *Not*I restriction enzymes. Subsequently, the 5' UTR, ribosome binding site and *pe/B* signal peptide, from a modified pORFES, were cloned into the digested pET41b(+)Hk to yield pBAK1.Hk (Figure 3.1). A single step cloning of these gene sequences into pET41b(+) yielded pBAK.1(Figure 3.3).

The sequences of pBAK.1Hk and pBAK.1 plasmids are shown in Figure 3.2 and 3.4, respectively. The sequence confirmed the presence of the *pe/B* leader sequence, the restriction sites *Nco*I, *Not*I and *Xho*I and the octa His tag. The scFv constructs were then cloned into the *Nco*I/*Not*I sites of the

plasmids. The generated plasmid maps for each construct are shown in the appendix.

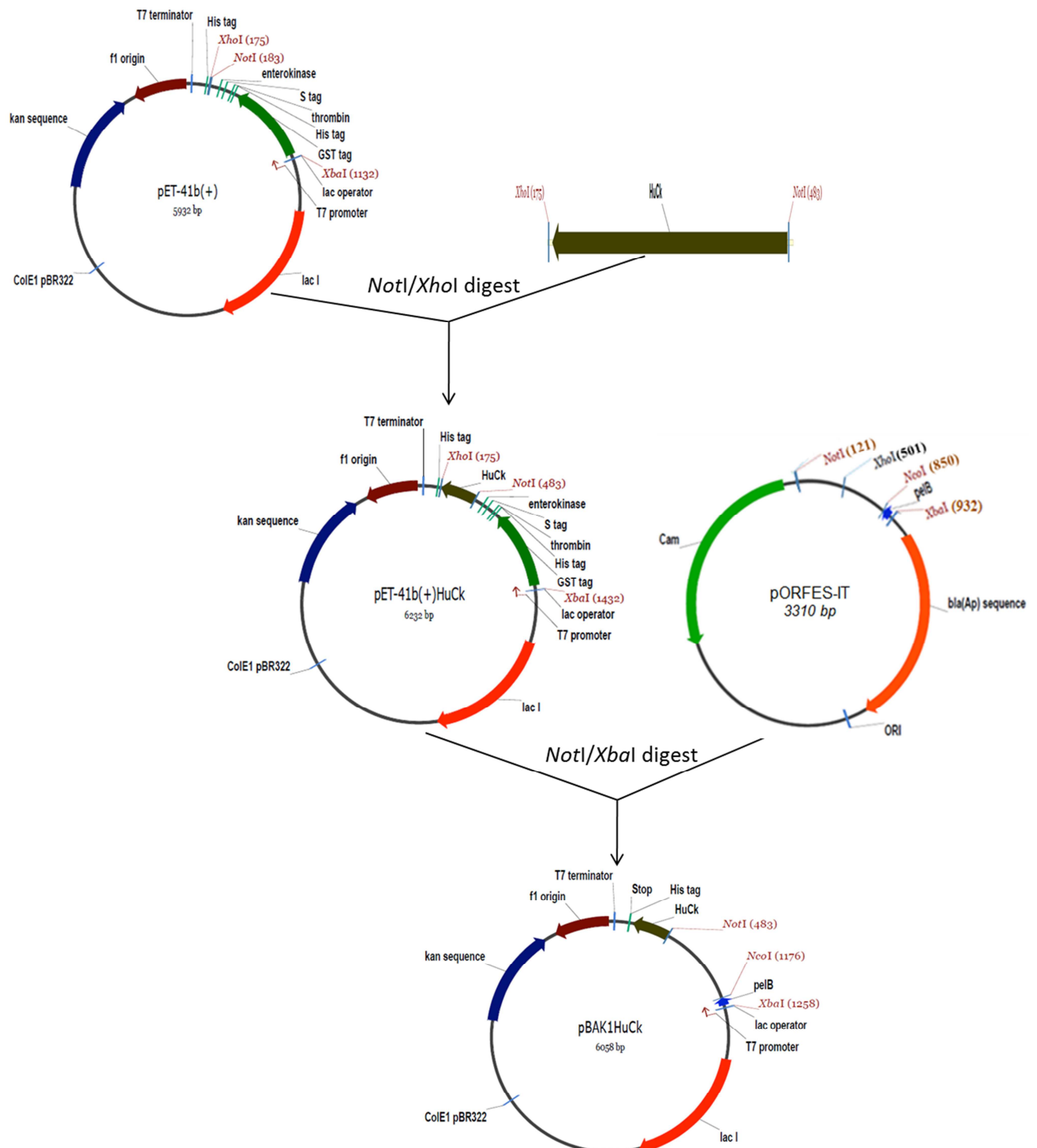


Figure 3.1: Cloning strategy and restriction maps of pET41b(+), pET41b(+)-HuCk, pORFES-IT and pBAK1HuCk. The plasmids are based on the pET41b(+) plasmid system and has the T7 promoter for expression of scFv and scFv-Hk. Relevant genetic elements are: lac operator, *peB* signal peptide, f1 origin of replication, T7 terminator, kanamycin resistance gene, ColE1pBR322 gene and *lacI* gene. The restriction sites and properties relevant for the construction and properties of the recombinant vector are shown.

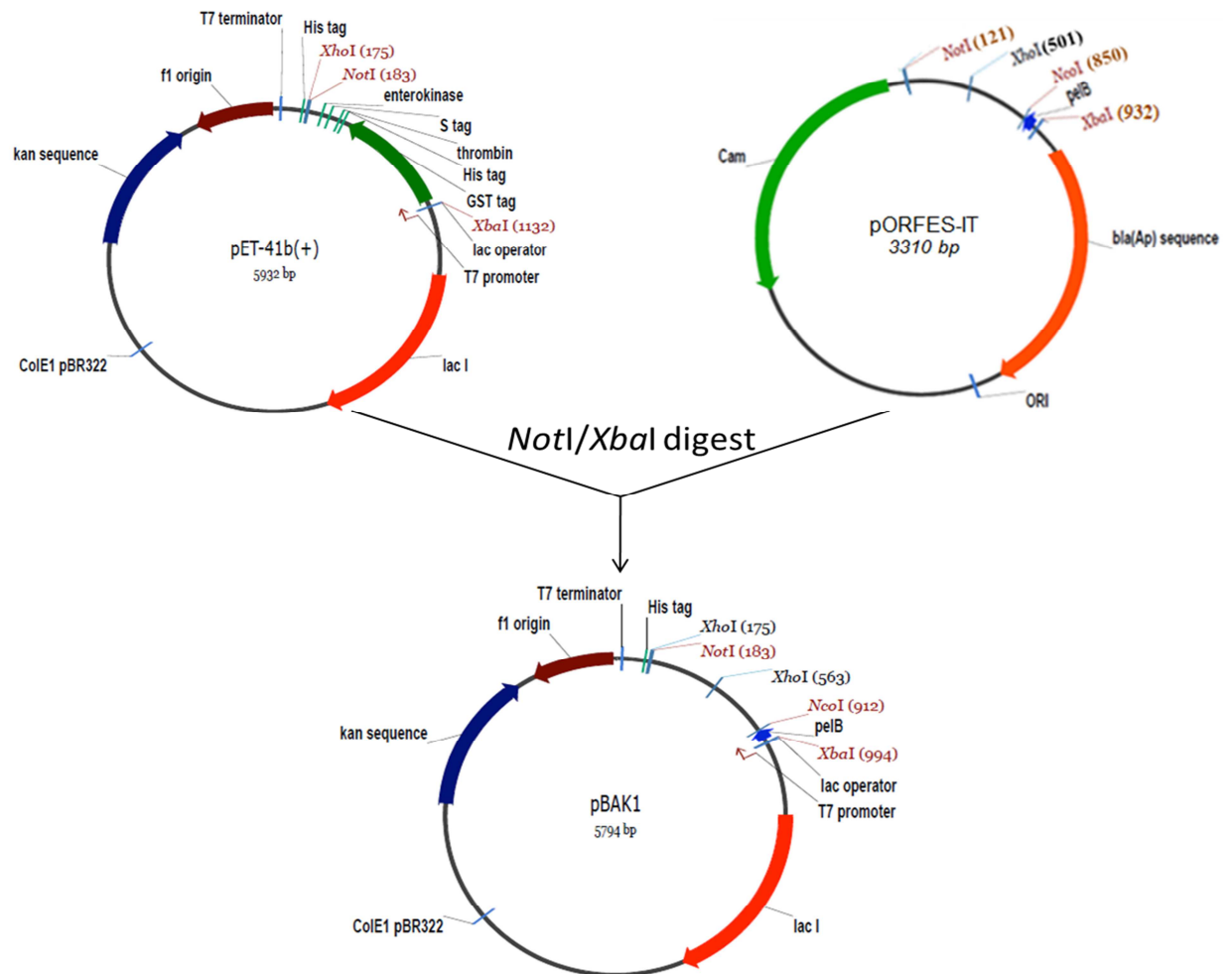


Figure 3.2: Cloning strategy and restriction maps of pET41b(+), pORFES and pBAK.1. The plasmids are based on the pET41b(+) plasmid system and has the T7 promoter for expression of scFv and scFv-Hk. Relevant genetic elements are: lac operator, *pelB* signal peptide, f1 origin of replication, T7 terminator, kanamycin resistance gene, ColE1pBR322 gene and *lacI* gene. The restriction sites and properties relevant for the construction and properties of the recombinant vector are shown.

3.2.1 Cloning of 4B7 scFv-1 V_H-V_L gene into pBAK.1 and pBAK.1Hk

To express 4B7 scFv-1 in the V_H-V_L orientation, the codon optimised gene synthesised as a pUC-19 insert was excised and subcloned into the *NcoI* and *NotI* restriction sites of pBAK.1 and pBAK.1Hk vectors. Transformants were colony screened by PCR using T7 promoter and terminator specific primers. Plasmids were purified and sequenced to ensure that the insert was inframe (Appendix). The expression plasmids encoding 4B7 scFv-1 were transformed

into *E. coli* BL21 (DE3) pRARE cells. Small scale expression in 50 mL LB induced with 0.3 mM IPTG was carried out. To investigate scFv secretion, periplasmic proteins were isolated and purified by IMAC. The expressed protein (cell pellet) and purified fractions were analysed by SDS-PAGE and Western blot. The blot was probed with monoclonal anti-His antibody as described in Section 2.4.10. The predicted molecular weight of the recombinant 4B7 scFv-1 was 27.8 kDa and 38.5 kDa for scFv-1Hk. SDS-PAGE and Western blot showed that most of the expressed protein was retained within the cytoplasm (Figure 3.3A). No secretion into the periplasm was observed on the Western blots (Figure 3.3B & C). The orientation of the 4B7 scFv-1 was reversed to $V_L - V_H$ and its expression and secretion investigated.

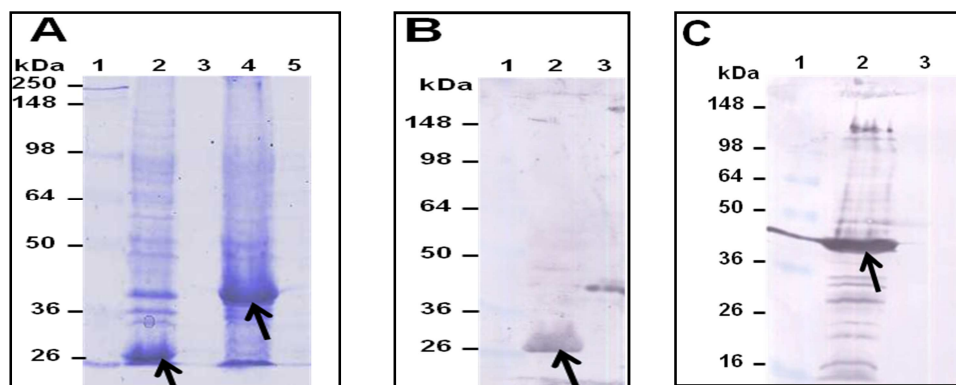


Figure 3.3: SDS-PAGE analysis under reducing conditions (A) and Western blot of small scale purification of 4B7 scFv-1 $V_H - V_L$ expressed from plasmids pBAK.1 (B) and pBAK.1Hk (C). 20 μ L of each fraction was loaded, electrophoresed on a 12% gel and stained with Coomassie Brilliant Blue R-250 (A) and transferred onto PVDF membrane and probed with monoclonal anti His-AP labelled antibody (B and C). Expressed recombinant proteins are indicated by arrows. **(A)** Lane 1: molecular weight markers, Lane 2: pBAK1 induced cell pellet, Lane 3: pBAK1 purified periplasmic extract, Lane 4: pBAK1Hk induced cell pellet, Lane 5: pBAK1Hk purified periplasmic extract. **(B)** Lane 1: molecular weight markers, Lane 2: pBAK1 induced cell pellet, Lane 3: pBAK1 purified periplasmic extract. **(C)** Lane 1: molecular weight markers, Lane 2: pBAK1Hk induced cell pellet, Lane 3: pBAK1Hk purified periplasmic extract.

3.2.2 Cloning of 4B7 scFv-0 and scFv-20 V_L - V_H genes into pSANG10-3F and pBAK.1Hk

To construct 4B7 scFv-0 in the V_L – V_H orientation, the variable domains were amplified with the primers **4B7VHF** and **4B7VHNot** for V_H and **4B7VLNco** and **4B7VLR** for V_L using 4B7 scFv-1 V_H – V_L pUC-19 as template. The scFv-0 was then assembled by overlap extension PCR using the primers **4B7VLNco** and **4B7VHNot**. The resulting PCR product was digested and inserted into the *Nco*I and *Not*I restriction sites of pSANG10-3F and pBAK.1Hk expression vectors and sequenced (Appendix).

The 4B7 scFv-0 and scFv-20 gene inserts in the expression plasmids, pSANG10-3F and pBAK.1Hk, were transformed into *E. coli* BL21 (DE) pRARE cells and recombinant protein expression evaluated. Protein expression was conducted as described in Section 2.4.2. Recombinant proteins isolated from the periplasm were purified in two stages: firstly, by IMAC on a nickel agarose column (Section 2.4.3) and secondly, by anion exchange chromatography (Section 2.4.5). The protein fractions from the two purifications steps were analysed by SDS-PAGE and Western blot.

The predicted molecular weights of 4B7 scFv-0 (Figure 3.4A) and scFv-20 (Figure 3.4B), using pSANG10-3F plasmid, on SDS-PAGE were consistent with the estimated values of 30 and 31.2 kDa, respectively. The level of scFv-0 expression, as indicated by the arrow of the induced band, was slightly lower than that of scFv-20. This corresponds with the scFv-0 level of secretion into the periplasm. The IMAC purified proteins also had other *E. coli* contaminants. Just below the secreted scFv-0 and scFv-20 is a 25 kDa *E. coli* protein.

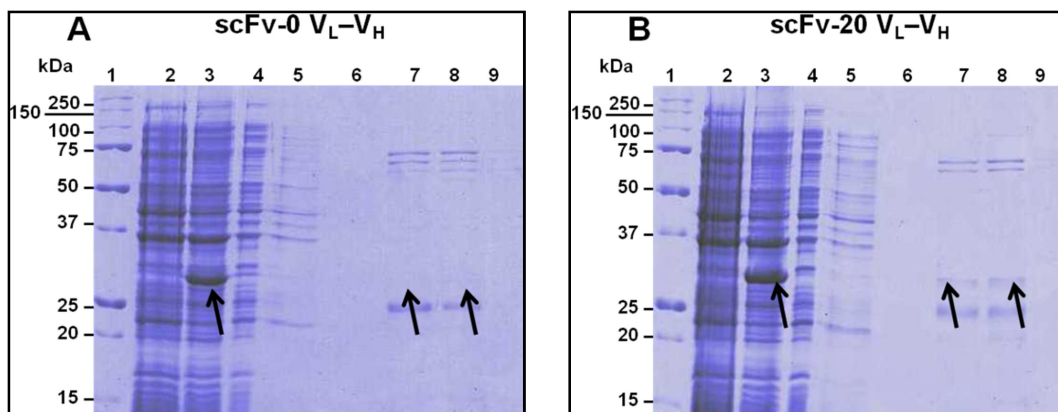


Figure 3.4: Expression and purification of 4B7 scFv-0 and scFv-20 using pSANG10-3F plasmid. SDS-PAGE analyses under reducing conditions of Ni-NTA affinity purification of scFv-0 (**A**) and scFv-20 (**B**) respectively. 20 μ L of each purification fraction was loaded, electrophoresed on a 12% gel and stained with Coomassie Brilliant blue R-250. (**A** and **B**) Lane 1: molecular weight marker; Lane 2: uninduced cell pellets; Lane 3: induced cell pellet; Lane 4: crude periplasmic fraction; Lane 5: Ni column flow through; Lane 6: Ni column wash with 10 mM Imidazole; Lanes 7-9: elutions with 500 mM Imidazole.

The IMAC purified scFv proteins were further purified by AEC based on the isoelectric points (pI) of the scFvs. The scFv-0 and scFv-20 both have the same pI of 4.96. The AEC purified proteins were concentrated and the purity compared with IMAC purified proteins on SDS-PAGE (Figure 3.5A). A duplicate gel was used for Western blotting (Figure 3.5B). The AEC purification did not result in homogeneously purified proteins as seen on SDS-PAGE. The Western blot (Figure 3.5B) showed two species of the purified scFv proteins. The higher molecular weight protein indicates that the signal peptide was not cleaved during translocation of the scFv into the periplasm. The scFv-0 and scFv-20 with uncleaved SP would have predicted molecular weights of 32.6 (pI 4.92) and 33.9 kDa (pI 4.92), respectively. For the scFv-20, the lower band is more pronounced and may be the processed protein.

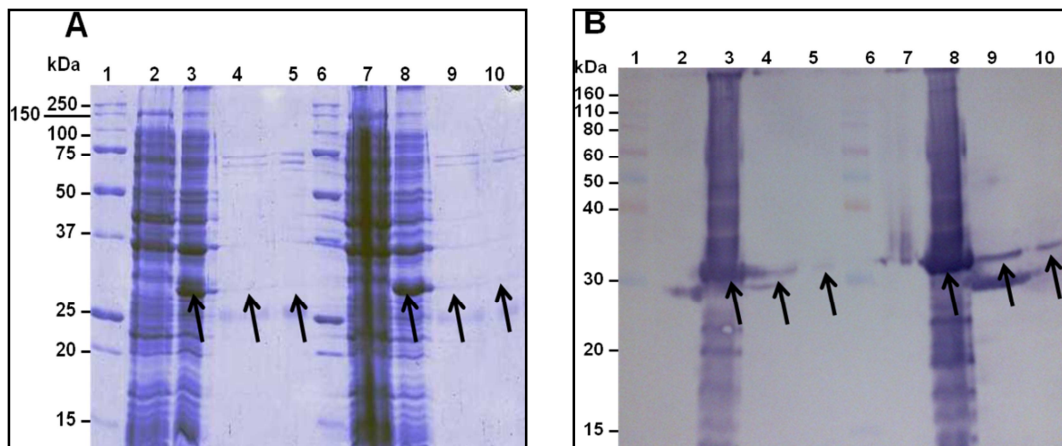


Figure 3.5: AEC of 4B7 scFv-0 and scFv-20 using pSANG10-3F plasmid. SDS-PAGE analyses under reducing conditions of Ni-NTA affinity and AEC purification of scFv-0 and scFv-20 (**A**). (**B**) Western blot of duplicate gel of (**A**). Proteins were probed with rabbit anti-tri FLAG antibody as primary antibody and goat anti-rabbit IgG-AP as secondary antibody. BCIP/NBT was used as substrate. **20 μ L** of each purification fraction was loaded, electrophoresed on a 12% gel and stained with Coomassie Brilliant blue R-250 (**A**). (**A** and **B**) Lane 1: molecular weight marker; Lane 2: scFv-0 uninduced cell pellets; Lane 3: scFv-0 induced cell pellet; Lane 4: IMAC purified scFv-0 (Figure 3.9A Lane 8); Lane 5: AEC purified scFv-0; Lane 6: molecular weight marker; lane 7: scFv-20 uninduced cell pellets; Lane 8: scFv-20 induced cell pellet (panel **B**, Lane 3); Lane 9: IMAC purified scFv-20 (Figure 3.9B, Lane 8) Lane 10: AEC purified scFv-20. Arrows indicate expressed recombinant proteins.

Expression of the 4B7 scFv-0 and 20 were also carried out in the pBAK.1Hk plasmid. The molecular weights of 4B7 scFv-0Hk (Figure 3.6A) and scFv-20Hk (Figure 3.6B) on SDS-PAGE were consistent with the estimated values of 38.4 (pI 5.59) and 39.6 (pI 5.59) kDa, respectively. The 25 kDa *E. coli* protein observed as a contaminant in the pSANG10-3F purified proteins was also observed for the scFv-0Hk and scFv-20Hk proteins. The affinity purified proteins were further purified by AEC (Figure 3.7A) similar to those of pSANG10-3F expressed proteins.

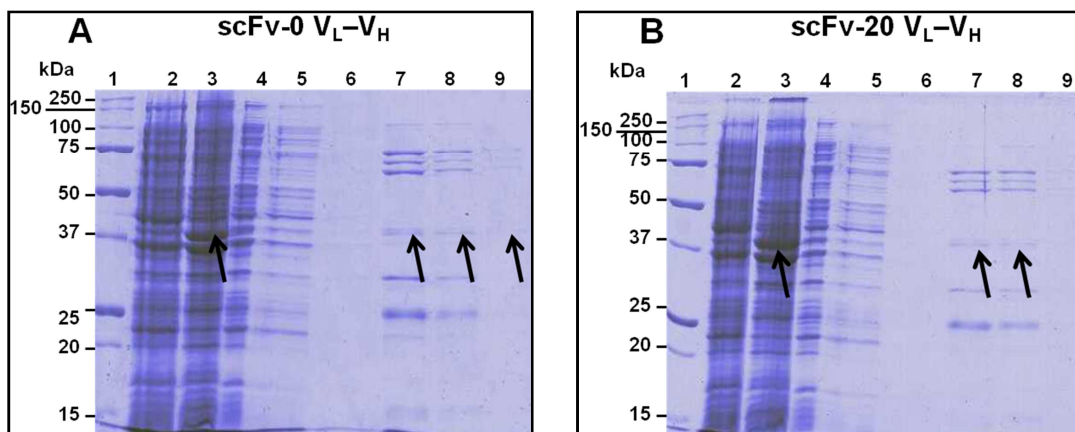


Figure 3.6: Expression and purification of 4B7 scFv-0 and 20 using pBAK.1Hk plasmid. SDS-PAGE analyses under reducing conditions of Ni-NTA affinity purification of scFv-0Hk (**A**) and scFv-20Hk (**B**) respectively. **20** μL of each purification fraction was loaded, electrophoresed on a 12% gel and stained with Coomassie Brilliant blue R-250. (**A** and **B**) Lane 1: molecular weight marker; Lane 2: uninduced cell pellets; Lane 3: induced cell pellet; Lane 4: crude periplasmic fraction; Lane 5: Ni column flow through; Lane 6: Ni column wash with 10 mM Imidazole; Lanes 7-9: elutions with 500 mM Imidazole.

On the Western blot (Figure 3.7B) faint bands corresponding to the predicted size of each scFv-Hk were observed in the uninduced proteins fractions. This was, however, not evident on the SDS-PAGE. The scFv-Hk proteins isolated by IMAC were not observed in the AEC eluted proteins.

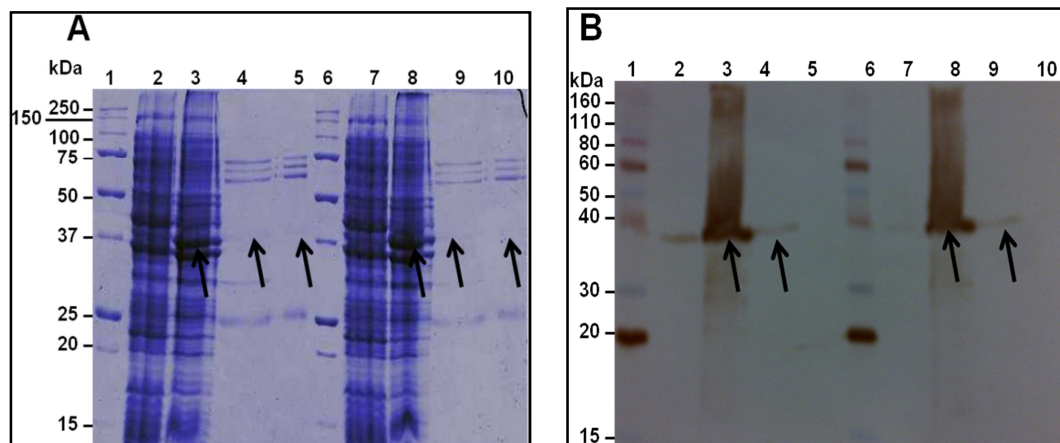


Figure 3.7: AEC of 4B7 scFv-0 and 20 using pBAK.1Hk plasmid. SDS-PAGE analyses under reducing conditions of Ni-NTA affinity and AEC purification of scFv-0Hk and scFv-20Hk (**A**). (**B**) Western blot of duplicate gel of (**A**). Proteins were probed with anti-His-HRP antibody. DAB was used as substrate. (**A** and **B**) Lane 1: molecular weight marker; Lane 2: scFv-0Hk uninduced cell pellets; Lane 3: scFv-0Hk induced cell pellet; Lane 4: IMAC purified scFv-0Hk (Figure 3.11A Lane 8); Lane 5: AEC purified scFv-0Hk; Lane 6: molecular weight marker; lane 7: scFv-20Hk uninduced cell pellets; Lane 8: scFv-20Hk induced cell pellet (panel **B**, Lane 3); Lane 9: IMAC purified scFv-20Hk (Figure 3.11B, Lane 8) Lane 10: AEC purified scFv-20Hk. Arrows indicate expressed recombinant proteins.

3.2.3 ELISA for functional analysis of 4B7 scFv-0 and scFv-20

The binding activity of the pSANG10-3F and pBAK.1Hk expressed scFv-0 and scFv-20 were evaluated in an ELISA as described in Section 2.4.11. Though the scFvs were expressed and secreted in pBAK.1 binding activity could not be assessed as the recombinant Pfs25 antigen used has a C-terminal His-tag. Dilutions of the scFv proteins were carried out with 1% BSA in PBST (0.1% Tween-20). PBST (0.05% Tween-20) was included in the washing steps to prevent non-specific binding. Negative controls were also incorporated in the ELISA to further demonstrate the specificity of 4B7 scFv-0 and scFv-20 to Pfs25. The negative controls were BSA (1% w/v) and Pf-NPNA-1 scFv (scFv-0 and scFv-12 used as controls for 4B7 scFv-0 and scFv-20, respectively).

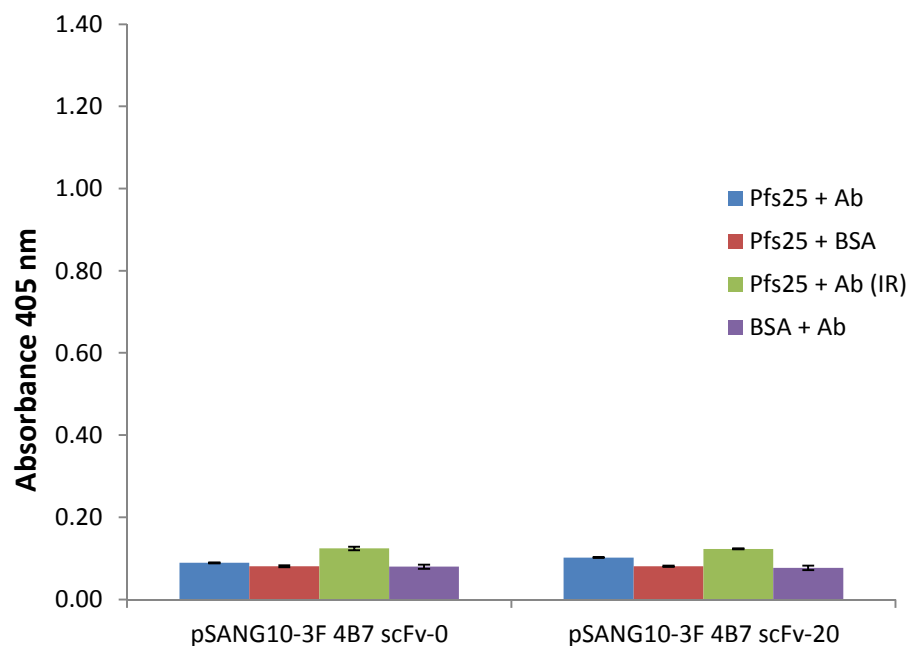


Figure 3.8: Specificity evaluation of 4B7 pSANG10-3F expressed scFv-0 and scFv-20 to Pfs25. Antigen was coated at 100ng per well and bound scFv detected with a rabbit anti-tri FLAG antibody (primary antibody) and goat anti-rabbit IgG-AP (secondary antibody). p-NPP was used as substrate and absorbance measured at 405 nm. The error bars indicate the standard errors of the means ($n = 3$). Ag: codes for Antigen, Ab: for Antibody and Ab (IR): for irrelevant or non-specific antibody (Pf-NPNA-1 scFv-0 and scFv-12 were used as controls for 4B7 scFv-0 and scFv-20, respectively).

Binding activity could not be established for the pSANG10-3F (Figure 3.8) and pBAK.1Hk (Figure 3.9) scFv proteins as the ELISA signals were very low. These results were not considered statistically significant. The Pf-NPNA-1 scFv and scFv-Hk used as controls had higher ELISA signal than the 4B7 scFvs. This was more evident when the Pf-NPNA-1 scFv-12Hk was probed with the goat anti-human kappa constant antibody.

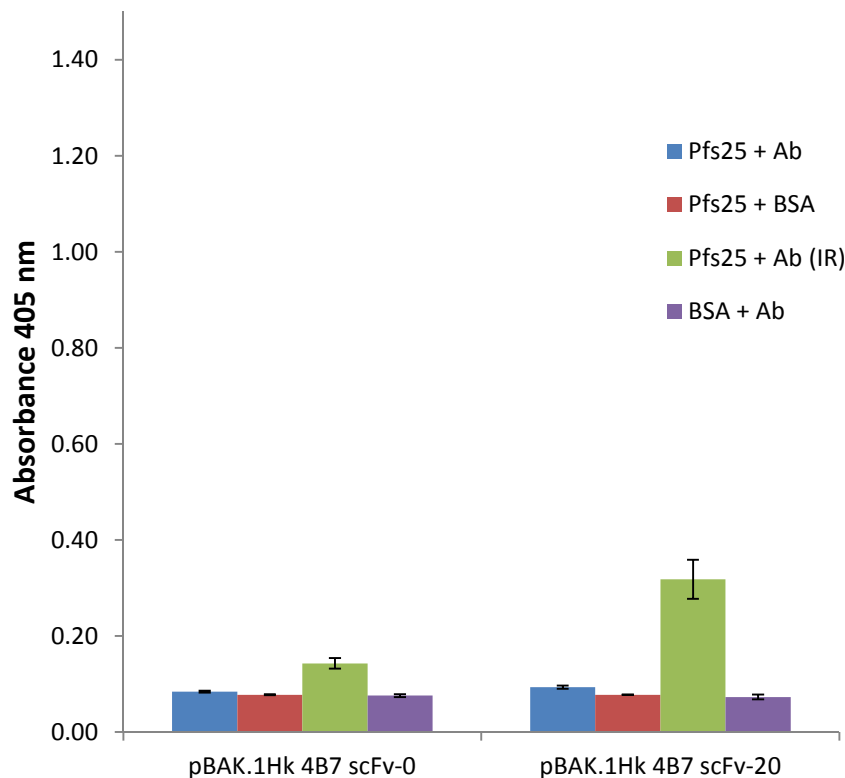


Figure 3.9: Specificity of soluble 4B7 scFv-0 and scFv-20 expressed from pBAK.1Hk to Pfs25. Antigen was coated at 100ng per well and bound scFv-Hk detected with monoclonal goat anti-Human kappa light chains (bound and free) –AP antibody. p-NPP was used as substrate and absorbance measured at 405 nm. The error bars indicate the standard errors of the means ($n = 3$). Ag: codes for Antigen, Ab: for Antibody and Ab (IR): for irrelevant or non-specific antibody (Pf-NPNA-1 scFv-0Hk and scFv-12Hk were used as controls for 4B7 scFv-0 and scFv-20, respectively).

3.2.4 Site directed mutagenesis of 4B7 (V_L - V_H) scFv-0 and scFv-20

Since no binding activity was observed for 4B7 scFv-0 and scFv-20 expressed from the two plasmids, the sequence was compared to another scFv sequence designated 4B7 (AJ) that was also obtained from the murine monoclonal antibody mAb 4B7. The previously expressed recombinant scFv designated 4B7 (AK) differed from 4B7 (AJ) by seven amino acids. There were four changes in the V_L FR (Q3E, I5T, L85F and G86V) and three in the V_H FR (Q18R, T92A and L114V).

Mutated Frame work residues	Effect
V _L Q3E; FR1	Conserved hydrophilic
V _L I5T; FR1	Hydrophobic → hydrophilic
V _L L85F; FR3	Conserved hydrophobic
V _L G86V; FR3	Hydrophilic → hydrophobic
V _H Q18R; FR1	Conserved hydrophilic
V _H T92A; FR3	Hydrophilic → hydrophobic
V _H L114V; FR4	Conserved hydrophobic

Table 3.1: Amino acid substitutions in FR of 4B7 scFv and properties of the substituted residues.

```

                                VLCDR1
4B7AK  MKYLLPTAAAGLLLLLAAQPAMADIQMTQSPSSMFASLGDRVSLSCRASQDIRGNLDFWFQQ
4B7AJ  MKYLLPTAAAGLLLLLAAQPAMADIEMTQSPSSMFASLGDRVSLSCRASQDIRGNLDFWFQQ
*****:*****

                                VLCDR2                                VLCDR3
4B7AK  KPGGTIKLLIYSTSNLNSGVPSRFRSGSGSGSDYSLTISSLESEDLGDIYCLQRNAYPLTF
4B7AJ  KPGGTIKLLIYSTSNLNSGVPSRFRSGSGSGSDYSLTISSLESEDFVDIYCLQRNAYPLTF
*****:*****

                                VHCDR1
4B7AK  GSGTKLEIKAEVKLVESGGGLVQPGGSKLSCAASGFTFSDYGMWFRQAPGKGPWFVAF
4B7AJ  GSGTKLEIKAEVKLVESGGGLVQPGGSKLSCAASGFTFSDYGMWFRQAPGKGPWFVAF
*****:*****

                                VHCDR2                                VHCDR3
4B7AK  INNLAYSIYYADTVTGRFTISRENAKNTLYLEMSSLRSEDITMYYCARGNLYYGLDYWGQ
4B7AJ  INNLAYSIYYADTVTGRFTISRENAKNTLYLEMSSLRSEDITMYYCARGNLYYGLDYWGQ
*****:*****

4B7AK  GTTLTVSSAAASAHHHHHKLDYKDHDGDYKDHDIDYKDDDDK
4B7AJ  GTTIVTVSSAAASAHHHHHKLDYKDHDGDYKDHDIDYKDDDDK
*****:*****

```

Figure 3.10: Amino acid sequence alignment of two variants of 4B7 scFv. Differences in amino acids are indicated in purple. The CDR sequences are in green. Sequences predicted to form hydrogen bonds with Pfs25 antigen during interaction are indicated in red.

Site directed mutagenesis was performed, using pSANG10-3F 4B7 scFv-0 in the V_L-V_H orientation as template. 4B7 scFv-20(AJ) was assembled as described (Section 2.3.3). The scFv-0(AJ) and 20(AJ) cassettes were cloned into the expression vectors pSANG10-3F and pBAK1.HK and expressed in BL21(DE3) pRARE cells. The expressed scFvs were purified by IMAC and purity assessed on a 12% SDS-PAGE gel (Figure 3.11A & B). As observed previously, higher molecular weight proteins (~66 kDa), a ~25 kDa *E. coli* protein and lower molecular weight proteins co-purified with the scFv-0 and scFv-20.

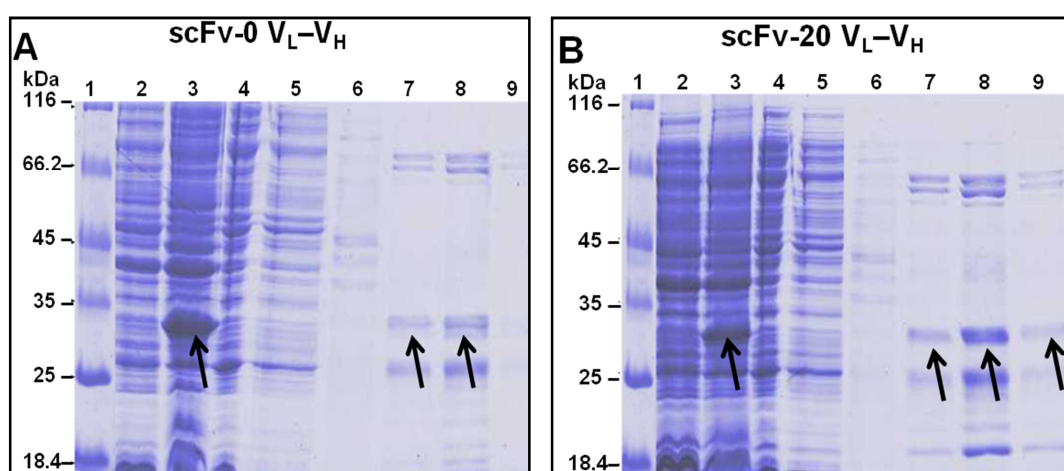


Figure 3.11: Expression and purification of 4B7 (AJ) scFv-0 and scFv-20 using pSANG10-3F plasmid. SDS-PAGE analyses under reducing conditions of Ni-NTA affinity purification of scFv-0 (**A**) and scFv-20 (**B**) respectively. 20 μ L of each purification fraction was loaded, electrophoresed on a 12% gel and stained with Coomassie Brilliant blue R-250. (**A** and **B**) Lane 1: molecular weight marker; Lane 2: uninduced cell pellets; Lane 3: induced cell pellet; Lane 4: crude periplasmic fraction; Lane 5: Ni column flow through; Lane 6: Ni column wash with 10 mM Imidazole; Lanes 7-9: elutions with 500 mM Imidazole.

Purified recombinant 4B7 scFv were also evaluated under non-reducing conditions (semi-native). Under reducing conditions only the monomeric forms of the proteins were observed on the Western blot (Figure 3.12, Lanes 2 and 3). However, under non-reducing conditions monomeric, dimeric and multimeric forms were observed for pSANG10-3F expressed 4B7 scFv-0 and 20 (Figure 3.12, Lanes 4 and 5). The dimeric protein had an apparent molecular mass of 60 kDa. The molecular mass of the multimeric form could not be estimated on the Western blot as it exceeded 260 kDa. The

electrophoretic mobility of each scFv under non-reducing conditions was faster than that of its corresponding scFvs under reducing conditions.

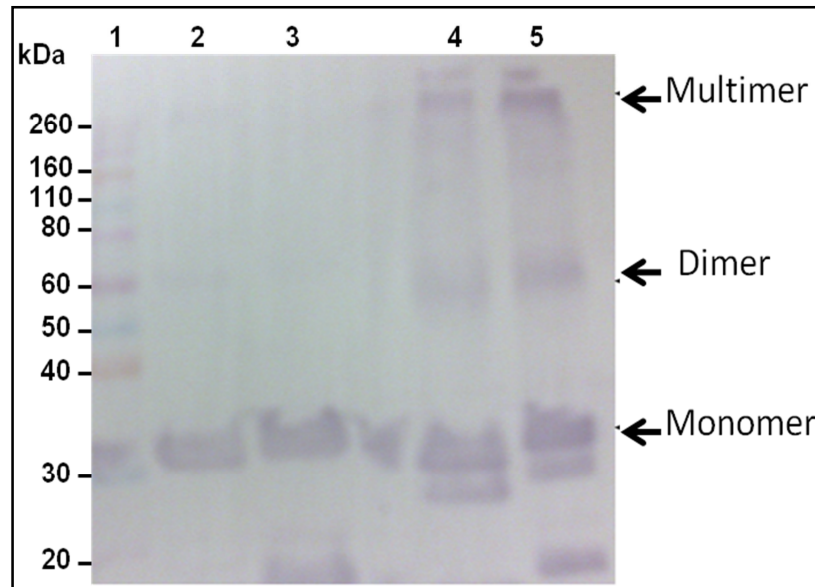


Figure 3.12: Western blot of IMAC purified proteins electrophoresed under reducing and non-reducing conditions. 20 μ L of each purification fraction was loaded, electrophoresed on a 12% gel at 4°C. Proteins were transferred onto PVDF membrane and were probed with rabbit anti-tri FLAG antibody as primary antibody and goat anti-rabbit IgG conjugated to alkaline phosphatase (AP) as secondary antibody. BCIP/NBT was used as substrate. Lane 1: molecular weight marker; Lane 2: IMAC purified scFv-0 under reducing conditions; Lane 3: IMAC purified scFv-20 under reducing conditions; Lane 4: IMAC purified scFv-0 under non-reducing conditions; Lane 5: IMAC purified scFv-20 under non-reducing conditions. Arrows indicate expressed recombinant proteins.

The spontaneous assembly of the scFv-0 and scFv-20 into multimeric assembly was further ascertained by size-exclusion chromatography (SEC). Prior to SEC the scFv-20, which showed higher level of expression, was subjected to anion exchange chromatography (AEC) (Figure 3.13) to obtain a homogenous product that will facilitate investigation of multimeric assembly. AEC was chosen based on the earlier determination of the pI of the expression protein. IMAC purified fraction 7 to 9 (Figure 3.11B) were pooled and applied on a 1 mL HiTrap Q sepharose column. Prior to application on the HiTrap column, the IMAC purified proteins were desalted with PBS to remove excess NaCl present in the elution buffer.

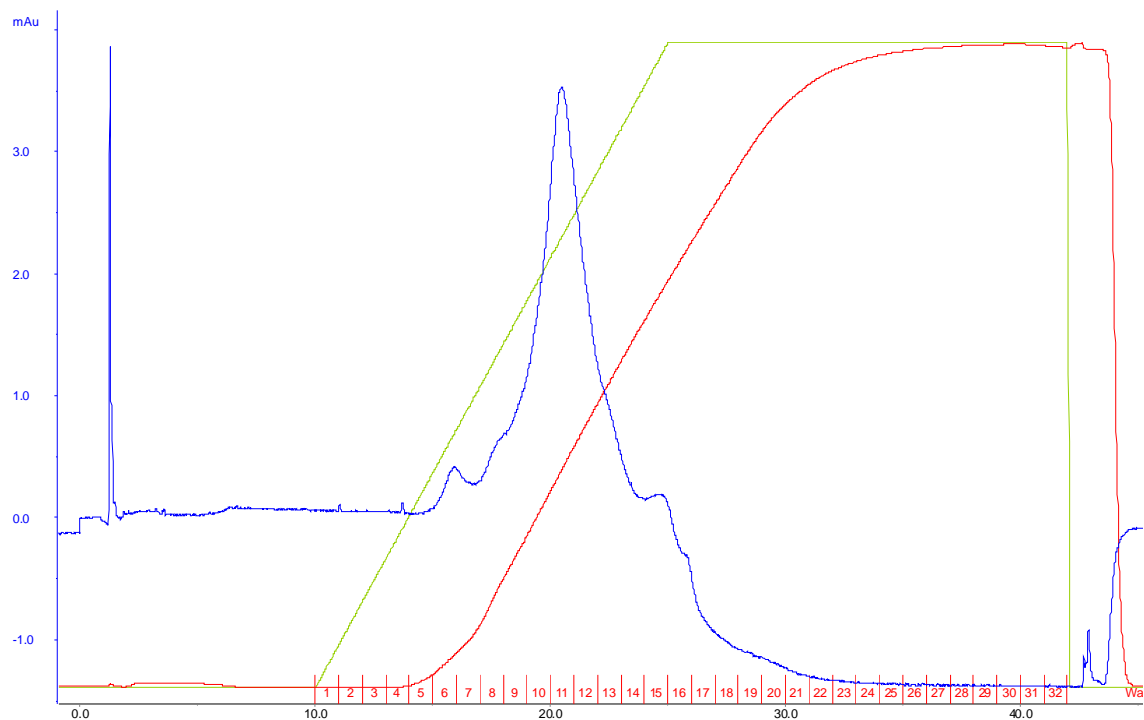


Figure 3.13: Anion exchange chromatography of 4B7 scFv-20 a 1 mL HiTrap Q Sepharose column. IMAC purified protein was applied to the column, the flow rate was 0.5 mL/min and the fractions collected at 1 mL intervals. The blue shows absorbance at 280 nm, the green line shows addition of buffer from 0 to 1M NaCl and the red line indicates the fractions collected. Peak fractions 10 -12 were collected for further analysis.

The peak fractions (10 to 12) were then analysed by SDS-PAGE to determine homogeneity of the proteins after AEC. Subsequently, the fractions were pooled, concentrated to 1 mL and applied to a Hi-Load 16/60 Superdex column pre-equilibrated with PBS and pre-calibrated with Sigma-Aldrich gel filtration standard proteins (cytochrome c, 12.4 kDa; carbonic anhydrase, 29 kDa; bovine serum albumin, 66 kDa and β -Amylase, 200 kDa). The major peaks of the scFv-20 showed a higher molecular mass protein (peak 1, ~50 min), a dimer (~66 kDa, 90min) and monomer (~33 kDa; 100 min) (Figure 3.14). Insufficient amount of material did not permit further investigation of these protein forms. Peaks 4 and 5 may indicate degraded proteins.

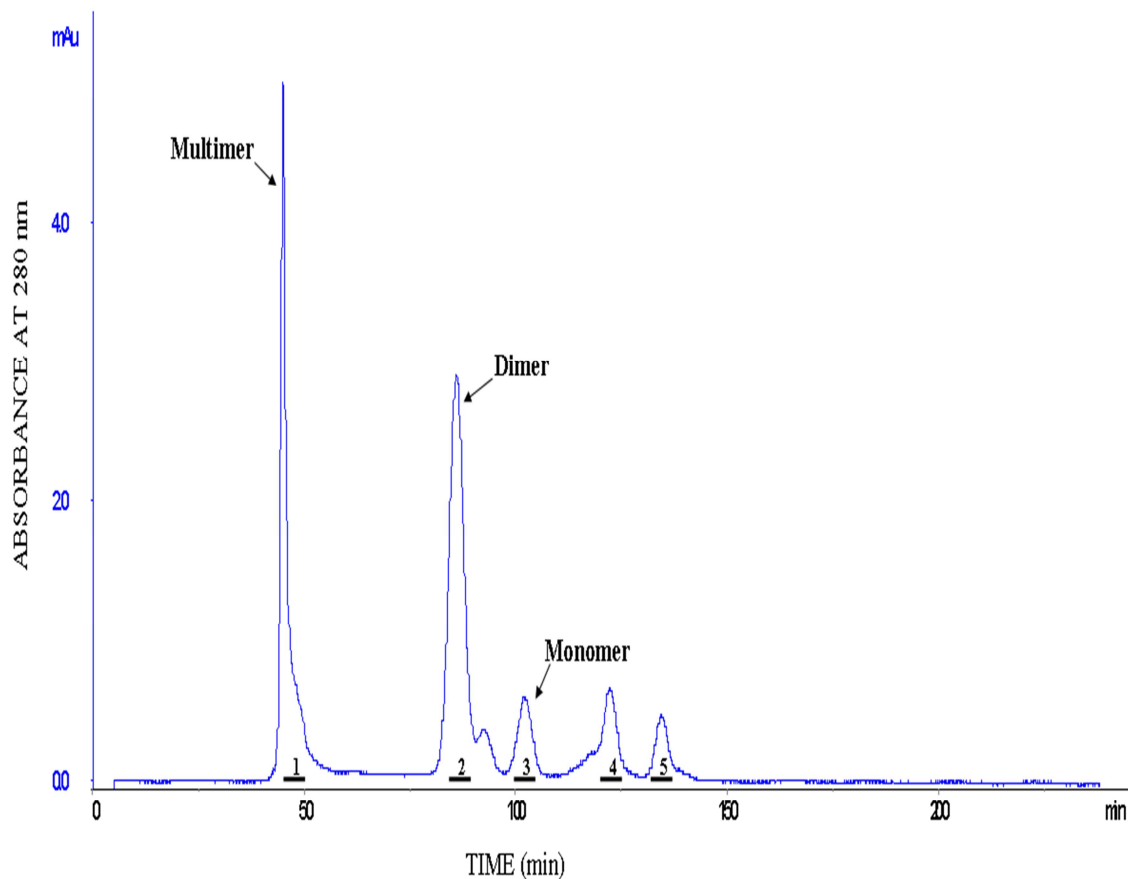


Figure 3.14: Size exclusion HPLC on a calibrated Hi-Load 16/60 Superdex column of purified 4B7 scFv-20. The V_L - V_H protein eluted as a monomer at 100.7 min and dimer at 90.6 mins. The elution times are consistent with the calculated molecular weight of 31.2 and 62.4 kDa. The column was equilibrated with 1X PBS (3.2 mM Na_2HPO_4 , 0.5 mM KH_2PO_4 , 1.3 mM KCl, 135 mM NaCl, pH 8.0), run at a flow rate of 1.0 ml/min. The high molecular mass multimer (peak 1), dimer (peak 2) and monomer (peak 3) were collected. Peaks 4 and 5 indicate degraded proteins.

To evaluate expression of the 4B7 (AJ) scFv fused to the human kappa constant domain, 4B7 (AJ) scFv-0 and scFv-20 gene fragments were cloned into pBAK.1Hk expression plasmid. Both constructs were expressed and purified under similar conditions as described earlier in sections 2.4.2 and 2.4.3, respectively. The scFv-0Hk was secreted with most of the expressed protein (38.4 kDa) retained in the cytoplasm (Figure 3.15A). On the other hand, scFv-20Hk (39.6 kDa) showed very high secretion level with less protein in the cytoplasm (Figure 3.16A). Both secreted proteins were subjected to SDS-PAGE under reducing and non-reducing conditions. The scFv-0Hk and scFv-20Hk both formed monomeric and multimeric forms (Figure 3.15B and 3.16B, respectively).

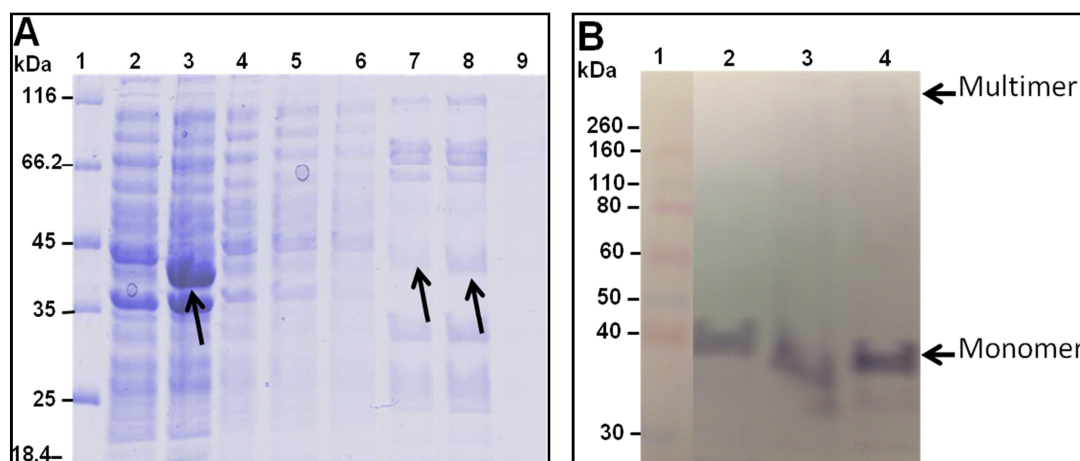


Figure 3.15: Expression and purification of 4B7 (AJ) scFv-0Hk. SDS-PAGE analyses of Ni-NTA affinity purification of scFv-0Hk (**A**) and Western blot (**B**) under reducing and non-reducing conditions, respectively. Proteins were probed with anti-Human kappa-AP antibody (1:30000). **20 μ L** of each purification fraction was loaded, electrophoresed on a 12% gel and stained with Coomassie Brilliant blue R-250. For Western blotting BCIP/NBT was used as substrate. (**A**) Lane 1: molecular weight marker; Lane 2: uninduced cell pellets; Lane 3: induced cell pellet; Lane 4: crude periplasmic fraction; Lane 5: Ni column flow through; Lane 6: Ni column wash with 10 mM Imidazole; Lanes 7-9: elutions with 500 mM Imidazole. (**B**) Lane 1: molecular weight marker; Lane 2: IMAC purified scFv-0Hk (panel **A** Lane 8) under reducing conditions; Lane 3 and 4: IMAC purified scFv-0Hk (panel **A** Lane 8) under non-reducing conditions.

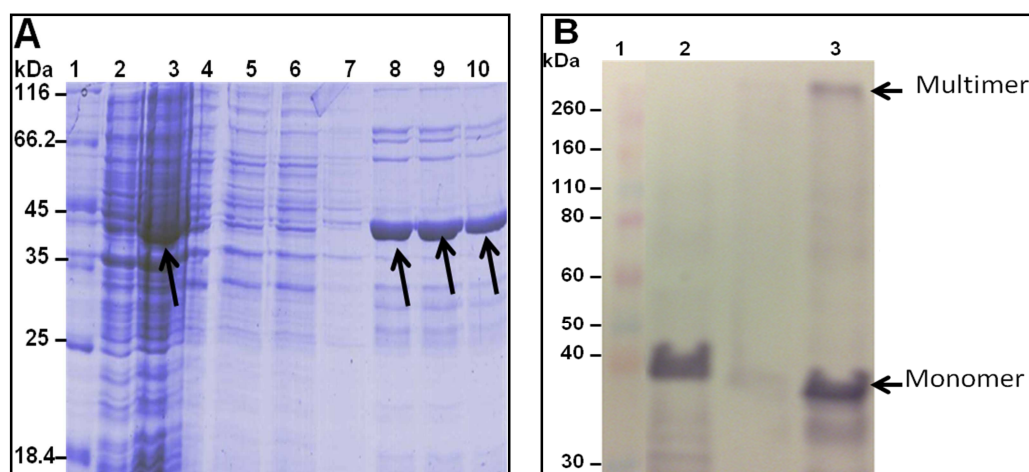


Figure 3.16: Expression and purification of 4B7 (AJ) scFv-20Hk. SDS-PAGE analyses of Ni-NTA affinity purification of scFv-20Hk (**A**) and Western blot (**B**) under reducing and non-reducing conditions, respectively. Proteins were probed with anti-Human kappa-AP antibody (1:30000). **20 μ L** of each purification fraction was loaded, electrophoresed on a 12% gel and stained with Coomassie Brilliant blue R-250. For Western blotting BCIP/NBT was used as substrate. (**A**) Lane 1: molecular weight marker; Lane 2: uninduced cell pellets; Lane 3: induced cell pellet; Lane 4: crude periplasmic fraction; Lane 5: Ni column flow through; Lane 6: Ni column wash with 10 mM Imidazole; Lanes 8-10: elutions with 500 mM Imidazole. (**B**) Lane 1: molecular weight marker; Lane 2: IMAC purified scFv-20Hk (panel **A** Lane 8) under reducing conditions; Lane 3: IMAC purified scFv-20Hk (panel **A** Lane 8) under non-reducing conditions.

3.2.5 ELISA of 4B7 (AJ) scFv-0 ($V_L - V_H$) and scFv-20 ($V_L - V_H$)

The binding activity of the pSANG10-3F and pBAK.1Hk expressed 4B7 (AJ) scFv-0 and scFv-20 were evaluated in an ELISA (Figure 3.17 and 3.18). The low signals obtained for both proteins could not suffice as binding to target antigen. However, the ELISA signal obtained for pSANG10-3F expressed 4B7 (AJ) scFv-0 was higher than that of scFv-20 and does not correlate with the level of expression of both scFvs. The differences in binding to the scFvs to Pfs25 and BSA were considered statistically significant ($p < 0.001$).

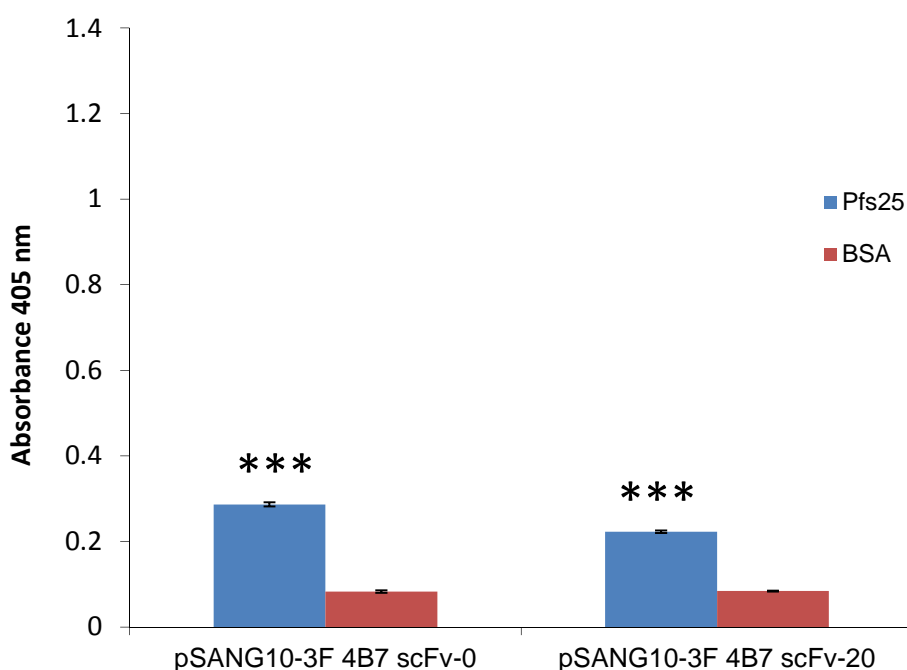


Figure 3.17: Specificity evaluation of 4B7 (AJ) pSANG10-3F expressed scFv-0 and scFv-20 to Pfs25. Antigen was coated at 100ng per well and bound scFv detected with a rabbit anti-tri FLAG antibody (primary antibody) and mouse anti-rabbit IgG-AP (secondary antibody). BSA was used as a negative control. p-NPP was used as substrate and absorbance measured at 405 nm. The error bars indicate the standard errors of the means triplicate well for two independent studies. Asterisk denotes statistical significance (triple asterisk denotes $p < 0.001$; paired t test)

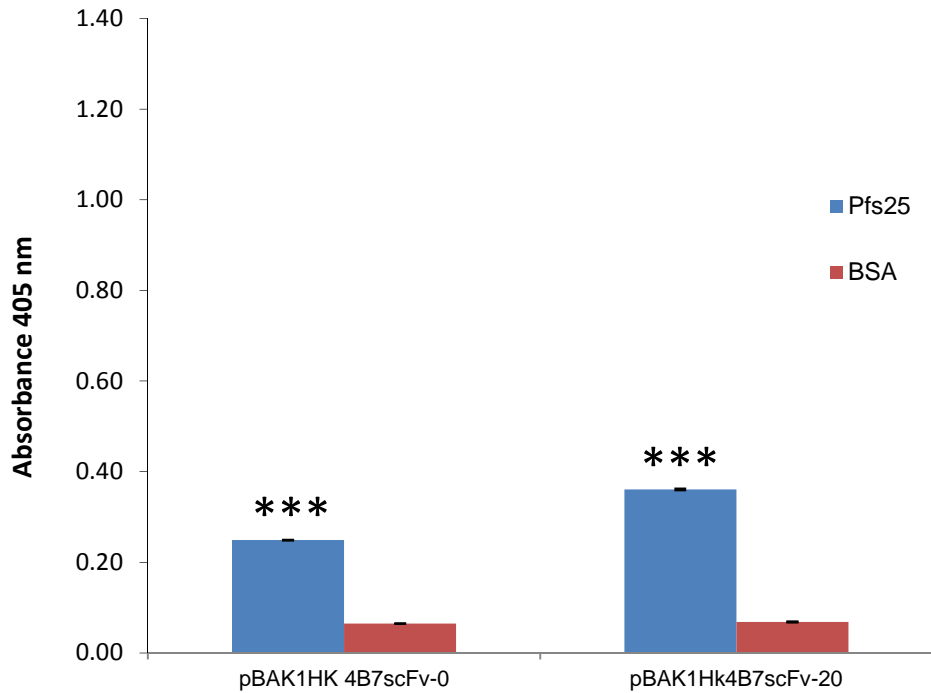


Figure 3.18: Specificity of soluble 4B7 (AJ) scFv-0 and scFv-20 expressed from pBAK.1Hk to Pfs25. Antigen was coated at 100ng per well and bound scFv-Hk detected with monoclonal goat anti-Human kappa light chains (bound and free) –AP antibody. p-NPP was used as substrate and absorbance measured at 405 nm. The error bars indicate the standard errors of the means of triplicate well for two independent studies. Asterisk denotes statistical significance (triple asterisk denotes $p < 0.001$; paired t test)

3.3 Discussion on expression and characterisation of 4B7 scFv

This section deals with three of the four objectives of this study, which are the characterisation of the scFv antibodies 4B7 and Pf-NPNa-1. Chapter two (section 2.3.3) describes the cloning and expression of the murine monoclonal antibody 4B7, that recognises the Pfs25 sexual stage protein expressed on the surface of ookinetes. The V_H and the V_L domains from the Fab antibody 4B7 originally isolated from hybridoma cells were used as the building blocks to construct the scFv 4B7 (Appendix, Figure II). However, bioinformatic analysis showed the presence of rare codons, which can impede prokaryotic expression, in the DNA sequence of 4B7. To address this problem, the sequence was codon optimised for expression in *E. coli*. Two scFv formats, $V_H - V_L$ or $V_L - V_H$ orientations of which the former is more common, were constructed in this study. Some studies have demonstrated the superiority, in terms of higher yields of soluble protein (Desplancq *et al.*, 1994; Tsumoto *et al.*, 1994; Ayala *et al.*, 1995; Hamilton *et al.*, 2001; Albrecht *et al.*, 2006) and higher binding characteristics (Lu *et al.*, 2004), of the $V_L - V_H$ orientation. Conversely, other studies have shown that the relative orientations of the V_H and V_L have no effect on the expression level but the $V_L - V_H$ orientation nearly abolished antigen binding (Albrecht *et al.*, 2006). Due to the variations in expression levels of the different scFv fragments cited, it has been suggested that the orientation of the V_H and V_L domains that results in optimum expression must be investigated for each fragment (Hu *et al.*, 2005). Hence, two versions of 4B7 scFv were generated in the $V_H - V_L$ or $V_L - V_H$ orientation to test the effect of domain order on expression and secretion. The scFv constructs were then expressed in *E. coli* and purified from periplasmic extracts by affinity chromatography. The V domain orientation had a significant effect on the secretion of the antibody into the periplasmic space of the bacterium. Although both scFv formats were expressed in the cytoplasm, periplasmic secretion was only detected for the scFv $V_L - V_H$ format (Section 3.2.2; Figure 3.6 A&B).

Using the pET-based vectors, to facilitate periplasmic secretion, the scFv 4B7 was initially expressed in the $V_H - V_L$ orientation, which upon investigation

showed barely detectable levels in *E. coli* (Figure 3.5). The expressed scFv was retained in the cytoplasm, suggesting its association with the bacterial membrane. Efforts were then directed into isolation and refolding of inclusion bodies. However, the refolded inclusion bodies showed no antigen binding. Lack of secretion of scFvs into the periplasm, due to association with the bacterial inner membrane, has been reported in numerous studies (Pantoliano *et al.*, 1991; Malby *et al.*, 1993; Ayala *et al.*, 1995). The lack of secretion of the anti-fluorescyl scFv 4.4.20 was attributed to the presence of charged residues within the amino terminus of the mature V_H domain (Pantoliano *et al.*, 1991). Malby *et al.* (1993) attributed the membrane association of the NC10 antibody to the presence of two lysines (positions 11 and 21) and an arginine (position 17). Ayala *et al.* (1995) also had a similar problem with the scFv CB-Hep.1 due to the presence of two lysines at position 3 and 19 and an arginine at position 16. The 4B7 scFv ($V_H - V_L$) used in this study has two lysines at positions 3 and 19 in its V_H . The presence of these residues may have disrupted the correct processing of the signal peptide and thus preventing the translocation of the protein into the periplasm. Three main mechanisms have been hypothesized to explain the membrane association effect: interaction of the positively charged amino acids with membrane phospholipids, translocation impairment due to increase pKa and incorrect positioning of the signal peptide sequence (Li *et al.*, 1988; Boyd and Beckwith, 1989; Ayala *et al.*, 1995). In the case of other proteins, membrane association has been attributed to the presence of positively charged amino acids, such as arginine and lysine, 20-30 residues downstream of the signal sequence (Li *et al.*, 1988; Boyd and Beckwith, 1989; Summers *et al.*, 1989; Kajava *et al.*, 2000). Li *et al.* (1988) reported a 50-fold decrease in protein translocation to the periplasm when amino acids arginine and glutamic acid at the N-terminal of the mature sequence of alkaline phosphatase were mutated to two arginines.

The presence of other charged residues, such as glutamate (E) and glutamine (Q) should be taken into consideration during bacterial expression of scFvs (Benhar and Pastan, 1995; de Haard *et al.*, 1998). These amino acid residues, which are mainly present in the framework regions, may give rise to an altered specificity or affinity of the antibody to its antigen by altering the

conformation of the CDR loops (McCartney *et al.*, 1995). The residues may also affect the yield and stability of the antibody (Johnson and Bird, 1991; Soderlind *et al.*, 1992; Kipriyanov *et al.*, 1997; de Haard *et al.*, 1998). The parent mAb 4B7 was isolated from hybridoma cell lines and the N-terminal sequences of the variable domains determined by N-terminal sequencing. However, only the first five amino acids (EVKLV) of the heavy chain and seven (DIQMIQS) of the light chain were obtained by N-terminal amino acid sequencing. The sixth amino acid of the V_H obtained by PCR was glutamate (E) (Stura *et al.*, 1994a). The presence of such a residue in the N-terminus of the scFv 4B7 in the V_H - V_L orientation may have impeded correct processing of the signal peptide and subsequent translocation of the expressed protein into the periplasm. A detailed search of the literature and Kabat database revealed that 45% of mouse V_H sequences have E at position 6, whereas 55% have Q at this position (Kabat and Wu, 1991; Kabat *et al.*, 1991). Thus, position 6 of V_H FR1 (H6) could be occupied by either a glutamate (E) or a glutamine (Q), which is buried and conserved within the immunoglobulin variable domain (Langedijk *et al.*, 1998; Honegger and Pluckthun, 2001). Although glutamate at this position of mAb 4B7 may be an inherent property of subgroup IIIA antibodies, previously determined by Stura *et al.* (1994a) by comparison with sequences in the Kabat database, its presence instead of Q in some bacterially expressed scFvs has resulted in drastic reduction in production yield, instability and loss of binding of the recombinant scFv to its antigen (McCartney *et al.*, 1995; Kipriyanov *et al.*, 1997; de Haard *et al.*, 1998; Li *et al.*, 2000a).

In the study of deHaard *et al.* (1998) antigen binding activity was restored by replacing E (introduced by PCR) with Q, which is well conserved in subgroup IIA to which the V_H of the anti-human chorionic gonadotropin belongs. Not only did the presence of E at this position affect the affinity of the antibody but also the level of bacterial expression. The restoration of the amino acid (E) to Q led to a 30-fold increase in the soluble OKT3 derived scFv (V_H subgroup IIA) (Kipriyanov *et al.*, 1997). This substitution led to a significant increase in the stability of the scFv but had no effect on its binding to CD3 antigen. Significant stabilisation and refolding yield (more than 10 fold) was also

observed for Tras-SE, a scFv derived from the murine monoclonal antibody 03/01/01 directed against the musk odorant traseolide (6-acetyl-1-isopropyl-2,3,3,5-tetramethyl-indane), when Q-H6 was restored (Langedijk *et al.*, 1998). In the case of the scFv and Fab fragment derived from the murine anti-gastric cancer mAb 3H11 (V_H subgroup IIB), the presence of E in the FR1 of V_H6 resulted in loss of antigen binding activity but had no effect on expression (Li *et al.*, 2000a; Li *et al.*, 2000b). Conversely, other studies have shown no effect on the properties of antibodies with E present in the V_H FR1 (Froyen *et al.*, 1995; Brégère *et al.*, 1997). Brégère *et al.* (1997) had contrasting results with the murine antibodies mAb19 (V_H subgroup IIB) and mAb93 (V_H subgroups VA, IIB or IIA) directed against the TrpB₂ subunit of *E. coli* tryptophan synthase. Substitution of the V_H -Q6 residue with E, introduced by the degeneracy of the primers, resulted in decreased affinity for TrpB₂ and increased degradation of the mAb93. However, the properties of the mAb19 were not affected by this change. In the case of Froyen *et al.* (1995), no functional (binding and neutralising) differences were observed between the scFvs D9D10 and D9D10N, derived from the same mouse anti-human interferon-gamma antibody D9D10, although they differed by three amino acids in the V_H (E in position 6 of D9D10) and three in the V_L (E in position 3 of D9D10). The variable domain sequences of D9D10 were obtained by PCR and that of D9D10N by traditional cDNA synthesis.

It is clear from the above studies that E in the V_H may be the natural sequence of a particular antibody subtype and its presence may or may not affect the properties of the antibody. This particular residue is, however, absent in the V_L FR1 of scFv 4B7. According to Spada *et al.* (1998) QV_L6 in lamda and kappa variable light chain domains is highly conserved as the cysteine residues in immunoglobulin domains (Spada *et al.*, 1998). Since it has suggested that the folding problems of scFv antibodies can be associated with the V_H (Knappik and Pluckthun, 1995) and the V_L of antibodies can act as a chaperone in the folding of the V_H (Freund *et al.*, 1996), the scFv orientation of 4B7 was changed to a V_L - V_H format (position 6 of the scFv 4B7 V_L is occupied by Q). In this study, switching of the scFv domain to a V_L - V_H format resulted in secretion of the expressed protein into the periplasm (Figure 3.6 A&B)

although three arginine residues (positions 18, 24 and 30) are located in the variable light chain domain. By changing the scFv orientation, Ayala *et al.* (1995) observed substantial improvement in the secretion of their scFv. Improvements in expression yields have also been observed in other studies when the scFv orientation was changed to a V_L - V_H format (Tsumoto *et al.*, 1994; Hamilton *et al.*, 2001). Hamilton *et al.* (2001) observed a 150% improvement in the expression level upon reversal of the variable domain orientation. In the case of anti-lysozyme scFv HyHEL10, Tsumoto *et al.* (1994) observed a higher level of expression of the V_L - V_H format compared to the V_H - V_L . High level expression of both formats of the scFv HyHEL10 were only observed after expression of the scFvs in an *E. coli* cell-free expression system that was supplemented with reduced and oxidized glutathione, protein disulfide isomerase (PDI), and chaperones (Merk *et al.*, 1999).

3.3.2 Site-directed mutagenesis of scFv 4B7 framework residues

The work presented in this thesis showed that although reversal of the 4B7 scFv orientation to a V_L - V_H format resulted in secretion, antigen binding activity could not be determined. Subsequently, sequence alignment the scFv 4B7 with that of another mAb, isolated from the same hybridoma cell line, designated 4B7 (AJ) showed seven differences (4 in FR of V_L and 3 in FR of V_H , Table 3.1) in their amino acid sequences. These amino acid differences were only identified in the framework residues (Figure 3.12). Framework residues, which form the conserved β -sheet framework of immunoglobulin domains, have been known to play a part in maintaining the conformation of the CDR loops (Chothia *et al.*, 1992) and in determining the protein structure and stability (Chowdhury *et al.*, 1998). Studies have shown that FR residues that interact with CDR residues can affect the antigen binding by altering the conformation of the CDR loops (Kettleborough *et al.*, 1991; Foote and Winter, 1992; Lavoie *et al.*, 1992; Xiang *et al.*, 1995). To improve the binding characteristics of an antibody two main approaches may be used: CDR grafting and directed evolution. The latter approach was chosen and site-directed mutagenesis was performed at the seven FR positions (V_L : Q3E, I5T,

L85F, G86V and V_H: Q18R, T92A, L114V) to evaluate any influence these residues may have on binding activity. The additive rather than the individual effects of these residues on secretion and antigen binding was investigated. Although substitutions in the CDRs have been shown to enhance affinity, it was considered important to maintain their canonical structures and rather mutate the framework residues. Replacement of the amino acids, which resulted in 4B7(AJ) scFv, did not lead to any dramatic alteration in antigen binding. Although both scFv variants were expressed, very little secretion was observed for scFv 4B7 compared to 4B7(AJ). With scFv 4B7 induced cells did not grow beyond the optical density at which induction was carried out. A likely explanation for this observation could be that the scFv 4B7 was toxic to the cells, which may lead to leakiness and eventual lysis of the cells. Knappik and Pluckthun (1995) identified beneficial framework residues that could affect cell physiology (cell growth and leakiness) during experimental analysis of two scFv antibodies that were 75% identical in the V_L and 78% in the V_H. (Knappik and Pluckthun, 1995). Based on the findings of Knappik and Pluckthun (1995), Forsberg *et al.* (1997) further showed the importance of the beneficial framework residues in preventing periplasmic leakiness, folding and yield of expressed protein (Forsberg *et al.*, 1997). However, none of the replacement residues were identified as beneficial residues when compared to the studies of Knappik and Pluckthun (1995) and Forsberg *et al.* (1997).

On the other hand, high secretion of the scFv 4B7(AJ) was observed on SDS-PAGE (Figure 3.11) and Western blot (Figure 3.12). Despite the high level of secretion very low antigen binding was observed (Figure 3.17 and 3.18). It is not known whether the changes made in the framework residues of the mutant 4B7 scFv had any effect on the expression level. However, it has been demonstrated that some framework residues play a key role in the CDR conformation (Krauss *et al.*, 2004). In the case of Krauss *et al.* (2004), alteration of the V_H-71Arg in FR3, considered a key determinant for the CDR-H1 and CDR-H2 structures, had a tremendous effect on the stability of the scFv huHMFG1. deHaard *et al.* (1999) also observed that the vernier zone residue 4 of the murine subgroup II kappa light chain plays a critical role in antigen recognition. However, none of the mutated framework residues of

scFv 4B7 can be considered as constituents of the 'Vernier' zone residues. Vernier residues, often located on the borders of the CDRs, comprise residues in the β -sheet framework that support the CDR loop structures. Although these residues are not in direct contact with the antigen they play an important role in fine tuning the antibody-antigen interaction (Foote and Winter, 1992).

As previously stated, Pfs25 consists of four epidermal growth factor-like domains that contain three putative N-linked glycosylation sites and 22 cysteine residues that form 11 disulphide bonds. The presence of these disulphide bonds presents difficulties during recombinant expression leading to production of heterogeneous molecules that lack correctly folded protein (Barr *et al.*, 1991; Kaslow and Shiloach, 1994; Stowers *et al.*, 2000; Zou *et al.*, 2003; Tsuboi *et al.*, 2008). Using wheat germ-cell free extracts Tsuboi *et al.* (2008) produced homogeneous recombinant Pfs25 that reacted with the anti-Pfs25 conformational dependent antibody 4B7. Pfs25 produced by this means was provided for use in ELISA. An oversight of this study was the inability to assess the binding of Pfs25. As a positive control the mAb 4B7, purified from mouse ascites, should have been used in the initial stages of this study to confirm antibody binding to recombinant Pfs25.

3.3.3 Assessment of 4B7 scFv-0 and 20 multimer formation

Monovalent binding of scFvs may limit their effectiveness and sensitivity during immunological applications such as ELISA. To provide increased avidity to target antigens, attention has focused on the design of linkers which generate multivalent scFv molecules (Iliades *et al.*, 1997; Kortt *et al.*, 1997). To achieve stable multimeric scFv molecules, the linker length joining the variable domains is shortened such that domain swapping occurs, in which the V_H is incapable of interacting with its adjoining V_L (Arndt *et al.*, 1998)(Arndt *et al.*, 1998). In this study, the different patterns of oligomerisation were investigated by constructing 4B7 scFv-0 and scFv-20. Unexpectedly, scFv-0 and scFv-20 both formed similar patterns of oligomerisation: monomer, dimer

and multimer under native conditions (native SDS-PAGE) (Figure 3.12) and by size exclusion chromatography (Figure 3.14). This observation contrasts previous studies which have shown the predominant species of scFv-0 antibodies to be trimers and tetramers. The oligomerisation of the scFv-20 was unexpected based on observations from previous studies (Holliger *et al.*, 1993; Desplancq *et al.*, 1994; Iliades *et al.*, 1997; Kortt *et al.*, 1997; Atwell *et al.*, 1999; Le Gall *et al.*, 1999; Dolezal *et al.*, 2000; Power *et al.*, 2003). This is in contrast with the general rule that monovalent forms of a scFv predominate when a linker length greater than 12 amino acids is used (Griffiths *et al.*, 1993; Kortt *et al.*, 1994; Whitlow *et al.*, 1994). On the other hand, linkers of 3 to 10 residues result in predominately dimeric forms whereas less than 3 residues results in the trimeric forms (Power *et al.*, 2003). Although similar patterns of multimeric assembly were observed for 4B7 scFv-0 and scFv-20, the scFv-20 showed increased expression level (Figure 3.11 A&B). The decrease in level of soluble affinity purified protein as the linker length was shortened was observed in Dolezal *et al.* (2000) investigation of the NC10 scFv.

Desplancq *et al.* (1994) observed only dimeric and monomeric forms of the tumor binding antibody B72.3 scFv-20 (V_L - V_H). The dimer-monomer formation by this antibody was concentration dependent. However, scFvs with less than 10 amino acids formed mainly dimers and oligomers. Although multimerisation results from non-covalent interactions, Desplancq *et al.* (1994) do not exclude the fact that the constraints posed on folding by the shorter linkers may lead to exposure of hydrophobic patches that are usually concealed within the immunoglobulin domain. In the case of Le Gall *et al.* (1999) the anti-CD19 (HD37) scFv-18 in the V_H - V_L orientation formed monomers, dimers and tetramers, whereas the scFv-0 formed trimers. When the anti-neuraminidase NC10 antibody was assembled in the scFv format, the scFv-15 (V_H - V_L or V_L - V_H) existed mainly as monomers. However, the NC10 scFv-0 (V_L - V_H) protein consisted of a mixture of tetramer (major component) and trimer (minor component) (Kortt *et al.*, 1994; Dolezal *et al.*, 2000). Similar oligomerisation patterns have been reported for the anti-sperm antibody, RASA, derived from the murine antibody S19 (Norton *et al.*, 2001). The RASA scFv-15 (V_H - V_L) consisted of monomer, dimer and trimers. The RASA scFv recognised the

human sperm agglutination antigen on Western blots and in indirect immunofluorescence assay.

3.3.4 Effect of HuCk on 4B7 scFv expression

The low periplasm yield of scFv antibodies have been attributed to aggregation prone intermediates of the unfolded polypeptide chain. This problem has been addressed by fusion of the scFv polypeptide to carrier proteins such as maltose-binding protein, alkaline phosphatase and human immunoglobulin-kappa constant domain (HuCk) (Hayhurst, 2000; Palmer *et al.*, 2006). This strategy is used as a means to improve the solubility and stability of heterologous proteins (Maynard *et al.*, 2000; Maynard *et al.*, 2002). To this end, the 4B7 scFv-0 and scFv-20 were fused to the HuCk in this study. Investigation of the expressed proteins revealed significant improvement in the total amount of protein detected and extracted from the periplasm of the scFv-20Hk (Figure 3.16). Enhanced secretion was also observed for a model scFv antibody (Appendix). The lower secretion of the scFv-0Hk (Figure 3.15) may be attributed to aggregation of the polypeptide within the cytoplasm before secretion commences. Aggregation may have occurred as a result of the close proximity of the variable domain brought about by the absence of a linker. It should be noted that the scFv-HuCk (V_L - V_H orientation) which showed improved expression level is in contrast to that of Hayhurst (2000) and McGregor *et al.* (1994), which are in the V_H - V_L orientation. This indicates that the improved expression, due to HuCk, is independent of scFv orientation.

The positive effects of HuCk on expression have been observed for other scFvs (Hayhurst, 2000; Maynard *et al.*, 2002; Palmer *et al.*, 2006) and single-chain $\alpha\beta$ T-receptors (Maynard *et al.*, 2005). However, the authors are of the view that the effect is dependent on the primary sequence of the scFv. Though speculative, the enhanced secretion by HuCk has been ascribed to effects on transcription, translation, mRNA structure and stability. In addition,

the HuCk may stabilise the scFv-HuCk fusion protein by shielding the hydrophobic residues on the surface of the scFv, thereby allowing a higher proportion of the expressed scFv to fold properly (Hayhurst, 2000; Maynard *et al.*, 2002; Palmer *et al.*, 2006). According to Hayhurst (2000), HuCk may also act as a ribosomal chaperone to prevent translational jamming, a consequence of the binding of hydrophobic residues of the scFv to the ribosome. Since transcription and translation are tightly coupled in bacteria, an increase in the translational activity may prevent the mRNA from degradation by exonucleases, resulting in further enhancement of translation (Sletta *et al.*, 2007).

The HuCk domain was added in an effort to increase the affinity, through avidity effects, of the 4B7 scFv. This investigation was undertaken as McGregor *et al.* (1994) found that the anti-herbicide atrazine scFv upon fusion to the HuCk domain existed in dimeric forms. However, the scFv-0Hk and scFv-20Hk both showed monomeric and multimeric forms (Figure 3.15B and 3.16B) in contrast to the study anti-herbicide atrazine scFv when fused to the kappa constant domain (McGregor *et al.*, 1994; Byrne *et al.*, 1996). In this study, the higher ordered oligomer could be due to an interaction between the variable domains and not the human kappa constant domain. On the other, the model scFv protein (Appendix) used in this study formed a monomer and dimer consistent with the study of McGregor *et al.* (1994).

Though an improvement in the expression level was observed no significant increase was observed in the antigen binding capacity of 4B7 scFv-HuCk (Figure 3.18) compared to its scFv counterpart (Figure 3.17). The scFv-0 and scFv-20 both showed slight antigen binding activity in ELISA. The ELISA signal obtained for pSANG10-3F expressed 4B7 (AJ) scFv-0 was slightly higher than that of scFv-20. A similar observation was made for scFv-0Hk and scFv-20Hk. These differences, based on expression levels, could be due to differences in protein concentration of the scFv and not due to avidity effects. Despite scFv-0 and scFv-20 showing similar oligomerisation patterns, the dimer and higher multimers may be exhibiting monovalent binding properties. Le Gall *et al.* (1999) reported monovalent binding of the anti-CD19 scFv-0

triabody. The authors attributed the monovalency to improper folding of the triabody which prevented formation of a trivalent molecule.

In summary, the 4B7 scFvs were easily expressed and secreted into *E. coli* periplasm after extensive bioinformatic analysis, domain swapping and application of site-directed mutagenesis. The secreted proteins formed monomers, dimers and higher multimeric forms. Fusion to HuCk also enhanced the secretion of recombinant protein into the periplasm. However, further investigation is required to enhance the affinity of this antibody to its target antigen.

3.4 Results for expression and characterisation of Pf-NPNA-1

3.4.1 Cloning, expression and purification of (NPNA)₉-MKC antigen

The (NPNA)₉-MKC (mouse kappa constant) gene sequence was synthesised as a pUC-57 insert, excised as *Nco*I and *Xho*I fragment and inserted into pBAK.1 digested with the same enzymes. The purified and sequenced pBAK.1- (NPNA)₉-MKC plasmid (Appendix) was transformed into *E. coli* BL21(DE3) cells and expressed as described in Section 2.4.1. The recombinant protein was purified from a 200 mL culture induced with 0.3 mM IPTG for 3 hours at 37°C using a HiTrap chelating 1 mL column (charged with Ni²⁺) connected to an ÄKTAprime plus purification system (GE Healthcare, UK). Bound protein was eluted with 500 mM imidazole. The elution profile of the antigen is shown in Figure 3.19.

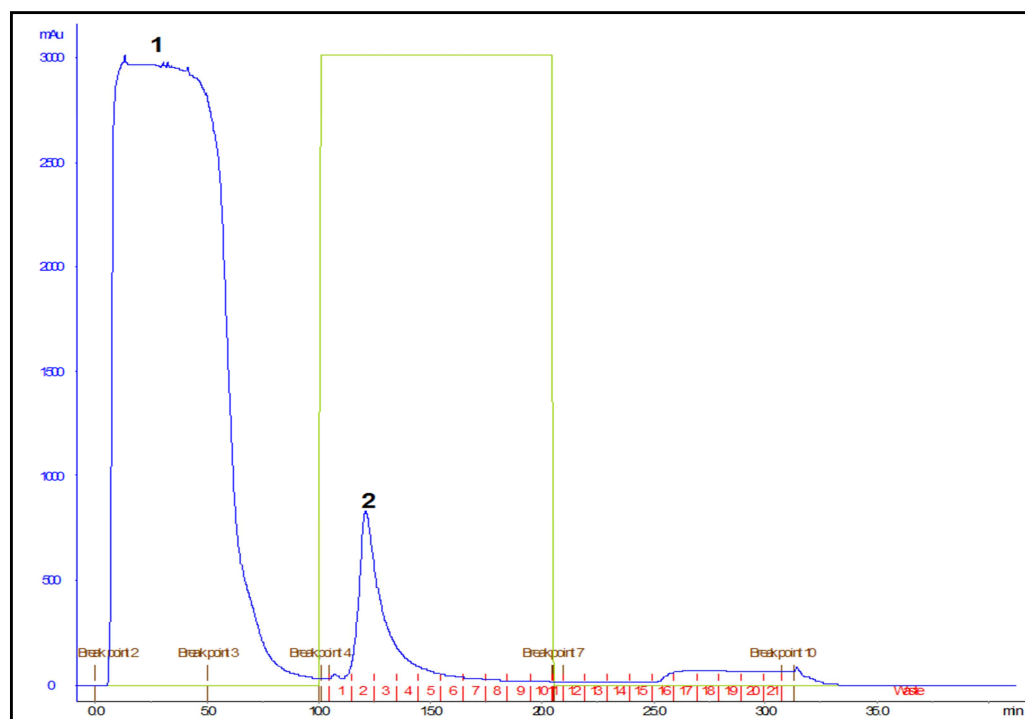


Figure 3.19: Ni-NTA purification of (NPNA)₉-MKC antigen. Crude lysate was loaded onto a 1 mL nickel resin at a flow rate of 1 mL/min and fractions were collected at 1 mL intervals. The blue line shows the absorbance at 280 nm, the green line shows addition of elution buffer and the fractions collected are shown in red. Peak 1 indicates unbound protein (flow through) and peak 2: bound proteins eluted with elution buffer (100 mM NaHPO₄, 500 mM NaCl, 500 mM Imidazole, pH 8).

The eluted fractions (1, 2, 3, 4) from peak 2 were analysed by SDS-PAGE. The predicted molecular weight of 20 kDa for the (NPNA)₉-MKC antigen was consistent with the protein bands observed on SDS-PAGE (Figure 3.20).

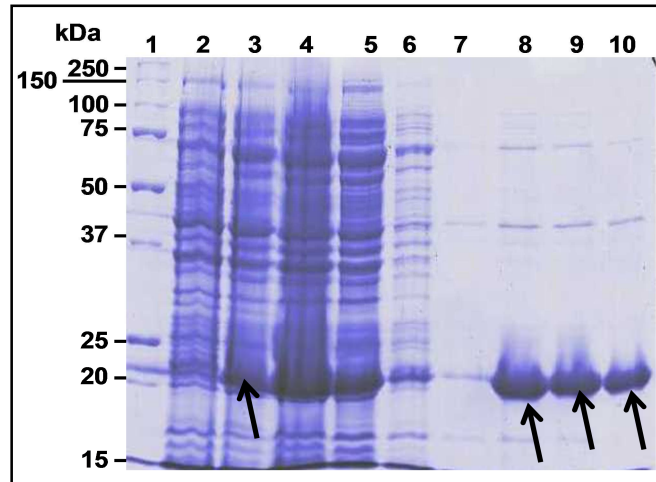


Figure 3.20: SDS-PAGE analysis of Ni-NTA affinity purified (NPNA)₉-MKC antigen from pBAK1. 10 μ L of each purification fraction was loaded and electrophoresed on a 12% gel and stained with Coomassie Brilliant blue R-250. Lane 1: molecular weight marker; Lane 2: uninduced cell pellets; Lane 3: induced cell pellet; Lane 4: crude lysate; Lane 5: Ni column flow through; Lane 6: Ni column wash with 10 mM Imidazole; Lanes 7-10: elutions with 500 mM Imidazole. Arrows indicate expressed recombinant proteins.

Protein concentration was estimated by using a Bradford assay with BSA as protein standard. The final protein concentration was estimated as 1.065 mg/ml. Secretion of the recombinant antigen into the periplasm was observed (data not shown).

3.4.2 Cloning of Pf-NPNA-1 scFv-12 V_H - V_L genes into pBAK.1 and pSANG10-3F

The Pf-NPNA-1 scFv-12 synthesised as a pUC-19 insert was subcloned into pBAK.1 and pSANG10-3F expression plasmids. Transformants were colony screened by PCR using T7 promoter and T7 terminator specific primers. Plasmids were purified and sequenced (Appendix) to ensure that the insert was in-frame.

The expression plasmids pBAK.1 Pf-NPNA-1 scFv-12 and pSANG10-3F Pf-NPNA-1 scFv-12 were transformed into *E. coli* BL21 (DE3) pRARE cells. Small scale expression in 50 mL LB induced with 0.3 mM IPTG was carried out. Periplasmic proteins were isolated and purified by IMAC. The expressed protein (cell pellet) and purified fractions were analysed by SDS-PAGE and Western blot. The blot was probed with monoclonal anti-His antibody as described in section 2.4.10.

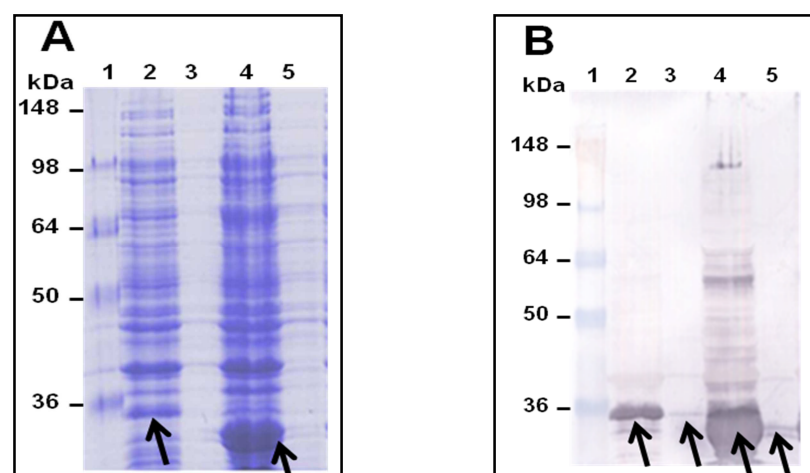


Figure 3.21: SDS-PAGE analysis under reducing conditions (A) and Western blotting (B) of small scale purification Pf-NPNA-1 V_H - V_L scFv-12 expressed from plasmids pSANG10-3F and pBAK1. 20 μ L of each fraction was loaded, electrophoresed on a 12% gel and stained with Coomassie Brilliant Blue R-250 (A) and a duplicate gel (B) transferred onto PVDF membrane and probed with monoclonal anti His-AP labelled antibody. Expressed recombinant proteins are indicated by the arrows. Lane 1: molecular weight markers, Lane 2: pSANG10-3F induced cell pellet, Lane 3: pSANG10-3F purified periplasmic extract, Lane 4: pBAK1 induced cell pellet, Lane 5: pBAK1 purified periplasmic extract.

The predicted molecular weight of the recombinant Pf-NPNA-1 scFv-12 was 27.2 kDa (from pBAK.1, Figure 3.21A) and 30.1 kDa (from pSANG10-3F, Figure 3.21A). Secretion of the recombinant protein from plasmids, pBAK.1 and pSANG10-3F, into the periplasmic space was observed on Western blot (Figure 3.21B).

3.4.3 Cloning of Pf-NPNA-1 scFv-0 V_H-V_L

A Pf-NPNA-1 scFv-0 (V_H-V_L) (Appendix) was generated in two PCR steps by using Pf-NPNA-1 scFv-12 as template. All PCR products were separated on a 1.5% agarose gel and gel purified. In the first step, the variable domains were amplified with the primers **NcoF** and **PfVHR** for V_H and **PfVLF** and **NotR** for V_L. The scFv-0 was then assembled by overlap extension PCR using gel purified V_H and V_L with the primers **NcoF** and **NotR**. The PCR product was gel purified, digested *NcoI* and *NotI* and subcloned into the pET-based vectors.

The Pf-NPNA-1 scFv-0 and scFv-12 gene inserts in the expression plasmids, pBAK.1, pSANG10-3F and pBAK.1Hk, were transformed into *E. coli* BL21 (DE) pRARE cells and recombinant protein expression evaluated. Protein expression was conducted as described in Section 2.4.2. Recombinant proteins isolated from the periplasm were purified in two stages: firstly, on a nickel agarose column and secondly by cation exchange chromatography. The protein fractions from the two purifications steps were analysed by SDS-PAGE and Western blot.

The predicted molecular weights of Pf-NPNA-1 scFv-0 (Figure 3.22A) and scFv-12 (Figure 3.22B) using plasmid pBAK.1 were estimated to be 27 (pI 8.64) and 27.7 kDa (pI 8.64), respectively. These were consistent with protein bands observed on SDS-PAGE. The level of expression of both scFv-0 and scFv-12 as observed on Western blot (Figure 3.23B) were the same; however, scFv-12 secretion into the periplasm was higher than that of scFv-0.

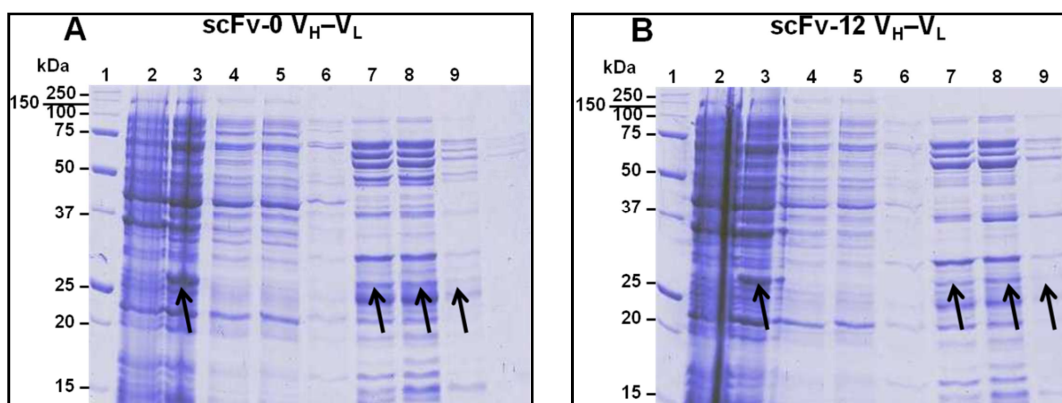


Figure 3.22: Expression and purification of Pf-NPNA-1 scFv-0 and 12 using pBAK.1 plasmid. SDS-PAGE analyses under reducing conditions of Ni-NTA affinity purification of scFv-0 (**A**) and scFv-12 (**B**) respectively. **20 μ L** of each purification fraction was loaded, electrophoresed on a 12% gel and stained with Coomassie Brilliant blue R-250. (**A** and **B**) Lane 1: molecular weight marker; Lane 2: uninduced cell pellets; Lane 3: induced cell pellet; Lane 4: crude periplasmic fraction; Lane 5: Ni column flow through; Lane 6: Ni column wash with 10 mM Imidazole; Lanes 7-9: elutions with 500 mM Imidazole.

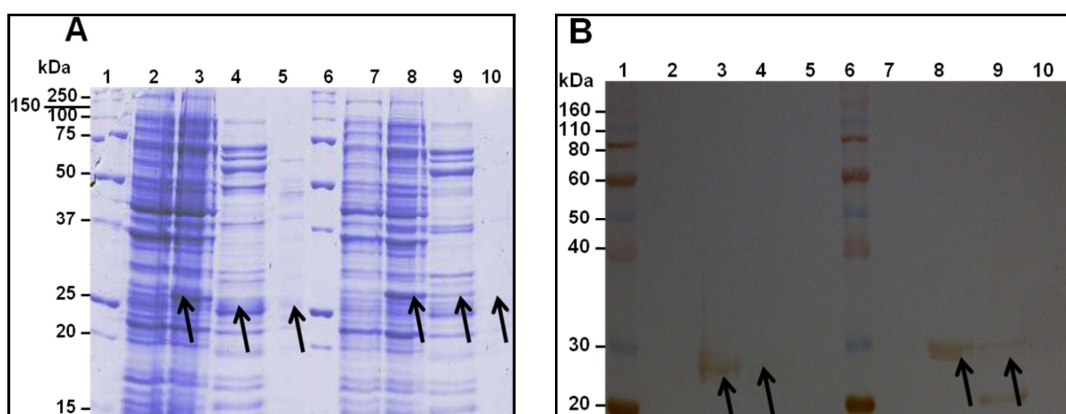


Figure 3.23: CEC of Pf-NPNA-1 scFv-0 and 12 using pBAK1 plasmid. SDS-PAGE analyses under reducing conditions of Ni-NTA affinity and CEC purification of scFv-0 and scFv-12 (**A**). (**B**) Western blot of duplicate gel of (**A**). **20 μ L** of each purification fraction was loaded and electrophoresed on a 12% gel. Proteins were probed with anti-His-HRP antibody. DAB was used as substrate. (**A** and **B**) Lane 1: molecular weight marker; Lane 2: scFv-0 uninduced cell pellets; Lane 3: scFv-0 induced cell pellet; Lane 4: IMAC purified scFv-0 (Figure 3.26A, Lane 8); Lane 5: CEC purified scFv-0; Lane 6: molecular weight marker; lane 7: scFv-12 uninduced cell pellets; Lane 8: scFv-12 induced cell pellet (panel **B**, Lane 3); Lane 9: IMAC purified scFv-12 (Figure 3.26B, Lane 8) Lane 10: CEC purified scFv-12. Arrows indicate expressed recombinant proteins.

Both scFvs were subjected to CEC and purity compared to IMAC purified proteins on SDS-PAGE (Figure 3.23A). However, no proteins were recovered from CEC as observed on Western blot (Figure 3.23B). Lane 4 (Figure 3.23B)

showed barely detectable levels for periplasmic expression of pBAK.1 Pf-NPNA-1 scFv-0. However, the IMAC purified protein sample showed binding activities in an ELISA (Figure 3.30). Degraded protein of the scFv-12 Pf-NPNA-1 was also observed (Figure 3.23B, Lane 9).

The molecular weights of Pf-NPNA-1 scFv-0 (Figure 3.24A) and scFv-12 (Figure 3.24B), using pSANG10-3F plasmid, on SDS-PAGE were consistent with the estimated values of 29.5 (pI 6.4) and 30.3 kDa (pI 6.4), respectively.

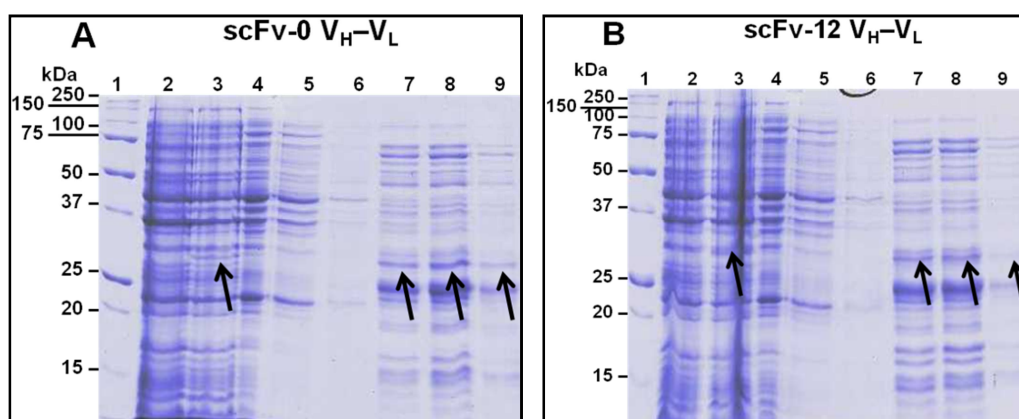


Figure 3.24: Expression and purification of Pf-NPNA-1 scFv-0 and 12 using pSANG10-3F plasmid. SDS-PAGE analyses under reducing conditions of Ni-NTA affinity purification of scFv-0Hk (A) and scFv-20Hk (B) respectively. 20 μ L of each purification fraction was loaded, electrophoresed on a 12% gel and stained with Coomassie Brilliant blue R-250. (A and B) Lane 1: molecular weight marker; Lane 2: uninduced cell pellets; Lane 3: induced cell pellet; Lane 4: crude periplasmic fraction; Lane 5: Ni column flow through; Lane 6: Ni column wash with 10 mM Imidazole; Lanes 7-9: elutions with 500 mM Imidazole.

The IMAC purified scFvs were then analysed under reducing and non-reducing conditions (Figure 3.25). Dimeric and multimeric forms of the scFvs were observed. It was more evident in the case of the scFv-12. Further confirmation of the multimeric patterns, by gel filtration, could not be carried out due to the low amount of protein purified from the periplasm. Functionality of the recombinant proteins were analysed in an ELISA (Figure 3.29).

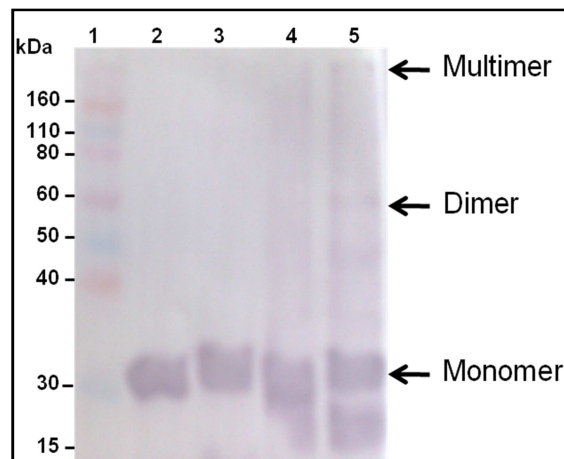


Figure 3.25: Western blot of expressed and purified Pf-NPNA-1 scFv-0 and scFv-12 using pSANG10-3F under reducing and non-reducing conditions. 20 μL of each purification fraction was loaded, electrophoresed on a 12% gel at 4°C. Proteins were transferred onto PVDF membrane and were probed with rabbit anti-tri FLAG antibody as primary antibody and goat anti-rabbit IgG conjugated to alkaline phosphatase (AP) as secondary antibody. BCIP/NBT was used as substrate. Lane 1: molecular weight marker; Lane 2: IMAC purified scFv-0 under reducing conditions; Lane 3: IMAC purified scFv-12 under reducing conditions; Lane 4: IMAC purified scFv-0 under non-reducing conditions; Lane 5: IMAC purified scFv-12 under non-reducing conditions. Arrows indicate expressed recombinant proteins.

The Pf-NPNA-1 scFv-0 and scFv-12 were also expressed in the pBAK.1Hk plasmid. The molecular weights observed on SDS-PAGE (Figure 3.26 A&B) were consistent with the predicted values of 37.5 (pI 8.62) and 38.2 kDa (pI 8.62) for scFv-0Hk and scFv-12Hk, respectively. The IMAC purified scFv-Hk proteins were further purified by CEC based on the pI. CEC purified proteins analysed on SDS-PAGE (Figure 3.27A) showed that they co-purified with an *E. coli* protein with an estimated size of 60 kDa and a lower molecular weight of about 27 kDa. Both the IMAC and CEC purified proteins were observed as doublets. The purified proteins were analysed on a Western blot (Figure 3.27B) and ELISA (Figure 3.28 and 3.31). Degraded protein, equivalent to the molecular weight of a scFv-12, was observed on the western blot (Figure 3.31, Lanes 9 & 10). This was absent for the scFv-0Hk.

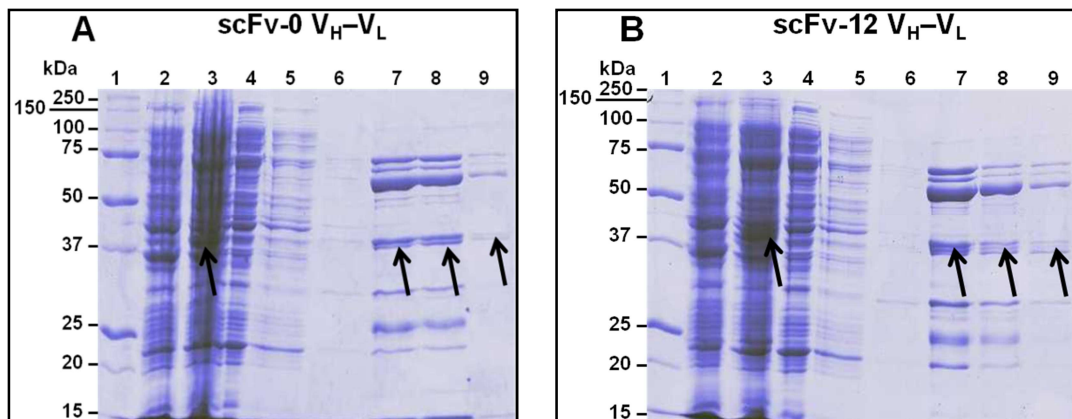


Figure 3.26: Expression and purification of Pf-NPNA-1 scFv-0 and 12 using pBAK.1Hk plasmid. SDS-PAGE analyses under reducing conditions of Ni-NTA affinity purification of scFv-0Hk (**A**) and scFv-12Hk (**B**) respectively. **20 μ L** of each purification fraction was loaded, electrophoresed on a 12% gel and stained with Coomassie Brilliant blue R-250. (**A** and **B**) Lane 1: molecular weight marker; Lane 2: uninduced cell pellets; Lane 3: induced cell pellet; Lane 4: crude periplasmic fraction; Lane 5: Ni column flow through; Lane 6: Ni column wash with 10 mM Imidazole; Lanes 7-9: elutions with 500 mM Imidazole.

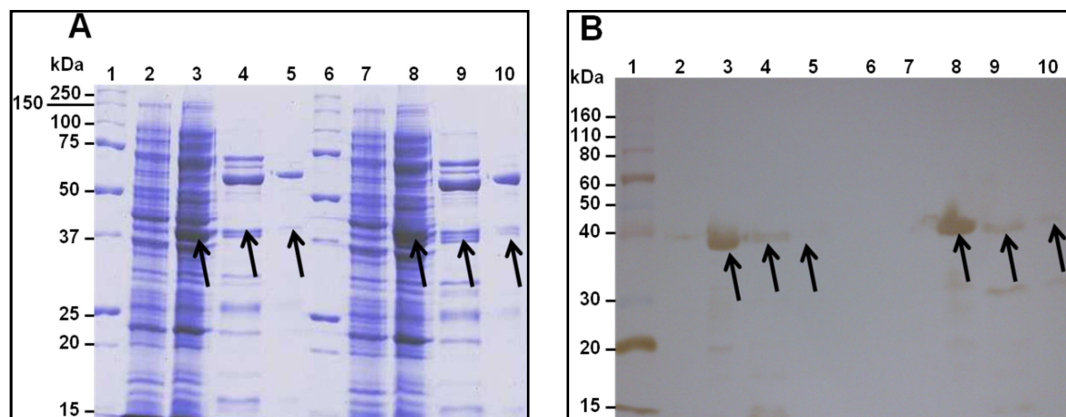


Figure 3.27: CEC of Pf-NPNA-1 scFv-0 and 12 using pBAK.1Hk plasmid. SDS-PAGE analyses of Ni-NTA affinity and CEC purification of scFv-0Hk and scFv-12Hk (**A**). (**B**) Western blot of duplicate gel of (**A**). **20 μ L** of each purification fraction was loaded and electrophoresed on a 12% gel. Proteins were probed with anti-His-HRP antibody. DAB was used as substrate. (**A** and **B**) Lane 1: molecular weight marker; Lane 2: scFv-0Hk uninduced cell pellets; Lane 3: scFv-0Hk induced cell pellet; Lane 4: IMAC purified scFv-0Hk (Figure 3.30A Lane 8); Lane 5: CEC purified scFv-0Hk; Lane 6: blank well; lane 7: scFv-12 uninduced cell pellets; Lane 8: scFv-12Hk induced cell pellet (panel **B**, Lane 3); Lane 9: IMAC purified scFv-12Hk (Figure 3.30B, Lane 8) Lane 10: CEC purified scFv-12. Arrows indicate expressed recombinant proteins.

3.4.4 ELISA for functional analyses of Pf-NPNA-1 scFv-0 and scFv-12

The binding activities and specificities of the pBAK.1, pSANG10-3F and pBAK.1Hk Pf-NPNA-1 scFv-0 and scFv-12 purified proteins to the Ni-NTA purified (NPNA)₉-MKC antigen and Woodchuck Hepatitis core antigen (WHcAg) containing the *P. falciparum* sporozoite major repeat motif [NANPNVDP(NANP)₃] peptide antigen were evaluated in ELISA as described in Section 2.4.11. Dilutions of the scFv proteins were carried out with 1% BSA in PBST (0.1% Tween-20). PBST (0.05% Tween-20) was included in the washing steps to prevent non-specific binding. Negative controls were also incorporated in the ELISA to further demonstrate the specificity of the Pf-NPNA-1 scFv-0 and scFv-12 to (NPNA)₉-MKC and WHcAg. The negative controls were BSA (1% w/v) and 4B7 scFv (scFv-0 and scFv-20 used as controls for Pf-NPNA-1 scFv-0 and 12, respectively).

Initial ELISA studies (Figure 3.28) were evaluated with the (NPNA)₉-MKC antigen using Pf-NPNA-1 scFv-0 and scFv-12 protein samples expressed from the vector pBAK.1HK. The scFv-Hk fusion proteins were then probed with goat anti-Human kappa light chains (bound and free)-AP antibody since both fusion proteins and the antigen bear C-terminal His-tags. The ELISA data of Pf-NPNA-1 scFv-0Hk was in agreement with the level of protein expression observed on both SDS-PAGE and Western blot. A low signal was detected for the scFv-0Hk in comparison to that of scFv-12Hk. The scFv-12Hk, on the other hand, showed specificity to the repeat motif on the (NPNA)₉-MKC antigen. Statistical significance of the ELISA data was calculated with GraphPad software using the paired t test.

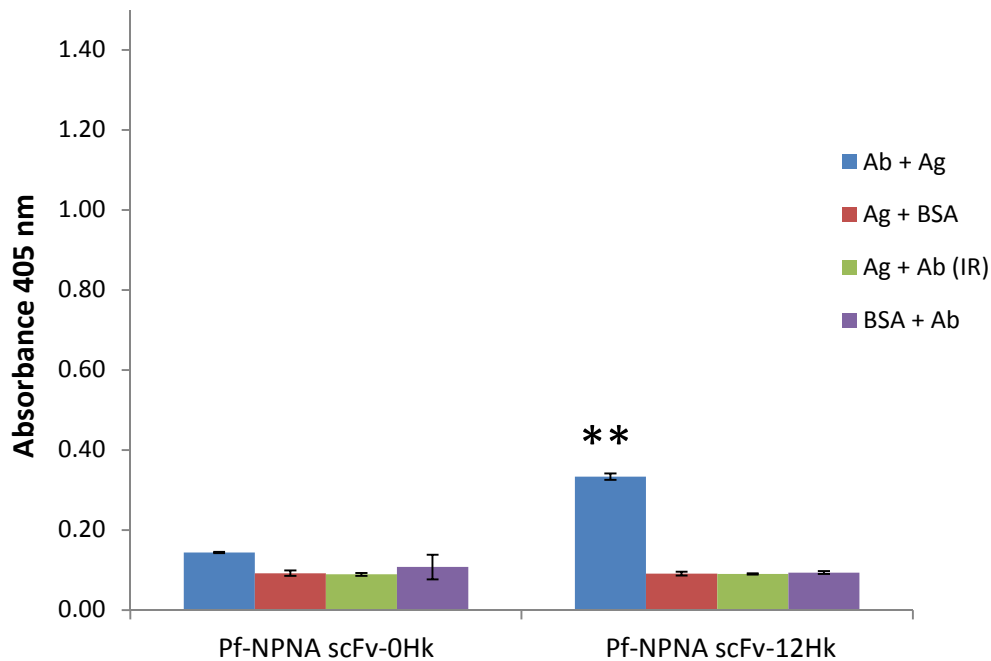


Figure 3.28: Specificity of soluble Pf-NPNA-1 scFv-0 and scFv-12 expressed from pBAK.1Hk to (NPNA)₉-MKC. Antigen was coated at 1µg per well and bound scFv-Hk detected with monoclonal goat anti-Human kappa light chains (bound and free) –AP antibody. p-NPP was used as substrate and absorbance measured at 405 nm. The error bars indicate the standard errors of the means ($n = 3$). Asterisk denotes statistical significance (double asterisk denotes $p < 0.01$; paired t test). Ag: codes for Antigen, Ab: for Antibody and Ab (IR): for irrelevant or non-specific antibody (4B7 scFv-0 and scFv-20).

Subsequently, the pSANG10-3F, pBAK.1 and pBAK.1Hk expressed and purified Pf-NPNA-1 scFv-0 and scFv-12 proteins were evaluated in ELISA using WHcAg (Figures 3.29, 3.30 and 3.31). Negative controls were set up as described for the scFv-Hk ELISA. The negative controls were 4B7 scFv-0 for Pf-NPNA-1 scFv-0 and 4B7 scFv-20 for Pf-NPNA-1 scFv-12, respectively. The WHcAg + BSA and BSA + Ab controls eliminated non-specific binding of BSA to antigen and of Pf-NPNA-1 scFvs to BSA, respectively. Furthermore, the absence of a signal in the WHcAg + BSA control wells indicated that the WHcAg lacked any terminal His tag. Comparison of the ELISA data for the Pf-NPNA-1 and 4B7 scFvs showed that the Pf-NPNA-1 scFvs specifically recognised the repeat epitope. The ELISA signals obtained for each antibody reflected the level of expression from the vectors pSANG10-3F, pBAK.1 and pBAK.1Hk.

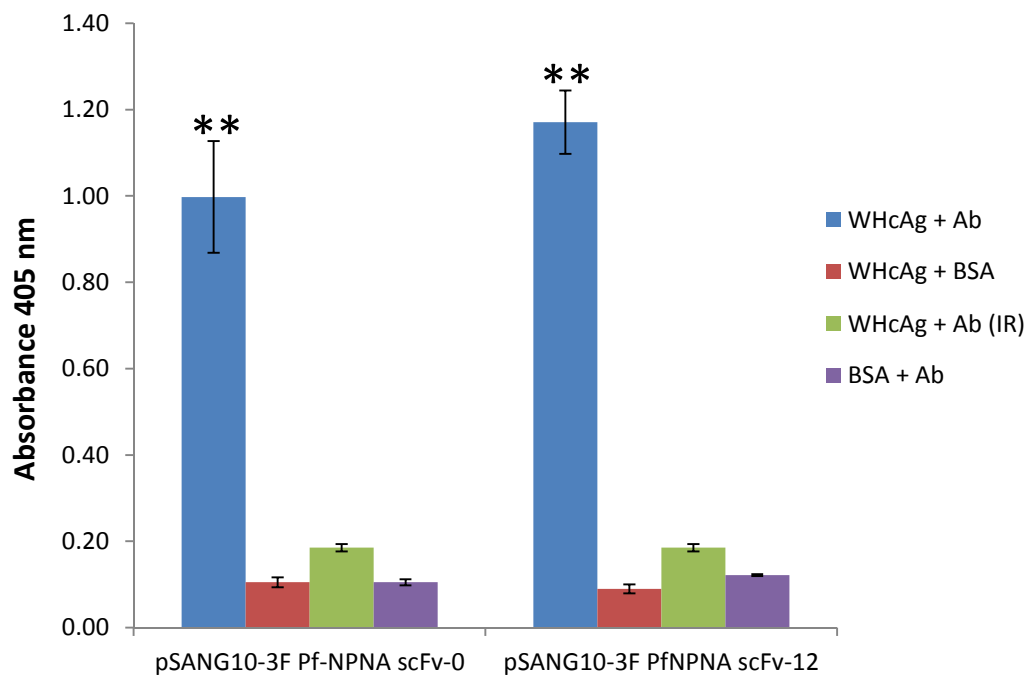


Figure 3.29: Specificity of soluble Pf-NPNA-1 scFv-0 and scFv-12 expressed from pSANG10-3F to WHcAg. Antigen was coated at 100 ng per well and bound scFv detected with monoclonal anti-His-AP antibody. p-NPP was used as substrate and absorbance measured at 405 nm. The error bars indicate the standard errors of the means ($n = 3$). Asterisk denotes statistical significance (double asterisk denotes $p < 0.01$; paired t test). Ag: codes for Antigen, Ab: for Antibody and Ab (IR): for irrelevant or non-specific antibody (4B7 scFv-0 and scFv-20).

Binding of pSANG10-3F Pf-NPNA-1 scFv-0 and scFv-12 to WHcAg were considered statistically significant by comparison with the negative controls using paired t test. For scFv-0 p-values were: 0.009 compared with 4B7 scFv-0 and 0.0076 compared with BSA. P-values for scFv-12 were 0.0015 when compared with 4B7 scFv-20 and 0.0017 when compared with BSA. These values were considered as statistically significant.

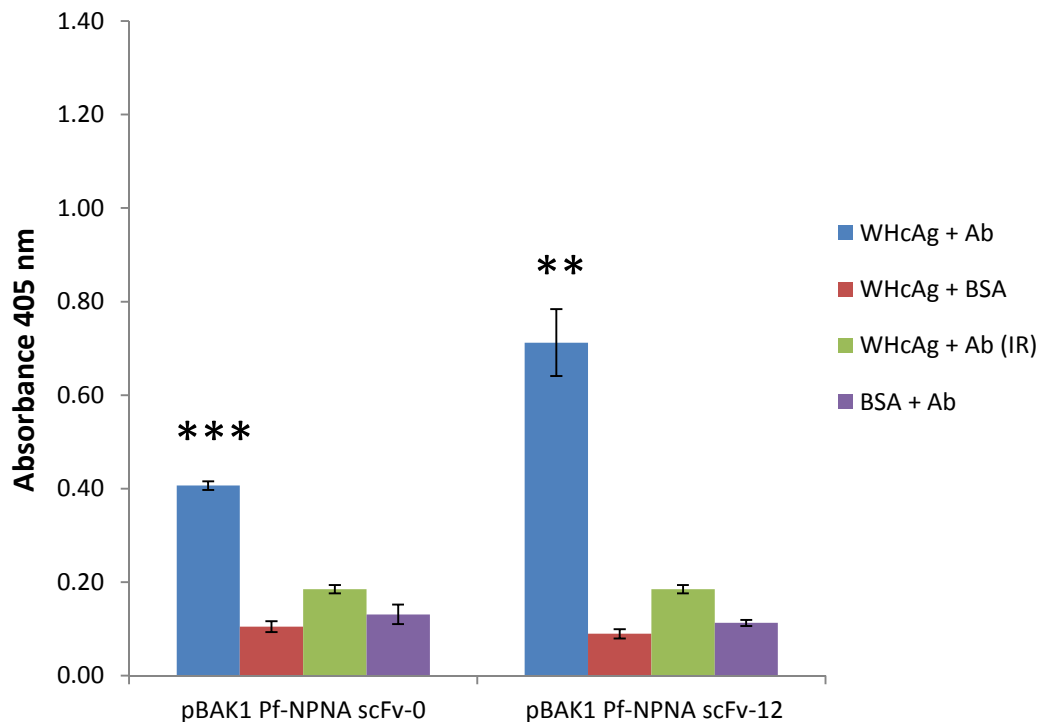


Figure 3.30: Specificity of soluble Pf-NPNA-1 scFv-0 and scFv-12 expressed from pBAK.1 to WHcAg. Antigen was coated at 100 ng per well and bound scFv detected with monoclonal anti-His-AP antibody. p-NPP was used as substrate and absorbance measured at 405 nm. The error bars indicate the standard errors of the means ($n = 3$). Asterisk denotes statistical significance (double asterisk denotes $p < 0.01$ and triple asterisk denotes $p < 0.001$; paired t test). Ag: codes for Antigen, Ab: for Antibody and Ab (IR): for irrelevant or non-specific antibody (4B7 scFv-0 and scFv-20).

The pBAK.1 expressed Pf-NPNA-1 scFv-0 and scFv-12 showed specificity to WHcAg. Statistical significance was as described above. For scFv-0 p-values were: 0.0008 compared with 4B7 scFv-0 and 0.0007 compared with BSA. P-values for scFv-12 were 0.0076 when compared with 4B7 scFv-20 and 0.0056 when compared with BSA. These values were considered as statistically significant.

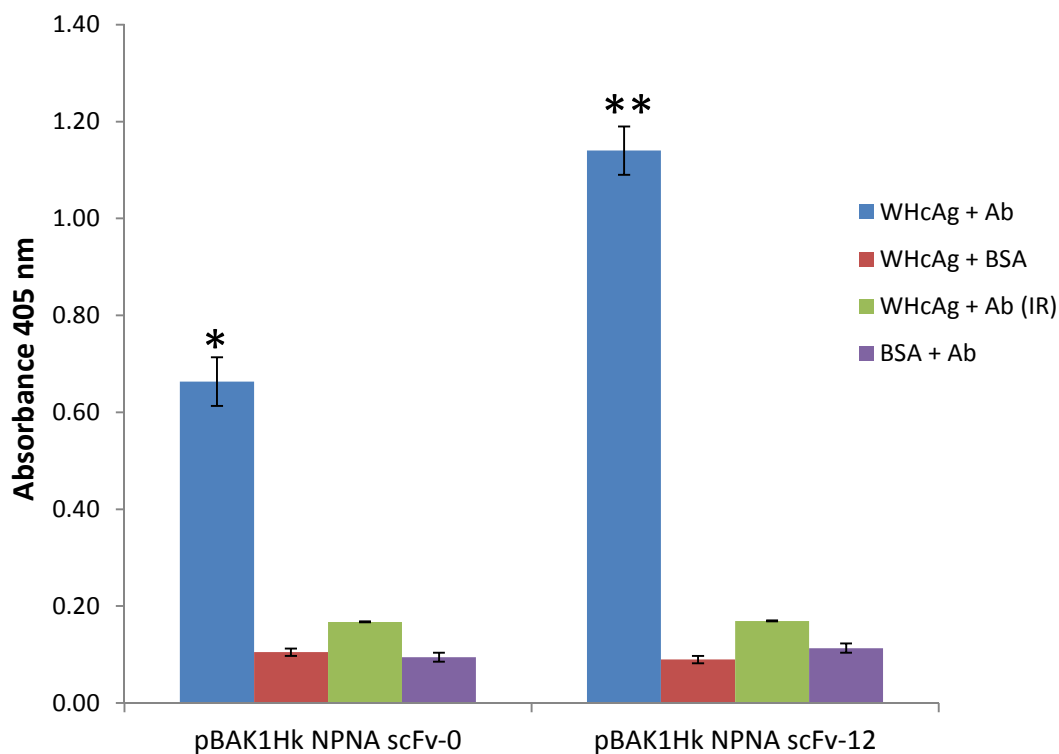


Figure 3.31: Specificity of soluble Pf-NPNA-1 scFv-0 and scFv-12 expressed from pBAK.1Hk to WHcAg. Antigen was coated at 100 ng per well and bound scFv detected with monoclonal anti-His-AP antibody. p-NPP was used as substrate and absorbance measured at 405 nm. The error bars indicate the standard errors of the means ($n = 3$). Asterisk denotes statistical significance (single asterisk denotes $p < 0.05$, and a double asterisk denotes $p < 0.01$; paired t test). Ag: codes for Antigen, Ab: for Antibody and Ab (IR): for irrelevant or non-specific antibody (4B7 scFv-0 and scFv-20).

Evaluation of scFv-0Hk and scFv-12Hk samples, previously analysed (Figure 3.28) with the (NPNA)₉-MKC antigen, showed superior binding activities with WHcAg (Figure 3.31). The higher ELISA signals obtained with WHcAg may be due to the number of NPNA repeats displayed by the viral component of the antigen. Binding to WHcAg was determined as statistically significant. The p values for scFv-0Hk were 0.0131 compared with 4B7 scFv-0Hk and 0.0103 compared with BSA. For scFv-12Hk the p-values were 0.0049 compared with 4B7 scFv-20Hk and 0.0044 when compared with BSA.

3.4.5 Indirect Immunofluorescence Assay (IFA) on *P. falciparum* sporozoites

The specificity of the Pf-NPNA-1 scFvs was demonstrated in an IFA using pBAK.1 Pf-NPNA-1 expressed scFv-0 and scFv-12. These protein samples were used based on an earlier observation, during this study, that some anti-His-tag antibodies recognise only C-terminal His-tag (data not shown). Although the pSANG10-3F expressed scFvs showed better binding, the protein samples could not be used in the IFA due to an internal His-tag (adjacent to the C-terminal tri-FLAG). The IFA revealed the needle-like structure of the sporozoites but were of variable shapes and sizes. As shown in the figure below, the scFv antibodies (positive controls) reacted with the entire surface membrane of the parasite, which is in agreement with the predominance of CSP on sporozoites. Although DAPI stain was added during the incubation step, nuclei staining of the sporozoites were not seen. No surface labelling was observed for the negative controls.

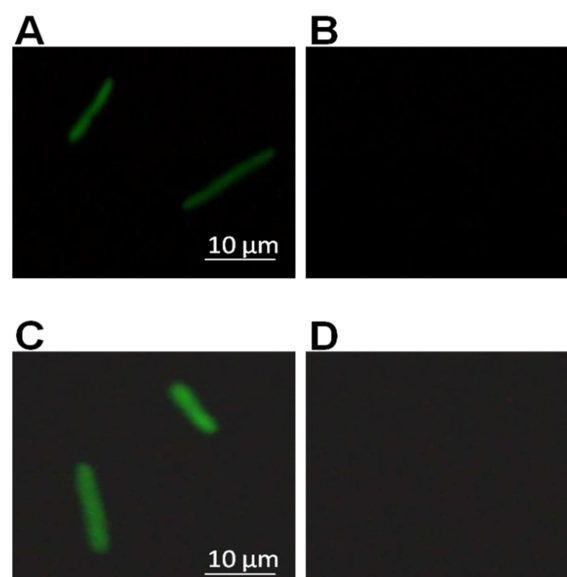


Figure 3.32: Indirect Immunofluorescence Assay (IFA) of pBAK.1 expressed Pf-NPNA-1 scFv-0 (A) and scFv-12 (C) on *P. falciparum* sporozoites. B and D are negative controls for scFv-0 and scFv-12, respectively. Fixed sporozoites were incubated with the affinity purified scFv and stained with polyclonal anti-His FITC conjugated antibody (Green). The parasites were visualized by fluorescence microscopy with a Zeiss Axioskop fluorescent microscope equipped with a 100X oil immersion objective. Scale bars, 10 μm.

3.5 Discussion on expression and characterisation of Pf-NPNA-1

This section of the thesis looked at the expression and functional analysis of the Pf-NPNA-1 antibody. The anti-PfCS protein repeat antibody, Pf-NPNA-1, previously isolated by repertoire cloning from individuals immunised by the bites of irradiated *Anopheles* mosquitoes, was constructed with a 27 amino acid linker between the V_H and V_L (Chappel *et al.*, 2004b). Other sporozoite antibodies as such as, N2H6D5 scFv, expressed via a Sindbis virus which efficiently blocked sporozoite entry of the salivary glands in the avian malaria model encoded a 15 amino acid linker (de Lara Capurro *et al.*, 2000). In the case of 13.1 scFv, the V_H and V_L were joined by a 20 linker peptide (Yoshida *et al.*, 2001). These scFvs encoded by such long linkers would favour only monomeric assembly (Holliger *et al.*, 1993). To facilitate multimeric assembly, two variants, scFv-0 and scFv-12, of the Pf-NPNA-1 antibody were constructed in the V_H - V_L orientation and expressed in the pET-based (pBAK.1, pSANG10-3F and pBAK.1Hk) expression vectors. There was no need to construct the scFvs in the reverse orientation (as in the case of the 4B7 scFvs) as initial studies with the Pf-NPNA-1 scFv-12 (Figure 3.21) showed expression and secretion into the periplasm.

The level of expression of the Pf-NPNA-1 scFv-0 was lower than that of scFv-12 when expressed from the vectors pBAK.1 (Figure 3.22 A&B) and pBAK.1Hk (Figure 3.24 A&B). These observations are in agreement with the lower expression levels of the 4B7 scFv-0 (Figure 3.11A and Figure 3.15A) when compared to those of scFv-20 (Figure 3.11B and Figure 3.16 A). Since scFv with no linkers are noted for their spontaneous assembly into higher oligomers (triabody), it is not known whether this phenomenon takes place before disulphide bond formation occurs. If multimeric assembly precedes disulfide bond formation, it is very likely that the polypeptides with exposed hydrophobic surfaces may aggregate in the periplasm. This may explain the low levels of soluble scFv-0 isolated from the periplasm in contrast to high levels of proteins that were retained within the cytoplasm. The over-expression of scFv in the cytoplasm could be attributed to the strong T7 promoter used. This may lead to lower processing efficiency of the bacterial

secretory machine. Eventually, clogging of the machinery may occur, preventing translocation of the recombinant scFv into the periplasm. It has been explained in a number of reviews that polypeptide to be secreted into the periplasm by the general secretory are initially expressed in an unfolded state. Hence, those polypeptides not transported quickly would aggregate due to interaction between its exposed hydrophobic surfaces. Due to the high level of protein retained within the cytoplasm, purification under denaturing conditions was considered and subsequently undertaken. Although, this strategy resulted in the isolation and purification of active proteins, it was found to be cumbersome and complicated.

In the study by Chappel *et al.* (2004b), the specificity of the monovalent scFv-27 was evaluated against three antigens containing the NPNA repeats. In this study, the binding activities of the Pf-NPNA-1 scFv-0 and scFv-12 were evaluated using two antigens: (NPNA)₉-MKC and WHcAg. The scFv-0Hk and scFv-12Hk binding to (NPNA)₉-MKC were first evaluated. Since both antigen and scFvs bear C-terminal His tags an anti-human kappa antibody was used to detect the scFvs. Analysis of fine specificity revealed weak binding to (NPNA)₉-MKC (Figure 3.28) in contrast to the strong binding to WHcAg (Figure 3.31). Although the Pf-NAPN-1 scFv-12Hk was functional, the scFv-0Hk did not have any antigen binding activity despite being detected on Western blot. Lack of scFv-0Hk binding may be attributed to incorrect folding of its polypeptide chains. The very high binding observed for the scFv-12Hk with the WHcAg, in contrast to the (NPNA)₉-MKC, is probably due to the viral nature of the antigen. This viral antigen is capable of displaying an array of the repeat epitope, thus allowing a higher number of scFv antibody binding and retention.

The fine specificity of the recombinant Pf-NPNA-1 scFv-0 and scFv-12 proteins expressed from pBAK.1 (Figure 3.30) and pSANG10-3F (Figure 3.29) (Martin *et al.*, 2006) were evaluated in an ELISA with WHc antigen. The CSP repeats on this antigen are displayed on a viral particle (Billaud *et al.*, 2005). This antigen lacks a C-terminal His tag, thus soluble scFvs were detected with an anti-His tag antibody. The low signals of scFv-0 (2.5 fold higher in

expression level could also be attributed to the distance between their SD and SC. The optimal spacing between the SD and the SC required for translation initiation varies from 5 to 13 nucleotides with an optimum of 8 to 10 nucleotides (Ringquist *et al.*, 1992; Chen *et al.*, 1994). This spacing is also dependent on the bases at the 3' end of 16S rRNA that take part in the interaction (Chen *et al.*, 1994). However, Scherer and colleagues suggested an optimum of 5 nucleotides in natural *E. coli* mRNA with the SD sequence UAAGGAGGU (Scherer *et al.*, 1980). The pBAK.1 and pSANG10-3F have 9 and 8 nucleotides, respectively between the SD and SC. Since secretion was higher for pSANG10-3F it is presumed that translation initiation may be more efficient in this vector. These observations agree well with the study of deBoer and colleagues who showed a 40% decrease in the translation efficiency of a chimeric leukocyte interferon when the aligned spacing between the SD and SC was increased from 4 to 8 or 13 nucleotides (de Boer *et al.*, 1983) and in the case of the recombinant growth hormone (Dalboge *et al.*, 1988).

Further to the fine specificity shown in ELISA, the Pf-NPNA-1 recombinant proteins were also evaluated for binding to *P. falciparum* sporozoites in an IFA. Although the pSANG-10 3F expressed proteins showed a strong signal in ELISA, these were not used for the IFA as it was previously determined that C-terminal anti-His tag antibodies, purchased from AbCam, did not detect proteins with an internal His-tag (data not shown). However, the pBAK.1 expressed proteins, which bear a C-terminal His-tag, labelled the entire surface of *P. falciparum* sporozoites when used in the IFA (Figure 3.32). These observations are in agreement with those of Chappel *et al.* (2004b). Sporozoites did not fluoresce when BSA was used as negative control. An appropriate positive control would have been the murine monoclonal anti-*falciparum* repeat antibody 2A10 (Zavala *et al.*, 1985b). A limitation of this study was the inability to detect the characteristic sky-blue fluorescence staining of the sporozoite nuclei when stained with DAPI.

Chapter 4

Results

**Expression of scFv 4B7 and Pf-NPNA-1
in *Asaia* sp.**

4.0 The genus *Asaia*

4.1 Introduction

Presently, the genus is made of five species: *Asaia bogorensis* (Yamada *et al.*, 2000), *Asaia siamensis* (Katsura *et al.*, 2001) *Asaia krungthepensis* (Yukphan *et al.*, 2004), *Asaia lannaensis* (Malimas *et al.*, 2008) and *Asaia spathodeae* (Kommanee *et al.*, 2010). They are obligate aerobes belonging to the family acetobacteraceae and phylum α -proteobacterium. Strains belonging to the genus *Asaia* have mostly been isolated from tropical flowers, which is a source of nectar for insects such as mosquitoes. *Asaia* species are capable of tolerating acidic conditions growing at pH values lower than 5 (pH 3.5). Phenotypically *Asaia* species, with the exception of *Asaia lannaensis*, exhibit no oxidation or very weak oxidation of ethanol to acetic acid as they lack membrane-bound NAD-dependent alcohol dehydrogenase (Ano *et al.*, 2008). All four species, however, do not grow on 0.35% acetic acid. These properties differentiate them from other acetic acid bacteria (AAB) such as *Acetobacter* and *Gluconobacter* (Yamada and Yukphan, 2008). The confirmation of the presence of NADP-dependent dehydrogenase activity for D-glucose and a quinoprotein glycerol dehydrogenase in *As. bogorensis* further substantiated their capability to oxidise sugars (D-glucose, D-Fructose and sucrose) and sugar alcohols (glycerol, mannitol and sorbitol) to produce acid (Ano *et al.*, 2008).

Recently Favia *et al.* (2007) identified an acetic acid bacterium from the midgut of *A. stephensi*. Based on 16S rRNA gene sequences, the isolated bacterium was identical to *Asaia bogorensis* (99.6%) and *Asaia siamensis* (99.8%) (Favia *et al.*, 2007). More recently, *Asaia krungthepensis* has also been isolated from other mosquito species (Chouaia *et al.*, 2010). *Asaia* sp. SF2.1 satisfies the prerequisites for any bacterial candidate to be considered for inclusion in a paratransgenic approach. Firstly, *Asaia* can easily be isolated and cultured in cell-free media and is present in high prevalence in mosquitoes. The ease of cultivation in the laboratory has facilitated its genetic manipulation, an important criterion for symbiotic control, to express a

recombinant GFP. Thirdly, the recombinant *Asaia* expressing GFP, when fed to mosquitoes, colonised the midgut, salivary glands and reproductive organs of male and female adult mosquitoes (Favia *et al.*, 2007; Damiani *et al.*, 2008; Crotti *et al.*, 2009; Damiani *et al.*, 2010). More recently, Chouaia *et al.* (2010) found that different strains (up to five) of *Asaia* can simultaneously associate with a single mosquito. This led them to suggest that multiple infections can occur during the life span of the mosquito. The authors are also of the view that *Asaia*, the leading bacterial candidate for use in paratransgenesis, does not exert any pathogenic effect on the host mosquito. Fourthly, fluorescently tagged strains have exhibited diversified modes of transmission: vertically to progeny via egg smearing and horizontally through feeding (Favia *et al.*, 2007) and paternally by venereal transfer from male to female (Damiani *et al.* 2008). It has been suggested that these different routes of transmission could offer alternative ways to release engineered bacteria into mosquito populations in the field (Ricci *et al.*, 2011). Lastly, *Asaia* is capable of colonising insects of diverse genera and order (Crotti *et al.*, 2009; Crotti *et al.*, 2010). More importantly, *Asaia* has been found in association with the malaria mosquito vectors *An. stephensi* (Favia *et al.*, 2007), *An. gambiae* (Damiani *et al.*, 2010), *An. maculipennis*, the virus vector *Aedes aegypti* (Crotti *et al.*, 2009) and *Aedes albopictus* (Chouaia *et al.*, 2010). These studies provide proof of principle that this bacterium can be used for symbiont control, that is, to express anti-parasite molecules within the mosquito to disrupt parasite development.

Although, transformation of *Asaia* sp. has been carried out and shown to express GFP, heterologous expression of disulphide containing proteins, such as scFv, has not been investigated. On the other hand, the *E. coli lacZ* (encoding β -galactosidase) and *lacY* (β -galactosidase permease) genes have been cloned into a shuttle vector and functionally expressed in two phylogenetically related strains of *Asaia*, *Gluconobacter oxydans* and *Acetobacter liquefaciens* (Mostafa *et al.*, 2002). Subsequently, El-mezawy *et al.* (2005) showed functional activity of an extracellularly expressed β -galactosidase gene of *Bifidobacterium infants* in *G. oxydans* with the plasmid

pBINF1 (El-mezawy *et al.*, 2005). In this section of the thesis, recombinant *Asaia* will be assessed for expression of the scFvs 4B7 and Pf-NPNA-1.

4.2 Assessment of antibiotic resistance

Wild type *Asaia* SF2.1 was streaked on a range of GLY agar kanamycin plates and growth monitored after two days. Growth was observed at kanamycin concentrations of 25 – 150 µg/mL. No growth was observed at 200 µg/mL. Subsequently, recombinant *Asaia* SF2.1 was grown at kanamycin concentration of 200 µg/mL.

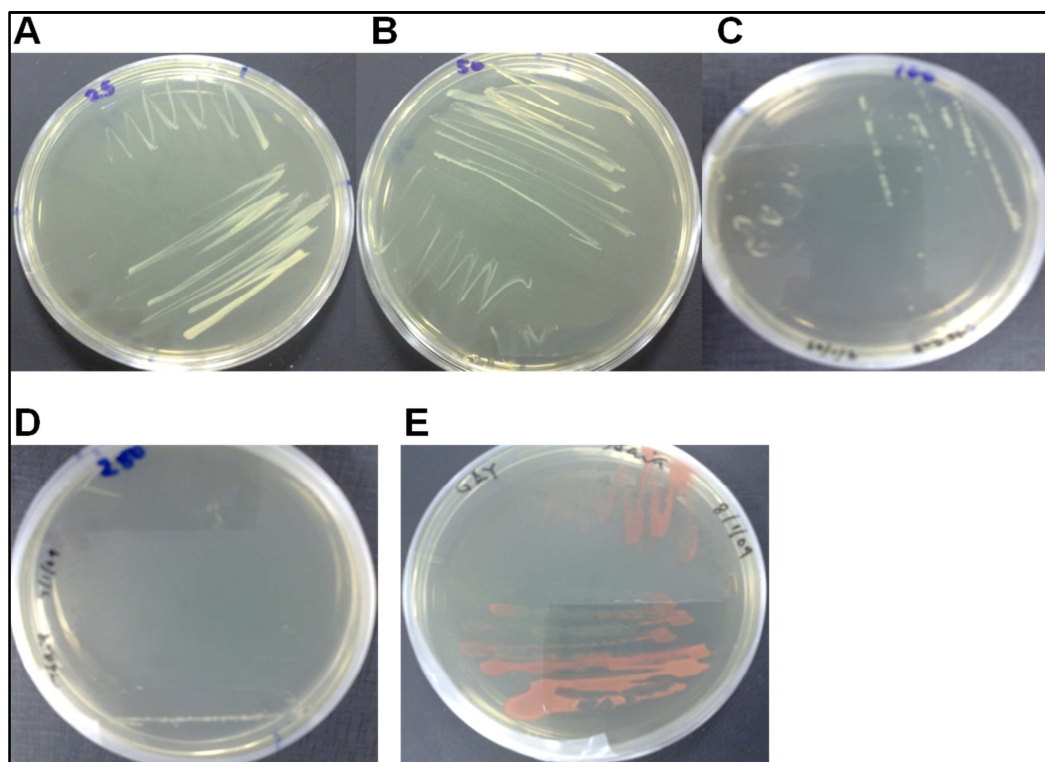


Figure 4.1: Assessment of kanamycin resistance of *Asaia* SF2.1. *Asaia* SF2.1 was streaked on GLY plates supplemented with varying concentrations of kanamycin (25 – 200 µg/mL). Growth was observed on GLY with kanamycin concentrations of 25 µg/mL (A), 50 µg/mL (B) and 100 µg/mL (C). No growth was observed at 200 µg/mL (D). E shows the characteristic pink colour of colonies of *Asaia* SF2.1 after days of storage in the fridge.

Antibiotic susceptibility of *Asaia* SF2.1 to other antibiotics was also investigated. *Asaia* was resistant to the antibiotics ampicillin, chloramphenicol and streptomycin at concentrations as high as 200 µg/mL.

4.3 Expression of recombinant proteins in *Asaia* SF2.1

The broad-host range vector pMAK031 2P (Figure 4.2) was used for transformation of *Asaia* SF2.1. The plasmid was constructed using pHM2 vector (Mostafa *et al.*, 2002) as the parental plasmid. This plasmid differs from pHM2 (8.86 kb), in that the *lacZ* and *lacY* genes were replaced with a GFP cassette, a gram negative (ORI) and gram positive (*OriR*) bacterial origin from the plasmid pRR1.1. The *nptII* kanamycin promoter (PnptII) allows constitutive expression of recombinant proteins. The plasmid also has a C-terminal His-tag and Tri-FLAG for purification and detection. It bears the *NcoI*, *NdeI* and *NotI* for directional cloning of recombinant protein genes.

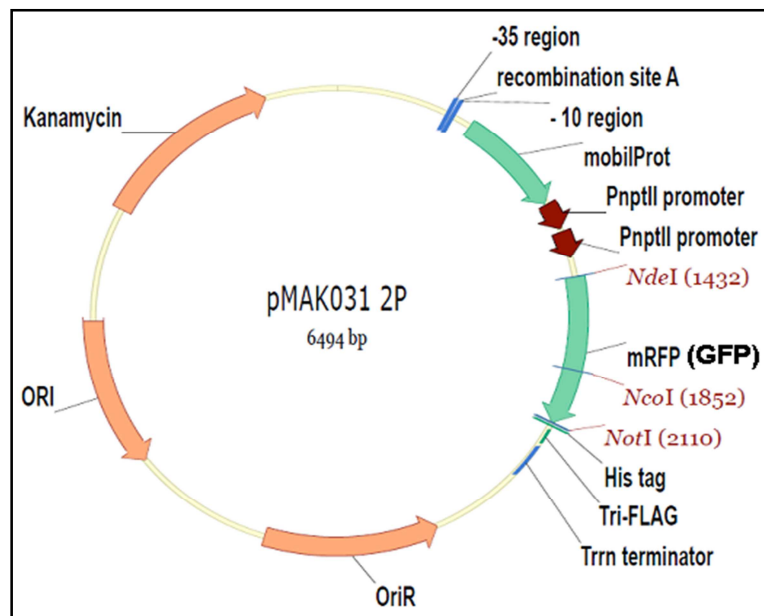


Figure 4.2: Vector map of plasmid pMAK031 2P with a GFP gene. ORI: origin of replication for gram-negative bacteria; OriR: origin of replication for gram-positive bacteria; mobilProt: mobilisation protein; PnptII: constitutive kanamycin (neomycin) phosphotransferase promoter; Trrn terminator: *rnnB* rRNA T1 transcriptional terminator; kanamycin: kanamycin resistance gene. Restriction sites (*NcoI*, *NotI*, *NdeI*) for cloning of scFv genes are coloured red. The 6X His and Tri-FLAG tags are shown.

The functionality of the pMAK031 2P plasmid was assessed by cloning a GFP gene into the *Nde*I and *Not*I and the resulting construct used to transform both gram negative (*E. coli* and *Asaia* SF2.1) and gram positive (*R. rhodnii* and *R. cornyebacterioides*) bacteria. Recombinant GFP expression was observed in both gram negative (Figure 4.3) and gram positive bacteria (data not shown).

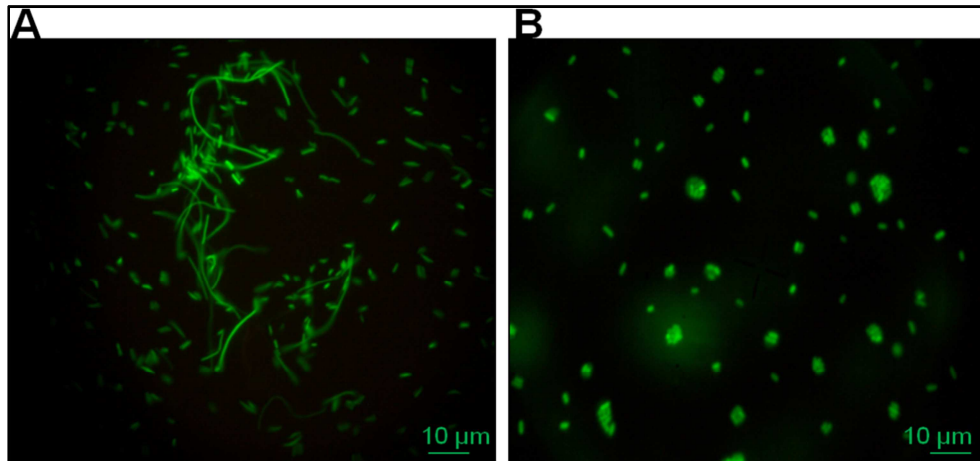


Figure 4.3: Fluorescence images of *E. coli* (A) and *Asaia* sp SF2.1 (B) transformed with pMAK031(2P)-GFP. A single colony of *E. coli* and *Asaia* sp SF2.1 were mounted on a glass slide using 20% glycerol in PBS and a coverslip. The fluorescent bacteria were visualized by fluorescence microscopy with a Zeiss Axioskop fluorescent microscope equipped with a 100X oil immersion objective.

4.3.2 Carbon utilisation of *Asaia*

Glycerol and glucose were used to evaluate the capability of *Asaia* to grow on different carbon sources. The glucose medium (LB-Glu) consisted of LB broth (pH 7.0) supplemented with 2% (v/v) glucose whereas glycerol formed the carbon component of GLY medium (pH 5.5). The growth of *Asaia* SF2.1 was examined in 100 ml of each medium in a 500-ml Erlenmeyer flask at 30°C with rotary shaking at 200 rpm. After 48 hours of growth the final pH in both media was ~4.6. As shown in Figure 4.4 growth of *Asaia* in GLY was higher compared to LB-Glu. GLY was subsequently used for recombinant expression of scFvs in *Asaia*.

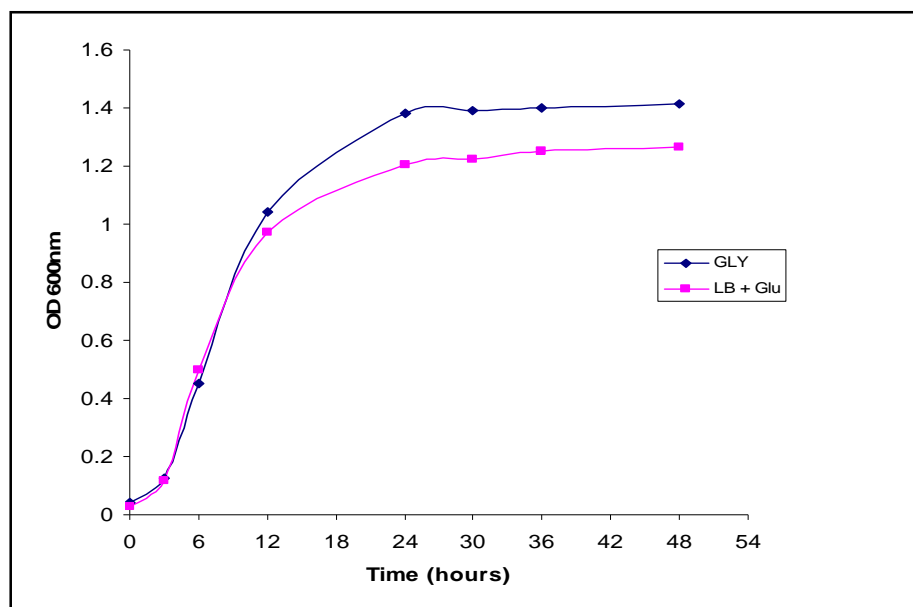


Figure 4.4: Growth profile of pMAK031 2P 4B7 scFv-0 transformed *Asaia* sp SF1 on different carbon sources. GLY (25 g/L glycerol, 10 g/L yeast extract, pH 5); LB + Glu (LB medium supplemented with 2% v/v glucose). Optical density measurements were taken over 48 hours. Mean values from two independent cultures are shown.

4.3.3 Cloning of 4B7 and Pf-NPNA-1 scFvs into pMAK031 2P

The pMAK031 2P-GFP was digested *NdeI/NotI* to facilitate cloning of the scFv genes.

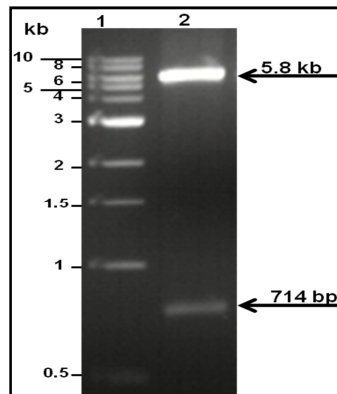


Figure 4.5: Restriction enzyme digestion of pMAK031 2P-GFP. 50 μ L of the digested reaction was loaded and subjected to electrophoresis on a 1.5% agarose at 100 V for 1 hour. The DNA was visualised using ethidium bromide under UV light at wavelength of 200 nm. The digested plasmid (~5.8kb) was excised and agarose gel purified. Lane 1: 1 kb DNA ladder, Lane 2: *NdeI/NotI* digested pMAK031 2P-GFP.

The Pf-NPNA-1 (scFv-0 and 12) and 4B7AJ (scFv-0 and 20) were digested from pSANG10-3F and subcloned into the *NdeI/NotI* digested pMAK031 2P plasmid (Figure 4.5). During this cloning step the *peB* signal peptide, from the pSANG10-3F vector, was cloned along with the scFvs. *E. coli* transformants were screened by colony PCR with primers **T7ABATG** (GC AGC TAA TAC GAC TCA CTA TAG GAA CAG ACC ACC ATG GCC) and **PfVLR** (TTT AAT TCC ACT TTG GTG CCG CCG CC) for Pf-NPNA-1 scFvs and **4B7VLNco** and **4B7VHNot** for 4B7AJ scFvs, respectively. Plasmids were then purified from positive clones, sequenced (Appendix) and used to transform *Asaia*.

Subsequently, constitutive expression in *Asaia* of each scFv was then evaluated in small scale cultures over three days, to determine optimal expression time. Constitutive expression was observed in 48 and 72 hours with optimal expression seen by day 2 (48 hours) for all scFvs (Figure 4.6). Protease degradation of the 4B7 scFv-20 was observed on a western blot

during this investigation. As a result, further characterisation of this construct was not assessed. Subsequently, recombinant expressions of the scFvs were carried out over 2 days.

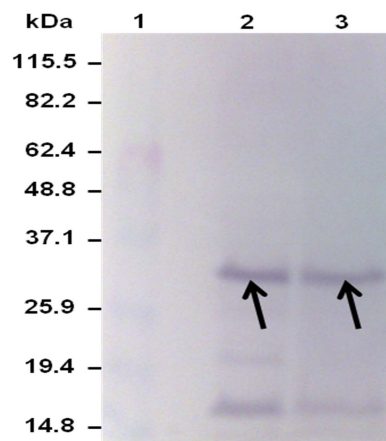


Figure 4.6: Impact of production time on expression scFv in small scale culture of *Asaia*. Aliquots (1 mL) of *Asaia* culture were collected at days 2 and 3 and centrifuged. Cell pellets were separated by reducing SDS-PAGE on a 12% gel and transferred onto PVDF membranes. Lane 1: molecular weight marker; lane 2: *Asaia* expressed 4B7 scFv-0 under reducing conditions (day 2) and lane 3: *Asaia* expressed 4B7 scFv-0 under reducing conditions (day 3). Proteins were probed with goat anti-tri FLAG antibody as primary antibody and mouse anti-rabbit IgG conjugated to alkaline phosphatase (AP) as secondary antibody. BCIP/NBT was used as substrate.

The 4B7 (AJ) scFv-0, Pf-NPNA-1 scFv-0 and scFv-12 were expressed and purified from 200 mL of GLY medium. The constitutively expressed 4B7 scFv-0 in *Asaia* was compared to that expressed in *E. coli*. Under reducing conditions, the molecular weight of the purified 4B7 scFv-0 was comparable in both expression systems (Figure 4.7B, Lanes 2 and 3). However, different multimeric patterns of the scFv-0 were observed under non-reducing conditions (Figure 4.7B, Lanes 4 and 5). The multimeric assembly (monomer, dimer and higher multimer) of the *E. coli* expressed scFv-0 was consistent with previous result (Figure 3.14). The *Asaia* expressed scFv-0 showed monomer and dimer formation under non-reducing conditions (Figure 4.7B, Lane 4).

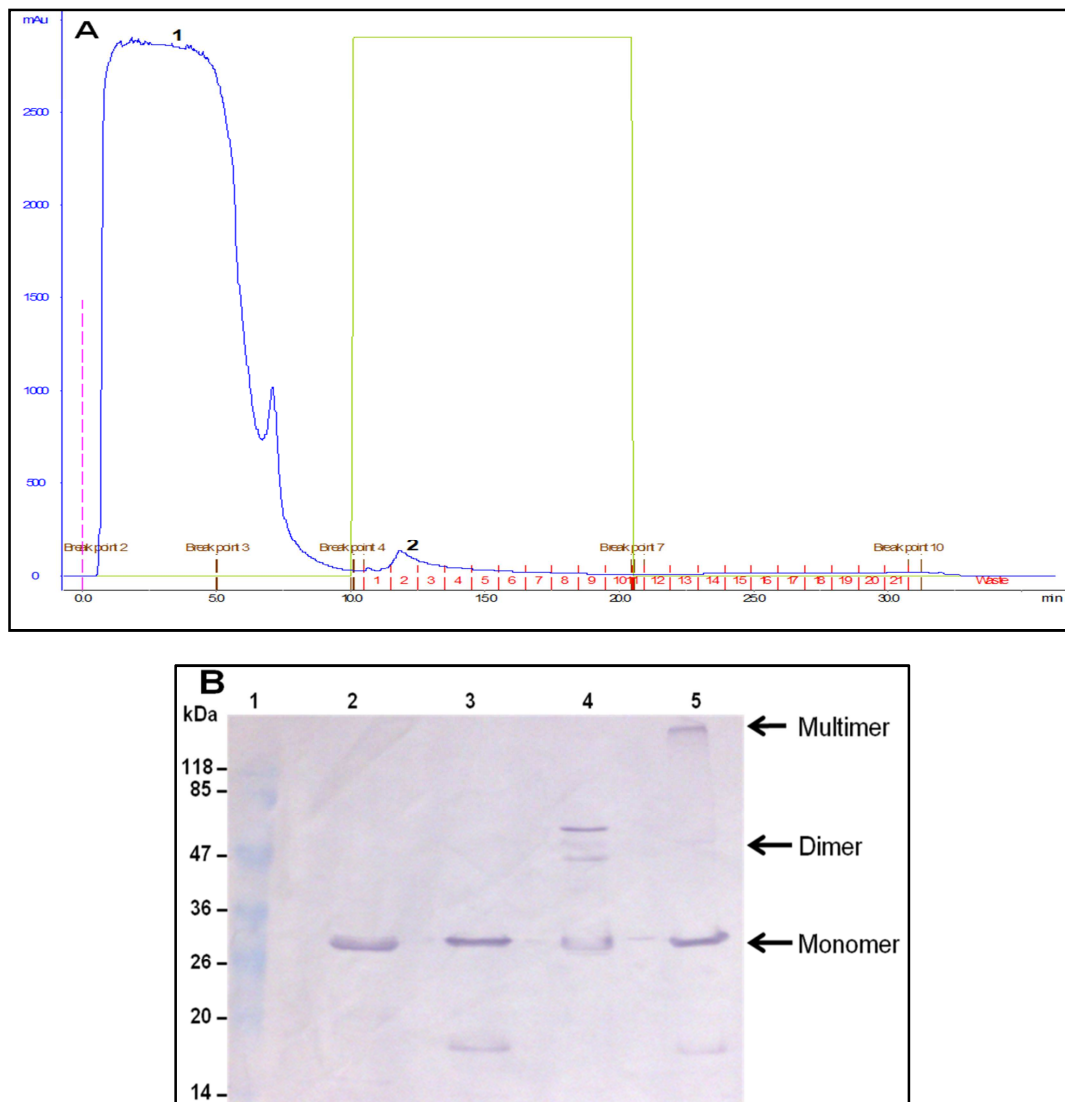


Figure 4.7: Purification of 4B7 scFv-0 on a 1 mL Ni²⁺ column (A) and Western blot of *E. coli* and *Asaia* sp. SF1 expressed and purified 4B7(AJ) scFv-0 under reducing and non-reducing conditions. (A) Crude lysate was loaded onto a 1 mL nickel resin at a flow rate of 1 mL/min and fractions were collected at 1 mL intervals. The blue line shows the absorbance at 280 nm, the green line shows addition of elution buffer and the fractions collected are shown in red. Peak 1 indicates unbound protein (flow through) and peak 2: bound proteins eluted with elution buffer (100 mM NaHPO₄, 500 mM NaCl, 500 mM Imidazole, pH 8). **(B)** Lane 1: molecular weight marker; lane 2: *Asaia* expressed 4B7 scFv-0 under reducing conditions; lane 3: *E. coli* expressed 4B7 scFv-0 under reducing conditions; lane 4: *Asaia* expressed 4B7 scFv-0 under non-reducing conditions and lane 5: *E. coli* expressed 4B7 scFv-0 under non-reducing conditions. Proteins were probed with goat anti-tri FLAG antibody as primary antibody and mouse anti-rabbit IgG conjugated to alkaline phosphatase (AP) as secondary antibody. BCIP/NBT was used as substrate.

The Pf-NPNA-1 scFv-0 and scFv-12 were also expressed in *Asaia*, purified and characterised. The chromatogram generated during purification and analyses of the purified scFv-0 and 12 on SDS-PAGE are shown in Figure 4.8 and 4.9, respectively.

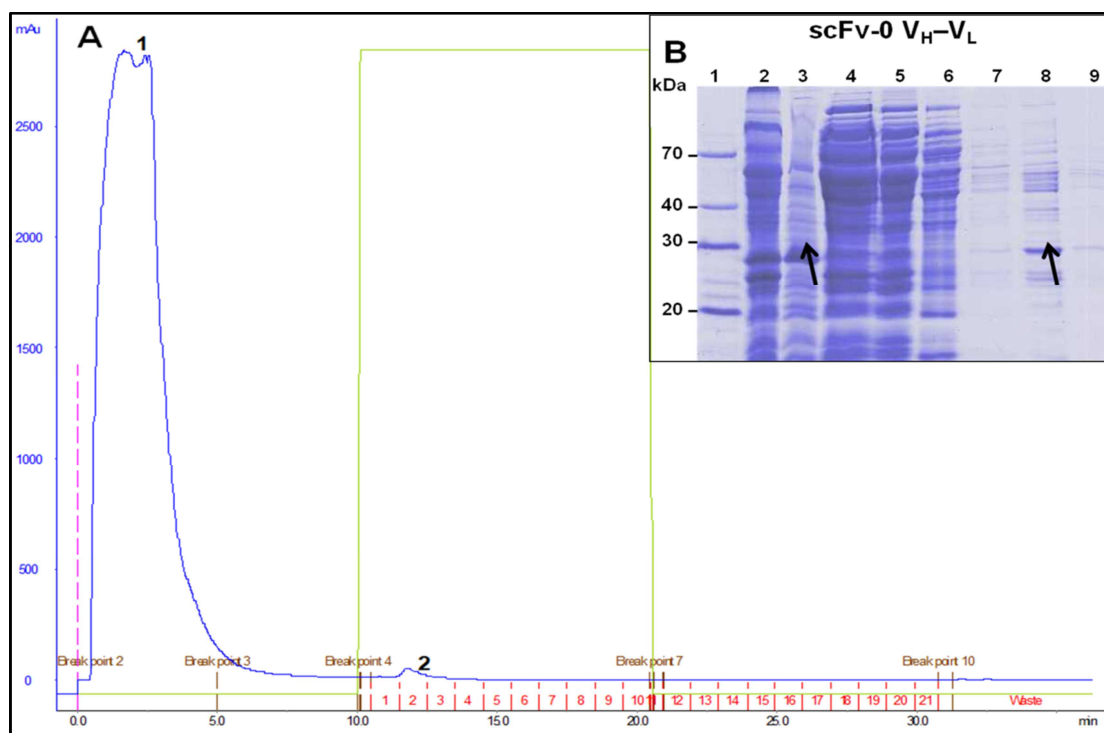


Figure 4.8: Purification of Pf-NPNA-1 scFv-0 on a 1 mL Ni²⁺ column (A) and SDS-PAGE of purified proteins under reducing conditions (B). (A) Crude lysate was loaded onto a 1 mL nickel resin at a flow rate of 1 mL/min and fractions were collected at 1 mL intervals. The blue line shows the absorbance at 280 nm, the green line shows addition of elution buffer and the fractions collected are shown in red. Peak 1 indicates unbound protein (flow through) and peak 2: bound proteins eluted with elution buffer (100 mM NaHPO₄, 500 mM NaCl, 500 mM Imidazole, pH 8). (B) **20μL** of proteins fractions were electrophoresed on a 12% gel and stained with Coomassie brilliant blue R-250. Lane 1: molecular weight maker; Lane 2: untransformed *Asaia*; Lane 3: transformed *Asaia*; Lane 4: crude lysate; Lane 5: flow through; Lane 6: wash; Lanes 7 - 9: elutions 1-3.

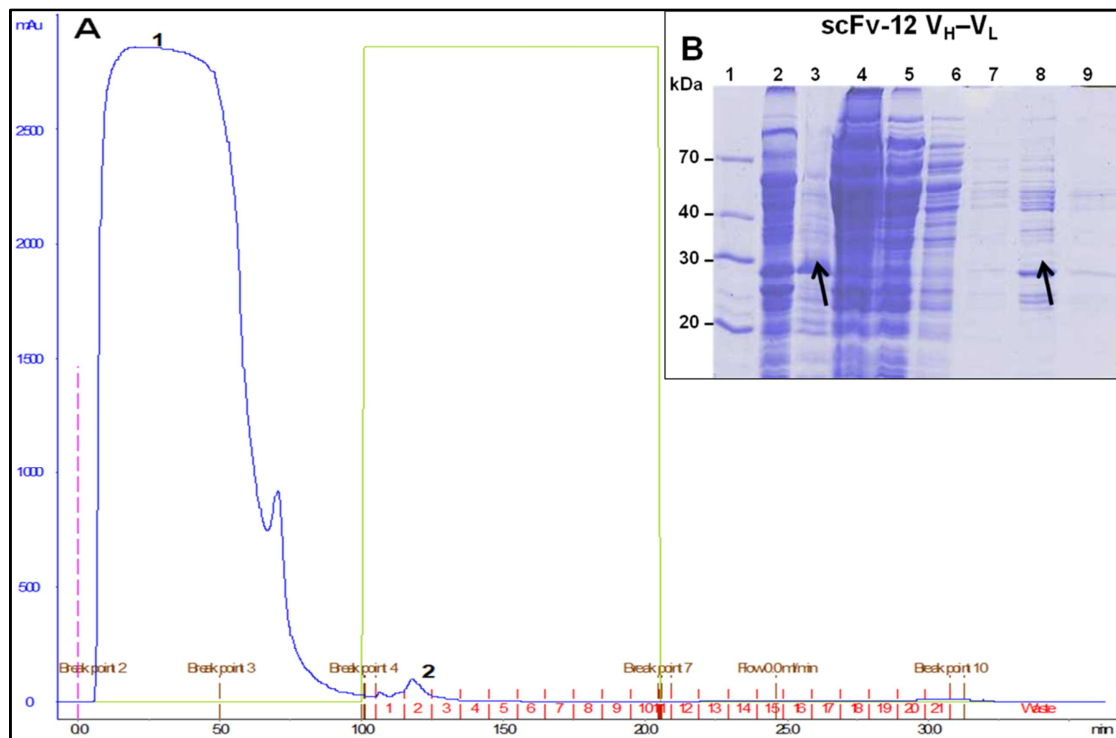


Figure 4.9: Purification of Pf-NPNA-1 scFv-12 on a 1 mL Ni²⁺ column (A) and SDS-PAGE of purified proteins under reducing conditions (B). (A) Crude lysate was loaded onto a 1 mL nickel resin at a flow rate of 1 mL/min and fractions were collected at 1 mL intervals. The blue line shows the absorbance at 280 nm, the green line shows addition of elution buffer and the fractions collected are shown in red. Peak 1 indicates unbound protein (flow through) and peak 2: bound proteins eluted with elution buffer (100 mM NaHPO₄, 500 mM NaCl, 500 mM Imidazole, pH 8). (B) Proteins were electrophoresed on a 12% gel and stained with Coomassie brilliant blue R-250. Lane 1: molecular weight maker; Lane 2: untransformed *Asaia*; Lane 3: transformed *Asaia*; Lane 4: crude lysate; Lane 5: flow through; Lane 6: wash; Lanes 7 - 9: elutions 1-3.

The peak fractions 2 (Lane 8 in Figures 4.8B and 4.9B) were run under reducing conditions, transferred onto PVDF membrane and probed with rabbit anti-tri FLAG antibody and goat anti-rabbit IgG-AP. The predicted molecular weight of the *Asaia* purified Pf-NPNA-1 scFv-0 (28.8 kDa) and scFv-12 (30.1 kDa) were consistent with those on the Western blot. A twin-arginine translocation (TAT) signal peptide was cloned from the CA19.9 scFv (donated by Dr. Anatoliy Markiv, UoW) and its expression analysed alongside that of *pe/B*-Sec dependant signal peptide. Both signal peptides were efficiently processed in *Asaia* resulting in similar molecular weights of Pf-NPNA-1 scFv-0 and 12 (Figure 4.10).

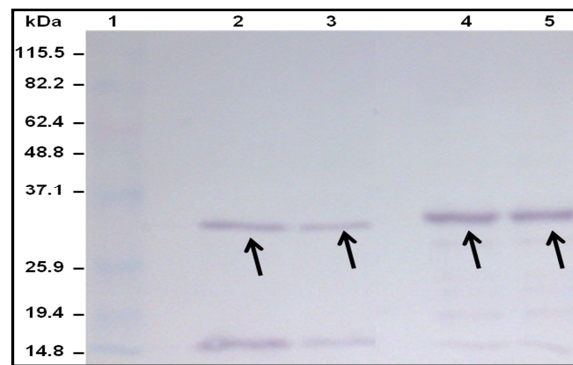


Figure 4.10: Western blot of purified Pf-NPNA-1 scFv-0 and 12 from *Asaia* sp. SF.1 with different signal peptides. Lane 1: molecular weight marker, lanes 2 and 3: Pf-NPNA-1 scFv-0 expressed with *peB* and TAT signal peptides, respectively; lanes 4 and 5: Pf-NPNA-1 scFv-12 expressed with *peB* and TAT signal peptides. Proteins were probed with rabbit anti-tri FLAG antibody as primary antibody and goat anti-rabbit IgG conjugated to alkaline phosphatase (AP) as secondary antibody. BCIP/NBT was used as substrate.

Binding of the constitutively expressed Pf-NPNA-1 scFv-0 and scFv-12 were evaluated in an ELISA (Figure 4.11) with WHcAg as antigen. The ELISA signals are lower than those obtained in chapter 3 (Figure 3.29 and 3.30).

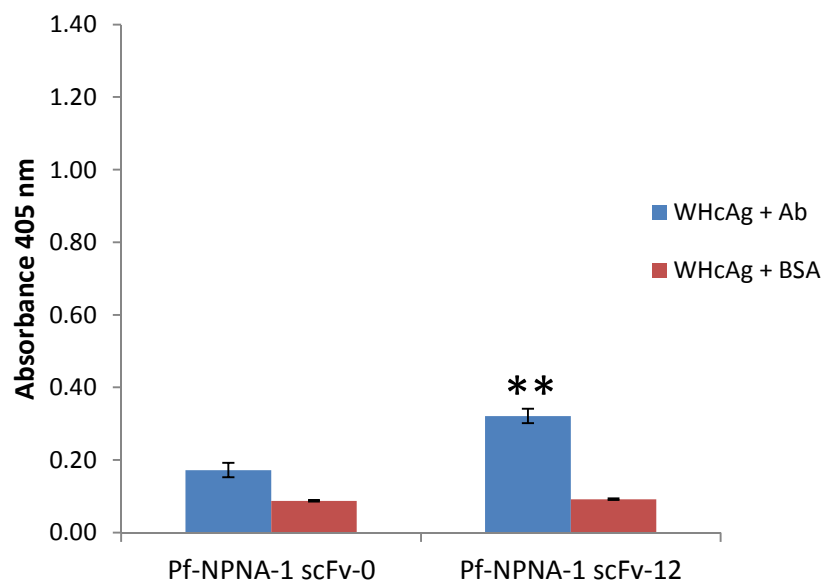


Figure 4.11: Specificity evaluation of Pf-NPNA-1 pMAK031 2P expressed scFv-0 and scFv-12 to WHcAg. Antigen was coated at 100ng per well and bound scFv detected with a rabbit anti-tri FLAG antibody (primary antibody) and mouse anti-rabbit IgG-AP (secondary antibody). BSA was used as a negative control. p-NPP was used as substrate and absorbance measured at 405 nm. The error bars indicate the standard errors of the means ($n = 3$). Double asterisk denotes $p < 0.01$.

4.4 Discussion on recombinant expression of scFvs in *Asaia* SF2.1

Recombinant expression of scFv 4B7 and Pf-NPNA-1 in *Asaia*, described in this chapter and the first of its kind, has shown that *Asaia* SF2.1 has the capacity to express disulphide containing proteins. Initial stages of the study examined the antibiotic susceptibility and resistance of *Asaia* to some commonly used antibiotics. *Asaia* was resistant to the antibiotics ampicillin, chloramphenicol, streptomycin and tetracycline. Susceptibility to kanamycin was only observed at a high concentration of 200 µg/mL. This is in contrast to the concentration of kanamycin (100 µg/mL) used by Favia *et al.* (2007). These observations, during the susceptibility and resistant studies, are in agreement with previous observations (Katsura *et al.*, 2001; Yukphan *et al.*, 2004; Malimas *et al.*, 2008; and Kommanee *et al.*, 2010). The natural habitat of *Asaia* is tropical flowers and fruits of south-east Asia. As a ubiquitous bacterium in the environment, *Asaia* could have acquired its antibiotic resistance through promiscuous exchange and shuffling of genes, genetic platforms and genetic vectors among other environmental bacteria isolates (Baquero *et al.*, 2008).

For the expression studies, two carbon sources (glucose and glycerol) were evaluated to study the growth kinetics of *Asaia*. *Asaia* has the capacity to oxidise both sugars and sugar alcohols. The overall growth of *Asaia* on both carbon sources was similar during the exponential phase, however, the final bacterial cell densities at the stationary phase was higher for glycerol compared to glucose. This indicates that glucose is quickly utilised during bacterial growth whereas glycerol may provide a steady source of carbon. After cultivation the final pH of both culture media was 4.6, which is similar to that observed by Ano *et al.* (2008). Yamada *et al.* (2002) have indicated that *Asaia* has the ability to produce acid from glucose and glycerol. In other AAB, the oxidation of D-glucose to D-gluconic acid and 2- or 5-keto-D-gluconic acid, are catalysed by the membrane-bound D-glucose dehydrogenase and 2-keto-D-gluconate dehydrogenase. On the other hand, oxidation of glycerol to dihydroxyacetone is catalysed by glycerol dehydrogenase. The confirmation of the presence of NADP-dependent dehydrogenase activity for D-glucose

and a quinoprotein glycerol dehydrogenase in *As. bogorensis* further substantiated their versatility to oxidise sugars and sugar alcohols to produce acid (Ano *et al.*, 2008).

The optimum expression time of 48 hours was chosen based on the fact that *Asaia* SF2.1 is a slow growing bacterium, with an estimated doubling time of 2 hours (Crotti *et al.*, 2009) and on the observations made in this study during the small scale expression studies. This slow growth rate was evident during transformational and growth curve studies (Figure 4.4). During the transformational studies, *Asaia* transformants could only be observed after 48 hours of incubation at 30°C. In addition, growth in GLY medium showed a higher cell density beyond 24 hours. An important consideration during heterologous expression is the translation of rare codons, as gram negative bacteria exhibit differential codon usage. In the case of *Asaia*, the fact that recombinant GFP (previously expressed in numerous *E. coli* strains) could be expressed (Favia *et al.*, 2007) indicated that the codon usage of this bacterium may be similar to that of *E. coli*. However, disulphide containing protein expression has not been attempted. In this study, the disulphide containing scFv antibodies (4B7 and Pf-NPNA-1) were successfully expressed and formed intact disulphide bonds, which were cleaved under reducing conditions (Figure 4.7 and Figure 4.10, respectively). In the case of the 4B7 scFv-0, comparative analyses of *Asaia* and *E. coli* expressed proteins showed the same molecular weight of 30 kDa (Figure 4.7, lanes 2 and 3, respectively). This observation indicates the presence of a signal peptidase in *Asaia*, which resulted in the correct processing of the Sec-dependent *pefB* signal peptide. On the other hand, recombinant protein expression was compared between the Sec-dependent *pefB* and a twin-arginine translocation (TAT) signal peptides (SP). The former SP transports an unfolded polypeptide from the cytoplasm into the periplasm via the Sec pathway, whereas the latter translocates folded proteins across the inner membrane independent of the Sec pathway (DeLisa *et al.*, 2003; Choi and Lee, 2004). Using the Pf-NPNA-1 scFv-0 and 12 as model proteins similar molecular weights were observed for the *pefB* and TAT fusion proteins (Figure 4.9). These observations further confirm that the Sec secretory and TAT pathways are functional in *Asaia*.

Although these preliminary studies have shown the presence of these secretory pathways in *Asaia*, further studies are required to identify the gene clusters that form the components of these pathways.

An interesting observation was made regarding the oligomeric patterns of the *Asaia* and *E. coli* expressed 4B7 scFv-0 recombinant proteins. Under reducing conditions, both proteins had the same predicted molecular weight of 30 kDa. Under non-reducing conditions the *E. coli* 4B7 scFv-0 protein showed monomer, dimer and multimeric forms, as previously observed (Chapter 3, Figure 3.12 and 3.13). However, the *Asaia* expressed 4B7 scFv-0 showed monomer, dimer and other multimeric species (Figure 4.7). Arndt *et al.* (1998) suggested that multimeric assembly of scFvs is dependent on factors such as the expression conditions, bacterial strain, folding methods and association constant for domain-domain interaction. Although the bacterial strains, the expression conditions (cultivation at 30°C compared to 20°C in *E. coli*; duration of cultivation for 48 hours compared to 24 hours) and protein isolation (osmotic shock compared to ultrasonic vibrations) differ, further studies are required to delineate the oligomeric patterns of recombinantly expressed scFvs in both strains.

Binding of the *Asaia* expressed 4B7 scFv-0 was not determined as previous binding studies of *E. coli* expressed and purified proteins did not show effective binding. However, Pf-NPNA-1 scFv-0 and 12, which effectively bound WHcAg after *E. coli* expression (Chapter 3, Figure 3.29), failed to show similar binding when expressed in *Asaia* SF2.1 (Figure 4.11). It is not clear whether the acidic extracellular medium, resulting from the oxidation of glycerol, had any effect on the binding of the scFv. Although the final pH of the extracellular medium was 4.6, purifications of the scFvs were conducted in buffers with basic pH (pH 8). As a result a small difference of 1.5 fold in ELISA signal was observed when crude Pf-NPNA-1 scFv-12 crude extract was compared to that of purified scFv. Low pH (2.3) environments have been shown to affect scFv binding. However, binding is restored by adjusting to neutral pH (6.3) (Yuan *et al.*, 2000). The observations of Yuan *et al.* (2000) are in agreement with other studies in which phage displayed scFvs are eluted with acidic pH buffers and then neutralised with basic buffers.

Therefore, further experiments in the form of stability studies, are required to investigate possible effects of pH on the structure and function of the scFv antibodies.

Chapter 5

General Discussion

5.1 Discussion

Malaria remains a global health problem. The causative agent, *Plasmodium*, remains elusive as current control strategies are incapable of curtailing transmission. Novel vector control strategies are being developed to block development of the parasite within the arthropod vector. Paratransgenesis, which utilises mosquito symbiotic microorganism to secrete anti-parasite molecules that block parasite development, is one proposed approach (Beard *et al.*, 1992; Beard *et al.*, 1998; Yoshida *et al.*, 2001; Riehle and Jacobs-Lorena, 2005; Riehle *et al.*, 2007). It has gained considerable interest and is being developed to control transmission. However, the success of this approach depends on identification of suitable symbiotic bacteria and efficient anti-parasite molecules. Recently an acetic acid bacterium, *Asaia* sp., was identified and shown to be associated with *Anopheles* mosquitoes (Favia *et al.*, 2007; Damiani *et al.*, 2008; Damiani *et al.*, 2010). Genetically modified *Asaia* expressing GFP was capable of colonising the gut, salivary gland, male and female reproduct organs. The GFP-tagged bacteria also showed similar distribution in both *A. stephensi* and *A. gambiae* (Damiani *et al.*, 2010). These characteristics make *Asaia* a suitable bacterial candidate for the delivery of anti-parasite molecules.

Although numerous anti-parasite molecules have been identified (Nirmala and James, 2003), there is the need to identify and evaluate other anti-parasite molecules that target surface ligands required by the parasite for successful establishment within the mosquito. The use of multiple effector molecules will also ensure the long term effectiveness of the approach by preventing development of resistant pathogens. The best targets have been identified as the midgut or late ookinete stages, because of the low numbers, and the salivary glands. Pfs25 expressed on the ookinetes and CS proteins expressed on the sporozoites are potential targets for blocking transmission. Parasite ligands are important targets for effector molecules (Barreau *et al.*, 1995; de Lara Capurro *et al.*, 2000) and has been suggested that targeting the parasite with effector molecules may be more beneficial, imposing less genetic load,

than targeting mosquito tissues (James, 2003). However, no ideal effector molecule has yet been found against *P. falciparum*.

Antibodies hold promise due to their specificity and affinity. The antibodies 4B7 (Barr *et al.*, 1991) and Pf-NPNA-1 (Chappel *et al.*, 2004b) have been isolated against Pfs25 and the repeats of Pf-CS protein, respectively. Application of these antibodies as effector molecules requires prior evaluation in a bacterial system (*E. coli* and subsequently *Asaia* SF2.1) for secretion and functional analysis. Thus, the first and foremost aim of this study was the construction of the antibodies 4B7 and Pf-NPNA-1 in the scFv format with different linker length connecting the variable domains. Varying the linker length between the variable domains has in previous studies, resulted in multimeric assembly. Secondly, the constructed scFvs were expressed in *E. coli* and secreted proteins evaluated for antigen binding. The third aim was evaluation of multimeric assembly by size exclusion chromatography of the purified proteins. Evidence of these multimeric assemblies will facilitate investigation into the contributive effects of antibody avidity to antigen binding. Finally, the scFvs were transferred into a broad-host range vector for expression in the acetic acid bacterium, *Asaia*.

All the scFv constructs were successfully expressed in *E. coli*. Two variants of the 4B7 antibody were expressed. Initial expression of the 4B7 scFv (V_H - V_L) did not show detectable secretion, which was attributed to the presence of charged residues in the N-terminus of the mature protein. The possibility of these charged residues to bind the cell membrane of *E. coli* and cause translocation impairment of the signal peptide were considered. Thus, the scFv constructed in the reverse orientation (V_L - V_H) showed slightly detectable secretion with no antigen binding. After extensive bioinformatic analyses and sequence comparisons, a second variant 4B7 (AJ) obtained by site-directed mutagenesis of framework residues showed detectable levels of secretion and slight antigen binding. These experiments were the first time soluble and functional 4B7 proteins had been produced in *E. coli*. On the other hand, the Pf-NPNA-1 scFv-0 and scFv-12 (V_H - V_L) variants could easily be expressed and secreted without changing the orientation of the variable domains. These

were purified by IMAC and antigen binding evaluated. Specificities of the purified proteins to the repeats of Pf-CS protein were observed in an ELISA. Furthermore, the purified proteins were able to label the entire surface of sporozoites in an IFA. These observations were in agreement with those observed for the Pf-NPNA-1 scFv-27. Unfortunately the low yield of recombinant proteins precluded kinetic analysis by SPR.

In this study, a two-step purification strategy was carried out to purify protein samples to homogeneity. IMAC, which has widespread acceptance and application, was used as the first purification step. It failed to sufficiently purify proteins expressed at low levels compared to proteins expressed at high levels. Contamination or co-elution of low level expressed proteins with *E. coli* native proteins, which exhibit high affinity for divalent cations, has been the subject of many reviews (Bolanos-Garcia and Davies, 2006; Robichon *et al.*, 2011). Native proteins such as wondrous histidine-rich protein (Whp/SlyD, 196 aa, 20.8 kDa, 18 histidines), chloramphenicol acetyltransferase (Cat, 219 aa, 25.5 kDa, 12 histidine), superoxide dismutase (SodA, 195 aa, 8 histidines), Glucosamine-6-phosphate synthase (Glms, 609 aa, 67kDa, 24 histidines), Formyl transferase (YfbG, 660 aa, 74.2 kDa,) and carbonic anhydrase (YadF, 220 aa, 25 kDa, 12 histidines) have been identified as problematic contaminants during IMAC purification (Muller *et al.*, 1998; Bolanos-Garcia and Davies, 2006; Robichon *et al.*, 2011). Most of these proteins were identified as contaminants during purification in this study. Experimental observations made by Bolanos-Garcia and Davies (2006) indicate that these *E. coli* native proteins do not elute under the wash conditions (imidazole concentration of 20 mM) used in this study but rather at imidazole concentrations greater than 50 mM. Elution with low pH or organic solvents (Franken *et al.*, 2000), in order to eliminate these contaminants, were not tested as these strategies might inactivate the proteins. On the other hand, the low pH approach, which results in protonation of the histidine side chain and eventual loss of affinity for divalent metals, may not be capable of discriminating between the eluted protein and contaminant. To address this problem, ion exchange chromatography, anion or cation based on the estimated pI of the protein, was chosen as the second purification strategy.

This strategy also failed to provide homogeneously purified protein except for proteins that were highly expressed. Alternatively, immunoaffinity chromatography using anti-His monoclonal antibodies, could have been used as the second purification step for the proteins expressed at low levels. This approach was employed by Muller *et al.* (1998) to sufficiently purify proteins to homogeneity. However, the approach is time-consuming and has to be optimised based on the properties of each protein. To improve the purity of target protein, genetic engineering of *E. coli* BL21(DE3) has successfully been performed to express native protein contaminants with tags that allowed their rapid removal during the flow through step of IMAC (Robichon *et al.*, 2011). Further studies are needed, in terms of purification strategy, to enhance the yield of recombinant scFv antibodies.

The different scFv antibody constructs facilitated the use of different detection methods. When scFvs are expressed from the pSANG10-3F plasmid, the His-tag was detected on blots and in ELISA with either the rabbit anti-hexahistidine tag antibody conjugated to HRP or the murine monoclonal anti-polyhistidine AP antibody. The tri-FLAG was detected on blots with rabbit anti-tri FLAG antibody as primary antibody and goat anti-rabbit IgG conjugated to AP as secondary antibody. Finally, the HuCk fusion proteins could be detected on blots and ELISA with the goat anti-human kappa light chain antibody conjugated to AP.

Since the recombinant scFv to be expressed via the symbiotic bacteria would lack natural effector functions, it is reasoned that an ability to agglutinate the target could be incorporated by creating a functional self assembling multimer. The multivalent scFv, through site-specific inhibition and cross-linking, could further enhance the potential to reduce vector competence. These cross-linking antibodies would function to immobilise the parasite, thus preventing it from reaching and invading the salivary glands. Reducing the peptide linker length between the V_H and V_L domains has previously been shown to favour spontaneous multimeric assembly (Hudson and Kortt, 1999; Power and Hudson, 2000; Kortt *et al.*, 2001; Power *et al.*, 2001; Power *et al.*, 2003) . Moreover, it has been suggested that the shorter linkers in dimers and trimers

are inaccessible to proteases (Hudson and Kortt, 1999) and may protect the antibody from degradation in the harsh environment of the midgut and salivary glands. The 4B7(AJ) scFv-0 and 20, when expressed in *E. coli* and purified, both showed similar oligomeric patterns: monomer, dimer and higher molecular weight forms. On the contrary, the *Asaia* expressed 4B7(AJ) scFv-0 showed a different oligomeric pattern: monomer and dimer. This observation was attributed to the differences in bacterial strains, expression conditions and folding methods (Arndt *et al.*, 1998). Oligomeric pattern of the *Asaia* expressed 4B7(AJ) scFv-20 could not be assessed as this construct got degraded. The degradation of this construct may possibly indicate the presence of proteases in *Asaia*, different from those of *E. coli*, that may have recognised a sequence within the 4B7 (AJ) scFv-20 gene fragment, which led to its degradation during expression.

After successful expression of the scFv antibodies in *E. coli*, the scFv DNA fragments were cloned into a newly constructed vector, pMAK031 2P. This new vector maintained the advantageous features of the original vector, pHM2- a constitutive kanamycin promoter and a broad-host range origin of replication that allowed switching between expression hosts (*E. coli* and *Asaia*). The new vector also allowed the direct cloning of V_H and V_K with the introduction of two rare-cutting restriction enzyme sites (*NcoI* and *NotI*). In this investigation scFv antibodies were successfully expressed in the acetic acid bacterium *Asaia* SF2.1. To my knowledge, this is the first report of recombinant expression of scFvs in *Asaia*. Western blots of expressed proteins indicated that the *pefB* signal peptide was correctly processed facilitating the scFv antibodies into the periplasm for correct folding. Although cysteine oxidation by Dsb proteins in the periplasm of *E. coli* have been investigated in greater detail, correct disulphide bond formation of scFv antibodies in *Asaia* have not been demonstrated. Proteolytic fragmentation and mass spectrometric analysis of the fragments would have been the most accurate procedure to demonstrate the correct intramolecular disulphide bond formation in the *Asaia* secreted scFv antibodies. This approach was not undertaken due to the low amounts of proteins secreted. However,

comparison of the electrophoretic mobility of *E. coli* and *Asaia* secreted proteins by reducing and non-reducing SDS-PAGE showed similar mobilities, an indication of correctly formed intramolecular disulphide bonds. On the other hand, the *Asaia* expressed Pf-NPNA-1 scFvs did not demonstrate similar binding properties to those of *E. coli* produced scFv antibodies.

Finally, it can be concluded that the recombinant 4B7 and Pf-NPNA-1 scFv antibodies cloned and expressed in these studies could potentially be included in the arsenal of effector molecules for application in symbiotic control of malaria.

Chapter 6

Conclusion and Future work

6.1 Conclusion

The aim of the study was to use *E. coli* as a model bacterium and the acetic acid bacterium, *Asaia* SF2.1, for expression, secretion and functional analysis of two scFv antibodies (4B7 and Pf-NPNA-1) previously identified as effector molecules. Plasmid constructs of both scFvs were first expressed in *E. coli* and subsequently in *Asaia*.

For the scFv 4B7, in the V_H - V_L orientation, periplasmic secretion could not be attained due to association of the protein to the bacterial cell wall and the presence of N-terminal charged residues. Subsequent orientation of the variable domains (V_L - V_H) led to detectable levels of secretion into the periplasm but no antigen binding. Site-directed mutagenesis of seven framework residues, obtained by sequence comparison of two 4B7 gene sequences that have 95% sequence identity between them, did not show significant improvement in antigen binding. However, two variants of the mutant 4B7, scFv-0 and scFv-20, both formed monomers, dimers and higher molecular weight forms. Fusion of the human kappa constant domain resulted in higher secretion of recombinant scFv-20. The fusion proteins, scFv-0Hk and scFv-20 both formed monomer and higher molecular multimer. Very low antigen binding was also observed for these fusion proteins.

The two variants of Pf-NPNA-1, scFv-0 and scFv-12, in the V_H - V_L format could easily be expressed and secreted in *E. coli* without the need to swap variable domains. The pSANG-103F expression plasmid showed a higher level of expression compared to the other two expression plasmids. This was in agreement with the ELISA studies. The fusion of HuCk did not improve the expression levels of the Pf-NPNA-1 scFv-0 and scFv-12. However, both scFv variants labelled the entire surface of sporozoites in an IFA.

Transfer of the 4B7 and Pf-NPNA-1 scFv gene fragments into the broad-host range plasmid, pMAK0312P, and transformation into *Asaia* SF2.1 showed the capability of this acetic acid bacterium to express disulphide containing proteins. Moreover, *Asaia* efficiently processed the *pelB* signal peptide to

allow translocation of the scFv antibodies into the periplasm for proper disulphide bond formation. Although the *Asaia* expressed Pf-NPNA-1 scFv-12 showed antigen binding, the binding was not comparable to those of *E. coli* expressed ones.

6.2 Future work

6.2.1 Multimeric assembly of scFv

Evidence from this study has shown that the 4B7 and Pf-NPNA-1 scFvs are capable of multimeric assembly. However, the higher ordered multimers could not be evaluated for antigen binding due to the low yield of recombinant proteins obtained after isolation and purification. A limitation of IMAC was the inability to efficiently purify proteins expressed at very low levels. For further characterisation of scFv multimers large scale expression as described by Power *et al.* (2003) could be carried out and the purification strategies optimised to obtain high yields of recombinant proteins. To avoid co-elution of native *E. coli* proteins during the purification process, the BL21(DE3) *E. coli* strains engineered by Robichon *et al.* (2011) could be used for expression of the recombinant proteins. The immunoaffinity chromatography strategy of Muller *et al.* (1998) could then be adopted for efficient and homogenous protein purification. After purification of the protein to homogeneity, multimeric assembly could be evaluated by size exclusion chromatography. Multimers may then be assayed for antigen binding by ELISA and competitive ELISA. Furthermore, the avidity effects of the multimers could be evaluated by SPR on a BIACORE.

6.2.2 Homology modelling and affinity enhancement of scFv 4B7

For antibodies that do not have completely resolved three dimensional structures, the availability of data on the canonical structures of previously resolved antibody structures has facilitated their structural prediction through homology modelling. Homology modelling has previously been used to change the binding properties or increase the affinity of antibodies by identifying key amino acids involved in the antigen-antibody interaction. Based on these models, mutational analysis studies by application of site-directed or random mutagenesis have helped in the identification of antibodies with improved properties (Casipit *et al.*, 1998; Hemminki *et al.*, 1998; Kusharyoto *et al.*, 2002; Farady *et al.*, 2009). In agreement with the study by Stura *et al.* (1994), Sharma (2008) through computer-aided modelling and docking experiments identified a major interaction of the EGF III domain of Pfs25 with the heavy chain of scFv 4B7. According to the model of the complex, six hydrogen bonds were formed in the heavy chain and one in the light of the antibody; outlined in the Table 6.1 below.

Amino acid	Position on antibody Fv
Thr 28	V _H FR1
Asn 53	V _H CDR2
Asn 74	V _H FR3
Leu 101	V _H CDR3
Asp 106	V _H CDR3
Tyr 49	V _L FR2

Table 6.1: Amino acids identified to form hydrogen bonds with the third EGF domain during interaction of scFv 4B7 with Pfs25 (Sharma, 2008).

Based on Sharma (2008) model, the amino acids listed above may be key residues that contribute to antigen binding. A rational design could then be undertaken to investigate the molecular basis of the antibody's specificity and to improve its affinity by site-directed mutagenesis. Hence, mutations of both heavy chain and light chain residues within the predicted binding pockets can be modelled and the corresponding effect experimentally determined by ELISA and surface Plasmon resonance (SPR).

6.2.3 Extracellular secretion of recombinant scFvs in *Asaia* sp. SF2.1

Evidence from the preliminary expression studies showed that *Asaia* sp. SF2.1 is capable of expressing the recombinant scFvs and proteolytic processing of the signal peptide. For paratransgenic application the *pelB* signal peptide used may not be useful as the expressed scFv would accumulate in periplasm and will be released only upon bacterial death. Ultimately, extracellular secretion of the scFv from *Asaia* into the surroundings of the midgut or salivary glands would bring the recombinant scFv in direct contact with the parasite. Currently, bacterial leader sequences known to transport proteins into the extracellular medium are being evaluated. Alternatively, three other strategies could be adopted for extracellular secretion or display of the scFv antibodies. Firstly, the extracellular proteome of *Asaia* could be analysed using proteomic techniques such as two-dimensional electrophoresis (2-DE) to identify naturally secreted proteins. Potentially, these proteins may be utilised as fusion partners for extracellular production of the recombinant scFvs. Recently, Qian and colleagues reported extracellular secretion of three model proteins from *E. coli* by fusing them to naturally excreted protein that were identified by a proteome-based approach (Qian *et al.*, 2008). Secondly, extracellular delivery of the scFv antibodies could be achieved by utilising the hemolysin export apparatus (Fernandez *et al.*, 2000; Fernandez and de Lorenzo, 2001; Li *et al.*, 2002; Fraile *et al.*, 2004). Proteins secreted by this pathway are directed to the extracellular medium without a periplasmic intermediate. This secretion system has been shown to support secretion of disulphide-containing proteins (Fernandez *et al.*, 2000; Fernandez and de Lorenzo, 2001). Advantages of the hemolysin secretion system are its low toxicity on the producing cell and reduction in protein aggregation (Fernández *et al.*, 2000). Thirdly, the Lpp'OmpA (lipoprotein-outer membrane protein A) surface display approach used by Riehle *et al.* (2007) could be also adopted. The display of peptides or proteins is facilitated by the fusion of a truncated form of OmpA and the signal peptide of the outer membrane lipoprotein. This approach was successfully used to display SM1 and PLA2 on the surface of *E. coli*.

6.2.4 Evaluation of scFv expression in *Anopheles* and its impact on parasite load

In this study, *in vitro* experiments have demonstrated the capability of *Asaia* to express disulphide-containing proteins. Overall, the expression and secretion studies satisfy two of the three key components of paratransgenesis suggested by Riehle *et al.* (2007): effector molecules that inhibit *Plasmodium* development; mechanism for expressing and secreting the effector molecule in the symbiotic bacterium. Further *in vivo* expression studies, within *Anopheles* midgut and salivary glands, could then be conducted to assess expression and the effect of the effector molecule on *Plasmodium* development. Colonisation of the mosquito by recombinant *Asaia* could be performed according to the method outlined by Favia *et al.* (2007). A time course experiment could be carried out by preparing gut and salivary gland extracts of *Asaia* fed mosquitoes (control and test strains) and the homogenates assayed by PCR and Western blot for the presence of recombinant *Asaia* SF2.1 and expression of recombinant scFvs. Subsequently, the impact of the *in vivo* expressed antibodies on *Plasmodium* development can be investigated in transmission blocking experiments as described (Lobo *et al.*, 1999).

REFERENCES

- Abraham, E.G., Donnelly-Doman, M., Fujioka, H., Ghosh, A., Moreira, L. and Jacobs-Lorena, M. (2005). Driving midgut-specific expression and secretion of a foreign protein in transgenic mosquitoes with AgAper1 regulatory elements. *Insect Mol Biol.* **14**, 271-9.
- Aksoy, S. (2003). Control of tsetse flies and trypanosomes using molecular genetics. *Vet Parasitol.* **115**, 125-45.
- Aksoy, S., Weiss, B. and Attardo, G. (2008). Paratransgenesis applied for control of tsetse transmitted sleeping sickness. *Adv Exp Med Biol.* **627**, 35-48.
- Alavi, Y., Arai, M., Mendoza, J., Tufet-Bayona, M., Sinha, R., Fowler, K., *et al.* (2003). The dynamics of interactions between Plasmodium and the mosquito: a study of the infectivity of Plasmodium berghei and Plasmodium gallinaceum, and their transmission by Anopheles stephensi, Anopheles gambiae and Aedes aegypti. *Int J Parasitol.* **33**, 933-43.
- Albrecht, H., Denardo, G.L. and Denardo, S.J. (2006). Monospecific bivalent scFv-SH: effects of linker length and location of an engineered cysteine on production, antigen binding activity and free SH accessibility. *J Immunol Methods.* **310**, 100 - 116.
- Ano, Y., Toyama, H., Adachi, O. and Matsushita, K. (2008). Energy metabolism of a unique acetic acid bacterium, Asaia bogorensis, that lacks ethanol oxidation activity. *Biosci Biotechnol Biochem.* **72**, 989-97.
- Anxolabehere, D., Kidwell, M.G. and Periquet, G. (1988). Molecular characteristics of diverse populations are consistent with the hypothesis of a recent invasion of Drosophila melanogaster by mobile P elements. *Mol Biol Evol.* **5**, 252-69.
- Arakawa, T., Komesu, A., Otsuki, H., Sattabongkot, J., Udomsangpetch, R., Matsumoto, Y., *et al.* (2005). Nasal immunization with a malaria transmission-blocking vaccine candidate, Pfs25, induces complete protective immunity in mice against field isolates of Plasmodium falciparum. *Infect Immun.* **73**, 7375-80.
- Arndt, K.M., Muller, K.M. and Pluckthun, A. (1998). Factors influencing the dimer to monomer transition of an antibody single-chain Fv fragment. *Biochemistry.* **37**, 12918-26.
- Arrighi, R.B., Nakamura, C., Miyake, J., Hurd, H. and Burgess, J.G. (2002). Design and activity of antimicrobial peptides against sporogonic-stage parasites causing murine malarial. *Antimicrob Agents Chemother.* **46**, 2104-10.
- Atwell, J.L., Breheney, K.A., Lawrence, L.J., McCoy, A.J., Kortt, A.A. and Hudson, P.J. (1999). scFv multimers of the anti-neuraminidase antibody NC10: length of the linker between VH and VL domains dictates precisely the transition between diabodies and triabodies. *Protein Eng.* **12**, 597-604.
- Ayala, M., Balint, R.F., Fernandez-De-Cossio, L., Canaan-Haden, J.W., Larrick, J.W. and Gavilondo, J.V. (1995). Variable region sequence modulates periplasmic export of a single-chain Fv antibody fragment in Escherichia coli. *Biotechniques.* **18**, 832, 835-8, 840-2.

- Ballou, W.R., Hoffman, S.L., Sherwood, J.A., Hollingdale, M.R., Neva, F.A., Hockmeyer, W.T., *et al.* (1987). Safety and efficacy of a recombinant DNA Plasmodium falciparum sporozoite vaccine. *Lancet*. **1**, 1277-81.
- Ballou, W.R. (2009). The development of the RTS,S malaria vaccine candidate: challenges and lessons. *Parasite Immunol*. **31**, 492-500.
- Bannister, L. and Mitchell, G. (2003). The ins, outs and roundabouts of malaria. *Trends Parasitol*. **19**, 209-13.
- Baquero, F., Martinez, J.L. and Canton, R. (2008). Antibiotics and antibiotic resistance in water environments. *Curr Opin Biotechnol*. **19**, 260-5.
- Bardwell, J.C. (1994). Building bridges: disulphide bond formation in the cell. *Mol Microbiol*. **14**, 199-205.
- Barr, P.J., Green, K.M., Gibson, H.L., Bathurst, I.C., Quakyi, I.A. and Kaslow, D.C. (1991). Recombinant Pfs25 protein of Plasmodium falciparum elicits malaria transmission-blocking immunity in experimental animals. *J Exp Med*. **174**, 1203-8.
- Barreau, C., Touray, M., Pimenta, P.F., Miller, L.H. and Vernick, K.D. (1995). Plasmodium gallinaceum: sporozoite invasion of Aedes aegypti salivary glands is inhibited by anti-gland antibodies and by lectins. *Exp Parasitol*. **81**, 332-43.
- Barreau, C., Conrad, J., Fischer, E., Lujan, H.D. and Vernick, K.D. (1999). Identification of surface molecules on salivary glands of the mosquito, Aedes aegypti, by a panel of monoclonal antibodies. *Insect Biochem Mol Biol*. **29**, 515-26.
- Beard, C.B., Mason, P.W., Aksoy, S., Tesh, R.B. and Richards, F.F. (1992). Transformation of an insect symbiont and expression of a foreign gene in the Chagas' disease vector Rhodnius prolixus. *Am J Trop Med Hyg*. **46**, 195-200.
- Beard, C.B., Durvasula, R.V. and Richards, F.F. (1998). Bacterial symbiosis in arthropods and the control of disease transmission. *Emerg Infect Dis*. **4**, 581-91.
- Beard, C.B., Dotson, E.M., Pennington, P.M., Eichler, S., Cordon-Rosales, C. and Durvasula, R.V. (2001). Bacterial symbiosis and paratransgenic control of vector-borne Chagas disease. *Int J Parasitol*. **31**, 621-7.
- Beard, C.B., Cordon-Rosales, C. and Durvasula, R.V. (2002). Bacterial symbionts of the triatominae and their potential use in control of Chagas disease transmission. *Annu Rev Entomol*. **47**, 123-41.
- Benhar, I. and Pastan, I. (1995). Identification of residues that stabilize the single-chain Fv of monoclonal antibodies B3. *J Biol Chem*. **270**, 23373-80.
- Better, M., Chang, C.P., Robinson, R.R. and Horwitz, A.H. (1988). Escherichia coli secretion of an active chimeric antibody fragment. *Science*. **240**, 1041-3.
- Bextine, B., Lauzon, C., Potter, S., Lampe, D. and Miller, T.A. (2004). Delivery of a genetically marked Alcaligenes sp. to the glassy-winged sharpshooter for use in a paratransgenic control strategy. *Curr Microbiol*. **48**, 327-31.
- Bhattarai, A., Ali, A.S., Kachur, S.P., Martensson, A., Abbas, A.K., Khatib, R., *et al.* (2007). Impact of artemisinin-based combination therapy and insecticide-treated nets on malaria burden in Zanzibar. *PLoS Med*. **4**, e309.

- Billaud, J.N., Peterson, D., Barr, M., Chen, A., Sallberg, M., Garduno, F., *et al.* (2005). Combinatorial approach to hepadnavirus-like particle vaccine design. *J Virol.* **79**, 13656-66.
- Bird, R.E., Hardman, K.D., Jacobson, J.W., Johnson, S., Kaufman, B.M., Lee, S.M., *et al.* (1988). Single-chain antigen-binding proteins. *Science.* **242**, 423-6.
- Blair, C.D., Adelman, Z.N. and Olson, K.E. (2000). Molecular strategies for interrupting arthropod-borne virus transmission by mosquitoes. *Clin Microbiol Rev.* **13**, 651-61.
- Blandin, S. and Levashina, E.A. (2004). Mosquito immune responses against malaria parasites. *Curr Opin Immunol.* **16**, 16-20.
- Blanford, S., Thomas, M.B. and Langewald, J. (1998). Behavioural fever in the Senegalese grasshopper, *Oedaleus senegalensis*, and its implications for biological control using pathogens. *Ecol. Entomol.* **23**, 9–14.
- Blanford, S. and Thomas, M.B. (1999). Host-thermal biology: the key to understanding host–pathogen interactions and microbial pest control? *Agr. Forest Entomol.* **1**, 195–202.
- Blanford, S. and Thomas, M.B. (2001). Adult survival, maturation, and reproduction of the desert locust *Schistocerca gregaria* infected with the fungus *Metarhizium anisopliae* var *acridum*. *J Invertebr Pathol.* **78**, 1-8.
- Blanford, S., Chan, B.H., Jenkins, N., Sim, D., Turner, R.J., Read, A.F., *et al.* (2005). Fungal pathogen reduces potential for malaria transmission. *Science.* **308**, 1638-41.
- Blanford, S., Read, A.F. and Thomas, M.B. (2009). Thermal behaviour of *Anopheles stephensi* in response to infection with malaria and fungal entomopathogens. *Malar J.* **8**, 72.
- Bolanos-Garcia, V.M. and Davies, O.R. (2006). Structural analysis and classification of native proteins from *E. coli* commonly co-purified by immobilised metal affinity chromatography. *Biochim Biophys Acta.* **1760**, 1304-13.
- Boulanger, N., Matile, H. and Betschart, B. (1988). Formation of the circumsporozoite protein of *Plasmodium falciparum* in *Anopheles stephensi*. *Acta Trop.* **45**, 55-65.
- Boyd, D. and Beckwith, J. (1989). Positively charged amino acid residues can act as topogenic determinants in membrane proteins. *Proc Natl Acad Sci U S A.* **86**, 9446-50.
- Bradford, M.M. (1976). A rapid and sensitive method for the quantitation of microgram quantities of protein utilizing the principle of protein-dye binding. *Anal Biochem.* **72**, 248-54.
- Brégère, F., England, P., Djavadi-Ohanian, L. and Bedouelle, H. (1997). Recognition of *E. coli* tryptophan synthase by single-chain Fv fragments: comparison of PCR-cloning variants with the parental antibodies. *J Mol Recognit.* **10**, 169-81.
- Brennan, J.D., Kent, M., Dhar, R., Fujioka, H. and Kumar, N. (2000). *Anopheles gambiae* salivary gland proteins as putative targets for blocking transmission of malaria parasites. *Proc Natl Acad Sci U S A.* **97**, 13859-64.

- Bukhari, T., Middelmann, A., Koenraadt, C.J., Takken, W. and Knols, B.G. (2010). Factors affecting fungus-induced larval mortality in *Anopheles gambiae* and *Anopheles stephensi*. *Malar J.* **9**, 22.
- Burkot, T.R., Da, Z.W., Geysen, H.M., Wirtz, R.A. and Saul, A. (1991). Fine specificities of monoclonal antibodies against the *Plasmodium falciparum* circumsporozoite protein: recognition of both repetitive and non-repetitive regions. *Parasite Immunol.* **13**, 161-70.
- Byrne, F.R., Grant, S.D., Porter, A.J. and Harris, W.J. (1996). Cloning, expression and characterisation of a single-chain antibody specific for the herbicide atrazine. *Food Agric. Immunol.* **8**, 19–29.
- Carlson, J., Olson, K., Higgs, S. and Beaty, B. (1995). Molecular genetic manipulation of mosquito vectors. *Annu Rev Entomol.* **40**, 359-88.
- Carlson, J., Suchman, E. and Buchatsky, L. (2006). Dengoviruses for control and genetic manipulation of mosquitoes. *Adv Virus Res.* **68**, 361-92.
- Carvalho, L.J., Daniel-Ribeiro, C.T. and Goto, H. (2002). Malaria vaccine: candidate antigens, mechanisms, constraints and prospects. *Scand J Immunol.* **56**, 327-43.
- Casipit, C.L., Tal, R., Wittman, V., Chavallaz, P.A., Arbuthnott, K., Weidanz, J.A., *et al.* (1998). Improving the binding affinity of an antibody using molecular modeling and site-directed mutagenesis. *Protein Sci.* **7**, 1671-80.
- Catteruccia, F., Nolan, T., Loukeris, T.G., Blass, C., Savakis, C., Kafatos, F.C., *et al.* (2000). Stable germline transformation of the malaria mosquito *Anopheles stephensi*. *Nature.* **405**, 959-62.
- Chappel, J.A., Hollingdale, M.R. and Kang, A.S. (2004a). IgG(4) Pf NPNA-1 a human anti-*Plasmodium falciparum* sporozoite monoclonal antibody cloned from a protected individual inhibits parasite invasion of hepatocytes. *Hum Antibodies.* **13**, 91-6.
- Chappel, J.A., Rogers, W.O., Hoffman, S.L. and Kang, A.S. (2004b). Molecular dissection of the human antibody response to the structural repeat epitope of *Plasmodium falciparum* sporozoite from a protected donor. *Malar J.* **3**, 28.
- Chen, H., Bjerknes, M., Kumar, R. and Jay, E. (1994). Determination of the optimal aligned spacing between the Shine-Dalgarno sequence and the translation initiation codon of *Escherichia coli* mRNAs. *Nucleic Acids Res.* **22**, 4953-7.
- Cheng, Q. and Aksoy, S. (1999). Tissue tropism, transmission and expression of foreign genes in vivo in midgut symbionts of tsetse flies. *Insect Mol Biol.* **8**, 125-32.
- Choi, J.H. and Lee, S.Y. (2004). Secretory and extracellular production of recombinant proteins using *Escherichia coli*. *Appl Microbiol Biotechnol.* **64**, 625-35.
- Chothia, C., Lesk, A.M., Gherardi, E., Tomlinson, I.M., Walter, G., Marks, J.D., *et al.* (1992). Structural repertoire of the human VH segments. *J Mol Biol.* **227**, 799-817.
- Chouaia, B., Rossi, P., Montagna, M., Ricci, I., Crotti, E., Damiani, C., *et al.* (2010). Molecular evidence for multiple infections as revealed by typing of *Asaia* bacterial symbionts of four mosquito species. *Appl Environ Microbiol.* **76**, 7444-50.

- Chowdhury, P.S., Vasmatzis, G., Beers, R., Lee, B. and Pastan, I. (1998). Improved stability and yield of a Fv-toxin fusion protein by computer design and protein engineering of the Fv. *J Mol Biol.* **281**, 917-28.
- Clyde, D.F., Most, H., Mccarthy, V.C. and Vanderberg, J.P. (1973). Immunization of man against sporozite-induced falciparum malaria. *Am J Med Sci.* **266**, 169-77.
- Clyde, D.F. (1975). Immunization of man against falciparum and vivax malaria by use of attenuated sporozoites. *Am J Trop Med Hyg.* **24**, 397-401.
- Collet, J.F. and Bardwell, J.C. (2002). Oxidative protein folding in bacteria. *Mol Microbiol.* **44**, 1-8.
- Conde, R., Zamudio, F.Z., Rodriguez, M.H. and Possani, L.D. (2000). Scorpine, an anti-malaria and anti-bacterial agent purified from scorpion venom. *FEBS Lett.* **471**, 165-8.
- Conte, J.E., Jr. (1997). A novel approach to preventing insect-borne diseases. *N Engl J Med.* **337**, 785-6.
- Corby-Harris, V., Drexler, A., De Jong, L.W., Antonova, Y., Pakpour, N., Ziegler, R., *et al.* (2010). Activation of Akt Signaling Reduces the Prevalence and Intensity of Malaria Parasite Infection and Lifespan in *Anopheles stephensi* Mosquitoes. *PLoS Pathog.* **6**, 1-10.
- Coutinho-Abreu, I.V., Zhu, K.Y. and Ramalho-Ortigao, M. (2010). Transgenesis and paratransgenesis to control insect-borne diseases: current status and future challenges. *Parasitol Int.* **59**, 1-8.
- Crotti, E., Damiani, C., Pajoro, M., Gonella, E., Rizzi, A., Ricci, I., *et al.* (2009). *Asaia*, a versatile acetic acid bacterial symbiont, capable of cross-colonizing insects of phylogenetically distant genera and orders. *Environ Microbiol.* **11**, 3252-64.
- Crotti, E., Rizzi, A., Chouaia, B., Ricci, I., Favia, G., Alma, A., *et al.* (2010). Acetic acid bacteria, newly emerging symbionts of insects. *Appl Environ Microbiol.* **76**, 6963-70.
- Dalboge, H., Carlsen, S., Jensen, E.B., Christensen, T. and Dahl, H.H. (1988). Expression of recombinant growth hormone in *Escherichia coli*: effect of the region between the Shine-Dalgarno sequence and the ATG initiation codon. *DNA.* **7**, 399-405.
- Damiani, C., Ricci, I., Crotti, E., Rossi, P., Rizzi, A., Scuppa, P., *et al.* (2008). Paternal transmission of symbiotic bacteria in malaria vectors. *Curr Biol.* **18**, R1087-8.
- Damiani, C., Ricci, I., Crotti, E., Rossi, P., Rizzi, A., Scuppa, P., *et al.* (2010). Mosquito-Bacteria Symbiosis: The Case of *Anopheles gambiae* and *Asaia*. *Microb Ecol.*
- De Boer, H.A., Comstock, L.J., Hui, A., Wong, E. and Vasser, M. (1983). Portable Shine-Dalgarno regions; nucleotides between the Shine-Dalgarno sequence and the start codon affect the translation efficiency. *Gene Amplif Anal.* **3**, 103-16.
- De Haard, H.J., Kazemier, B., Van Der Bent, A., Oudshoorn, P., Boender, P., Van Gemen, B., *et al.* (1998). Absolute conservation of residue 6 of immunoglobulin heavy chain variable regions of class IIA is required for correct folding. *Protein Eng.* **11**, 1267-76.
- De Lara Capurro, M., Coleman, J., Beerntsen, B.T., Myles, K.M., Olson, K.E., Rocha, E., *et al.* (2000). Virus-expressed, recombinant single-chain

- antibody blocks sporozoite infection of salivary glands in *Plasmodium gallinaceum*-infected *Aedes aegypti*. *Am J Trop Med Hyg.* **62**, 427-33.
- Delisa, M.P., Tullman, D. and Georgiou, G. (2003). Folding quality control in the export of proteins by the bacterial twin-arginine translocation pathway. *Proc Natl Acad Sci U S A.* **100**, 6115-20.
- Desplancq, D., King, D.J., Lawson, A.D. and Mountain, A. (1994). Multimerization behaviour of single chain Fv variants for the tumour-binding antibody B72.3. *Protein Eng.* **7**, 1027-33.
- Dimopoulos, G., Richman, A., Muller, H.M. and Kafatos, F.C. (1997). Molecular immune responses of the mosquito *Anopheles gambiae* to bacteria and malaria parasites. *Proc Natl Acad Sci U S A.* **94**, 11508-13.
- Dinglasan, R.R., Kalume, D.E., Kanzok, S.M., Ghosh, A.K., Muratova, O., Pandey, A., *et al.* (2007). Disruption of *Plasmodium falciparum* development by antibodies against a conserved mosquito midgut antigen. *Proc Natl Acad Sci U S A.* **104**, 13461-6.
- Dolezal, O., Pearce, L.A., Lawrence, L.J., McCoy, A.J., Hudson, P.J. and Kortt, A.A. (2000). ScFv multimers of the anti-neuraminidase antibody NC10: shortening of the linker in single-chain Fv fragment assembled in V(L) to V(H) orientation drives the formation of dimers, trimers, tetramers and higher molecular mass multimers. *Protein Eng.* **13**, 565-74.
- Dong, Y., Taylor, H.E. and Dimopoulos, G. (2006). AgDscam, a hypervariable immunoglobulin domain-containing receptor of the *Anopheles gambiae* innate immune system. *PLoS Biol.* **4**, e229.
- Duffy, P.E., Pimenta, P. and Kaslow, D.C. (1993). Pgs28 belongs to a family of epidermal growth factor-like antigens that are targets of malaria transmission-blocking antibodies. *J Exp Med.* **177**, 505-10.
- Duffy, P.E. and Kaslow, D.C. (1997). A novel malaria protein, Pfs28, and Pfs25 are genetically linked and synergistic as *falciparum* malaria transmission-blocking vaccines. *Infect Immun.* **65**, 1109-13.
- Durvasula, R.V., Gumbs, A., Panackal, A., Kruglov, O., Aksoy, S., Merrifield, R.B., *et al.* (1997). Prevention of insect-borne disease: an approach using transgenic symbiotic bacteria. *Proc Natl Acad Sci U S A.* **94**, 3274-8.
- Durvasula, R.V., Gumbs, A., Panackal, A., Kruglov, O., Taneja, J., Kang, A.S., *et al.* (1999). Expression of a functional antibody fragment in the gut of *Rhodnius prolixus* via transgenic bacterial symbiont *Rhodococcus rhodnii*. *Med Vet Entomol.* **13**, 115-9.
- Durvasula, R.V., Sundaram, R.K., Kirsch, P., Hurwitz, I., Crawford, C.V., Dotson, E., *et al.* (2008). Genetic transformation of a *Corynebacterial* symbiont from the Chagas disease vector *Triatoma infestans*. *Exp Parasitol.* **119**, 94-8.
- El-Mezawy, A., Soliman, N.E. and Mostafa, H.E. (2005). Cloning and expression of extracellular β -galactosidase gene in *Gluconobacter oxydans*. *Arab J. Biotech.* **8**, 223 - 230.
- Elliot, S.L., Blanford, S. and Thomas, M.B. (2002). Host-pathogen interactions in a varying environment: temperature, behavioural fever and fitness. *Proc Biol Sci.* **269**, 1599-607.

- Fang, W., Vega-Rodriguez, J., Ghosh, A.K., Jacobs-Lorena, M., Kang, A. and St Leger, R.J. (2011). Development of transgenic fungi that kill human malaria parasites in mosquitoes. *Science*. **331**, 1074-7.
- Farady, C.J., Sellers, B.D., Jacobson, M.P. and Craik, C.S. (2009). Improving the species cross-reactivity of an antibody using computational design. *Bioorg Med Chem Lett*. **19**, 3744-7.
- Farenhorst, M. and Knols, B.G. (2007). Fungal entomopathogens for the control of adult mosquitoes: a look at the issues. *Proc Neth Entomol Soc Meeting*. **18**, 51–59.
- Farenhorst, M., Mouatcho, J.C., Kikankie, C.K., Brooke, B.D., Hunt, R.H., Thomas, M.B., *et al.* (2009). Fungal infection counters insecticide resistance in African malaria mosquitoes. *Proc Natl Acad Sci U S A*. **106**, 17443-7.
- Farenhorst, M., Knols, B.G., Thomas, M.B., Howard, A.F., Takken, W., Rowland, M., *et al.* (2010). Synergy in efficacy of fungal entomopathogens and permethrin against West African insecticide-resistant *Anopheles gambiae* mosquitoes. *PLoS One*. **5**, e12081.
- Favia, G., Ricci, I., Damiani, C., Raddadi, N., Crotti, E., Marzorati, M., *et al.* (2007). Bacteria of the genus *Asaia* stably associate with *Anopheles stephensi*, an Asian malarial mosquito vector. *Proc Natl Acad Sci U S A*. **104**, 9047-51.
- Federici, B.A. (1995). The future of microbial insecticides as vector control agents. *J Am Mosq Control Assoc*. **11**, 260-8.
- Fernandez, L.A., Sola, I., Enjuanes, L. and De Lorenzo, V. (2000). Specific secretion of active single-chain Fv antibodies into the supernatants of *Escherichia coli* cultures by use of the hemolysin system. *Appl Environ Microbiol*. **66**, 5024-9.
- Fernandez, L.A. and De Lorenzo, V. (2001). Formation of disulphide bonds during secretion of proteins through the periplasmic-independent type I pathway. *Mol Microbiol*. **40**, 332-46.
- Fidock, D.A., Nomura, T., Talley, A.K., Cooper, R.A., Dzekunov, S.M., Ferdig, M.T., *et al.* (2000). Mutations in the *P. falciparum* digestive vacuole transmembrane protein PfCRT and evidence for their role in chloroquine resistance. *Mol Cell*. **6**, 861-71.
- Foote, J. and Winter, G. (1992). Antibody framework residues affecting the conformation of the hypervariable loops. *J Mol Biol*. **224**, 487-99.
- Forsberg, G., Forsgren, M., Jaki, M., Norin, M., Sterky, C., Enhörning, A., *et al.* (1997). Identification of Framework Residues in a Secreted Recombinant Antibody Fragment That Control Production Level and Localization in *Escherichia coli*. *J Biol Chem*. **272**, 12430–12436.
- Fraile, S., Munoz, A., De Lorenzo, V. and Fernandez, L.A. (2004). Secretion of proteins with dimerization capacity by the haemolysin type I transport system of *Escherichia coli*. *Mol Microbiol*. **53**, 1109-21.
- Franken, K.L., Hiemstra, H.S., Van Meijgaarden, K.E., Subronto, Y., Den Hartigh, J., Ottenhoff, T.H., *et al.* (2000). Purification of his-tagged proteins by immobilized chelate affinity chromatography: the benefits from the use of organic solvent. *Protein Expr Purif*. **18**, 95-9.
- Freund, C., Honegger, A., Hunziker, P., Holak, T.A. and Pluckthun, A. (1996). Folding nuclei of the scFv fragment of an antibody. *Biochemistry*. **35**, 8457-64.

- Frevert, U., Sinnis, P., Cerami, C., Shreffler, W., Takacs, B. and Nussenzweig, V. (1993). Malaria circumsporozoite protein binds to heparan sulfate proteoglycans associated with the surface membrane of hepatocytes. *J Exp Med.* **177**, 1287-98.
- Frevert, U., Galinski, M.R., Hugel, F.U., Allon, N., Schreier, H., Smulevitch, S., *et al.* (1998). Malaria circumsporozoite protein inhibits protein synthesis in mammalian cells. *Embo J.* **17**, 3816-26.
- Froyen, G., Hendrix, D., Ronsse, I., Fiten, P., Martens, E. and Billiau, A. (1995). Effect of VH and VL consensus sequence-specific primers on the binding and neutralizing potential of a single-chain Fv directed towards HULFN-gamma. *Mol Immunol.* **32**, 515-21.
- Garcia, J.E., Puentes, A. and Patarroyo, M.E. (2006). Developmental biology of sporozoite-host interactions in *Plasmodium falciparum* malaria: implications for vaccine design. *Clin Microbiol Rev.* **19**, 686-707.
- Ghosh, A., Edwards, M.J. and Jacobs-Lorena, M. (2000). The journey of the malaria parasite in the mosquito: hopes for the new century. *Parasitol Today.* **16**, 196-201.
- Ghosh, A.K., Ribolla, P.E. and Jacobs-Lorena, M. (2001). Targeting *Plasmodium* ligands on mosquito salivary glands and midgut with a phage display peptide library. *Proc Natl Acad Sci U S A.* **98**, 13278-81.
- Gonzalez-Ceron, L., Santillan, F., Rodriguez, M.H., Mendez, D. and Hernandez-Avila, J.E. (2003). Bacteria in midguts of field-collected *Anopheles albimanus* block *Plasmodium vivax* sporogonic development. *J Med Entomol.* **40**, 371-4.
- Griffiths, A.D., Malmqvist, M., Marks, J.D., Bye, J.M., Embleton, M.J., McCafferty, J., *et al.* (1993). Human anti-self antibodies with high specificity from phage display libraries. *Embo J.* **12**, 725-34.
- Grossman, G.L., Rafferty, C.S., Clayton, J.R., Stevens, T.K., Mukabayire, O. and Benedict, M.Q. (2001). Germline transformation of the malaria vector, *Anopheles gambiae*, with the piggyBac transposable element. *Insect Mol Biol.* **10**, 597-604.
- Gwadz, R.W., Kaslow, D., Lee, J.Y., Maloy, W.L., Zasloff, M. and Miller, L.H. (1989). Effects of magainins and cecropins on the sporogonic development of malaria parasites in mosquitoes. *Infect Immun.* **57**, 2628-33.
- Hajek, A.E. and St Leger, R.J. (1994). Interactions between fungal pathogens and insect hosts. *Annu Rev Entomol.* **39**, 293-322.
- Hamilton, S., Odili, J., Gundogdu, O., Wilson, G.D. and Kupsch, J.M. (2001). Improved production by domain inversion of single-chain Fv antibody fragment against high molecular weight proteoglycan for the radioimmunotargeting of melanoma. *Hybrid Hybridomics.* **20**, 351-60.
- Hanahan, D. (1983). Studies on transformation of *Escherichia coli* with plasmids. *J Mol Biol.* **166**, 557-80.
- Hay, S.I., Guerra, C.A., Gething, P.W., Patil, A.P., Tatem, A.J., Noor, A.M., *et al.* (2009). A world malaria map: *Plasmodium falciparum* endemicity in 2007. *PLoS Med.* **6**, e1000048.
- Hayhurst, A. (2000). Improved expression characteristics of single-chain Fv fragments when fused downstream of the *Escherichia coli* maltose-binding protein or upstream of a single immunoglobulin-constant domain. *Protein Expr Purif.* **18**, 1-10.

- Hemingway, J., Hawkes, N.J., Mccarroll, L. and Ranson, H. (2004). The molecular basis of insecticide resistance in mosquitoes. *Insect Biochem Mol Biol.* **34**, 653-65.
- Hemminki, A., Niemi, S., Hautoniemi, L., Soderlund, H. and Takkinen, K. (1998). Fine tuning of an anti-testosterone antibody binding site by stepwise optimisation of the CDRs. *Immunotechnology.* **4**, 59-69.
- Hillesland, H., Read, A., Subhadra, B., Hurwitz, I., Mckelvey, R., Ghosh, K., *et al.* (2008). Identification of aerobic gut bacteria from the kala azar vector, *Phlebotomus argentipes*: a platform for potential paratransgenic manipulation of sand flies. *Am J Trop Med Hyg.* **79**, 881-6.
- Hoffman, S.L., Wistar, R., Jr., Ballou, W.R., Hollingdale, M.R., Wirtz, R.A., Schneider, I., *et al.* (1986). Immunity to malaria and naturally acquired antibodies to the circumsporozoite protein of *Plasmodium falciparum*. *N Engl J Med.* **315**, 601-6.
- Hoffman, S.L., Goh, L.M., Luke, T.C., Schneider, I., Le, T.P., Doolan, D.L., *et al.* (2002). Protection of humans against malaria by immunization with radiation-attenuated *Plasmodium falciparum* sporozoites. *J Infect Dis.* **185**, 1155-64.
- Holliger, P., Prospero, T. and Winter, G. (1993). "Diabodies": small bivalent and bispecific antibody fragments. *Proc Natl Acad Sci U S A.* **90**, 6444-8.
- Honegger, A. and Pluckthun, A. (2001). The influence of the buried glutamine or glutamate residue in position 6 on the structure of immunoglobulin variable domains. *J Mol Biol.* **309**, 687-99.
- Horton, R.M., Hunt, H.D., Ho, S.N., Pullen, J.K. and Pease, L.R. (1989). Engineering hybrid genes without the use of restriction enzymes: gene splicing by overlap extension. *Gene.* **77**, 61-8.
- Howard, A.F., N'guessan, R., Koenraadt, C.J., Asidi, A., Farenhorst, M., Akogbeto, M., *et al.* (2010). The entomopathogenic fungus *Beauveria bassiana* reduces instantaneous blood feeding in wild multi-insecticide-resistant *Culex quinquefasciatus* mosquitoes in Benin, West Africa. *Parasit Vectors.* **3**, 87.
- Hu, X., O'dwyer, R. and Wall, J.G. (2005). Cloning, expression and characterisation of a single-chain Fv antibody fragment against domoic acid in *Escherichia coli*. *J Biotechnol.* **120**, 38-45.
- Huber, M., Cabib, E. and Miller, L.H. (1991). Malaria parasite chitinase and penetration of the mosquito peritrophic membrane. *Proc Natl Acad Sci U S A.* **88**, 2807-10.
- Hudson, P.J. and Kortt, A.A. (1999). High avidity scFv multimers; diabodies and triabodies. *J Immunol Methods.* **231**, 177-89.
- Huse, W.D., Sastry, L., Iverson, S.A., Kang, A.S., Alting-Mees, M., Burton, D.R., *et al.* (1989). Generation of a large combinatorial library of the immunoglobulin repertoire in phage lambda. *Science.* **246**, 1275-81.
- Iliades, P., Kortt, A.A. and Hudson, P.J. (1997). Triabodies: single chain Fv fragments without a linker form trivalent trimers. *FEBS Lett.* **409**, 437-41.
- Ito, J., Ghosh, A., Moreira, L.A., Wimmer, E.A. and Jacobs-Lorena, M. (2002). Transgenic anopheline mosquitoes impaired in transmission of a malaria parasite. *Nature.* **417**, 452-5.

- Jacobs-Lorena, M. (2003). Interrupting malaria transmission by genetic manipulation of anopheline mosquitoes. *J Vector Borne Dis.* **40**, 73-7.
- James, A.A. (2003). Blocking malaria parasite invasion of mosquito salivary glands. *J Exp Biol.* **206**, 3817-21.
- Jaynes, J.M., Burton, C.A., Barr, S.B., Jeffers, G.W., Julian, G.R., White, K.L., *et al.* (1988). In vitro cytotoxic effect of novel lytic peptides on *Plasmodium falciparum* and *Trypanosoma cruzi*. *Faseb J.* **2**, 2878-83.
- Johnson, S. and Bird, R.E. (1991). Construction of single-chain Fv derivatives monoclonal antibodies and their production in *Escherichia coli*. *Methods Enzymol.* **203**, 88-98.
- Jones, T.R., Ballou, W.R. and Hoffman, S.L. (1993). Antibodies to the circumsporozoite protein and protective immunity to malaria sporozoites. *Prog Clin Parasitol.* **3**, 103-17.
- Kabat, E.A. and Wu, T.T. (1991). Identical V region amino acid sequences and segments of sequences in antibodies of different specificities. Relative contributions of VH and VL genes, minigenes, and complementarity-determining regions to binding of antibody-combining sites. *J Immunol.* **147**, 1709-19.
- Kabat, E.A., Wu, T.T., Perry, H.M., Gottesman, K.S. and Foeller, C. (1991). Sequences of proteins of immunological interest. *NIH Publications.* **5th ed**, 91-3242. .
- Kajava, A.V., Zolov, S.N., Kalinin, A.E. and Nesmeyanova, M.A. (2000). The net charge of the first 18 residues of the mature sequence affects protein translocation across the cytoplasmic membrane of gram-negative bacteria. *J Bacteriol.* **182**, 2163-9.
- Kanzok, S.M. and Jacobs-Lorena, M. (2006). Entomopathogenic fungi as biological insecticides to control malaria. *Trends Parasitol.* **22**, 49-51.
- Kappe, S.H., Buscaglia, C.A. and Nussenzweig, V. (2004). *Plasmodium* sporozoite molecular cell biology. *Annu Rev Cell Dev Biol.* **20**, 29-59.
- Kaslow, D.C. and Shiloach, J. (1994). Production, purification and immunogenicity of a malaria transmission-blocking vaccine candidate: TBV25H expressed in yeast and purified using nickel-NTA agarose. *Biotechnology (N Y).* **12**, 494-9.
- Kaslow, D.C. (2002). Transmission-blocking vaccines. *Chem Immunol.* **80**, 287-307.
- Katsura, K., Kawasaki, H., Potacharoen, W., Saono, S., Seki, T., Yamada, Y., *et al.* (2001). *Asaia siamensis* sp. nov., an acetic acid bacterium in the alpha-proteobacteria. *Int J Syst Evol Microbiol.* **51**, 559-63.
- Kettleborough, C.A., Saldanha, J., Heath, V.J., Morrison, C.J. and Bendig, M.M. (1991). Humanization of a mouse monoclonal antibody by CDR-grafting: the importance of framework residues on loop conformation. *Protein Eng.* **4**, 773-83.
- Kikankie, C.K., Brooke, B.D., Knols, B.G., Koekemoer, L.L., Farenhorst, M., Hunt, R.H., *et al.* (2010). The infectivity of the entomopathogenic fungus *Beauveria bassiana* to insecticide-resistant and susceptible *Anopheles arabiensis* mosquitoes at two different temperatures. *Malar J.* **9**, 71.
- Kim, W., Koo, H., Richman, A.M., Seeley, D., Vizioli, J., Klocko, A.D., *et al.* (2004). Ectopic expression of a cecropin transgene in the human

- malaria vector mosquito *Anopheles gambiae* (Diptera: Culicidae): effects on susceptibility to *Plasmodium*. *J Med Entomol.* **41**, 447-55.
- Kipriyanov, S.M., Moldenhauer, G., Martin, A.C., Kupriyanova, O.A. and Little, M. (1997). Two amino acid mutations in an anti-human CD3 single chain Fv antibody fragment that affect the yield on bacterial secretion but not the affinity. *Protein Eng.* **10**, 445-53.
- Klass, J.I., Blanford, S. and Thomas, M.B. (2007). Development of a model for evaluating the effects of environmental temperature and thermal behaviour on biological control of locusts and grasshoppers using pathogens. *Agr. Forest Entomol.* **9**, 189–199.
- Knappik, A. and Pluckthun, A. (1995). Engineered turns of a recombinant antibody improve its in vivo folding. *Protein Eng.* **8**, 81-9.
- Knols, B.G. and Thomas, M.B. (2006). Fungal entomopathogens for adult mosquito control - A look at the prospects. *Outlooks Pest Manag.* **17**, 257–259.
- Knols, B.G., Bukhari, T. and Farenhorst, M. (2010). Entomopathogenic fungi as the next-generation control agents against malaria mosquitoes. *Future Microbiol.* **5**, 339-41.
- Kokoza, V., Ahmed, A., Cho, W.L., Jasinskiene, N., James, A.A. and Raikhel, A. (2000). Engineering blood meal-activated systemic immunity in the yellow fever mosquito, *Aedes aegypti*. *Proc Natl Acad Sci U S A.* **97**, 9144-9.
- Kokoza, V., Ahmed, A., Woon Shin, S., Okafor, N., Zou, Z. and Raikhel, A.S. (2010). Blocking of *Plasmodium* transmission by cooperative action of Cecropin A and Defensin A in transgenic *Aedes aegypti* mosquitoes. *Proc Natl Acad Sci U S A.* **107**, 8111-6.
- Kommanee, J., Tanasupawat, S., Yukphan, P., Malimas, T., Muramatsu, Y., Nakagawa, Y., *et al.* (2010). *Asaia spathodeae* sp. nov., an acetic acid bacterium in the alpha-Proteobacteria. *J Gen Appl Microbiol.* **56**, 81-7.
- Kortt, A.A., Malby, R.L., Caldwell, J.B., Gruen, L.C., Ivancic, N., Lawrence, M.C., *et al.* (1994). Recombinant anti-sialidase single-chain variable fragment antibody. Characterization, formation of dimer and higher-molecular-mass multimers and the solution of the crystal structure of the single-chain variable fragment/sialidase complex. *Eur J Biochem.* **221**, 151-7.
- Kortt, A.A., Lah, M., Oddie, G.W., Gruen, C.L., Burns, J.E., Pearce, L.A., *et al.* (1997). Single-chain Fv fragments of anti-neuraminidase antibody NC10 containing five- and ten-residue linkers form dimers and with zero-residue linker a trimer. *Protein Eng.* **10**, 423-33.
- Kortt, A.A., Dolezal, O., Power, B.E. and Hudson, P.J. (2001). Dimeric and trimeric antibodies: high avidity scFvs for cancer targeting. *Biomol Eng.* **18**, 95-108.
- Krauss, J., Arndt, M.A., Zhu, Z., Newton, D.L., Vu, B.K., Choudhry, V., *et al.* (2004). Impact of antibody framework residue VH-71 on the stability of a humanised anti-MUC1 scFv and derived immunoenzyme. *Br J Cancer.* **90**, 1863-70.
- Kurien, B.T. and Scofield, R.H. (1998). Heat mediated quick Coomassie blue protein staining and destaining of SDS-PAGE gels. *Indian J Biochem Biophys.* **35**, 385-9.

- Kusharyoto, W., Pleiss, J., Bachmann, T.T. and Schmid, R.D. (2002). Mapping of a hapten-binding site: molecular modeling and site-directed mutagenesis study of an anti-atrazine antibody. *Protein Eng.* **15**, 233-41.
- Kuzina, L.V., Peloquin, J.J., Vacek, D.C. and Miller, T.A. (2001). Isolation and identification of bacteria associated with adult laboratory Mexican fruit flies, *Anastrepha ludens* (Diptera: Tephritidae). *Curr Microbiol.* **42**, 290-4.
- Lacey, L.A. and Undeen, A.H. (1986). Microbial control of black flies and mosquitoes. *Annu Rev Entomol.* **31**, 265-96.
- Laemmli, U.K. (1970). Cleavage of structural proteins during the assembly of the head of bacteriophage T4. *Nature.* **227**, 680-5.
- Langedijk, A.C., Honegger, A., Maat, J., Planta, R.J., Van Schaik, R.C. and Pluckthun, A. (1998). The nature of antibody heavy chain residue H6 strongly influences the stability of a VH domain lacking the disulfide bridge. *J Mol Biol.* **283**, 95-110.
- Lavoie, T.B., Drohan, W.N. and Smith-Gill, S.J. (1992). Experimental analysis by site-directed mutagenesis of somatic mutation effects on affinity and fine specificity in antibodies specific for lysozyme. *J Immunol.* **148**, 503-13.
- Le Calvez, H., Green, J.M. and Baty, D. (1996). Increased efficiency of alkaline phosphatase production levels in *Escherichia coli* using a degenerate PelB signal sequence. *Gene.* **170**, 51-5.
- Le Gall, F., Kipriyanov, S.M., Moldenhauer, G. and Little, M. (1999). Di-, tri- and tetrameric single chain Fv antibody fragments against human CD19: effect of valency on cell binding. *FEBS Lett.* **453**, 164-8.
- Li, J., Wang, Y., Wang, Z. and Dong, Z. (2000a). Influences of amino acid sequences in FR1 region on binding activity of the scFv and Fab of an antibody to human gastric cancer cells. *Immunol Lett.* **71**, 157-65.
- Li, J., Wang, Y., Wang, Z. and Dong, Z. (2000b). Effect of VL and VH consensus sequence-specific primers on the binding and expression of a mini-molecule antibody directed towards human gastric cancer. *Chin Med Sci J.* **15**, 133-9.
- Li, P., Beckwith, J. and Inouye, H. (1988). Alteration of the amino terminus of the mature sequence of a periplasmic protein can severely affect protein export in *Escherichia coli*. *Proc Natl Acad Sci U S A.* **85**, 7685-9.
- Li, Y., Chen, C.X., Von Specht, B.U. and Hahn, H.P. (2002). Cloning and hemolysin-mediated secretory expression of a codon-optimized synthetic human interleukin-6 gene in *Escherichia coli*. *Protein Expr Purif.* **25**, 437-47.
- Lindh, J.M., Terenius, O. and Faye, I. (2005). 16S rRNA gene-based identification of midgut bacteria from field-caught *Anopheles gambiae* sensu lato and *A. funestus* mosquitoes reveals new species related to known insect symbionts. *Appl Environ Microbiol.* **71**, 7217-23.
- Lindh, J.M., Borg-Karlson, A.K. and Faye, I. (2008). Transstadial and horizontal transfer of bacteria within a colony of *Anopheles gambiae* (Diptera: Culicidae) and oviposition response to bacteria-containing water. *Acta Trop.* **107**, 242-50.

- Lobo, C.A., Dhar, R. and Kumar, N. (1999). Immunization of mice with DNA-based Pfs25 elicits potent malaria transmission-blocking antibodies. *Infect Immun.* **67**, 1688-93.
- Lu, D., Jimenez, X., Witte, L. and Zhu, Z. (2004). The effect of variable domain orientation and arrangement on the antigen-binding activity of a recombinant human bispecific diabody. *Biochem Biophys Res Commun.* **318**, 507-13.
- Luckhart, S., Vodovotz, Y., Cui, L. and Rosenberg, R. (1998). The mosquito *Anopheles stephensi* limits malaria parasite development with inducible synthesis of nitric oxide. *Proc Natl Acad Sci U S A.* **95**, 5700-5.
- Makrides, S.C. (1996). Strategies for achieving high-level expression of genes in *Escherichia coli*. *Microbiol Rev.* **60**, 512-38.
- Malby, R.L., Caldwell, J.B., Gruen, L.C., Harley, V.R., Ivancic, N., Kortt, A.A., *et al.* (1993). Recombinant antineuraminidase single chain antibody: expression, characterization, and crystallization in complex with antigen. *Proteins.* **16**, 57-63.
- Malimas, T., Yukphan, P., Takahashi, M., Kaneyasu, M., Potacharoen, W., Tanasupawat, S., *et al.* (2008). *Asaia lannaensis* sp. nov., a new acetic acid bacterium in the Alphaproteobacteria. *Biosci Biotechnol Biochem.* **72**, 666-71.
- Malkin, E., Dubovsky, F. and Moree, M. (2006). Progress towards the development of malaria vaccines. *Trends Parasitol.* **22**, 292-5.
- Marrelli, M.T., Moreira, C.K., Kelly, D., Alphey, L. and Jacobs-Lorena, M. (2006). Mosquito transgenesis: what is the fitness cost? *Trends Parasitol.* **22**, 197-202.
- Marshall, J.M. and Taylor, C.E. (2009). Malaria control with transgenic mosquitoes. *PLoS Med.* **6**, e20.
- Martin, C.D., Rojas, G., Mitchell, J.N., Vincent, K.J., Wu, J., Mccafferty, J., *et al.* (2006). A simple vector system to improve performance and utilisation of recombinant antibodies. *BMC Biotechnol.* **6**, 46.
- Martinez-Torres, D., Chandre, F., Williamson, M.S., Darriet, F., Berge, J.B., Devonshire, A.L., *et al.* (1998). Molecular characterization of pyrethroid knockdown resistance (kdr) in the major malaria vector *Anopheles gambiae* s.s. *Insect Mol Biol.* **7**, 179-84.
- Maynard, J., Adams, E.J., Krogsgaard, M., Petersson, K., Liu, C.W. and Garcia, K.C. (2005). High-level bacterial secretion of single-chain alphabeta T-cell receptors. *J Immunol Methods.* **306**, 51-67.
- Maynard, J.A., Maassen, C.B., Leppla, S.H., Brasky, K., Patterson, J.L., Iverson, B.L., *et al.* (2002). Protection against anthrax toxin by recombinant antibody fragments correlates with antigen affinity. *Nat Biotechnol.* **20**, 597-601.
- Mccartney, J.E., Tai, M.S., Hudziak, R.M., Adams, G.P., Weiner, L.M., Jin, D., *et al.* (1995). Engineering disulfide-linked single-chain Fv dimers [(sFv')₂] with improved solution and targeting properties: anti-digoxin 26-10 (sFv')₂ and anti-c-erbB-2 741F8 (sFv')₂ made by protein folding and bonded through C-terminal cysteinyl peptides. *Protein Eng.* **8**, 301-14.
- Mcgregor, D.P., Molloy, P.E., Cunningham, C. and Harris, W.J. (1994). Spontaneous assembly of bivalent single chain antibody fragments in *Escherichia coli*. *Mol Immunol.* **31**, 219-26.

- Menard, R., Sultan, A.A., Cortes, C., Altszuler, R., Van Dijk, M.R., Janse, C.J., *et al.* (1997). Circumsporozoite protein is required for development of malaria sporozoites in mosquitoes. *Nature*. **385**, 336-40.
- Meredith, J.M., Basu, S., Nimmo, D.D., Larget-Thiery, I., Warr, E.L., Underhill, A., *et al.* (2011). Site-specific integration and expression of an anti-malarial gene in transgenic *Anopheles gambiae* significantly reduces *Plasmodium* infections. *PLoS One*. **6**, e14587.
- Merk, H., Stiege, W., Tsumoto, K., Kumagai, I. and Erdmann, V.A. (1999). Cell-free expression of two single-chain monoclonal antibodies against lysozyme: effect of domain arrangement on the expression. *J Biochem*. **125**, 328-33.
- Miura, K., Keister, D.B., Muratova, O.V., Sattabongkot, J., Long, C.A. and Saul, A. (2007). Transmission-blocking activity induced by malaria vaccine candidates Pfs25/Pvs25 is a direct and predictable function of antibody titer. *Malar J*. **6**, 107.
- Moorthy, V.S., Good, M.F. and Hill, A.V. (2004). Malaria vaccine developments. *Lancet*. **363**, 150-6.
- Moreira, C.K., Marrelli, M.T. and Jacobs-Lorena, M. (2004a). Gene expression in *Plasmodium*: from gametocytes to sporozoites. *Int J Parasitol*. **34**, 1431-40.
- Moreira, C.K., Rodrigues, F.G., Ghosh, A., Varotti Fde, P., Miranda, A., Daffre, S., *et al.* (2007). Effect of the antimicrobial peptide gomesin against different life stages of *Plasmodium* spp. *Exp Parasitol*. **116**, 346-53.
- Moreira, L.A., Edwards, M.J., Adhami, F., Jasinskiene, N., James, A.A. and Jacobs-Lorena, M. (2000). Robust gut-specific gene expression in transgenic *Aedes aegypti* mosquitoes. *Proc Natl Acad Sci U S A*. **97**, 10895-8.
- Moreira, L.A., Ito, J., Ghosh, A., Devenport, M., Zieler, H., Abraham, E.G., *et al.* (2002). Bee venom phospholipase inhibits malaria parasite development in transgenic mosquitoes. *J Biol Chem*. **277**, 40839-43.
- Moreira, L.A., Wang, J., Collins, F.H. and Jacobs-Lorena, M. (2004b). Fitness of anopheline mosquitoes expressing transgenes that inhibit *Plasmodium* development. *Genetics*. **166**, 1337-41.
- Mostafa, H.E., Heller, K.J. and Geis, A. (2002). Cloning of *Escherichia coli* lacZ and lacY genes and their expression in *Gluconobacter oxydans* and *Acetobacter liquefaciens*. *Appl Environ Microbiol*. **68**, 2619-23.
- Muller, K.M., Arndt, K.M., Bauer, K. and Pluckthun, A. (1998). Tandem immobilized metal-ion affinity chromatography/immunoaffinity purification of His-tagged proteins--evaluation of two anti-His-tag monoclonal antibodies. *Anal Biochem*. **259**, 54-61.
- Myung, J.M., Marshall, P. and Sinnis, P. (2004). The *Plasmodium* circumsporozoite protein is involved in mosquito salivary gland invasion by sporozoites. *Mol Biochem Parasitol*. **133**, 53-9.
- Nagasawa, H., Procell, P.M., Atkinson, C.T., Campbell, G.H., Collins, W.E. and Aikawa, M. (1987). Localization of circumsporozoite protein of *Plasmodium ovale* in midgut oocysts. *Infect Immun*. **55**, 2928-32.
- Nagasawa, H., Aikawa, M., Procell, P.M., Campbell, G.H., Collins, W.E. and Campbell, C.C. (1988). *Plasmodium malariae*: distribution of

- circumsporozoite protein in midgut oocysts and salivary gland sporozoites. *Exp Parasitol.* **66**, 27-34.
- Nardin, E.H., Nussenzweig, V., Nussenzweig, R.S., Collins, W.E., Harinasuta, K.T., Tapchaisri, P., *et al.* (1982). Circumsporozoite proteins of human malaria parasites *Plasmodium falciparum* and *Plasmodium vivax*. *J Exp Med.* **156**, 20-30.
- Ndiaye, J.L., Randrianarivelosia, M., Sagara, I., Brasseur, P., Ndiaye, I., Faye, B., *et al.* (2009). Randomized, multicentre assessment of the efficacy and safety of ASAQ--a fixed-dose artesunate-amodiaquine combination therapy in the treatment of uncomplicated *Plasmodium falciparum* malaria. *Malar J.* **8**, 125.
- Nirmala, X. and James, A.A. (2003). Engineering *Plasmodium*-refractory phenotypes in mosquitoes. *Trends Parasitol.* **19**, 384-7.
- Nolan, T., Bower, T.M., Brown, A.E., Crisanti, A. and Catteruccia, F. (2002). piggyBac-mediated germline transformation of the malaria mosquito *Anopheles stephensi* using the red fluorescent protein dsRED as a selectable marker. *J Biol Chem.* **277**, 8759-62.
- Norton, E.J., Diekman, A.B., Westbrook, V.A., Flickinger, C.J. and Herr, J.C. (2001). RASA, a recombinant single-chain variable fragment (scFv) antibody directed against the human sperm surface: implications for novel contraceptives. *Hum Reprod.* **16**, 1854-60.
- Nussenzweig, R.S., Vanderberg, J., Most, H. and Orton, C. (1967). Protective immunity produced by the injection of x-irradiated sporozoites of *plasmodium berghei*. *Nature.* **216**, 160-2.
- Otten, M., Aregawi, M., Were, W., Karema, C., Medin, A., Bekele, W., *et al.* (2009). Initial evidence of reduction of malaria cases and deaths in Rwanda and Ethiopia due to rapid scale-up of malaria prevention and treatment. *Malar J.* **8**, 14.
- Padua, L.E., Ohba, M. and Aizawa, K. (1980). The isolates of *Bacillus thuringiensis* serotype 10 with a highly preferential toxicity to mosquito larvae. *J Invertebr Pathol.* **36**, 180-6.
- Palmer, E., Liu, H., Khan, F., Taussig, M.J. and He, M. (2006). Enhanced cell-free protein expression by fusion with immunoglobulin Ckappa domain. *Protein Sci.* **15**, 2842-6.
- Pantoliano, M.W., Bird, R.E., Johnson, S., Asel, E.D., Dodd, S.W., Wood, J.F., *et al.* (1991). Conformational stability, folding, and ligand-binding affinity of single-chain Fv immunoglobulin fragments expressed in *Escherichia coli*. *Biochemistry.* **30**, 10117-25.
- Perera, O.P., Harrell, I.R. and Handler, A.M. (2002). Germ-line transformation of the South American malaria vector, *Anopheles albimanus*, with a piggyBac/EGFP transposon vector is routine and highly efficient. *Insect Mol Biol.* **11**, 291-7.
- Peterson, E., Owens, S.M. and Henry, R.L. (2006). Monoclonal antibody form and function: manufacturing the right antibodies for treating drug abuse. *Aaps J.* **8**, E383-90.
- Pettigrew, M.M. and O'Neill, S.L. (1997). Control of Vector-Borne Disease by Genetic Manipulation of Insect Populations: Technological Requirements and Research Priorities. *Australian Journal of Entomology.* **36**, 309-317.

- Picot, S., Olliaro, P., De Monbrison, F., Bienvenu, A.L., Price, R.N. and Ringwald, P. (2009). A systematic review and meta-analysis of evidence for correlation between molecular markers of parasite resistance and treatment outcome in falciparum malaria. *Malar J.* **8**, 89.
- Pinto, J., Lynd, A., Vicente, J.L., Santolamazza, F., Randle, N.P., Gentile, G., *et al.* (2007). Multiple origins of knockdown resistance mutations in the Afrotropical mosquito vector *Anopheles gambiae*. *PLoS One.* **2**, e1243.
- Possani, L.D., Zurita, M., Delepierre, M., Hernandez, F.H. and Rodriguez, M.H. (1998). From noxiustoxin to Shiva-3, a peptide toxic to the sporogonic development of *Plasmodium berghei*. *Toxicon.* **36**, 1683-92.
- Power, B.E. and Hudson, P.J. (2000). Synthesis of high avidity antibody fragments (scFv multimers) for cancer imaging. *J Immunol Methods.* **242**, 193-204.
- Power, B.E., Caine, J.M., Burns, J.E., Shapira, D.R., Hattarki, M.K., Tahtis, K., *et al.* (2001). Construction, expression and characterisation of a single-chain diabody derived from a humanised anti-Lewis Y cancer targeting antibody using a heat-inducible bacterial secretion vector. *Cancer Immunol Immunother.* **50**, 241-50.
- Power, B.E., Doughty, L., Shapira, D.R., Burns, J.E., Bayly, A.M., Caine, J.M., *et al.* (2003). Noncovalent scFv multimers of tumor-targeting anti-Lewis(y) hu3S193 humanized antibody. *Protein Sci.* **12**, 734-47.
- Pumpuni, C.B., Beier, M.S., Nataro, J.P., Guers, L.D. and Davis, J.R. (1993). *Plasmodium falciparum*: inhibition of sporogonic development in *Anopheles stephensi* by gram-negative bacteria. *Exp Parasitol.* **77**, 195-9.
- Pumpuni, C.B., Demaio, J., Kent, M., Davis, J.R. and Beier, J.C. (1996). Bacterial population dynamics in three anopheline species: the impact on *Plasmodium* sporogonic development. *Am J Trop Med Hyg.* **54**, 214-8.
- Qian, Z.G., Xia, X.X., Choi, J.H. and Lee, S.Y. (2008). Proteome-based identification of fusion partner for high-level extracellular production of recombinant proteins in *Escherichia coli*. *Biotechnol Bioeng.* **101**, 587-601.
- Quakyi, I.A., Miller, L.H., Good, M.F., Ahlers, J.D., Isaacs, S.N., Nunberg, J.H., *et al.* (1995). Synthetic peptides from *P. falciparum* sexual stage 25-kDa protein induce antibodies that react with the native protein: the role of IL-2 and conformational structure on immunogenicity of Pfs25. *Pept Res.* **8**, 335-44.
- Rani, A., Sharma, A., Rajagopal, R., Adak, T. and Bhatnagar, R.K. (2009). Bacterial diversity analysis of larvae and adult midgut microflora using culture-dependent and culture-independent methods in lab-reared and field-collected *Anopheles stephensi*-an Asian malarial vector. *BMC Microbiol.* **9**, 96.
- Rathore, D., Hrstka, S.C., Sacci, J.B., Jr., De La Vega, P., Linhardt, R.J., Kumar, S., *et al.* (2003). Molecular mechanism of host specificity in *Plasmodium falciparum* infection: role of circumsporozoite protein. *J Biol Chem.* **278**, 40905-10.
- Ren, X., Hoiczyk, E. and Rasgon, J.L. (2008). Viral paratransgenesis in the malaria vector *Anopheles gambiae*. *PLoS Pathog.* **4**, e1000135.

- Ricci, I., Mosca, M., Valzano, M., Damiani, C., Scuppa, P., Rossi, P., *et al.* (2011). Different mosquito species host *Wickerhamomyces anomalus* (*Pichia anomala*): perspectives on vector-borne diseases symbiotic control. *Antonie Van Leeuwenhoek*. **99**, 43-50.
- Riehle, M.A., Srinivasan, P., Moreira, C.K. and Jacobs-Lorena, M. (2003). Towards genetic manipulation of wild mosquito populations to combat malaria: advances and challenges. *J Exp Biol*. **206**, 3809-16.
- Riehle, M.A. and Jacobs-Lorena, M. (2005). Using bacteria to express and display anti-parasite molecules in mosquitoes: current and future strategies. *Insect Biochem Mol Biol*. **35**, 699-707.
- Riehle, M.A., Moreira, C.K., Lampe, D., Lauzon, C. and Jacobs-Lorena, M. (2007). Using bacteria to express and display anti-Plasmodium molecules in the mosquito midgut. *Int J Parasitol*. **37**, 595-603.
- Ringquist, S., Shinedling, S., Barrick, D., Green, L., Binkley, J., Stormo, G.D., *et al.* (1992). Translation initiation in *Escherichia coli*: sequences within the ribosome-binding site. *Mol Microbiol*. **6**, 1219-29.
- Robichon, C., Luo, J., Causey, T.B., Benner, J.S. and Samuelson, J.C. (2011). Engineering *Escherichia coli* BL21(DE3) derivative strains to minimize *E. coli* protein contamination after purification by immobilized metal affinity chromatography. *Appl Environ Microbiol*. **77**, 4634-46.
- Rodrigues, F.G., Santos, M.N., De Carvalho, T.X., Rocha, B.C., Riehle, M.A., Pimenta, P.F., *et al.* (2008). Expression of a mutated phospholipase A2 in transgenic *Aedes fluviatilis* mosquitoes impacts *Plasmodium gallinaceum* development. *Insect Mol Biol*. **17**, 175-83.
- Rosenberg, R. (1985). Inability of *Plasmodium knowlesi* sporozoites to invade *Anopheles freeborni* salivary glands. *Am J Trop Med Hyg*. **34**, 687-91.
- Sacarlal, J., Aide, P., Aponte, J.J., Renom, M., Leach, A., Mandomando, I., *et al.* (2009). Long-term safety and efficacy of the RTS,S/AS02A malaria vaccine in Mozambican children. *J Infect Dis*. **200**, 329-36.
- Sambrook, J.a.R., D. W. , (2001). *Molecular Cloning: A Laboratory Manual*. Cold Spring Harbor, New York, Cold Spring Harbor Laboratory Press.
- Sastry, L., Alting-Mees, M., Huse, W.D., Short, J.M., Sorge, J.A., Hay, B.N., *et al.* (1989). Cloning of the immunological repertoire in *Escherichia coli* for generation of monoclonal catalytic antibodies: construction of a heavy chain variable region-specific cDNA library. *Proc Natl Acad Sci U S A*. **86**, 5728-32.
- Saxena, A.K., Wu, Y. and Garboczi, D.N. (2007). Plasmodium p25 and p28 surface proteins: potential transmission-blocking vaccines. *Eukaryot Cell*. **6**, 1260-5.
- Scherer, G.F., Walkinshaw, M.D., Arnott, S. and Morre, D.J. (1980). The ribosome binding sites recognized by *E. coli* ribosomes have regions with signal character in both the leader and protein coding segments. *Nucleic Acids Res*. **8**, 3895-907.
- Scholte, E.J., Knols, B.G. and Takken, W. (2004). Autodissemination of the entomopathogenic fungus *Metarhizium anisopliae* amongst adults of the malaria vector *Anopheles gambiae* s.s. *Malar J*. **3**, 45.
- Scholte, E.J., Ng'habi, K., Kihonda, J., Takken, W., Paaijmans, K., Abdulla, S., *et al.* (2005). An entomopathogenic fungus for control of adult African malaria mosquitoes. *Science*. **308**, 1641-2.

- Scholte, E.J., Knols, B.G. and Takken, W. (2006). Infection of the malaria mosquito *Anopheles gambiae* with the entomopathogenic fungus *Metarhizium anisopliae* reduces blood feeding and fecundity. *J Invertebr Pathol.* **91**, 43-9.
- Scott, J., Teasdale, J.D., Paykel, E.S., Johnson, A.L., Abbott, R., Hayhurst, H., *et al.* (2000). Effects of cognitive therapy on psychological symptoms and social functioning in residual depression. *Br J Psychiatry.* **177**, 440-6.
- Shahabuddin, M., Toyoshima, T., Aikawa, M. and Kaslow, D.C. (1993). Transmission-blocking activity of a chitinase inhibitor and activation of malarial parasite chitinase by mosquito protease. *Proc Natl Acad Sci U S A.* **90**, 4266-70.
- Shahabuddin, M., Fields, I., Bulet, P., Hoffmann, J.A. and Miller, L.H. (1998). *Plasmodium gallinaceum*: differential killing of some mosquito stages of the parasite by insect defensin. *Exp Parasitol.* **89**, 103-12.
- Shahabuddin, M. and Costero, A. (2001). Spatial distribution of factors that determine sporogonic development of malaria parasites in mosquitoes. *Insect Biochem Mol Biol.* **31**, 231-40.
- Sharma, B. (2008). Structure and mechanism of a transmission blocking vaccine candidate protein Pfs25 from *P. falciparum*: a molecular modeling and docking study. *In Silico Biol.* **8**, 193-206.
- Shi, Y.P., Alpers, M.P., Povoas, M.M. and Lal, A.A. (1992). Single amino acid variation in the ookinete vaccine antigen from field isolates of *Plasmodium falciparum*. *Mol Biochem Parasitol.* **50**, 179-80.
- Shin, S.W., Kokoza, V.A. and Raikhel, A.S. (2003). Transgenesis and reverse genetics of mosquito innate immunity. *J Exp Biol.* **206**, 3835-43.
- Siden-Kiamos, I. and Louis, C. (2004). Interactions between malaria parasites and their mosquito hosts in the midgut. *Insect Biochem Mol Biol.* **34**, 679-85.
- Sidhu, A.B., Verdier-Pinard, D. and Fidock, D.A. (2002). Chloroquine resistance in *Plasmodium falciparum* malaria parasites conferred by *pfcrt* mutations. *Science.* **298**, 210-3.
- Sidjanski, S.P., Vanderberg, J.P. and Sinnis, P. (1997). *Anopheles stephensi* salivary glands bear receptors for region I of the circumsporozoite protein of *Plasmodium falciparum*. *Mol Biochem Parasitol.* **90**, 33-41.
- Singh, B., Kim Sung, L., Matusop, A., Radhakrishnan, A., Shamsul, S.S., Cox-Singh, J., *et al.* (2004). A large focus of naturally acquired *Plasmodium knowlesi* infections in human beings. *Lancet.* **363**, 1017-24.
- Skerra, A. and Pluckthun, A. (1988). Assembly of a functional immunoglobulin Fv fragment in *Escherichia coli*. *Science.* **240**, 1038-41.
- Sletta, H., Tondervik, A., Hakvag, S., Aune, T.E., Nedal, A., Aune, R., *et al.* (2007). The presence of N-terminal secretion signal sequences leads to strong stimulation of the total expression levels of three tested medically important proteins during high-cell-density cultivations of *Escherichia coli*. *Appl Environ Microbiol.* **73**, 906-12.
- Soderlind, E., Simonsson, A.C. and Borrebaeck, C.A. (1992). Phage display technology in antibody engineering: design of phagemid vectors and in vitro maturation systems. *Immunol Rev.* **130**, 109-24.
- Spada, S., Honegger, A. and Pluckthun, A. (1998). Reproducing the natural evolution of protein structural features with the selectively infective

- phage (SIP) technology. The kink in the first strand of antibody kappa domains. *J Mol Biol.* **283**, 395-407.
- Stowers, A.W., Keister, D.B., Muratova, O. and Kaslow, D.C. (2000). A region of *Plasmodium falciparum* antigen Pfs25 that is the target of highly potent transmission-blocking antibodies. *Infect Immun.* **68**, 5530-8.
- Straif, S.C., Mbogo, C.N., Toure, A.M., Walker, E.D., Kaufman, M., Toure, Y.T., *et al.* (1998). Midgut bacteria in *Anopheles gambiae* and *An. funestus* (Diptera: Culicidae) from Kenya and Mali. *J Med Entomol.* **35**, 222-6.
- Stratmann, T. and Kang, A.S. (2005). Cognate peptide-receptor ligand mapping by directed phage display. *Proteome Sci.* **3**, 7.
- Stura, E.A., Kang, A.S., Stefanko, R.S., Calvo, J.C., Kaslow, D.C. and Satterthwait, A.C. (1994a). Crystallization, sequence and preliminary crystallographic data for transmission-blocking anti-malaria Fab 4B7 with cyclic peptides from the Pfs25 protein of *P. falciparum*. *Acta Crystallogr D Biol Crystallogr.* **50**, 535-42.
- Stura, E.A., Satterthwait, A.C., Calvo, J.C., Stefanko, R.S., Langeveld, J.P. and Kaslow, D.C. (1994b). Crystallization of an intact monoclonal antibody (4B7) against *Plasmodium falciparum* malaria with peptides from the Pfs25 protein antigen. *Acta Crystallogr D Biol Crystallogr.* **50**, 556-62.
- Subhadra, B., Hurwitz, I., Fieck, A., Rao, D.V., Rao, G.S. and Durvasula, R. (2010). Development of paratransgenic *Artemia* as a platform for control of infectious diseases in shrimp mariculture. *J Appl Microbiol.* **108**, 831-40.
- Summers, R.G., Harris, C.R. and Knowles, J.R. (1989). A conservative amino acid substitution, arginine for lysine, abolishes export of a hybrid protein in *Escherichia coli*. Implications for the mechanism of protein secretion. *J Biol Chem.* **264**, 20082-8.
- Tomas, A.M., Margos, G., Dimopoulos, G., Van Lin, L.H., De Koning-Ward, T.F., Sinha, R., *et al.* (2001). P25 and P28 proteins of the malaria ookinete surface have multiple and partially redundant functions. *Embo J.* **20**, 3975-83.
- Towbin, H., Staehelin, T. and Gordon, J. (1979). Electrophoretic transfer of proteins from polyacrylamide gels to nitrocellulose sheets: procedure and some applications. *Proc Natl Acad Sci U S A.* **76**, 4350-4.
- Tsuboi, T., Kaslow, D.C., Cao, Y.M., Shiwaku, K. and Torii, M. (1997). Comparison of *Plasmodium yoelii* ookinete surface antigens with human and avian malaria parasite homologues reveals two highly conserved regions. *Mol Biochem Parasitol.* **87**, 107-11.
- Tsuboi, T., Takeo, S., Iriko, H., Jin, L., Tsuchimochi, M., Matsuda, S., *et al.* (2008). Wheat germ cell-free system-based production of malaria proteins for discovery of novel vaccine candidates. *Infect Immun.* **76**, 1702-8.
- Tsumoto, K., Nakaoki, Y., Ueda, Y., Ogasahara, K., Yutani, K., Watanabe, K., *et al.* (1994). Effect of the order of antibody variable regions on the expression of the single-chain HyHEL10 Fv fragment in *E. coli* and the thermodynamic analysis of its antigen-binding properties. *Biochem Biophys Res Commun.* **201**, 546-51.

- Vaughan, J.A., Noden, B.H. and Beier, J.C. (1992). Population dynamics of *Plasmodium falciparum* sporogony in laboratory-infected *Anopheles gambiae*. *J Parasitol.* **78**, 716-24.
- Vaughan, J.A., Noden, B.H. and Beier, J.C. (1994). Prior blood feeding effects on susceptibility of *Anopheles gambiae* (Diptera: Culicidae) to infection with cultured *Plasmodium falciparum* (Haemosporida: Plasmodiidae). *J Med Entomol.* **31**, 445-9.
- Vekemans, J., Leach, A. and Cohen, J. (2009). Development of the RTS,S/AS malaria candidate vaccine. *Vaccine.* **27 Suppl 6**, G67-71.
- Vermeulen, A.N., Roeffen, W.F., Henderik, J.B., Ponnudurai, T., Beckers, P.J. and Meuwissen, J.H. (1985). *Plasmodium falciparum* transmission blocking monoclonal antibodies recognize monovalently expressed epitopes. *Dev Biol Stand.* **62**, 91-7.
- Vinetz, J.M., Dave, S.K., Specht, C.A., Brameld, K.A., Xu, B., Hayward, R., *et al.* (1999). The chitinase PfCMT1 from the human malaria parasite *Plasmodium falciparum* lacks proenzyme and chitin-binding domains and displays unique substrate preferences. *Proc Natl Acad Sci U S A.* **96**, 14061-6.
- Wall, J.G. and Pluckthun, A. (1999). The hierarchy of mutations influencing the folding of antibody domains in *Escherichia coli*. *Protein Eng.* **12**, 605-11.
- Warburg, A., Touray, M., Krettli, A.U. and Miller, L.H. (1992). *Plasmodium gallinaceum*: antibodies to circumsporozoite protein prevent sporozoites from invading the salivary glands of *Aedes aegypti*. *Exp Parasitol.* **75**, 303-7.
- Ward, T.W., Jenkins, M.S., Afanasiev, B.N., Edwards, M., Duda, B.A., Suchman, E., *et al.* (2001). *Aedes aegypti* transducing dengue virus pathogenesis and expression in *Aedes aegypti* and *Anopheles gambiae* larvae. *Insect Mol Biol.* **10**, 397-405.
- Whitlow, M., Filpula, D., Rollence, M.L., Feng, S.L. and Wood, J.F. (1994). Multivalent Fvs: characterization of single-chain Fv oligomers and preparation of a bispecific Fv. *Protein Eng.* **7**, 1017-26.
- Winger, L.A., Tirawanchai, N., Nicholas, J., Carter, H.E., Smith, J.E. and Sinden, R.E. (1988). Ookinete antigens of *Plasmodium berghei*. Appearance on the zygote surface of an Mr 21 kD determinant identified by transmission-blocking monoclonal antibodies. *Parasite Immunol.* **10**, 193-207.
- Winzeler, E.A. (2006). Applied systems biology and malaria. *Nat Rev Microbiol.* **4**, 145-51.
- Witkowski, B., Lelievre, J., Barragan, M.J., Laurent, V., Su, X.Z., Berry, A., *et al.* (2010). Increased tolerance to artemisinin in *Plasmodium falciparum* is mediated by a quiescence mechanism. *Antimicrob Agents Chemother.* **54**, 1872-7.
- Wu, X.C., Ng, S.C., Near, R.I. and Wong, S.L. (1993). Efficient production of a functional single-chain antidigoxin antibody via an engineered *Bacillus subtilis* expression-secretion system. *Biotechnology (N Y).* **11**, 71-6.
- Wu, Y., Ellis, R.D., Shaffer, D., Fontes, E., Malkin, E.M., Mahanty, S., *et al.* (2008). Phase 1 trial of malaria transmission blocking vaccine candidates Pfs25 and Pvs25 formulated with montanide ISA 51. *PLoS One.* **3**, e2636.

- Xiang, J., Sha, Y., Jia, Z., Prasad, L. and Delbaere, L.T. (1995). Framework residues 71 and 93 of the chimeric B72.3 antibody are major determinants of the conformation of heavy-chain hypervariable loops. *J Mol Biol.* **253**, 385-90.
- Yamada, Y., Katsura, K., Kawasaki, H., Widyastuti, Y., Saono, S., Seki, T., *et al.* (2000). *Asaia bogorensis* gen. nov., sp. nov., an unusual acetic acid bacterium in the alpha-Proteobacteria. *Int J Syst Evol Microbiol.* **50 Pt 2**, 823-9.
- Yamada, Y. and Yukphan, P. (2008). Genera and species in acetic acid bacteria. *Int J Food Microbiol.* **125**, 15-24.
- Yoshida, S., Matsuoka, H., Luo, E., Iwai, K., Arai, M., Sinden, R.E., *et al.* (1999). A single-chain antibody fragment specific for the Plasmodium berghei ookinete protein Pbs21 confers transmission blockade in the mosquito midgut. *Mol Biochem Parasitol.* **104**, 195-204.
- Yoshida, S., Ioka, D., Matsuoka, H., Endo, H. and Ishii, A. (2001). Bacteria expressing single-chain immunotoxin inhibit malaria parasite development in mosquitoes. *Mol Biochem Parasitol.* **113**, 89-96.
- Yoshida, S., Shimada, Y., Kondoh, D., Kouzuma, Y., Ghosh, A.K., Jacobs-Lorena, M., *et al.* (2007). Hemolytic C-type lectin CEL-III from sea cucumber expressed in transgenic mosquitoes impairs malaria parasite development. *PLoS Pathog.* **3**, e192.
- Yuan, Q., Hu, W., Pestka, J.J., He, S.Y. and Hart, L.P. (2000). Expression of a functional antizearalenone single-chain Fv antibody in transgenic Arabidopsis plants. *Appl Environ Microbiol.* **66**, 3499-505.
- Yukphan, P., Potacharoen, W., Tanasupawat, S., Tanticharoen, M. and Yamada, Y. (2004). *Asaia krungthepensis* sp. nov., an acetic acid bacterium in the alpha-Proteobacteria. *Int J Syst Evol Microbiol.* **54**, 313-6.
- Zavala, F., Masuda, A., Graves, P.M., Nussenzweig, V. and Nussenzweig, R.S. (1985a). Ubiquity of the repetitive epitope of the CS protein in different isolates of human malaria parasites. *J Immunol.* **135**, 2790-3.
- Zavala, F., Tam, J.P., Hollingdale, M.R., Cochrane, A.H., Quakyi, I., Nussenzweig, R.S., *et al.* (1985b). Rationale for development of a synthetic vaccine against Plasmodium falciparum malaria. *Science.* **228**, 1436-40.
- Zheng, L., Baumann, U. and Reymond, J.L. (2004). An efficient one-step site-directed and site-saturation mutagenesis protocol. *Nucleic Acids Res.* **32**, e115.
- Zieler, H., Keister, D.B., Dvorak, J.A. and Ribeiro, J.M. (2001). A snake venom phospholipase A(2) blocks malaria parasite development in the mosquito midgut by inhibiting ookinete association with the midgut surface. *J Exp Biol.* **204**, 4157-67.
- Zollner, G.E., Ponsa, N., Garman, G.W., Poudel, S., Bell, J.A., Sattabongkot, J., *et al.* (2006). Population dynamics of sporogony for Plasmodium vivax parasites from western Thailand developing within three species of colonized Anopheles mosquitoes. *Malar J.* **5**, 68.
- Zou, L., Miles, A.P., Wang, J. and Stowers, A.W. (2003). Expression of malaria transmission-blocking vaccine antigen Pfs25 in Pichia pastoris for use in human clinical trials. *Vaccine.* **21**, 1650-7.

APPENDIX

Plasmid	Source
pSANG103F	Martin <i>et al.</i> (2006)
pET41b(+)	Dr. Mark Clements (Univ. of Westminster)
pBSK CA19.9	Dr. Anatoliy Markiv (Univ. of Westminster)
pBAK1	This study
pBAK1.HK	This study
pMAK031 2P	This study

Table I: Plasmids used in this study and their sources.

Primer Name	Sequence
	PCR of HuCk from Phage library as <i>NotI/HindIII</i>
BAK.1	ACT GCG GCC GCA CCA TCT GTC TTC ATC TTC
BAK.2	AGA AGC TTG CTC GAG TCC CCT GTT GAA GCT CTT TGT GAC
	4B7 Primers
4B7VHNot	AAGCTTGCGGCCGCGCTGCTCACGGTCAGGGTGGTGC CCTGGCC
4B7VLNcoI	GCCATGGCCGATATTCAGATGATTCAGAGCCCGAGC
4B7VLR	CGCTTTATTTTCCAGTTTGGTGCCGCTGCC
4B7VHF	GAAGTGAAACTGGTGGAAGCGGCGGCGGC
4B7VHR	CGC GCT GCT CAC GGT CAG GGT GG
4B7VLF	GAT ATT CAG ATG ATT CAG AGC C
4B7VHLink5F	GGAGGTGGCGGAAGCGAAGTGAACTGGTGGAAAGC GGCGGCGGC
4B7VLLink5R	CTACCGCCACCTCCCGCTTTAATTTCCAGTTTGGTG CCGCTGCC

4B7VLVHLink30	GGAGGTGGCGGTAGTGGAGGTGGCGGAAGCGGAGG TGGCGGTAGTGGAGGTGGCGGAAGCGGAGGTGGCG GTAGTGGAGGTGGCGGAAGC
	4B7 Site-directed mutagenesis
4B7VLQ3EI5TF	GATATTGAGATGACCCAGAGCCCGAGCAGCATGTTTGC CG
4B7VLQ3EI5TR	GCTCTGGGTCATCTCAATATCGGCCATGGCCGGCTGG GC
4B7VLL85FG86AF	GCGAAGATTTTGCCGATTATTATTGCCTGCAGCGCAAC
4B7VLL85FG86AR	GCAATAATAATCGGCAAATCTTCGCTTTCCAGGCTGC
4B7VHQ20RF	GGCGGCAGCCGCAAACCTGAGCTGCGCGGCGAGCGGC
4B7VHQ20RR	GCTCAGTTTGC GGCTGCCGCCCGGCTGCACCAGGCC
4B7VHT94AF	GAAGATACCGCCATGTATTATTGCGCGCGCGGC
4B7VHT94AR	GCAATAATACATGGCGGTATCTTCGCTGCGCAG
4B7VH	GGCACCACCGTGACCGTGAGCAGCGCGGCCGCATCC GC
4B7VHL114VN otIR	GCGGATGCGGCCGCGCTGCTCACGGTCACGGTGGTG CC
	Pf-NPNA-1 Primers
NcoF	TCT AGA GCG GCC CAG CCG GCC ATG GCC
PfVHR	GCT GCT CAC GGT CAC CAG GGT GCC
PfVLF	GAA ATT GTG CTG ACC CAG AGC CCG
PfVLR	TTT AAT TCC ACT TTG GTG CCG CCG CC
Not R	ATT ACG CCA AGC TTG CGG CCG C
	pMAK031 2P plasmid
KANF	TAA CCG GAA TTG CCA GCT GG
KANR	GCG TTC ACC GAC AAA CAA CA
T7ABATG	GC AGC TAA TAC GAC TCA CTA TAG GAA CAG ACC ACC ATG GCC

Table II: Primers used in this study

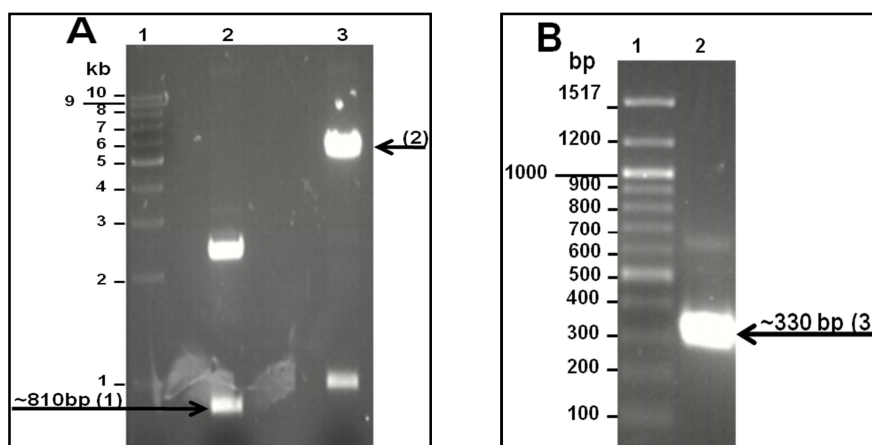


Figure I: Restriction enzyme digestion of (A) pORFES-IT and pET41b(+) and **(B) PCR amplified HuCk gene.** 50 μ L of each digested reaction was loaded and subjected to electrophoresis on a 1% agarose at 100 V for 1 hour. The DNA was visualised using ethidium bromide under UV light at wavelength of 200 nm. **A:** Lane 1: 1 kb DNA step ladder, Lane 2: XbaI/NotI digested pORFES-IT, Lane 3: XbaI/NotI digested pET41b(+); Lane 4: 100 bp DNA ladder. Inserts were excised and agarose gel purified. **B:** Lane 1: 100 bp DNA ladder, Lane 2: NotI/XhoI digested PCR amplified HuCk.

XbaI	<i>pelB</i> leader sequence					
1	TCTAGATCAG	GAGAACAGTC	ATAATGAAAT	ACCTATTGCC	TACGGCAGCC	
			M K Y	L L P	T A A	Frame 3
			sfiI		NcoI	
51	GCTGGATTGT	TATTACTCGC	GGCCCAGCCG	GCCATGGCCG	AGGTGCAGCT	Frame 3
	A G L L	L L A	A Q P	A M A	E V Q L	
101	GTTGGAGTCT	GGGGGAGGCT	TGGTACAGCC	TGGGGGGTCC	CTGAGACTCT	Frame 3
	L E S	G G G L	V Q P	G G S	L R L S	
151	CCTGTGCAGC	CTCTGGATTG	ACCTTTAGCA	GCTATGCCAT	GAGCTGGGTC	Frame 3
	C A A	S G F	T F S S	Y A M	S W V	
201	CGCCAGGCTC	CAGGGAAGGG	GCTGGAGTGG	GTCTCAATTA	TTGGGTCTGA	Frame 3
	R Q A P	G K G	L E W	V S I I	G S E	
251	GGGTTGGCCT	ACAATTTACG	CAGACTCCGT	GAAGGGCAGG	TTCACCATCT	Frame 3
	G W P	T I Y A	D S V	K G R	F T I S	
301	CCAGAGACAA	TTCCAAGAAC	ACGCTGTATC	TGCAAATGAA	CAGCCTGAGA	Frame 3
	R D N	S K N	T L Y L	Q M N	S L R	
351	GCCGAGGACA	CGGCCGTATA	TTACTGTGCG	AAAGGTGGGT	CGATGTTTGA	Frame 3
	A E D T	A V Y	Y C A	K G G S	M F D	
				XhoI		
401	CTACTGGGGC	CAGGGAACCC	TGGTCACCGT	CTCGAGCGGT	GGAGCGGTT	Frame 3
	Y W G	Q G T L	V T V	S S G	G G G S	
451	CAGGCGGAGG	TGGCAGCGGC	GGTGGCGGGT	CGACGGACAT	CCAGATGACC	Frame 3
	G G G	G S G	G G G S	T D I	Q M T	
501	CAGTCTCCAT	CCTCCCTGTC	TGCATCTGTA	GGAGACAGAG	TCACCATCAC	Frame 3
	Q S P S	S L S	A S V	G D R V	T I T	

```

551 TTGCCGGGCA AGTCAGAGCA TTAGCAGCTA TTTAAATTGG TATCAGCAGA
    C R A S Q S I S S Y L N W Y Q Q K Frame 3

601 AACCAGGGAA AGCCCCTAAG CTCCTGATCT ATCGTGCATC CAGCTTGCAA
    P G K A P K L L I Y R A S S L Q Frame 3

651 AGTGGGGTCC CATCAAGGTT CAGTGGCAGT GGATCTGGGA CAGATTTTCC
    S G V P S R F S G S G S G T D F T Frame 3

701 TCTCACCATC AGCAGTCTGC AACCTGAAGA TTTTGCAACT TACTACTGTC
    L T I S S L Q P E D F A T Y Y C Q Frame 3

751 AACAGTCGAG TAATACGCCT TATACGTTTCG GCCAAGGGAC CAAGGTGGAA
    Q S S N T P Y T F G Q G T K V E Frame 3
    NotI
801 ATTAAACGCA CTGCGGCCGC ACCATCTGTC TTCATCTTCC CGCCATCTGA
    I K R T A A A P S V F I F P P S D Frame 3

851 TGAGCAGTTG AAATCTGGAA CTGCCTCTGT TGTGTGCCTG CTGAATAACT
    E Q L K S G T A S V V C L L N N F Frame 3

901 TCTATCCCAG AGAGGCCAAA GTACAGTGGA AGGTGGATAA CGCCCTCCAA
    Y P R E A K V Q W K V D N A L Q Frame 3

951 TCGGGTAACT CCCAGGAGAG TGTCACAGAG CAGGACAGCA AGGACAGCAC
    S G N S Q E S V T E Q D S K D S T Frame 3

1001 CTACAGCCTC AGCAACACCC TGACGCTGAG CAAAGCAGAC TACGAGAAAC
    Y S L S N T L T L S K A D Y E K H Frame 3

1051 ACAAAGTCTA CGCCTGCGAA GTCACCCATC AGGGCCTGAG CTCGCCCGTC
    K V Y A C E V T H Q G L S S P V Frame 3
    XhoI
1101 ACAAAGAGCT TCAACAGGGG ACTCGAGCAC CACCACCACC ACCACCACCA
    T K S F N R G L E H H H H H H H H Frame 3

1151 CTAA
    * Frame 3

```

Figure II: Nucleotide and deduced amino acid sequence of pBAK.1Hk plasmid. The leader sequence, restriction sites and octa his tag are indicated. The sequence for the human kappa constant domain is represented by the purple colour.

```

XbaI                               pelB leader sequence
1 TCTAGATCAG GAGAACAGTC ATAATGAAAT ACCTATTGCC TACGGCAGCC
                               M K Y L L P T A A      Frame 3

SfiI                               NcoI
51 GCTGGATTGT TATTACTCGC GGCCAGCCG GCCATGGCCG AGGTGCAGCT
   A G L L L L A A Q P A M A E V Q L      Frame 3

101 GTTGGAGTCT GGGGGAGGCT TGGTACAGCC TGGGGGGTCC CTGAGACTCT
    L E S G G G L V Q P G G S L R L S      Frame 3

151 CCTGTGCAGC CTCTGGATTC ACCTTTAGCA GCTATGCCAT GAGCTGGGTC
    C A A S G F T F S S Y A M S W V      Frame 3

201 CGCCAGGCTC CAGGGAAGGG GCTGGAGTGG GTCTCAATTA TTGGGTCTGA
    R Q A P G K G L E W V S I I G S E      Frame 3

251 GGGTTGGCCT ACAATTTACG CAGACTCCGT GAAGGGCAGG TTCACCATCT
    G W P T I Y A D S V K G R F T I S      Frame 3

301 CCAGAGACAA TTCCAAGAAC ACGCTGTATC TGCAAATGAA CAGCCTGAGA
    R D N S K N T L Y L Q M N S L R      Frame 3

351 GCCGAGGACA CGGCCGTATA TTA CTGTGCG AAAGGTGGGT CGATGTTTGA
    A E D T A V Y Y C A K G G S M F D      Frame 3

XhoI
401 CTACTGGGGC CAGGGAACCC TGGTCACCGT CTCGAGCGGT GGAGGCGGTT
    Y W G Q G T L V T V S S G G G G S      Frame 3

451 CAGGCGGAGG TGGCAGCGGC GGTGGCGGGT CGACGGACAT CCAGATGACC
    G G G G S G G G G S T D I Q M T      Frame 3

501 CAGTCTCCAT CCTCCCTGTC TGCATCTGTA GGAGACAGAG TCACCATCAC
    Q S P S S L S A S V G D R V T I T      Frame 3

551 TTGCCGGGCA AGTCAGAGCA TTAGCAGCTA TTTAAATTGG TATCAGCAGA
    C R A S Q S I S S Y L N W Y Q Q K      Frame 3

601 AACCAGGGAA AGCCCCTAAG CTCCTGATCT ATCGTGCATC CAGCTTGCAA
    P G K A P K L L I Y R A S S L Q      Frame 3

651 AGTGGGGTCC CATCAAGGTT CAGTGGCAGT GGATCTGGGA CAGATTTAC
    S G V P S R F S G S G S G T D F T      Frame 3

701 TCTCACCATC AGCAGTCTGC AACCTGAAGA TTTTGCAACT TACTACTGTC
    L T I S S L Q P E D F A T Y Y C Q      Frame 3

751 AACAGTCGAG TAATACGCCT TATACGTTCG GCCAAGGGAC CAAGGTGGAA
    Q S S N T P Y T F G Q G T K V E      Frame 3

NotI                               XhoI                               His8 Tag
801 ATCAAACGGG CGGCCGCACT CGAGCACCAC CACCACCACC ACCACCCTAA
    I K R A A A L E H H H H H H H H *      Frame 3

```

Figure III: Nucleotide and deduced amino acid sequence of pBAK.1 plasmid.
The leader sequence, restriction sites and octa his tag are indicated.

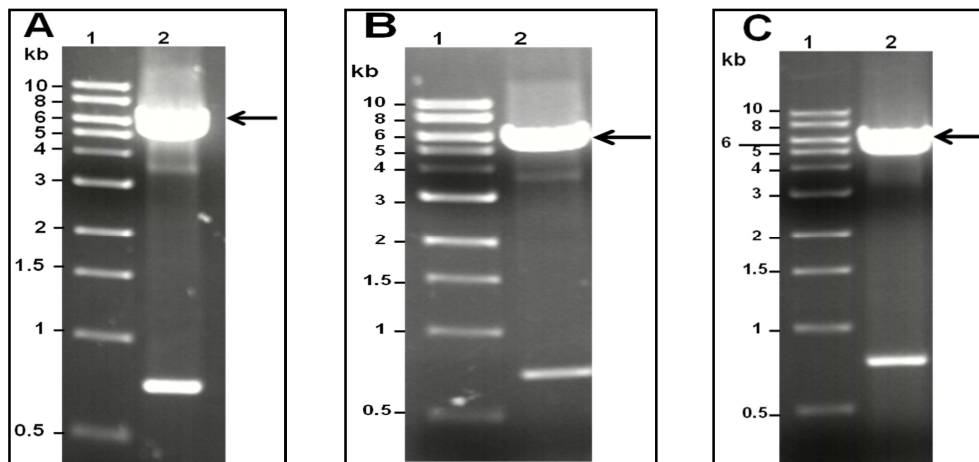


Figure IV: NcoI/NotI restriction enzyme digestion of expression plasmids: pBAK1 (A), pSANG10-3F (B) and pBAK1Hk (C). 50 μ L of each digested reaction was loaded and subjected to electrophoresis on a 1% agarose at 100 V for 1 hour. The DNA was visualised using ethidium bromide under UV light at wavelength of 200 nm. **(A)** Lane 1: 1 kb DNA ladder, Lane 2: digested pBAK1 **(B)** Lane 1: 1 kb DNA ladder, Lane 2: digested pSANG10-3F, **(C)** Lane 1: 1 kb DNA ladder, Lane 2: digested pBAK1Hk.

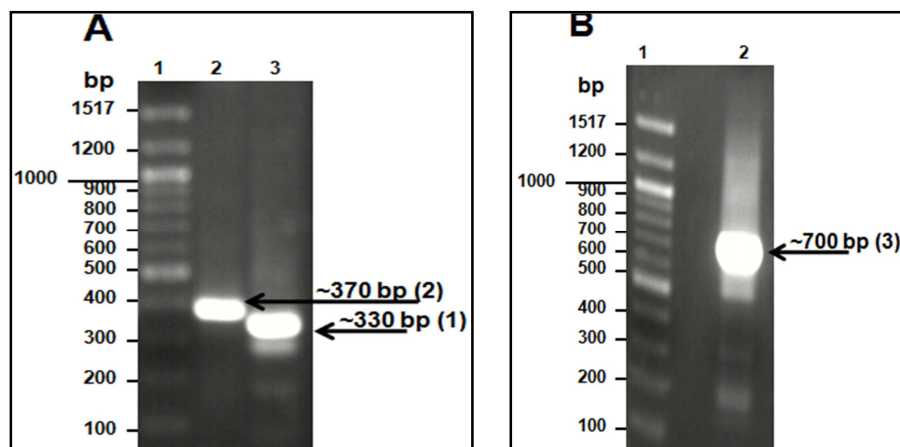


Figure V: PCR amplification of variable domains (A) and overlap extension PCR (B) of 4B7. 25 μ L of each PCR product was loaded and subjected to electrophoresis on a 1.5% agarose at 100 V for 1 hour. The DNA was visualised using ethidium bromide under UV light at wavelength of 200 nm. **(A)** Lane 1: 100 bp DNA ladder, Lane 2: 4B7 V_H (370 bp), Lane 3: 4B7 V_L (330 bp); **(B)** Lane 1: 100 bp DNA ladder, Lane 2: 4B7 $V_H - V_L$ (700 bp).

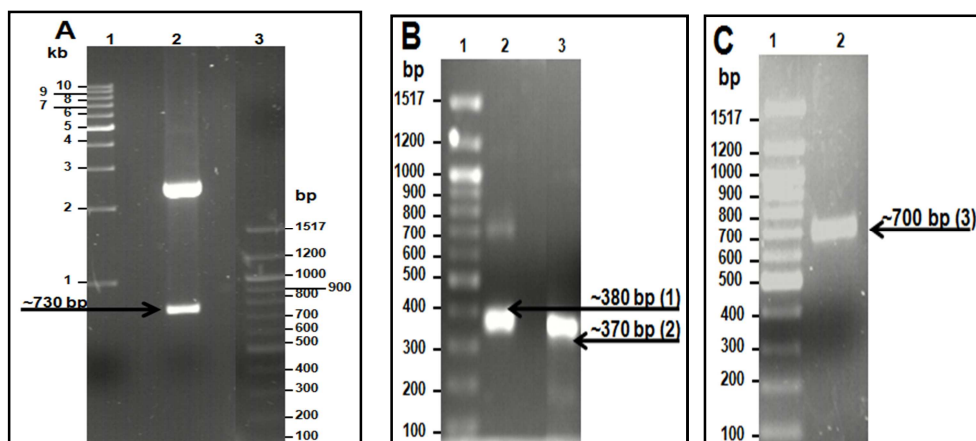


Figure VI: NcoI/NotI restriction enzyme digestion of pUC19-PfNPNA scFv-12 (A), PCR amplification of variable domains (B) and overlap extension PCR (C) of Pf-NPNA scFv-0. 50 μ L of digested reaction and 25 μ L of each PCR product was loaded and subjected to electrophoresis on a 1% and 1.5% agarose at 100 V for 1 hour. The DNA was visualised using ethidium bromide under UV light at wavelength of 200 nm. **(A)** Lane 1: 1 kb DNA ladder, Lane 2: digested pUC19-PfNPNA scFv-12 and Lane 3: 100 bp DNA ladder **(B)** Lane 1: 100 bp DNA ladder, Lane 2: Pf-NPNA V_H (380 bp), Lane 3: Pf-NPNA V_L (370 bp); **(C)** Lane 1: 100 bp DNA ladder, Lane 2: Pf-NPNA scFv-0 V_H – V_L (700 bp).

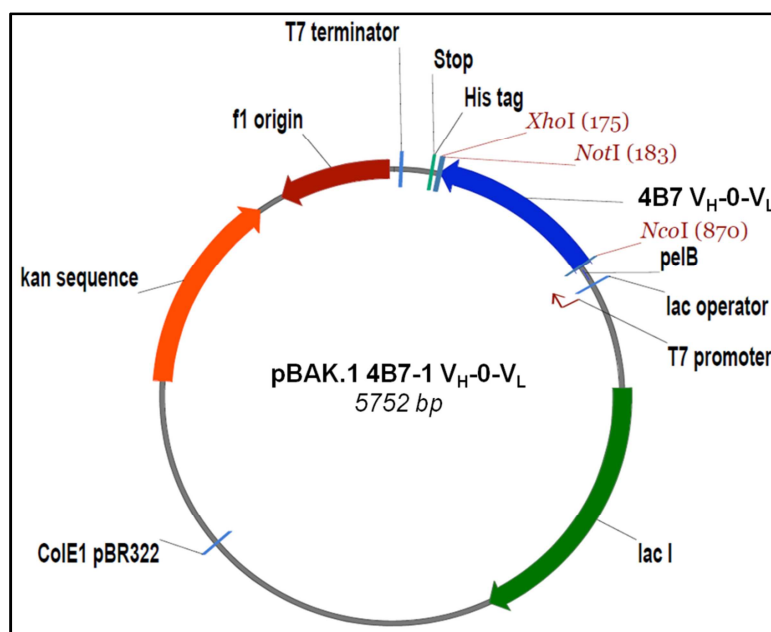


Figure VII: Physical maps of 4B7 scFv-0 V_H – V_L in pBAK.1. The plasmid is based on the pET41b(+) plasmid system and has the T7 promoter for expression of scFv. Relevant genetic elements are: lac operator, *peB* signal peptide, f1 origin of replication, T7 terminator, kanamycin resistance gene, ColE1pBR322 gene and *lacI* gene.

```

XbaI                                pelB leader sequence
1 TCTAGATCAG GAGAACAGTC ATAATGAAAT ACCTATTGCC TACGGCAGCC
            M K Y L L P T A A       Frame 3

                                sfiI      NcoI   $\overrightarrow{V_H}$ 
51 GCTGGATTGT TATTACTCGC GGCCAGCCG GCCATGGCCG AAGTGAACT
            A G L L L L A A Q P A M A E V K L       Frame 3

101 GGTGGAAAGC GGC GGCGGCC TGGTGCAGCC GGGCGGCAGC CAGAAACTGA
      V E S G G G L V Q P G G S Q K L S Frame 3
      CDR-H1
151 GCTGCGCGGC GAGCGGCTTT ACCTTTAGCG ATTATGGCAT GCGTGGTTT
      C A A S G F T F S D Y G M A W F Frame 3

201 CGCCAGGCGC CGGGCAAAGG CCCGGAATGG GTGGCGTTTA TTAACAACCT
      R Q A P G K G P E W V A F I N N L Frame 3
      CDR-H2
251 GCGTATAGC ATTTATTATG CGGATACCGT GACCGGCCGC TTTACCATTA
      A Y S I Y Y A D T V T G R F T I S Frame 3

301 GCCGCGAAAA CGCGAAAAAC ACCCTGTATC TGGAAATGAG CAGCCTGCGC
      R E N A K N T L Y L E M S S L R Frame 3
      CDR-H3
351 AGCGAAGATA CCACCATGTA TTATTGCGCG CGCGGCAACC TGTATTATGG
      S E D T T M Y Y C A R G N L Y Y G Frame 3
       $\overrightarrow{V_L}$ 
401 CCTGGATTAT TGGGGCCAGG GCACCACCCT GACCGTGAGC AGCGCGGATA
      L D Y W G Q G T T L T V S S A D I Frame 3

451 TTCAGATGAT TCAGAGCCCG AGCAGCATGT TTGCGAGCCT GGGCGATCGC
      Q M I Q S P S S M F A S L G D R Frame 3
      CDR-L1
501 GTGAGCCTGA GCTGCCGCGC GAGCCAGGAT ATTCGCGGCA ACCTGGATTG
      V S L S C R A S Q D I R G N L D W Frame 3

551 GTTTCAGCAG AAACCGGGCG GCACCATTAA ACTGCTGATT TATAGCACCA
      F Q Q K P G G T I K L L I Y S T S Frame 3
      CDR-L2
601 GCAACCTGAA CAGCGGCGTG CCGAGCCGCT TTAGCGGCAG CGGCAGCGGC
      N L N S G V P S R F S G S G S G Frame 3

651 AGCGATTATA GCCTGACCAT TAGCAGCCTG GAAAGCGAAG ATCTGGGCGA
      S D Y S L T I S S L E S E D L G D Frame 3
      CDR-L3
701 TTATTATTGC CTGCAGCGCA ACGCGTATCC GCTGACCTTT GGCAGCGGCA
      Y Y C L Q R N A Y P L T F G S G T Frame 3
      NotI      XhoI
751 CCAAACCTGGA AATTAAGCG GCCGACTCG AGCACCACCA CCACCACCAC
      K L E I K A A A L E       H H H H H H       Frame 3

801 CACCACTAG
            H H       * Frame 3

```

Figure VIII: Nucleotide and deduced amino acid sequence of pBAK.1 4B7 scFv-0 ($V_H - V_L$). The amino acid sequences corresponding to the complementary determining regions (CDRs) are in green. The leader sequence, restriction sites and octa his tag are indicated.

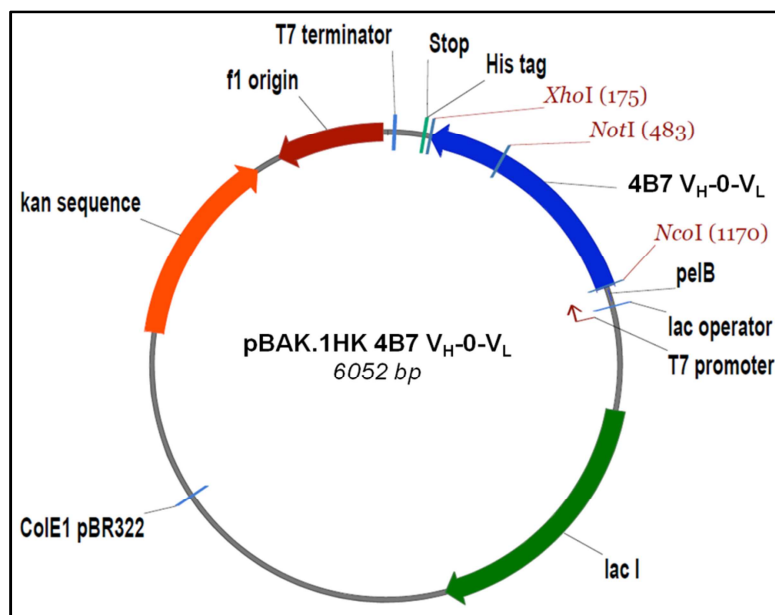


Figure IX: Physical maps of 4B7 scFv-0 V_H- V_L in pBAK.1HK. The plasmid is based on the pET41b(+) plasmid system and has the T7 promoter for expression of scFvHK. Relevant genetic elements are: lac operator, *pelB* signal peptide, f1 origin of replication, T7 terminator, kanamycin resistance gene, ColE1pBR322 gene and lacI gene.

```

XbaI
1  TCTAGATCAG  GAGAACAGTC  ATAATGAAAT  ACCTATTGCC  TACGGCAGCC
                               M  K  Y  L  L  P  T  A  A      Frame 3
                               NcoI
51  GCTGGATTGT  TATTACTCGC  GGCCAGCCG  GCCATGGCCG  AAGTGAAACT
    A  G  L  L  L  L  A  A  Q  P  A  M  A  E  V  K  L      Frame 3
101 GGTGAAAAGC  GCGGCGGCC  TGGTGCAGCC  GGGCGGCAGC  CAGAAACTGA
    V  E  S  G  G  G  L  V  Q  P  G  G  S  Q  K  L  S      Frame 3
151 GCTGCGCGGC  GAGCGGCTTT  ACCTTTAGCG  ATTATGGCAT  GCGTGGGTTT
    C  A  A  S  G  F  T  F  S  D  Y  G  M  A  W  F      Frame 3
201 CGCCAGGCGC  CGGGCAAAGG  CCCGGAATGG  GTGGCGTTTA  TTAACAACCT
    R  Q  A  P  G  K  G  P  E  W  V  A  F  I  N  N  L      Frame 3
251 GCGTATAGC  ATTTATTATG  CGGATACCGT  GACCGGCCGC  TTTACCATTA
    A  Y  S  I  Y  Y  A  D  T  V  T  G  R  F  T  I  S      Frame 3
301 GCCGCGAAAA  CGCGAAAAAC  ACCCTGTATC  TGGAAATGAG  CAGCCTGCGC
    R  E  N  A  K  N  T  L  Y  L  E  M  S  S  L  R      Frame 3
351 AGCGAAGATA  CCACCATGTA  TTATTGCGCG  CGCGGCAACC  TGTATTATGG
    S  E  D  T  T  M  Y  Y  C  A  R  G  N  L  Y  Y  G      Frame 3
401 CCTGGATTAT  TGGGGCCAGG  GCACCACCCT  GACCGTGAGC  AGCGCGGATA
    L  D  Y  W  G  Q  G  T  T  L  T  V  S  S  A  D  I      Frame 3
451 TTCAGATGAT  TCAGAGCCCG  AGCAGCATGT  TTGCGAGCCT  GGGCGATCGC
    Q  M  I  Q  S  P  S  S  M  F  A  S  L  G  D  R      Frame 3
501 GTGAGCCTGA  GCTGCCGCGC  GAGCCAGGAT  ATTCGCGGCA  ACCTGGATTG
  
```

```

V S L S C R A S Q D I R G N L D W Frame 3
551 GTTTCAGCAG AAACCGGGCG GCACCATTAA ACTGCTGATT TATAGCACCA
    F Q Q K P G G T I K L L I Y S T S Frame 3
601 GCAACCTGAA CAGCGGCGTG CCGAGCCGCT TTAGCGGCAG CGGCAGCGGC
    N L N S G V P S R F S G S G S G Frame 3
651 AGCGATTATA GCCTGACCAT TAGCAGCCTG GAAAGCGAAG ATCTGGGCGA
    S D Y S L T I S S L E S E D L G D Frame 3
701 TTATTATTGC CTGCAGCGCA ACGCGTATCC GCTGACCTTT GGCAGCGGCA
    Y Y C L Q R N A Y P L T F G S G T Frame 3
NotI
751 CCAAATGGA AATTAAAGCG GCCGCACCAT CTGTCTTCAT CTTCCC GCCA
    K L E I K A A A P S V F I F P P Frame 3
801 TCTGATGAGC AGTTGAAATC TGGAAGTACC TCTGTTGTGT GCCTGCTGAA
    S D E Q L K S G T A S V V C L L N Frame 3
851 TAACTTCTAT CCCAGAGAGG CCAAAGTACA GTGGAAGGTG GATAACGCC
    N F Y P R E A K V Q W K V D N A L Frame 3
901 TCCAATCGGG TAACTCCCAG GAGAGTGTC AAGAGCAGGA CAGCAAGGAC
    Q S G N S Q E S V T E Q D S K D Frame 3
951 AGCACCTACA GCCTCAGCAG CACCCTGACG CTGAGCAAAG CAGACTACGA
    S T Y S L S S T L T L S K A D Y E Frame 3
1001 GAAACACAAA CTCTACGCCT GCGAAGTCAC CCATCAGGGC CTGAGCTCGC
    K H K L Y A C E V T H Q G L S S P Frame 3
XhoI
1051 CCGTCACAAA GAGCTTCAAC AGGGGACTCG AGCACCACCA CCACCACCAC
    V T K S F N R G L E H H H H H H Frame 3
1101 CACCACTAAT
    H H * Frame 3

```

Figure X: Nucleotide and deduced amino acid sequence of pBAK.1Hk 4B7 scFv-0 ($V_H - V_L$). The amino acid sequences corresponding to the complementary determining regions (CDRs) are in green. The leader sequence, restriction sites and octa his tag are indicated.

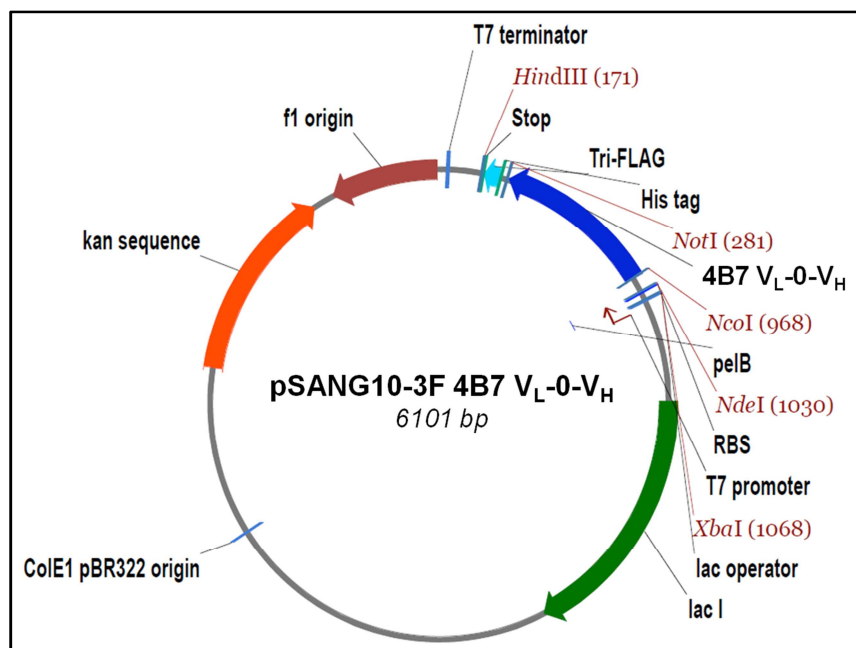


Figure XI: Physical map of 4B7 scFv-0 V_L-V_H in pSANG10-3F. The plasmid is based on the pET26(+) plasmid system and has the T7 promoter for expression of scFv-0. Relevant genetic elements are: lac operator, *pelB* signal peptide, f1 origin of replication, T7 terminator, kanamycin resistance gene, ColE1pBR322 gene and lacI gene.

XbaI	NdeI	
1 TCTAGAATAA TTTTGTTTAA CTTTAAGAAG GAGATATACA TATGAAATAC	<u>M K Y</u>	Frame 3
<i>pelB</i> leader sequence		
51 CTGCAGCCGA CCGCTGCTGC TGGTCTGCTG CTCCTCGCTG CCCAGCCGCGC	NcoI	Frame 3
<u>L Q P T A A A G L L L L A A Q P A</u>		
V _L →		
101 CATGCCGAT ATTCAGATGA TTCAGAGCCC GAGCAGCATG TTTGCGAGCC		Frame 3
<u>M A D I Q M I Q S P S S M F A S L</u>		
CDR-L1		
151 TGGGCGATCG CGTGAGCCTG AGCTGCCGCG CGAGCCAGGA TATTCGCGGC		Frame 3
<u>G D R V S L S C R A S Q D I R G</u>		
CDR-L2		
201 AACCTGGATT GGTTCAGCA GAAACCGGGC GGCACCATTA AACTGCTGAT		Frame 3
<u>N L D W F Q Q K P G G T I K L L I</u>		
CDR-L3		
251 TTATAGCACC AGCAACCTGA ACAGCGGCGT GCCGAGCCGC TTTAGCGGCA		Frame 3
<u>Y S T S N L N S G V P S R F S G S</u>		
CDR-L3		
301 GCGGCAGCGG CAGCGATTAT AGCCTGACCA TTAGCAGCCT GGAAAGCGAA		Frame 3
<u>G S G S D Y S L T I S S L E S E</u>		
CDR-L3		
351 GATCTGGGCG ATTATTATTG CCTGCAGCGC AACCGGTATC CGCTGACCTT		Frame 3
<u>D L G D Y Y C L Q R N A Y P L T F</u>		
V _H →		
401 TGGCAGCGGC ACCAAACTGG AAATTTAAAGC GGAAGTGAAA CTGGTGGAAA		Frame 3
<u>G S G T K L E I K A E V K L V E S</u>		
451 GCGGCGGCGG CCTGGTGCAG CCGGGCGGCA GCCAGAAACT GAGCTGCGCG		Frame 3
<u>G G G L V Q P G G S Q K L S C A</u>		

```

                                CDR-H1
501 GCGAGCGGCT TTACCTTTAG CGATTATGGC ATGGCGTGGT TTCGCCAGGC
    A S G F T F S D Y G M A W F R Q A   Frame 3
                                CDR-H2
551 GCCGGGCAAA GGCCCGGAAT GGGTGGCGTT TATTAACAAC CTGGCGTATA
    P G K G P E W V A F I N N L A Y S   Frame 3
601 GCATTTATTA TGCGGATACC GTGACCGGCC GCTTTACCAT TAGCCGCGAA
    I Y Y A D T V T G R F T I S R E   Frame 3
651 AACGCGAAAA ACACCCTGTA TCTGAAAATG AGCAGCCTGC GCAGCGAAGA
    N A K N T L Y L E M S S L R S E D   Frame 3
                                CDR-H3
701 TACCACCATG TATTATTGCG CGCGCGGCAA CCTGTATTAT GGCCTGGATT
    T T M Y Y C A R G N L Y Y G L D Y   Frame 3
                                NotI
751 ATTGGGGCCA GGGCACCACC CTGACCGTGA GCAGCGCGGC CGCATCCGCA
    W G Q G T T L T V S S A A A S A   Frame 3
    His6 tag                               Tri-FLAG
801 CATCATCATC ACCATCACAA GCTGGACTAC AAAGACCATG ACGGTGATTA
    H H H H H H K L D Y K D H D G D Y   Frame 3
                                HindIII
851 TAAAGATCAT GACATCGATT ACAAGGATGA CGATGACAAG TAATAAAAGC
    K D H D I D Y K D D D D K * Frame 3

```

Figure XII: Nucleotide and deduced amino acid sequence of pSANG10-3F 4B7 scFv-0 (V_L-V_H). The amino acid sequences corresponding to the complementary determining regions (CDRs) are in green. The sequences coding for the six histidines and the Tri-FLAG in the carboxy terminal part of the scFv are underlined.

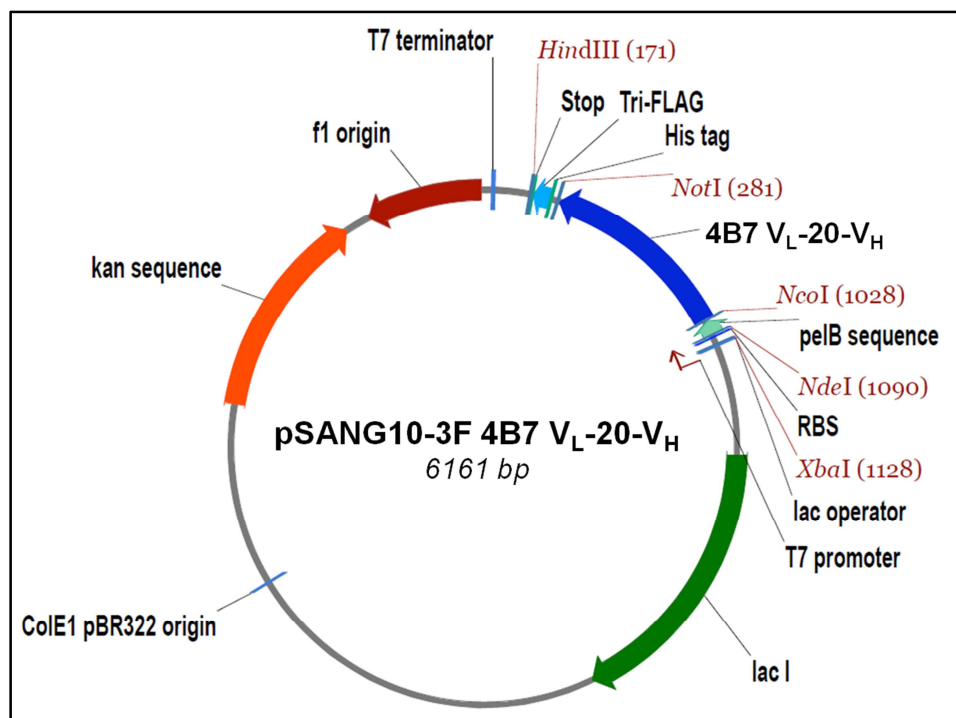


Figure XIII: Physical map of 4B7 scFv-20 V_L-V_H in pSANG10-3F. The plasmid is based on the pET26(+) plasmid system and has the T7 promoter for expression of scFv-20. Relevant genetic elements are: lac operator, *peIb* signal peptide, f1 origin of replication, T7 terminator, kanamycin resistance gene, ColE1pBR322 gene and lacI gene.

XbaI	NdeI	
1 TCTAGAATAA TTTTGTTTAA CTTTAAGAAG GAGATATACA TATGAAATAC		M K Y Frame 3
		peIb leader sequence NcoI
51 CTGCTGCCGA CCGCTGCTGC TGGTCTGCTG CTCCTCGCTG CCCAGCCGGC		L L P T A A A G L L L L A A Q P A Frame 3
		V _L →
101 CATGGCCGAT ATTCAGATGA TTCAGAGCCC GAGCAGCATG TTTGCGAGCC		M A D I Q M I Q S P S S M F A S L Frame 3
		CDR-L1
151 TGGGCGATCG CGTGAGCCTG AGCTGCCGCG CGAGCCAGGA TATTCGCGGC		G D R V S L S C R A S Q D I R G Frame 3
201 AACCTGGATT GGTTCAGCA GAAACCGGGC GGCACCATTA AACTACTGAT		N L D W F Q Q K P G G T I K L L I Frame 3
		CDR-L2
251 TTATAGCACC AGCAACCTGA ACAGCGGCGT GCCGAGCCGC TTTAGCGGCA		Y S T S N L N S G V P S R F S G S Frame 3
301 GCGGCAGCGG CAGCGATTAT AGCCTGACCA TTAGCAGCCT GGAAAGCGAA		G S G S D Y S L T I S S L E S E Frame 3
		CDR-L3
351 GATCTGGGCG ATTATTATTG CCTGCAGCGC AACCGGTATC CGCTGACCTT		D L G D Y Y C L Q R N A Y P L T F Frame 3
401 TGGCAGCGGC ACCAACTGG AAATTAAGC GGGAGGTGGC GGTAGTGGAG		G S G T K L E I K A G G G G S G G G Frame 3
		20 aa linker V _H →
451 GTGGCGGAAG CCGAGGTGGC GGTAGTGGAG GTGGCGGAAG CGAAGTGAAA		G G S G G G G S G G G G S E V K Frame 3
501 CTGGTGGAAA GCGGCGGCGG CCTGGTGCAG CCGGCGGCA GCCAGAAACT		L V E S G G G L V Q P G G S Q K L Frame 3

```

                                CDR-H1
551 GAGCTGCGCA GCGAGCGGCT TTACCTTTAG CGATTATGGC ATGGCGTGGT
    S C A A S G F T F S D Y G M A W F Frame 3
                                CDR-H2
601 TTCGCCAGGC GCCGGGCAAA GGCCCGGAAT GGGTGGCGTT TATTAACAAC
    R Q A P G K G P E W V A F I N N Frame 3
651 CTGGCGTATA GCATTTATTA TGCGGATACC GTGACCGGCC GCTTTACCAT
    L A Y S I Y Y A D T V T G R F T I Frame 3
701 TAGCCGCGAA AACGCAAAAA ACACCCTGTA TCTGGAAATG AGCAGCCTGC
    S R E N A K N T L Y L E M S S L R Frame 3
                                CDR-H3
751 GCAGCGAAGA TACCACCATG TATTATTGCG CGCGCGGCAA CCTGTATTAT
    S E D T T M Y Y C A R G N L Y Y Frame 3
                                NotI
801 GGCCTGGATT ATTGGGGCCA GGGCACCACC CTGACCGTGA GCAGCGCGGC
    G L D Y W G Q G T T L T V S S A A Frame 3
                                His6 tag                                Tri-FLAG
851 CGCATCCGCA CATCATCATC ACCATCACAA GCTGGACTAC AAAGACCATG
    A S A H H H H H H K L D Y K D H D Frame 3
901 ACGGTGATTA TAAAGATCAT GACATCGATT ACAAGGATGA CGATGACAAG
    G D Y K D H D I D Y K D D D D K Frame 3
                                HindIII
951 TAATAAAAGC TT
    * Frame 3

```

Figure XIV: Nucleotide and deduced amino acid sequence of pSANG10-3F 4B7 scFv-20 (V_L-V_H). The amino acid sequences corresponding to the complementary determining regions (CDRs) are in green. The sequences coding for the six histidines and the Tri-FLAG in the carboxy terminal part of the scFv are underlined.

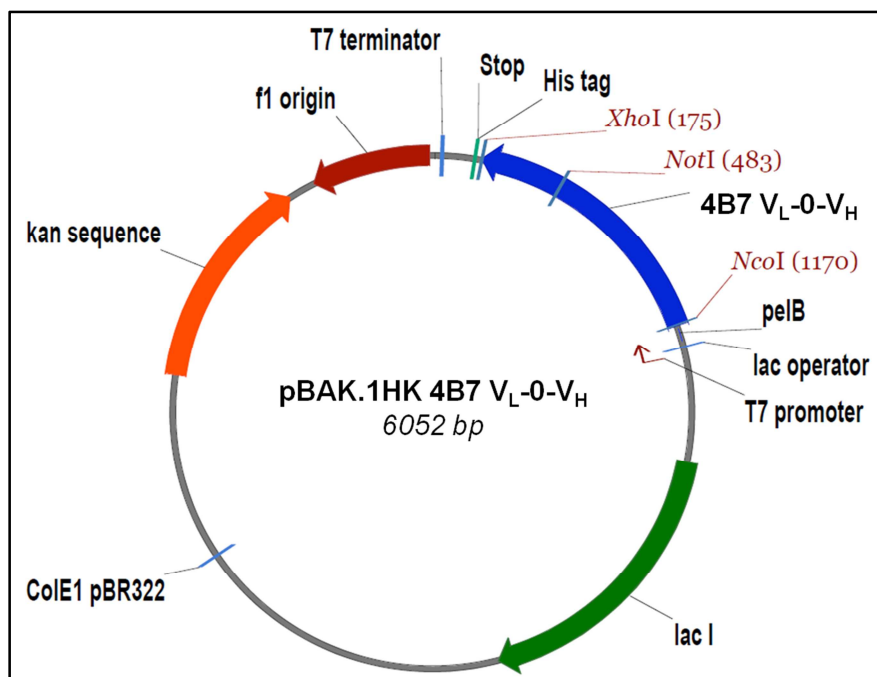


Figure XV: Physical maps of 4B7 scFv-0 V_L-V_H in pBAK.1HK. The plasmid is based on the pET41b(+) plasmid system and has the T7 promoter for expression of scFv-Hk. Relevant genetic elements are: lac operator, *pelB* signal peptide, f1 origin of replication, T7 terminator, kanamycin resistance gene, ColE1pBR322 gene and lacI gene.

XbaI

```

1 TCTAGATCAG GAGAACAGTC ATAATGAAAT ACCTATTGCC TACGGCAGCC
      M K Y L L P T A A      Frame 3
      NcoI
51 GCTGGATTGT TATTACTCGC GGCCAGCCG GCCATGGCCG ATATTGAGAT
      A G L L L L A A Q P A M A D I E M      Frame 3
101 GACCCAGAGC CCGAGCAGCA TGTTTTCGAG CCTGGGCGAT CGCGTGAGCC
      T Q S P S S M F A S L G D R V S L      Frame 3
151 TGAGCTGCCG CGCGAGCCAG GATATTCGCG GCAACCTGGA TTGGTTTCAG
      S C R A S Q D I R G N L D W F Q      Frame 3
201 CAGAAACCGG GCGGCACCAT TAAACTGCTG ATTTATAGCA CCAGCAACCT
      Q K P G G T I K L L I Y S T S N L      Frame 3
251 GAACAGCGGC GTGCCGAGCC GCTTTAGCGG CAGCGGCAGC GGCAGCGATT
      N S G V P S R F S G S G S G S D Y      Frame 3
301 ATAGCCTGAC CATTAGCAGC CTGGAAAAGCG AAGATTTTGT CGATTATTAT
      S L T I S S L E S E D F V D Y Y      Frame 3
351 TGCCTGCAGC GCAACGCGTA TCCGCTGACC TTTGGCAGCG GCACCAAACCT
      C L Q R N A Y P L T F G S G T K L      Frame 3
401 GGAAATTAAA GCGGAAAGTGA AACTGGTGGG AAGCGGCGGC GGCCTGGTGC
      E I K A E V K L V E S G G G L V Q      Frame 3
451 AGCCGGGCGG CAGCCAGAAA CTGAGCTGCG CGGCGAGCGG CTTTACCTTT
  
```

```

      P G G   S Q K   L S C A   A S G   F T F   Frame 3
501 AGCGATTATG GCATGGCGTG GTTTCGCCAG GCGCCGGGCA AAGGCCCGGA
      S D Y G   M A W   F R Q   A P G K   G P E   Frame 3
551 ATGGGTGGCG TTTATTAACA ACCTGGCGTA TAGCATTAT TATGCCGATA
      W V A   F I N N   L A Y   S I Y   Y A D T   Frame 3
601 CCGTGACCGG CCGCTTTACC ATTAGCCGCG AAAACGCGAA AAACACCCTG
      V T G   R F T   I S R E   N A K   N T L   Frame 3
651 TATCTGGAAA TGAGCAGCCT GCGCAGCGAA GATACCACCA TGTATTATTG
      Y L E M   S S L   R S E   D T T M   Y Y C   Frame 3
701 CGCGCGCGGC AACCTGTATT ATGGCCTGGA TTATTGGGGC CAGGGCACCA
      A R G   N L Y Y   G L D   Y W G   Q G T T   Frame 3
      NotI
751 CCCTGACCGT GAGCAGCGCG GCCGCACCAT CTGTCTTCAT CTTCCCGCCA
      L T V   S S A   A A P S   V F I   F P P   Frame 3
801 TCTGATGAGC AGTTGAAAATC TGGAAGTACC TCTGTTGTGT GCCTGCTGAA
      S D E Q   L K S   G T A   S V V C   L L N   Frame 3
851 TAACTTCTAT CCCAGAGAGG CCAAAGTACA GTGGAAGGTG GATAACGCCC
      N F Y   P R E A   K V Q   W K V   D N A L   Frame 3
901 TCCAATCGGG TAACTCCCAG GAGAGTGTC AAGAGCAGGA CAGCAAGGAC
      Q S G   N S Q   E S V T   E Q D   S K D   Frame 3
951 AGCACCTACA GCCTCAGCAG CACCCTGACG CTGAGCAAAG CAGACTACGA
      S T Y S   L S S   T L T   L S K A   D Y E   Frame 3
1001 GAAACACAAA CTCTACGCCT GCGAAGTCAC CCATCAGGGC CTGAGCTCGC
      K H K   L Y A C   E V T   H Q G   L S S P   Frame 3
      XhoI
1051 CCGTCACAAA GAGCTTCAAC AGGGGACTCG AGCACCACCA CCACCACCAC
      V T K   S F N   R G L E   H H H   H H H   Frame 3
1101 CACCACTAAT
      H H *   Frame 3

```

Figure XVI: Nucleotide and deduced amino acid sequence of pBAK.1 4B7 scFv-0 V_L-V_H. The amino acid sequences corresponding to the complementary determining regions (CDRs) are in green. The leader sequence, restriction sites and octa his tag are indicated.

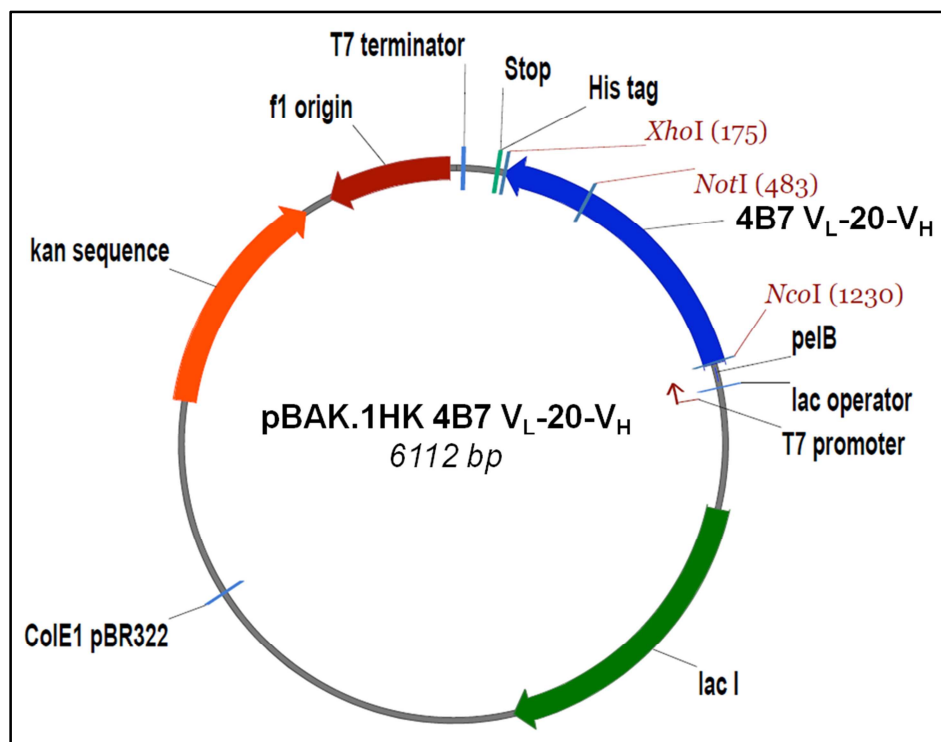


Figure XVII: Physical maps of 4B7 scFv-20 V_L-V_H in pBAK.1Hk. The plasmid is based on the pET41b(+) plasmid system and has the T7 promoter for expression of scFv-Hk. Relevant genetic elements are: *lac* operator, *peI*B signal peptide, *f1* origin of replication, T7 terminator, kanamycin resistance gene, *ColE1pBR322* gene and *lacI* gene.

```

XbaI
1  TCTAGATCAG GAGAACAGTC ATAATGAAAT ACCTATTGCC TACGGCAGCC
      M K Y L L P T A A      Frame 3
      SfiI      NcoI
51  GCTGGATTGT TATTACTCGC GGCCCAGCCG GCCATGGCCG ATATTGAGAT
      A G L L L L A A Q P A M A D I E M      Frame 3
101 GACCCAGAGC CCGAGCAGCA TGTTTTCGAG CCTGGGCGAT CGCGTGAGCC
      T Q S P S S M F A S L G D R V S L      Frame 3
151 TGAGCTGCCG CGCGAGCCAG GATATTCGCG GCAACCTGGA TTGGTTTCAG
      S C R A S Q D I R G N L D W F Q      Frame 3
201 CAGAAACCGG GCGGCACCAT TAAACTGCTG ATTTATAGCA CCAGCAACCT
      Q K P G G T I K L L I Y S T S N L      Frame 3
251 GAACAGCGGC GTGCCGAGCC GCTTTAGCGG CAGCGGCAGC GGCAGCGATT
      N S G V P S R F S G S G S G S D Y      Frame 3
301 ATAGCCTGAC CATTAGCAGC CTGGAAAAGCG AAGATTTTGT CGATTATTAT
      S L T I S S L E S E D F V D Y Y      Frame 3
351 TGCCTGCAGC GCAACGCGTA TCCGCTGACC TTTGGCAGCG GCACCAAACCT
      C L Q R N A Y P L T F G S G T K L      Frame 3
401 GGAAATTA AAA GCGGGAGGTG GCGGTAGTGG AGGTGGCGGA AGCGGAGGTG
      E I K A G G G G S G G G G S G G G      Frame 3

```

451 GCGGTAGCGG AGGTGGCGGA AGCGAAGTGA AACTGGTGA AAGCGGCGGC
 G S G G G G S E V K L V E S G G Frame 3

501 GGCCTGGTGC AGCCGGGCGG CAGCCGCAAA CTGAGCTGCG CGGCGAGCGG
 G L V Q P G G S R K L S C A A S G Frame 3

551 CTTTACCTTT AGCGATTATG GCATGGCGTG GTTTCGCCAG GCGCCGGGCA
 F T F S D Y G M A W F R Q A P G K Frame 3

601 AAGCCCCGGA ATGGGTGGCG TTTATTAACA ACCTGGCGTA TAGCATTAT
 G P E W V A F I N N L A Y S I Y Frame 3

651 TATGCGGATA CCGTGACCGG CCGCTTTACC ATTAGCCGCG AAAACGCGAA
 Y A D T V T G R F T I S R E N A K Frame 3

701 AAACACCCTG TATCTGAAA TGAGCAGCCT GCGCAGCGAA GATACCGCCA
 N T L Y L E M S S L R S E D T A M Frame 3

751 TGTATTATTG CGCGCGCGGC AACCTGTATT ATGGCCTGGA TTATTGGGGC
 Y Y C A R G N L Y Y G L D Y W G Frame 3

NotI

801 CAGGGCACCA CCGTGACCGT GAGCAGCGCG GCCGCACCAT CTGTCTTCAT
 Q G T T V T V S S A A A P S V F I Frame 3

851 CTTCCCGCCA TCTGATGAGC AGTTGAAATC TGGAAGTGC TCTGTTGTGT
 F P P S D E Q L K S G T A S V V C Frame 3

901 GCCTGCTGAA TAACTTCTAT CCCAGAGAGG CCAAAGTACA GTGGAAGGTG
 L L N N F Y P R E A K V Q W K V Frame 3

951 GATAACGCC TCCAATCGGG TAACTCCAG GAGAGTGTC CAGAGCAGGA
 D N A L Q S G N S Q E S V T E Q D Frame 3

1001 CAGCAAGGAC AGCACCTACA GCCTCAGCAG CACCCTGACG CTGAGCAAAG
 S K D S T Y S L S S T L T L S K A Frame 3

1051 CAGACTACGA GAAACACAAA CTCTACGCCT GCGAAGTCAC CCATCAGGGC
 D Y E K H K L Y A C E V T H Q G Frame 3

XhoI

1101 CTGAGCTCGC CCGTCACAAA GAGCTTCAAC AGGGGACTCG AGCACCACCA
 L S S P V T K S F N R G L E H H H Frame 3

1151 CCACCACCAC CACCACTAAT TGATTAATAC CTAGGCTGCT AAAC
 H H H H H * Frame 3

Figure XVIII: Nucleotide and deduced amino acid sequence of pBAK.1Hk 4B7 scFv-20 (V_L-V_H). The amino acid sequences corresponding to the complementary determining regions (CDRs) are in green. The sequences coding for the six histidines and the Tri-FLAG in the carboxy terminal part of the scFv are underlined.

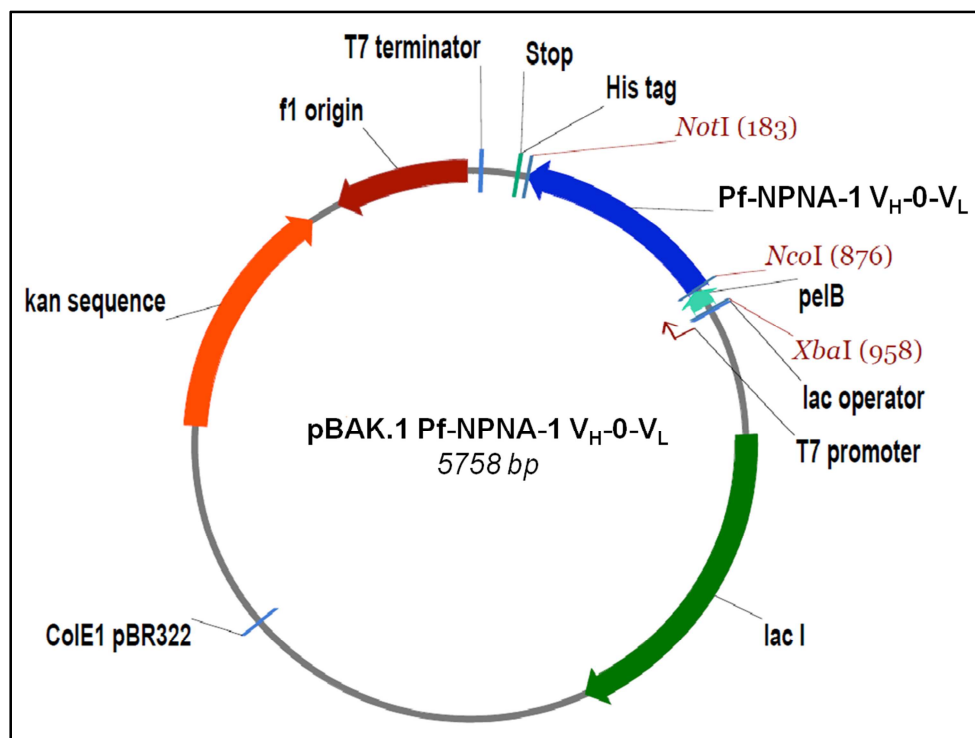


Figure XIX: Physical pBAK.1 with Pf-NPNA-1 scFv-0 insert. The plasmid is based on the pET41b(+) plasmid system and has the T7 promoter for expression of scFv-0. Relevant genetic elements are: lac operator, *pelB* signal peptide, f1 origin of replication, T7 terminator, kanamycin resistance gene, ColE1pBR322 gene and lacI gene.

XbaI		<i>pelB</i> leader sequence				
1	TCTAGATCAA	GGAGAACAGT	CATAATGAAA	TACCTATTGC	CTACGGCAGC	
			M K Y L L P	T A A		Frame 1
			SfiI	NcoI	V _H →	
51	CGCTGGATTG	TTATTACTCG	CGGCCAGCC	GGCCATGGCC	CAGGTGCAGC	
	A G L L L L A	A A Q P	A M A	Q V Q L		Frame 1
101	TGGTGCAGAG	CGGCGGCGGC	GTGGTGCAGC	CGGGCCGCAG	CCTGCGCCTG	
	V Q S G G G	V V Q P	G R S L R L			Frame 1
			CDR-H1			
151	AGCTGCGCGG	CGAGCGGCTT	TATTTTATAG	AACTATGCGA	TGGATTGGGT	
	S C A A S G F	I F S	N Y A M	D W V		Frame 1
201	GCGCCAGGCG	CCGGGCAAAG	GCCTGGATTG	GGTGGCGGTG	GTGAGCTATG	
	R Q A P G K G	L D W V A V	V S Y D			Frame 1
		CDR-H2				
251	ATGCGCGCAA	CCAGTATTAT	GCGGATAGCG	TGAAAGGCCG	CTTTACCATT	
	A R N Q Y Y	A D S V	K G R	F T I		Frame 1
301	AGCCGCGATA	ACAGCAAAA	CACCCTGTAT	CTGCGCATGA	ACAGCCTGCG	
	S R D N S K N	T L Y L R M N	S L R			Frame 1
			CDR-H3			
351	CGCGGAAGAT	ACCGCGGTGT	ATTATTGCGC	GCGCGATCGC	GATAGCTCGA	
	A E D T A V Y	Y C A R D R	D S S S			Frame 1
				V _L →		
401	GCTATTTTGA	TAGCTGGGGC	CAGGGCACCC	TGGTGACCGT	GAGCAGCGAA	
	Y F D S W G	Q G T L	V T V S S E			Frame 1

```

451 ATTGTGCTGA CCCAGAGCCC GAGCACCTG AGCGCGAGCG TGGGCGATCG
    I V L T Q S P S T L S A S V G D R      Frame 1
                                CDR-L1
501 CGTGACCACC ACCTGCCGCG CGAGCCAGGG CATTAGCAAC TGGCTGGCGT
    V T T T C R A S Q G I S N W L A W      Frame 1
                                CDR-L2
551 GGTATCAGCA GAAACCGGGC CGCGCGCCGA AACTGCTGAT TGTGAAAGCG
    Y Q Q K P G R A P K L L I V K A      Frame 1
                                CDR-L3
601 AGCAGCCTGG AAAGCGACGT GCCGAGCCGC TTTAGCGGCA GCGGCAGCGG
    S S L E S D V P S R F S G S G S G      Frame 1
                                CDR-L3
651 CACCGAATTT ACCCTGACCA TTAGCAGCCT GCAGCCGGAT GATTTGCGA
    T E F T L T I S S L Q P D D F A T      Frame 1
                                CDR-L3
701 CCTATTATTG CCAGCAGTAT AACAGCTATA GCGGCCTGAC CTTTGGCGGC
    Y Y C Q Q Y N S Y S G L T F G G      Frame 1
                                NotI      XhoI      His8 Tag
751 GGCACCAAAG TGGAAATTAA ACGCGCGGCC GCACTCGAGC ACCACCACCA
    G T K V E I K R A A A L E H H H H      Frame 1

801 CCACCACCAC CACTAA
    H H H H * Frame 1

```

Figure XX: Nucleotide and deduced amino acid sequence of pBAK.1 Pf-NPNA scFv-0 ($V_H - V_L$). The amino acid sequences corresponding to the complementary determining regions (CDRs) are in green. The leader sequence, restriction sites and octa his tag are indicated.

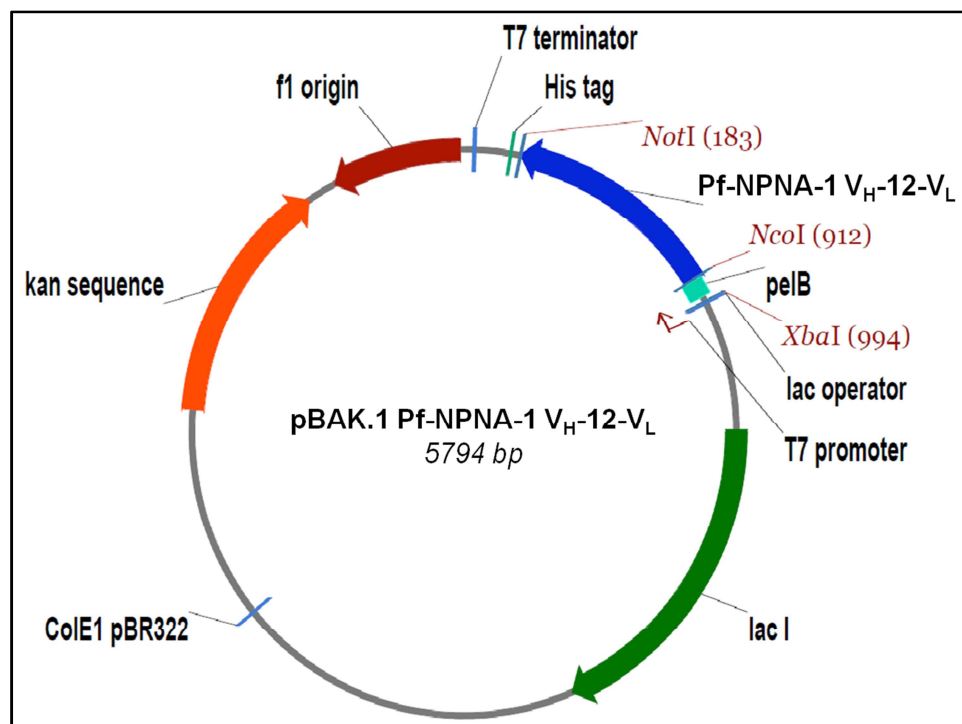


Figure XXI: Physical pBAK.1 with Pf-NPNA-1 scFv-12 insert. The plasmid is based on the pET41b(+) plasmid system and has the T7 promoter for expression of scFv-12. Relevant genetic elements are: lac operator, *peB* signal peptide, f1 origin of replication, T7 terminator, kanamycin resistance gene, ColE1pBR322 gene and *lacI* gene.

XbaI		<i>peB</i> leader sequence				
1	TCTAGATCAA	GGAGAACAGT	CATAATGAAA	TACCTATTGC	CTACGGCAGC	Frame 1
			<u>M K Y L L P</u>	<u>T A A</u>		
			sfiI	NcoI	V _H →	
51	CGCTGGATTG	TTATTACTCG	CGGCCAGCC	GGCCATGGCC	CAGGTGCAGC	Frame 1
	<u>A G L L L L A</u>	<u>A Q P</u>	<u>A M A</u>	<u>Q V Q L</u>		
101	TGGTGCAGAG	CGGCGCGGC	GTGGTGCAGC	CGGGCCGCAG	CCTGCGCCTG	Frame 1
	V Q S G G G	V V Q P	G R S L R L			
			CDR-H1			
151	AGCTGCGCGG	CGAGCGGCTT	TATTTTTAGC	AACTATGCGA	TGGATTGGGT	Frame 1
	S C A A S G F	I F S	N Y A M	D W V		
201	GCGCCAGGCG	CCGGGCAAAG	GCCTGGATTG	GGTGGCGGTG	GTGAGCTATG	Frame 1
	R Q A P G K G	L D W V A V	V S Y D			
		CDR-H2				
251	ATGCGCGCAA	CCAGTATTAT	GCGGATAGCG	TGAAAGGCCG	CTTTACCATT	Frame 1
	<u>A R N Q Y Y</u>	<u>A D S V</u>	<u>K G R</u>	<u>F T I</u>		
301	AGCCGCGATA	ACAGCAAAAA	CACCCTGTAT	CTGCGCATGA	ACAGCCTGCG	Frame 1
	S R D N S K N	T L Y L R M N	S L R			
			CDR-H3		XhoI	
351	CGCGGAAGAT	ACCGCGGTGT	ATTATTGCGC	GCGCGATCGC	GATAGCTCGA	Frame 1
	A E D T A V Y	Y C A R D R	D S S S			
401	GCTATTTTTGA	TAGCTGGGGC	CAGGGCACCC	TGGTGACCGT	GAGCAGCGGC	

```

      Y F D S W G Q G T L V T V S S G      Frame 1
      12 aa linker                               VL→
451 GGTGGCAGCG GTGGCCGGTAG CGGCCGGTGGC AGCGAAATTG TGCTGACCCA
      G G S G G G S G G G S E I V L T Q      Frame 1

501 GAGCCCGAGC ACCCTGAGCG CGAGCGTGGG CGATCGCGTG ACCACCACCT
      S P S T L S A S V G D R V T T T C      Frame 1
      CDR-L1
551 GCCGCGCGAG CCAGGGCATT AGCAACTGGC TGGCGTGGTA TCAGCAGAAA
      R A S Q G I S N W L A W Y Q Q K      Frame 1
      CDR-L2
601 CCGGGCCGCG CGCCGAAACT GCTGATTGTG AAAGCGAGCA GCCTGGAAAG
      P G R A P K L L I V K A S S L E S      Frame 1

651 CGGCGTGCCG AGCCGCTTTA GCGGCAGCGG CAGCGGCACC GAATTTACCC
      G V P S R F S G S G S G T E F T L      Frame 1

701 TGACCATTAG CAGCCTGCAG CCGGATGATT TTGCGACCTA TTATTGCCAG
      T I S S L Q P D D F A T Y Y C Q      Frame 1
      CDR-L3
751 CAGTATAACA GCTATAGCGG CCTGACCTTT GGCGGCGGCA CCAAAGTGGA
      Q Y N S Y S G L T F G G G T K V E      Frame 1
      NotI XhoI His8 Tag
801 AATTAAACGC GCGGCCGCAC TCGAGCACCA CCACCACCAC CACCACCACT
      I K R A A A L E H H H H H H H H *      Frame 1

851 AA

```

Figure XXII: Nucleotide and deduced amino acid sequence of pBAK.1 Pf-NPNA scFv-12 (V_H – V_L). The amino acid sequences corresponding to the complementary determining regions (CDRs) are in green. The leader sequence, restriction sites and octa his tag are indicated.

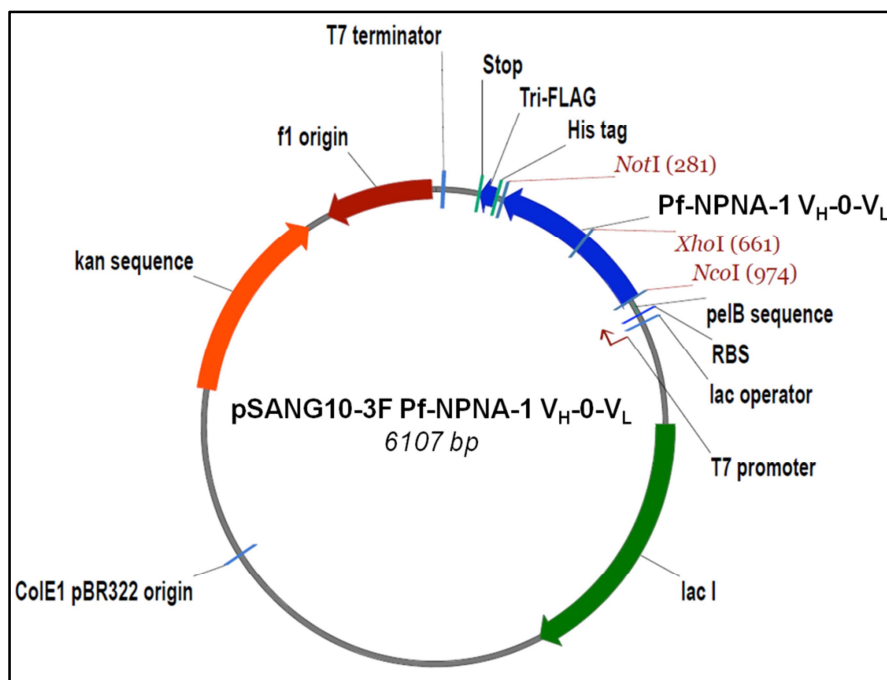


Figure XXIII: Physical map of Pf-NPNA-1 scFv-0 V_H-V_L in pSANG10-3F. The plasmid is based on the pET26(+) plasmid system and has the T7 promoter for expression of scFv-20. Relevant genetic elements are: lac operator, *peIB* signal peptide, f1 origin of replication, T7 terminator, kanamycin resistance gene, ColE1pBR322 gene and *lacI* gene.

XbaI	TTTTGTTTAA	CTTTAAGAAG	GAGATATACA	TATGAAATAC	
1	TCTAGAATAA	TTTTGTTTAA	CTTTAAGAAG	GAGATATACA	TATGAAATAC
				M K Y	Frame 3
				NcoI	
51	CTGCTGCCGA	CCGCTGCTGC	TGGTCTGCTG	CTCCTCGCTG	CCCAGCCGGC
	L L P T	A A A	G L L	L L A A	Q P A
					Frame 3
101	CATGGCCCAG	GTGCAGCTGG	TGCAGAGCGG	CGGCGGCGTG	GTGCAGCCGG
	M A Q	V Q L V	Q S G	G G V	V Q P G
					Frame 3
151	GCCGAGCCT	GCGCCTGAGC	TGCGCGGCGA	GCGGCTTTAT	TTTTAGCAAC
	R S L	R L S	C A A S	G F I	F S N
					Frame 3
201	TATGCGATGG	ATTGGGTGCG	CCAGGCGCCG	GGCAAAGGCC	TGGATTGGGT
	Y A M D	W V R	Q A P	G K G L	D W V
					Frame 3
251	GGCGGTGGTG	AGCTATGATG	CGCGCAACCA	GTATTATGCG	GATAGCGTGA
	A V V	S Y D A	R N Q	Y Y A	D S V K
					Frame 3
301	AAGGCCGCTT	TACCATTAGC	CGCGATAACA	GCAAAAACAC	CCTGTATCTG
	G R F	T I S	R D N S	K N T	L Y L
					Frame 3
351	CGCATGAACA	GCCTGCGCGC	GGAAGATACC	GCGGTGTATT	ATTGCGCGCG
	R M N S	L R A	E D T	A V Y Y	C A R
					Frame 3
401	CGATCGCGAT	AGCTCGAGCT	ATTTTGATAG	CTGGGGCCAG	GGCACCCTGG
	D R D	S S S Y	F D S	W G Q	G T L V
					Frame 3
451	TGACCGTGAG	CAGCGAAATT	GTGCTGACCC	AGAGCCCGAG	CACCCTGAGC

```

      T V S   S E I   V L T Q   S P S   T L S           Frame 3
501 GCGAGCGTGG GCGATCGCGT GACCACCACC TGCCGCGCGA GCCAGGGCAT
    A S V G   D R V   T T T   C R A S   Q G I           Frame 3
551 TAGCAACTGG CTGGCGTGGT ATCAGCAGAA ACCGGGCCGC GCGCCGAAAC
    S N W   L A W Y   Q Q K   P G R   A P K L           Frame 3
601 TGCTGATTGT GAAAGCGAGC AGCCTGGAAA GCGACGTGCC GAGCCGCTTT
    L I V   K A S   S L E S   D V P   S R F           Frame 3
651 AGCGGCAGCG GCAGCGGCAC CGAATTTACC CTGACCATTA GCAGCCTGCA
    S G S G   S G T   E F T   L T I S   S L Q           Frame 3
701 GCCGGATGAT TTTGCGACCT ATTATTGCCA GCAGTATAAC AGCTATAGCG
    P D D   F A T Y   Y C Q   Q Y N   S Y S G           Frame 3
                                           NotI
751 GCCTGACCTT TGGCGGCGGC ACCAAAGTGG AAATTAAACG CGCGGCCGCA
    L T F   G G G   T K V E   I K R   A A A           Frame 3
801 TCCGCACATC ATCATCACCA TCACAAGCTG GACTACAAAG ACCATGACGG
    S A H H   H H H   H K L   D Y K D   H D G           Frame 3
851 TGATTATAAA GATCATGACA TCGATTACAA GGATGACGAT GACAAGTAAT
    D Y K   D H D I   D Y K   D D D   D K *           Frame 3
      HindIII
901 TAAGCTTTAA TAAGTCGAGC ACCACCACCA CCACCACTGA GATCCGGCTG

```

Figure XXIV: Nucleotide and deduced amino acid sequence of pSANG10-3F NPNA scFv-0 (V_H - V_L). The amino acid sequences corresponding to the complementary determining regions (CDRs) are in green. The sequences coding for the six histidines and the Tri-FLAG in the carboxy terminal part of the scFv are underlined.

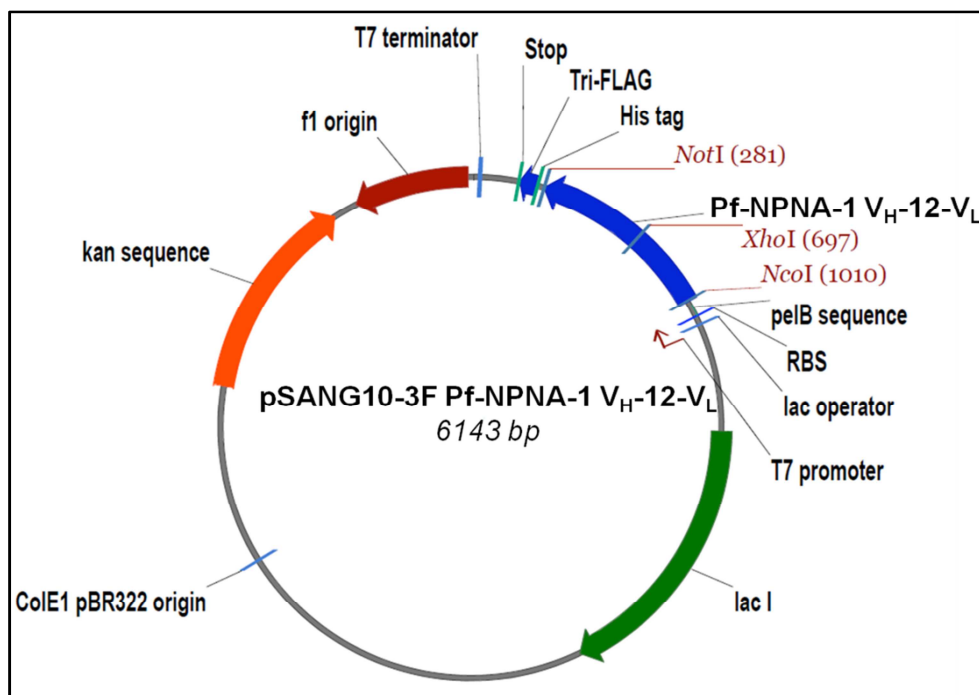


Figure XXV: Physical map of Pf-NPNA-1 scFv-12 V_H-V_L in pSANG10-3F. The plasmid is based on the pET26(+) plasmid system and has the T7 promoter for expression of scFv-20. Relevant genetic elements are: lac operator, *pelB* signal peptide, f1 origin of replication, T7 terminator, kanamycin resistance gene, ColE1pBR322 gene and *lacI* gene.

XbaI

1 TCTAAGAATA ATTTTGTTTA ACTTTAAGAA GGAGATATAC ATATGAAATA
M K Y Frame 1

51 CCTGCTGCCG ACCGCTGCTG CTGGTCTGCT GCTCCTCGCT GCCCAGCCGG
L L P T A A A G L L L L A A Q P A Frame 1

NcoI

101 CCATGGCCCA GGTGCAGCTG GTGCAGAGCG GCGGCGGCGT GGTGCAGCCG
M A Q V Q L V Q S G G G V V Q P Frame 1

151 GGCCGCAGCC TGC GCCTGAG CTGCGCGGCG AGCGGCTTTA TTTT TAGCAA
G R S L R L S C A A S G F I F S N Frame 1

201 CTATGCGATG GATTGGGTGC GCCAGGCGCC GGGCAAAGGC CTGGATTGGG
Y A M D W V R Q A P G K G L D W V Frame 1

251 TGGCGGTGGT GAGCTATGAT GCGCGCAACC AGTATTATGC GGATAGCGTG
A V V S Y D A R N Q Y Y A D S V Frame 1

301 AAAGGCCGCT TTACCATTAG CCGCGATAAC AGCAAAAACA CCCTGTATCT
K G R F T I S R D N S K N T L Y L Frame 1

351 GCGCATGAAC AGCCTGCGCG CGGAAGATAC CGCGGTGTAT TATTGCGCGC
R M N S L R A E D T A V Y Y C A R Frame 1

XhoI

401 GCGATCGCGA TAGCTCGAGC TATTTTGATA GCTGGGGCCA GGGCACCCCTG
D R D S S S Y F D S W G Q G T L Frame 1

```

451 GTGACCGTGA GCAGCGGCGG TGGCAGCGGT GCGCGTAGCG GCGGTGGCAG
   V T V S S G G G S G G G S G G G S Frame 1

501 CGAAATTGTG CTGACCCAGA GCCCGAGCAC CCTGAGCGCG AGCGTGGGCG
   E I V L T Q S P S T L S A S V G D Frame 1

551 ATCGCGTGAC CACCACCTGC CGCGCGAGCC AGGGCATTAG CAACTGGCTG
   R V T T T C R A S Q G I S N W L Frame 1

601 GCGTGGTATC AGCAGAAACC GGGCCGCGCG CCGAAACTGC TGATTGTGAA
   A W Y Q Q K P G R A P K L L I V K Frame 1

651 AGCGAGCAGC CTGGAAAAGCG GCGTGCCGAG CCGCTTTAGC GGCAGCGGCA
   A S S L E S G V P S R F S G S G S Frame 1

701 GCGGCACCGA ATTTACCCTG ACCATTAGCA GCCTGCAGCC GGATGATTTT
   G T E F T L T I S S L Q P D D F Frame 1

751 GCGACCTATT ATTGCCAGCA GTATAACAGC TATAGCGGCC TGACCTTTGG
   A T Y Y C Q Q Y N S Y S G L T F G Frame 1
                                     NotI
801 CGGCGGCACC AAAGTGGAAA TTAAACGCGC GGCCGCATCC GCACATCATC
   G G T K V E I K R A A A S A H H H Frame 1

851 ATCACCATCA CAAGCTGGAC TACAAAGACC ATGACGGTGA TTATAAAGAT
   H H H K L D Y K D H D G D Y K D Frame 1
                                     HindIII
901 CATGACATCG ATTACAAGGA TGACGATGAC AAGTAATAAA AGCTTTAATA
   H D I D Y K D D D D K * Frame 1

```

Figure XXVI: Nucleotide and deduced amino acid sequence of pSANG10-3F NPNA scFv-12 (V_H-V_L). The amino acid sequences corresponding to the complementary determining regions (CDRs) are in green. The sequences coding for the six histidines and the Tri-FLAG in the carboxy terminal part of the scFv are underlined.

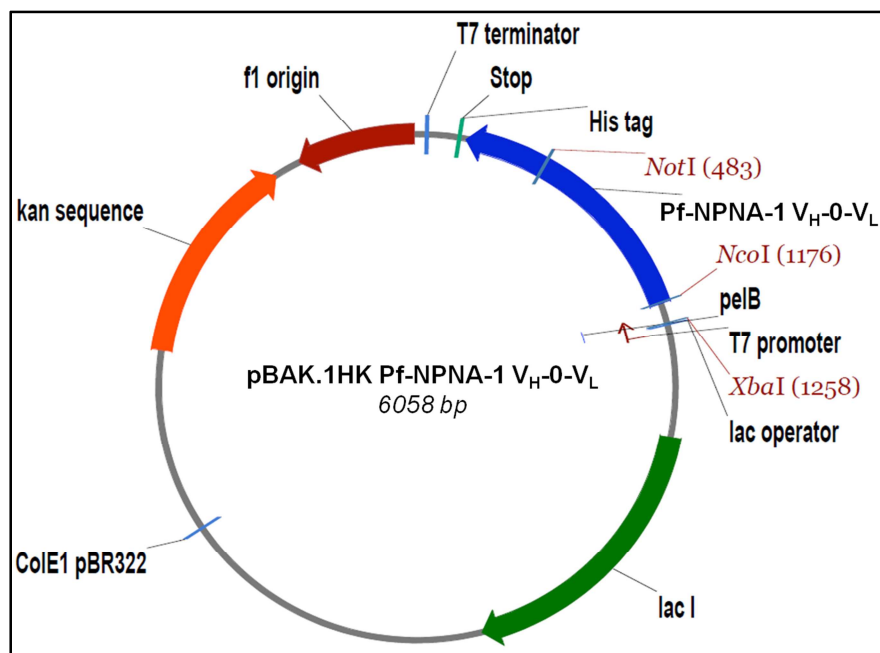


Figure XXVII: Physical pBAK.1HK with Pf-NPNA-1 scFv-0 insert. The plasmid is based on the pET41b(+) plasmid system and has the T7 promoter for expression of scFv-0Hk. Relevant genetic elements are: lac operator, *peB* signal peptide, f1 origin of replication, T7 terminator, kanamycin resistance gene, ColE1pBR322 gene and *lacI* gene.

```

XbaI
1 TCTAGATCAA GGAGAACAGT CATAATGAAA TACCTATTGC CTACGGCAGC
                               M K Y L L P T A A Frame 1

                               SfiI           NcoI
51 CGAAGGGGTG TTATTACTCG CGGCCAGCC GGCCATGGCC CAGGTGCAGC
   E G V L L L A A Q P A M A Q V Q L Frame 1

101 TGGTGCAGAG CGGCGGCGGC GTGGTGCAGC CGGGCCGCAG CCTGCGCCTG
    V Q S G G G V V Q P G R S L R L Frame 1

151 AGCTGCGCGG CGAGCGGCTT TATTTTTAGC AACTATGCGA TGGATTGGGT
    S C A A S G F I F S N Y A M D W V Frame 1

201 GCGCCAGGCG CCGGGCAAAG GCCTGGATTG GGTGGCGGTG GTGAGCTATG
    R Q A P G K G L D W V A V V S Y D Frame 1

251 ATGCGCGCAA CCAGTATTAT GCGGATAGCG TGAAAGGCCG CTTTACCATT
    A R N Q Y Y A D S V K G R F T I Frame 1

301 AGCCGCGATA ACAGCAAAAA CACCCTGTAT CTGCGCATGA ACAGCCTGCG
    S R D N S K N T L Y L R M N S L R Frame 1

                               XhoI
351 CGCGGAAGAT ACCGCGGTGT ATTATTGCGC GCGCGATCGC GATAGCTCGA
    A E D T A V Y Y C A R D R D S S S Frame 1

401 GCTATTTTGA TAGCTGGGGC CAGGGCACCC TGGTGACCGT GAGCAGCGAA
    Y F D S W G Q G T L V T V S S E Frame 1

451 ATTGTGCTGA CCCAGAGCCC GAGCACCTG AGCGGAGCG TGGGCGATCG

```

```

      I V L T Q S P S T L S A S V G D R Frame 1
501 CGTGACCACC ACCTGCCGCG CGAGCCAGGG CATTAGCAAC TGGCTGGCGT
      V T T T C R A S Q G I S N W L A W Frame 1
551 GGTATCAGCA GAAACCGGGC CGCGCGCCGA AACTGCTGAT TGTGAAAGCG
      Y Q Q K P G R A P K L L I V K A Frame 1
601 AGCAGCCTGG AAAGCGGCGT GCCGAGCCGC TTTAGCGGCA GCGGCAGCGG
      S S L E S G V P S R F S G S G S G Frame 1
651 CACCGAATTT ACCCTGACCA TTAGCAGCCT GCAGCCGGAT GATTTTGCGA
      T E F T L T I S S L Q P D D F A T Frame 1
701 CCTATTATTG CCAGCAGTAT AACAGCTATA GCGGCCTGAC CTTTGGCGGC
      Y Y C Q Q Y N S Y S G L T F G G Frame 1

                                NotI
751 GGCACCAAAG TGGA AATTAA ACGCGCGGCC GCACCATCTG TCTTCATCTT
      G T K V E I K R A A A P S V F I F Frame 1
801 CCCGCCATCT GATGAGCAGT TGAAATCTGG AACTGCCTCT GTTGTGTGCC
      P P S D E Q L K S G T A S V V C L Frame 1
851 TGCTGAATAA CTTCTATCCC AGAGAGGCCA AAGTACAGTG GAAGGTGGAT
      L N N F Y P R E A K V Q W K V D Frame 1
901 AACGCCCTCC AATCGGGTAA CTCCCAGGAG AGTGTCACAG AGCAGGACAG
      N A L Q S G N S Q E S V T E Q D S Frame 1
951 CAAGGACAGC ACCTACAGCC TCAGCAGCAC CCTGACGCTG AGCAAAGCAG
      K D S T Y S L S S T L T L S K A D Frame 1
1001 ACTACGAGAA ACACAAACTC TACGCCTGCG AAGTCACCCA TCAGGGCCTG
      Y E K H K L Y A C E V T H Q G L Frame 1

                                XhoI
1051 AGCTCGCCCG TCACAAAGAG CTTCAACAGG GGACTCGAGC ACCACCACCA
      S S P V T K S F N R G L E H H H H Frame 1

1101 CCACCACCAC CACTAATTGA TTAATACCTA GGCTGCTAAA CAAAGCCC GA
      H H H H * Frame 1

```

Figure XXVIII: Nucleotide and deduced amino acid sequence of pBAK.1Hk Pf-NPNA scFv-0 ($V_H - V_L$). The amino acid sequences corresponding to the complementary determining regions (CDRs) are in green. The leader sequence, restriction sites and octa his tag are indicated.

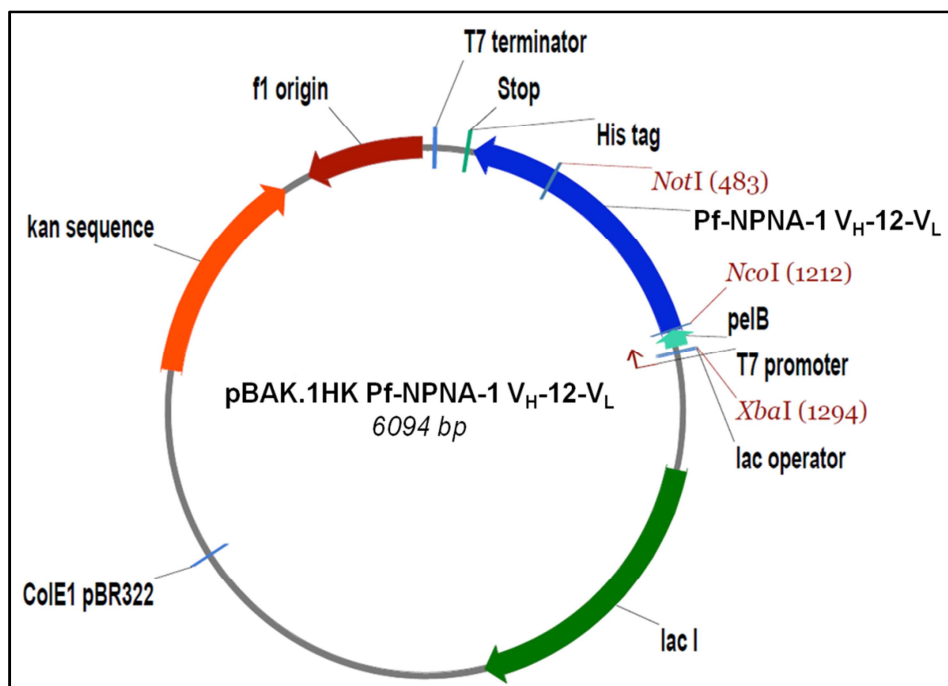


Figure XXIX: Physical pBAK.1HK with Pf-NPNA-1 scFv-12 insert. The plasmid is based on the pET41b(+) plasmid system and has the T7 promoter for expression of scFv-12Hk. Relevant genetic elements are: lac operator, *pelB* signal peptide, f1 origin of replication, T7 terminator, kanamycin resistance gene, ColE1pBR322 gene and *lacI* gene.

XbaI

```

1 TCTAGATCAG GAGAACAGTC ATAATGAAAT ACCTATTGCC TACGGCAGCC
      M K Y L L P T A A Frame 3
      SfiI NcoI
51 GCTGGATTGT TATTACTCGC GGCCAGCCG GCCATGGCCC AGGTGCAGCT
  A G L L L L A A Q P A M A Q V Q L Frame 3
101 GGTGCAGAGC GCGGGCGGCG TGGTGCAGCC GGGCCGCAGC CTGCGCCTGA
  V Q S G G G V V Q P G R S L R L S Frame 3
151 GCTGCGCGGC GAGCGGCTTT ATTTTATAGCA ACTATGCGAT GGATTGGGTG
  C A A S G F I F S N Y A M D W V Frame 3
201 CGCCAGGCGC CGGGCAAAGG CCTGGATTGG GTGGCGGTGG TGAGCTATGA
  R Q A P G K G L D W V A V V S Y D Frame 3
251 TGC GCGCAAC CAGTATTATG CGGATAGCGT GAAAGGCCGC TTTACCATTA
  A R N Q Y Y A D S V K G R F T I S Frame 3
301 GCCGCGATAA CAGCAAAAAC ACCCTGTATC TGCGCATGAA CAGCCTGCGC
      R D N S K N T L Y L R M N S L R Frame 3
      XhoI
351 GCGGAAGATA CCGCGGTGTA TTATTGCGCG CGCGATCGCG ATAGCTCGAG
  A E D T A V Y Y C A R D R D S S S Frame 3
401 CTATTTTGAT AGCTGGGGCC AGGGCACCCCT GGTGACCGTG AGCAGCGGCG
  Y F D S W G Q G T L V T V S S G G Frame 3

```

```

451 GTGGCAGCGG TGGCGGTAGC GCGGGTGGCA GCGAAATTGT GCTGACCCAG
    G S G G G S G G G S E I V L T Q Frame 3

501 AGCCCGAGCA CCCTGAGCGC GAGCGTGGGC GATCGCGTGA CCACCACCTG
    S P S T L S A S V G D R V T T T C Frame 3

551 CCGCGCGAGC CAGGGCATTG GCAACTGGCT GCGGTGGTAT CAGCAGAAAC
    R A S Q G I S N W L A W Y Q Q K P Frame 3

601 CGGGCCGCGC GCCGAAACTG CTGATTGTGA AAGCGAGCAG CCTGGAAAGC
    G R A P K L L I V K A S S L E S Frame 3

651 GCGGTGCCGA GCCGCTTTAG CGGCAGCGGC AGCGGCACCG AATTTACCCT
    G V P S R F S G S G S G T E F T L Frame 3

701 GACCATTAGC AGCCTGCAGC CGGATGATTT TGCGACCTAT TATTGCCAGC
    T I S S L Q P D D F A T Y Y C Q Q Frame 3

751 AGTATAACAG CTATAGCGGC CTGACCTTTG GCGGCGGCAC CAAAGTGGAA
    Y N S Y S G L T F G G G T K V E Frame 3
    NotI
801 ATTAAACGCG CGGCCGCACC ATCTGTCTTC ATCTTCCC GC CATCTGATGA
    I K R A A A P S V F I F P P S D E Frame 3

851 GCAGTTGAAA TCTGGAAGT CCTCTGTTGT GTGCCTGCTG AATAACTTCT
    Q L K S G T A S V V C L L N N F Y Frame 3

901 ATCCCAGAGA GGCCAAAGTA CAGTGAAGG TGGATAACGC CCTCCAATCG
    P R E A K V Q W K V D N A L Q S Frame 3

951 GGTAACTCCC AGGAGAGTGT CACAGAGCAG GACAGCAAGG ACAGCACCTA
    G N S Q E S V T E Q D S K D S T Y Frame 3

1001 CAGCCTCAGC AGCACCTGA CGCTGAGCAA AGCAGACTAC GAGAAACACA
    S L S S T L T L S K A D Y E K H K Frame 3

1051 AACTCTACGC CTGCGAAGTC ACCCATCAGG GCCTGAGCTC GCCCGTCACA
    L Y A C E V T H Q G L S S P V T Frame 3
    XhoI
1101 AAGAGCTTCA ACAGGGGACT CGAGCACCAC CACCACCACC ACCACCACTA
    K S F N R G L E H H H H H H H H * Frame 3

```

Figure XXX: Nucleotide and deduced amino acid sequence of pBAK.1Hk Pf-NPNA scFv-12 (V_H – V_L). The amino acid sequences corresponding to the complementary determining regions (CDRs) are in green. The leader sequence, restriction sites and octa his tag are indicated.

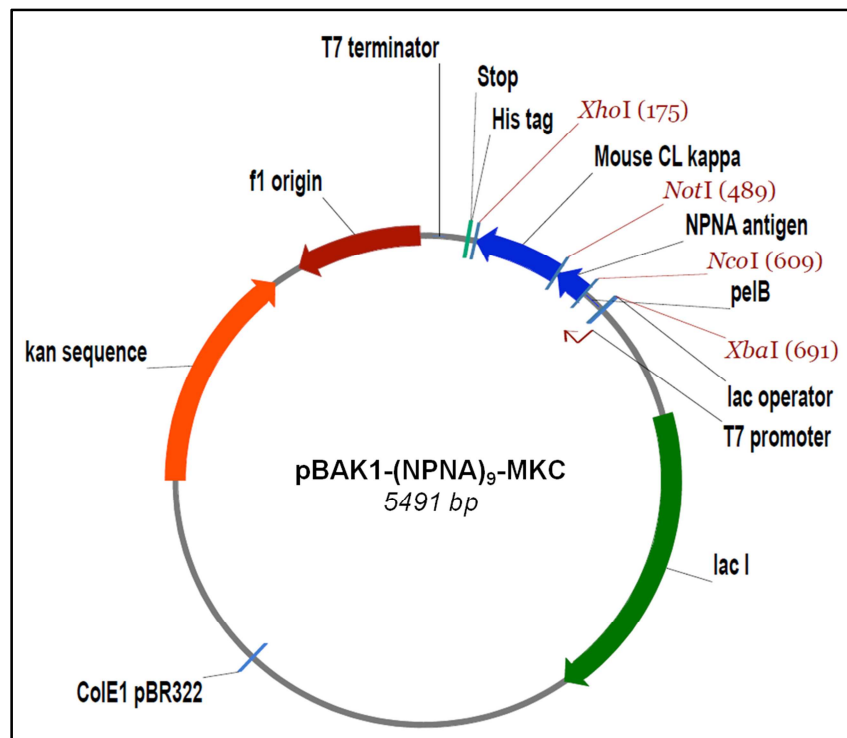


Figure XXXI: Physical map of pBAK.1-(NPNA)₉-MKC. The plasmid is based on the pET41b(+) plasmid system and has the T7 promoter for expression of the antigen (NPNA)₉-MKC. MKC stands for mouse kappa constant chain. Relevant genetic elements are: lac operator, *peI*B signal peptide, f1 origin of replication, T7 terminator, kanamycin resistance gene, ColE1pBR322 gene and *lacI* gene.

	XbaI		pelB leader sequence		
1	TCTAGATCAA	GGAGAACAGT	CATAATGAAA	TACCTATTGC	CTACGGCAGC
			<u>M K Y L L P T A A</u>		Frame 1
			sfiI	NcoI	
51	CGCTGGATTG	TTATTACTCG	CGGCCAGCC	GGCCATGGCG	AACGCAAATC
	<u>A G L L L L A</u>	<u>A Q P A M A</u>			N A N P
					Frame 1
101	CGAACGCCAA	TCCGAACGCT	AATCCGAACG	CTAATCCGAA	CGCAAATCCG
	N A N P N A	N P N A	N P N A	N P N A	N P N
					Frame 1
151	AACGCGAATC	CGAACGCTAA	TCCGAACGCA	AATCCGAACG	CGAATCCGAA
	N A N P N A	N P N A	N P N A	N P N A	N P N
					Frame 1
			NotI		
201	CGCGCCGCA	CCAACTGTAT	CCATCTTCCC	ACCATCCAGT	GAGCAGTTAA
	A A A	P T V S	I F P	P S S	E Q L T
					Frame 1
251	CATCTGGAGG	TGCCTCAGTC	GTGTGCTTCT	TGAACAACTT	CTACCCCAA
	S G G	A S V	V C F L	N N F	Y P K
					Frame 1
301	GACATCAATG	TCAAGTGGAA	GATTGATGGC	AGTGAACGAC	AAAATGGCGT
	D I N V	K W K	I D G	S E R Q	N G V
					Frame 1
351	CCTGAACAGT	TGGA CTGATC	AGGACAGCAA	AGACAGCACC	TACAGCATGA
	L N S	W T D Q	D S K	D S T	Y S M S
					Frame 1

```

401 GCAGCACCTT CACGTTGACC AAGGACGAGT ATGAACGACA TAACAGCTAT
    S T L T L T K D E Y E R H N S Y      Frame 1

451 ACCTGTGAGG CCACTCACAA GACATCAACT TCACCCATTG TCAAGAGCTT
    T C E A T H K T S T S P I V K S F      Frame 1
        XhoI           His8 Tag

501 CAACAGGAAT GAGTCTCTCG AGCACCACCA CCACCACCAC CACCACTAA
    N R N E S L E H H H H H H H H *      Frame 1
  
```

Figure XXXII: Nucleotide and deduced amino acid sequence of pBAK.1(NPNA)₉-MKC. MKC sequence is in green. The leader sequence, restriction sites and octa his tag are indicated.

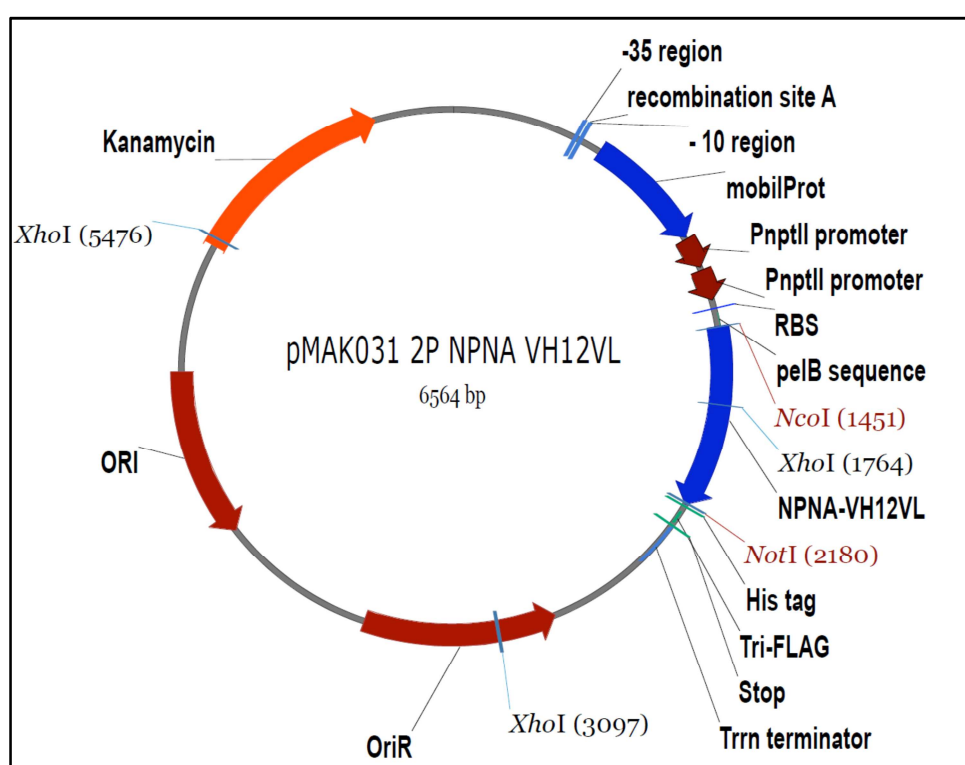


Figure XXXIII: Vector map of plasmid pMAK031 2P Pf-NPNA-1 scFv-12 insert. ORI: origin of replication for gram-negative bacteria; OriR: origin of replication for gram-positive bacteria; mobilProt: mobilisation protein; PnptII: constitutive kanamycin (neomycin) phosphotransferase promoter; Trn terminator: *rrnB* rRNA T1 transcriptional terminator; kanamycin: kanamycin resistance gene. Restriction sites (*NcoI*, *NotI*, *NdeI*) for cloning of scFv genes are coloured red. The 6X His and Tri-FLAG tags are shown.

HindIII

1051 TAAAGATCAT GACATTGATT ACAAGGATGA CGATGACAAG TAATAAAAGC
 K D H D I D Y K D D D D K * Frame 2

Figure XXXIV: Nucleotide and deduced amino acid sequence of pMAK031 2P Pf-NPNA scFv-12 (V_H – V_L). The amino acid sequences corresponding to the complementary determining regions (CDRs) are in green. The leader sequence, restriction sites and octa his tag are indicated

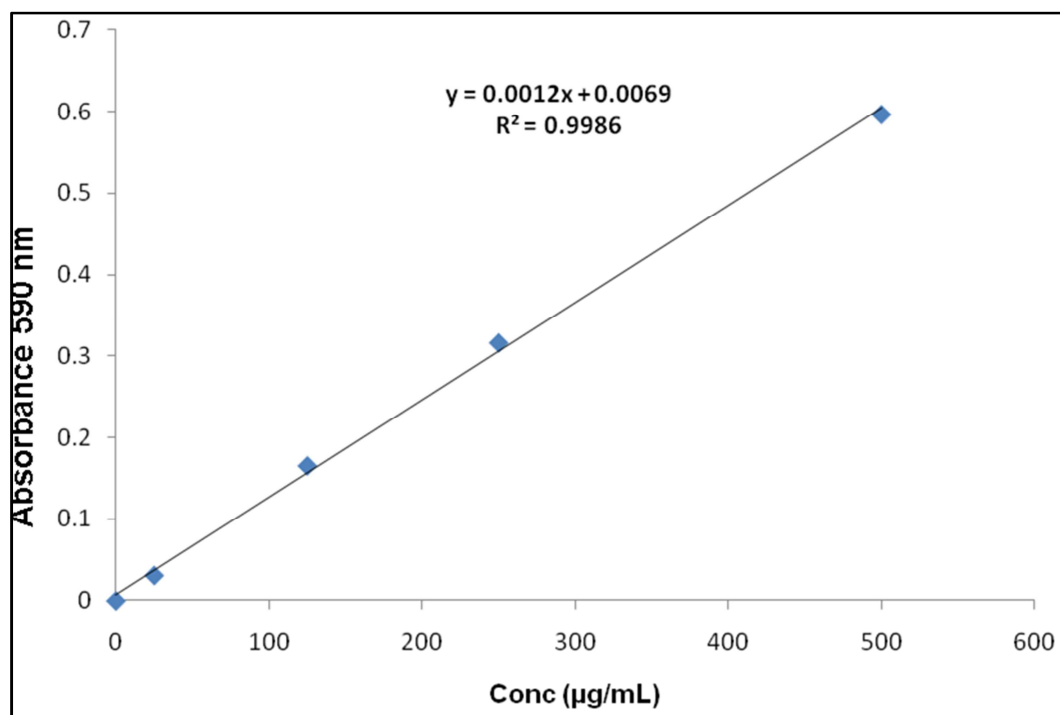


Figure XXXV: Bradford protein calibration curve. Protein standards were prepared in the range of 0 to 500 µg/mL. Absorbance was measured at 590 nm.

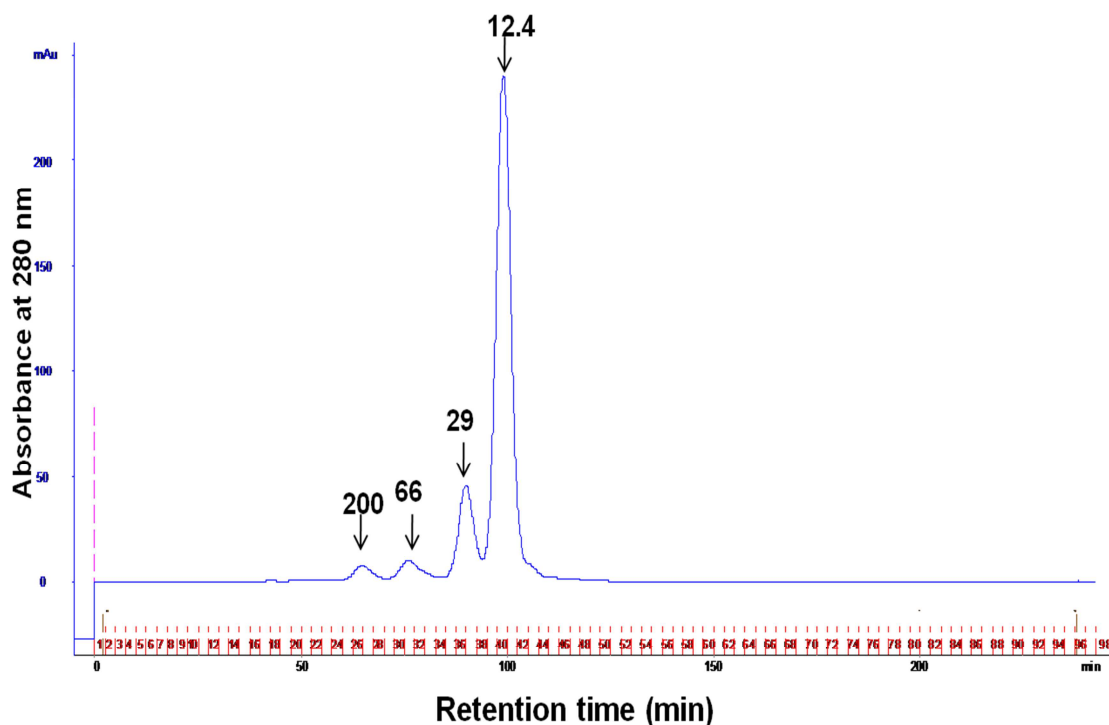


Figure XXXVI: Chromatographic separation of protein standards on HiLoad 16/60 Superdex column. The protein standards, cytochrome c (12.4 kDa), carbonic anhydrase (29 kDa), bovine serum albumin (66 kDa) and β -Amylase (200 kDa) were run under the conditions described in section. The column was eluted with 240 mL of 1X PBS (3.2 mM Na_2HPO_4 , 0.5 mM KH_2PO_4 , 1.3 mM KCl, 135 mM NaCl, pH 8.0), run at a flow rate of 1.0 ml/min.

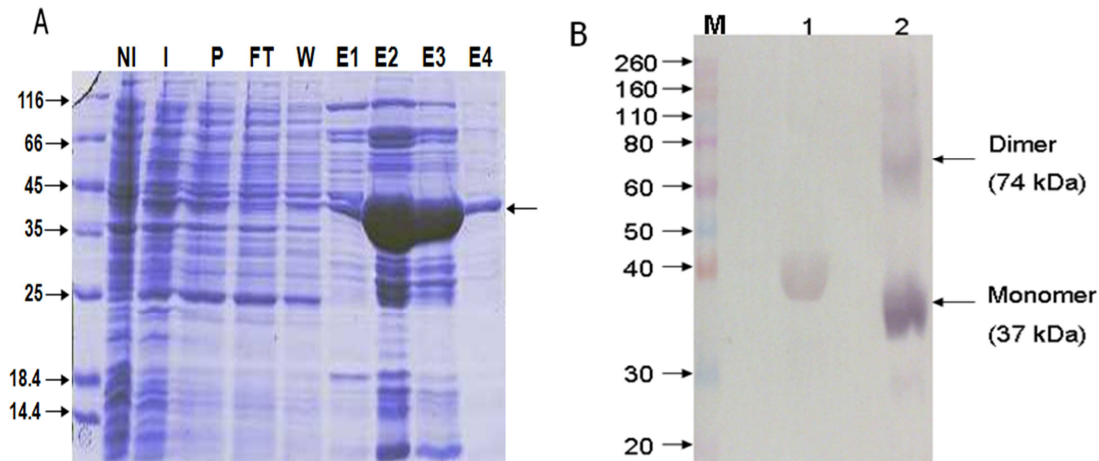


Figure XXXVII: SDS-PAGE (A) and Western blot (B) analyses of Ni-NTA affinity purified scFv NPNA $\text{VH}_{12}\text{VL Hk}$. **A:** Proteins were electrophoresed on a 12% gel and stained with Coomassie brilliant blue R-250. M: protein marker (kDa); NI: non-induced cell pellets; I: induced cell pellets; P: periplasmic fraction; FT: flow through; W: wash; E1- E4: Elutions 1-4. Arrow indicates expressed protein (37 kDa). **B:** Semi-native and western blot demonstrating multimerisation of scFv NPNA $\text{VH}_{12}\text{VL Hk}$. Ni-NTA purified protein (elution 2, Figure A) was analysed under reducing (lane 1) and non-reducing conditions (lane 2). M: molecular weight maker (kDa); Protein was probed with goat Anti-Human kappa light chain monoclonal antibody (1:30000) conjugated to alkaline phosphatase (AP). BCIP/NBT was used as substrate. Arrows indicate the monomeric and dimeric forms of the NPNA scFv-12Hk.

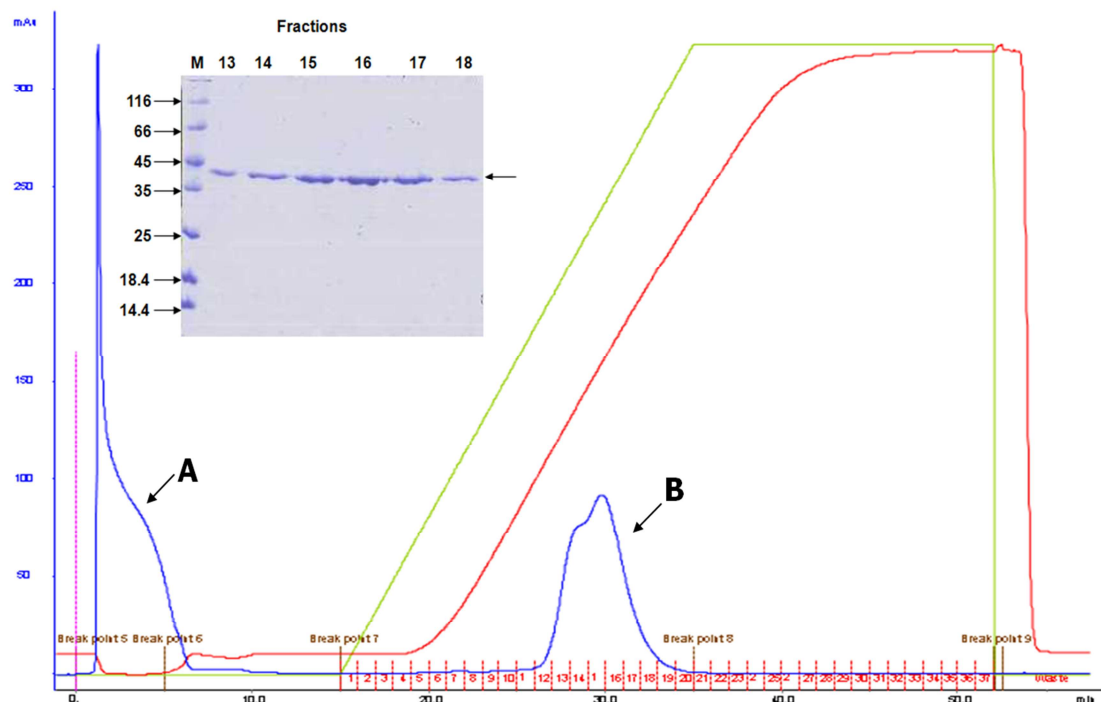


Figure XXXVIII: Cation exchange chromatography profile of Ni-NTA purified scFv NPNA VH₁₂VL Hk. The Ni-NTA purified proteins were desalted on a Sephadex G-20 column before being applied on a 1 mL HiTrap™ SP FF cation exchange column. Proteins were eluted with a 1 M NaCl gradient. Eluted fractions (13 to 18) were analysed on SDS-PAGE (Insert).

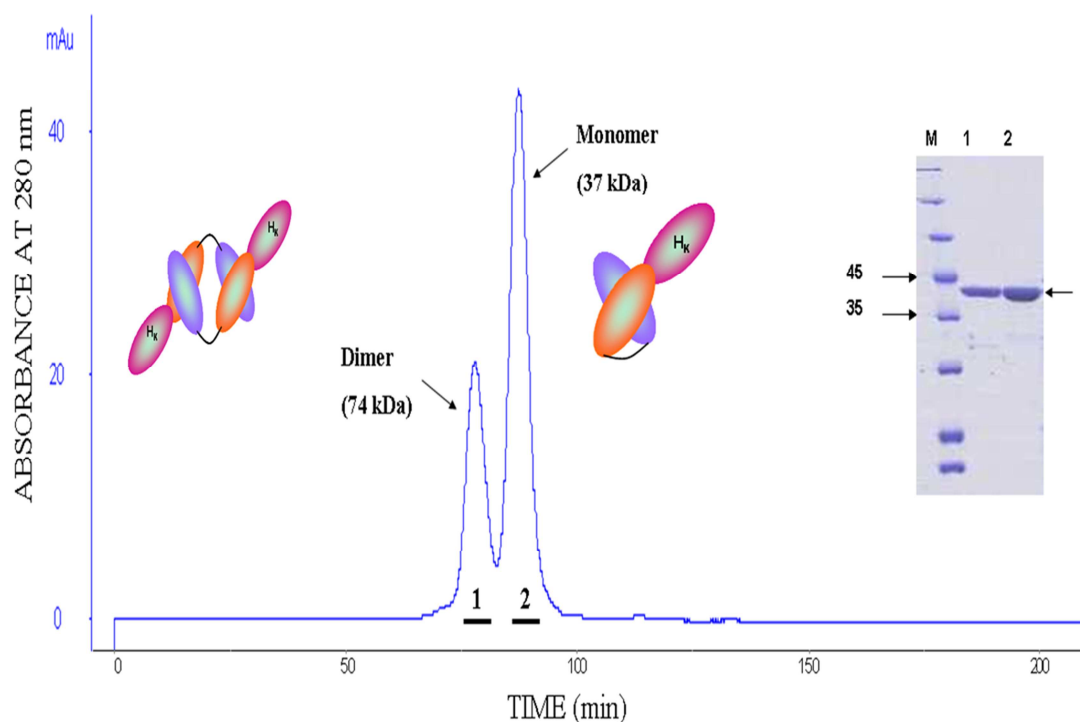


Figure XXXIX: Size exclusion HPLC on a calibrated Hi-Load 16/60 Superdex column of purified NPNA scFv fused to HuCk (fractions 13 – 18, Fig.). The column was eluted with 1X PBS (3.2 mM Na₂HPO₄, 0.5 mM KH₂PO₄, 1.3 mM KCl, 135 mM NaCl, pH 8.0), run at a flow rate of 1.0 ml/min. The dimer (peak 1) and monomer (peak 2) of the protein were analysed on SDS-PAGE (insert).

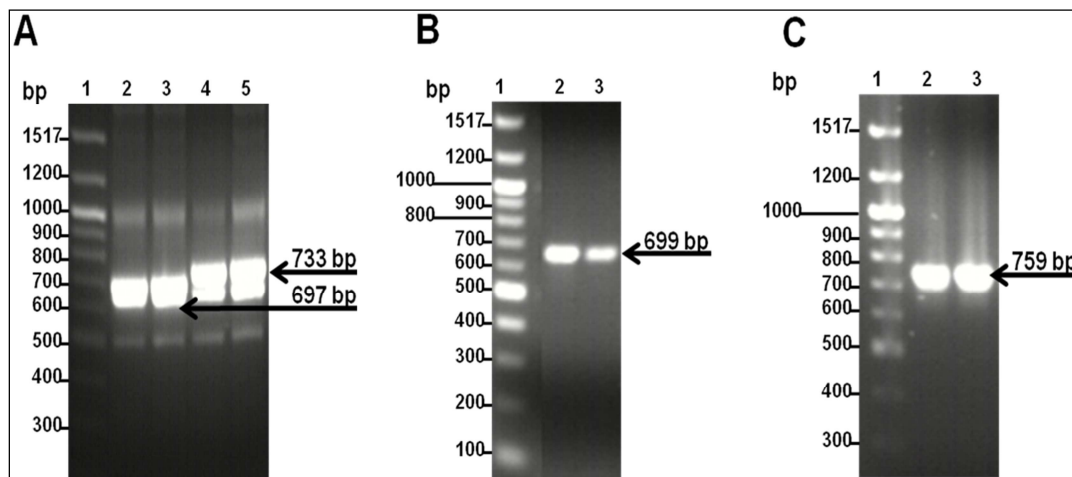


Figure XL: Agarose gel electrophoresis of PCR screened Pf-NPNA-1 scFv-0 and 12 (A) and 4B7 scFv-0 (B and C) scFvs in *Asaia* SF2.1. 25 μ L of each digested reaction was loaded and subjected to electrophoresis on a 1% agarose at 100 V for 1 hour. The DNA was visualised using ethidium bromide under UV light at wavelength of 200 nm. **A:** Pf-NPNA-1 scFv-0 (lane 2 and 3) and scFv-12 (lane 4 and 5) amplified with T7ABATG and PfVLR primers, **B:** 4B7(AJ) scFv-0 (lane 2 and 3) and **C:** 4B7(AJ) scFv-20 (lane 2 and 3) amplified with primers 4B7VLNco and 4B7VHNot. Lane 1: 100 bp DNA ladder (in all gels).

